A STUDY OF REACTIVE ION ETCHING OF GALLIUM ARSENIDE IN MIXTURES OF METHANE AND HYDROGEN PLASMAS

HOSSEIN FARIBORZ SAHAFI

A thesis submitted in partial fulfilment of the
requirements of the Middlesex University for
the degree of Doctor of Philosophy

December 1992

Middlesex University in collaboration with
GEC-Marconi Materials Technology Limited

I dedicate this work to
my parents Hassan and Farangis
my wife Sonia
and my daughter Pardis.

CONTENTS

ACKNOWLEDGEMENTS

I would like to thank the following people for their help during the progress of this research project.

My profound thanks to Dr Alan Webb and Dr Ali Rezazadeh without whom this project would not have started and ended successfully.

I would like to thank Professor George Goldspink, Dr Margaret Carter and Professor John Butcher for their excellent supervision of this project and invaluable advice.

It is a pleasure to acknowledge Messrs Dharmendra Jagjivan, David Court and Paul Kershaw for their help on equipment installations and electron microscope work.

It is a great pleasure to thank Messrs John White and Donald Thorpe for their advice on vacuum and electrical maintenance of the systems.

I would also like to thank Mrs Doreen Humm who organised all the official papers for the University committees.

Last but by no means least I would like to thank my father Mr Hassan Sahafi for his financial support throughout my life, especially during the past three years.

ABSTRACT

The aim of this research was to investigate the reactive ion etching (RIE) of gallium arsenide (GaAs) in mixtures of methane and hydrogen (CH_4/H_2) plasma and to evaluate thier advantages over chlorinated plasmas. This was performed in order to find the optimum etching conditions for GaAs such as, the best etch rate with greatest degree of anisotropy, the finest smooth side walls and the lowest surface roughness. The induced damage to GaAs due to RIE was investigated by current-voltage (I-V) and capacitance-voltage (C-V) measurements. From a study of the behaviour of the DC self bias voltage and an analysis of electrical characterization, a possible model of the mechanism of etching GaAs in methane and hydrogen mixtures was proposed. The main contributions of this research are as follows:

Etching of GaAs while maintaining the total flow rate of the gas mixture and its residence time in the chamber constant.

Studying the effect of the physical component of the etching mechanism on GaAs by investigating the variation in the DC self bias voltage for all process parameters.

Analyzing the effect of process parameters on the deposition rate of carbon polymers on the surface of the inorganic mask during GaAs etching.

Investigating the effect of process parameters and carbon polymer deposition on SiO_2 mask erosion during GaAs etching.

Examining the electrical characteristics of highly doped p-GaAs following RIE in CH_4/H_2 plasma and comparing with those of H_2 etched samples.

CHAPTER 1
INTRODUCTION

Dry etching is an important field of research in the microelectronics industry. This is because of the need for smaller device size and anisotropic pattern transfer (Singer, 1988). The process is also much cleaner than the alternative of wet etching as the use of acids and deionized (DI) water is minimized.

Silicon based technology uses dry etching for fabrication of integrated circuits (IC's) (Ephrath, 1982). Extensive research on dry etching of silicon (Si), silicon oxide (SiO_2), silicon nitride (Si_3N_4) and metallisation layers has been carried out by industries and research institutes (Sato and Nakamura, 1982 and Mullins, 1982). This was because of the extensive use of silicon technology in the microelectronics industry.

Over the past few years, mainly because of advances in optoelectronics, the need for fast devices and IC's made of III-V compounds has increased (Cooper III et al., 1989). These include devices such as metal-semiconductor field effect transistors (MESFET's) (Chen and Kensall, 1982) and high electron mobility transistors (HEMT's). Photonic devices such as semiconductor lasers, light emitting diodes (LED's), wave guides and photo-detectors are frequently used in optoelectronic circuits for communications (Yamada et al., 1985). Monolithic microwave integrated circuits (MMIC's) are also employed extensively (Hipwood and Wood, 1985).

For this reason, research into dry etching of III-V compounds has increased so that devices of high quality can be fabricated with minimum damage to their structures. In this chapter dry etching mechanisms are discussed and the advantages and handicaps of this process are explained.

1.1 Gallium arsenide

Gallium arsenide (GaAs), is considered to be an important semiconductor material for many reasons. The most important factor is the mobility of the electrons which is more than 5.6 times greater than the electron mobility in Si. This indicates that GaAs is an ideal material for fast devices such as HEMT's. The peak of the valence band in GaAs is vertically below the minimum of the conduction band. This classifies the material as a direct band semiconductor which is ideal for photonic devices such as semiconductor lasers (Sze, 1981).

For the bulk growth of GaAs, two techniques are commonly used (Thomas et al., 1986). The first is called the Liquid Encapsulated Czochralski method (LEC). This method is generally used to grow <100> oriented GaAs wafers which are mainly used for fast devices. The second method is called the Horizontal Bridgman method (HB). This method is mainly used for the growth of <111> oriented GaAs wafers and the largest consumer is the optoelectronics industry because the wafers grown by this method have a lower density of dislocations.

There are many techniques for the fabrication of epitaxial layers. If the layers do not have to be ultrathin, methods such as Liquid Phase Epitaxy (LPE) (Thompson and Kirkby, 1974), or Vapour Phase Epitaxy (VPE) (Olsen and Zamerowski, 1983) may be used. However, for the growth of ultrathin layers such as fabrication of quantum well devices, techniques such as Molecular Beam Epitaxy (MBE) (Foxon, 1978), and Metal Organic Chemical Vapour Deposition (MOCVD) (Moss, 1983), are necessary.

Two methods are available for etching GaAs (Thomas, et al., 1986). Firstly, wet etching, which involves the use of mixtures of deionized (DI) water, hydrogen peroxide (H_2O_2) and either sulphuric or hydrochloric acid (H_2SO_4 or HCl). This method allows a fast etch rate and very good selectivity.

Secondly, dry etching takes place in a vacuum chamber where ionized gases and/or reactive chemical radicals attack and etch the surface. There are many gases which can be used for this purpose but they will not be detailed here as the choice of the gas is dependent on the mechanism of etching.

1.2 Wet and dry etching

Three main problems arise when a wet etching technique is applied. First, reduction of device dimensions to nanometre scales makes the wet etching technique impracticable (Roosmalen, 1984). At about 3 μm, surface tension forces become significant. When the masked wafers are immersed in the etchant liquid, the surface tension force causes air bubbles to be trapped between the masking material and the etching liquid (see Figure 1.1). The result is failure to etch the surface of the semiconductor.

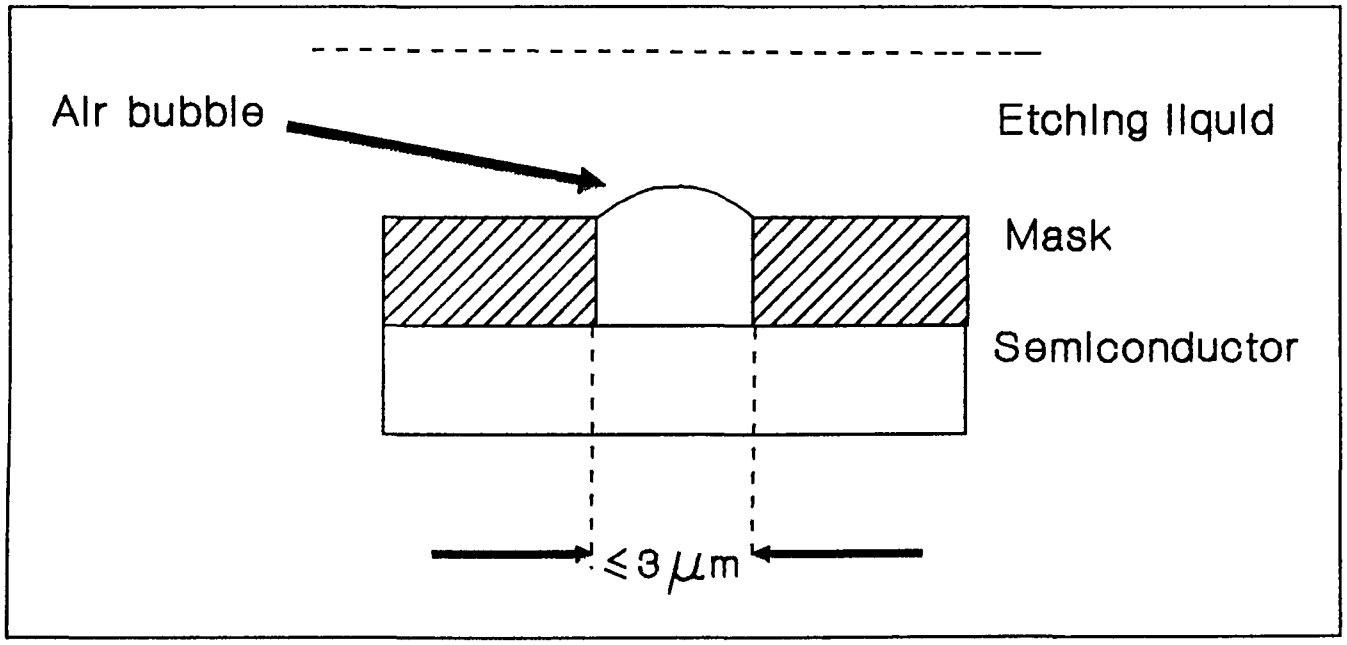

Figure 1.1. Air bubble trapped between the semiconductor surface, mask walls and etchant liquid.

Secondly, at dimensions larger than 3 μm, wet etching causes under- cutting of the mask (Coburn, 1982). This is because the liquid etches both laterally and vertically (isotropically). The dimensions of the etched patterns will then be larger than the initial mask pattern.

Finally, for optoelectronic devices there is a need for crystallographic orientation selectivity and anisotropic etching (vertical pattern transfer) (Ibbotson[a] and Flamm, 1988). The wet etching technique can perform crystallographic etching however it cannot perform anisotropic etching. Figure 1.2 shows the semiconductor surface before etching and possible etch profiles after etching. The profile is dependent on the technique implemented and the process parameters.

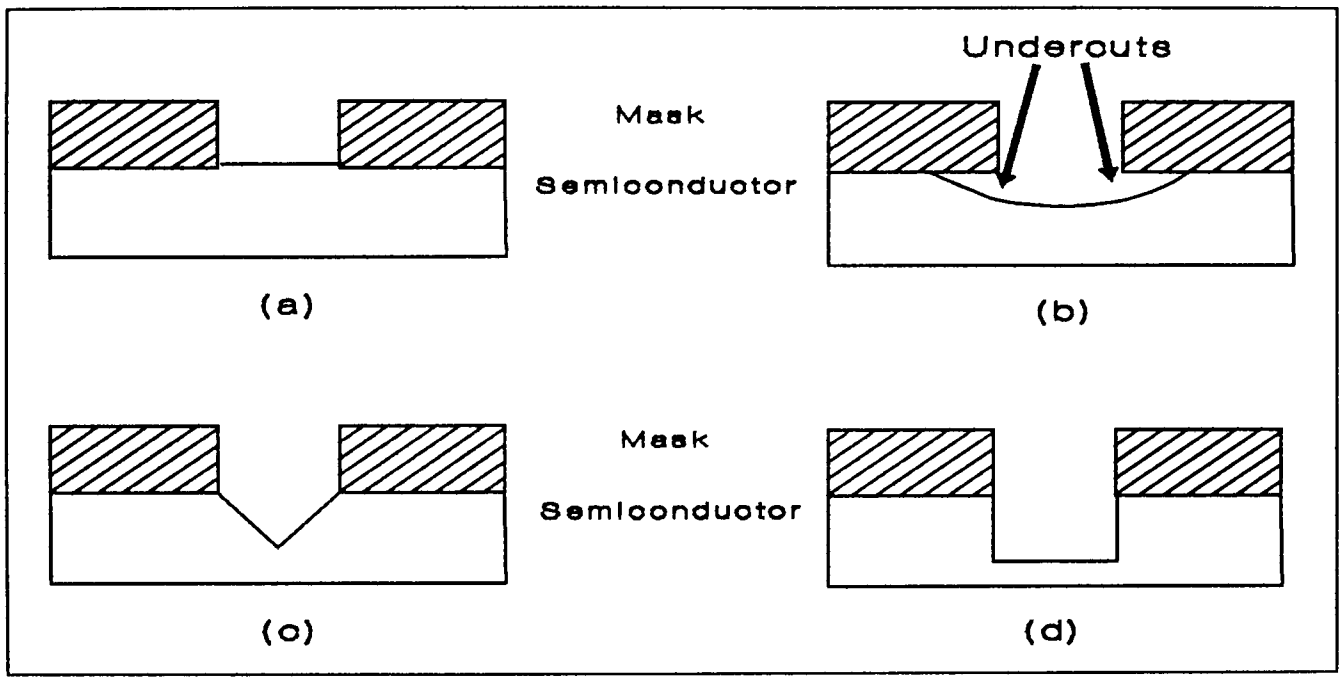

Figure 1.2. (a) Unetched. (b) Isotropic. (c) Crystallographic. (d) Anisotropic etching.

The advantages of wet etching are good selectivity, fast etch rate and crystallographic etching. Dry etching can perform crystallographic etching but at submicron dimensions. This depends on the etching parameters and the material which is etched. Table 1.1 shows the advantages and disadvantages of wet and dry etching.

The dry etching technique can overcome all the wet etching disadvantages stated in the table 1.1, but it has its disadvantages too. These are semiconductor damage such as surface and bulk modification and film deposition. Semiconductor damage occurs because of ion bombardment (Pang, 1984 and Yuba et al., 1988). These are generally, ion impregnation

and intrinsic bond damage. Film deposition is usually due to the non-active component of the etching gas used. The volatile species produced after etching may dissociate and a non-volatile component may land on the surface of the semiconductor.

Table 1.1. Advantages and disadvantages of wet and dry etching.

WET ETCHING		DRY ETCHING	
ADVANTAGES	DISADVANTAGES	ADVANTAGES	DISADVANTAGES
Good selectivity	Undercutting of mask	Submicron patterning	Surface damage
Fast etch rate	Isotropic etching	Anisotropic etching	Bulk damage
Crystallo-graphic etching	Failure to etch ≤ 3 μm	*Crystallo-graphic etching	Film deposition

*-Depending on the etching gas, etching parameters and material.

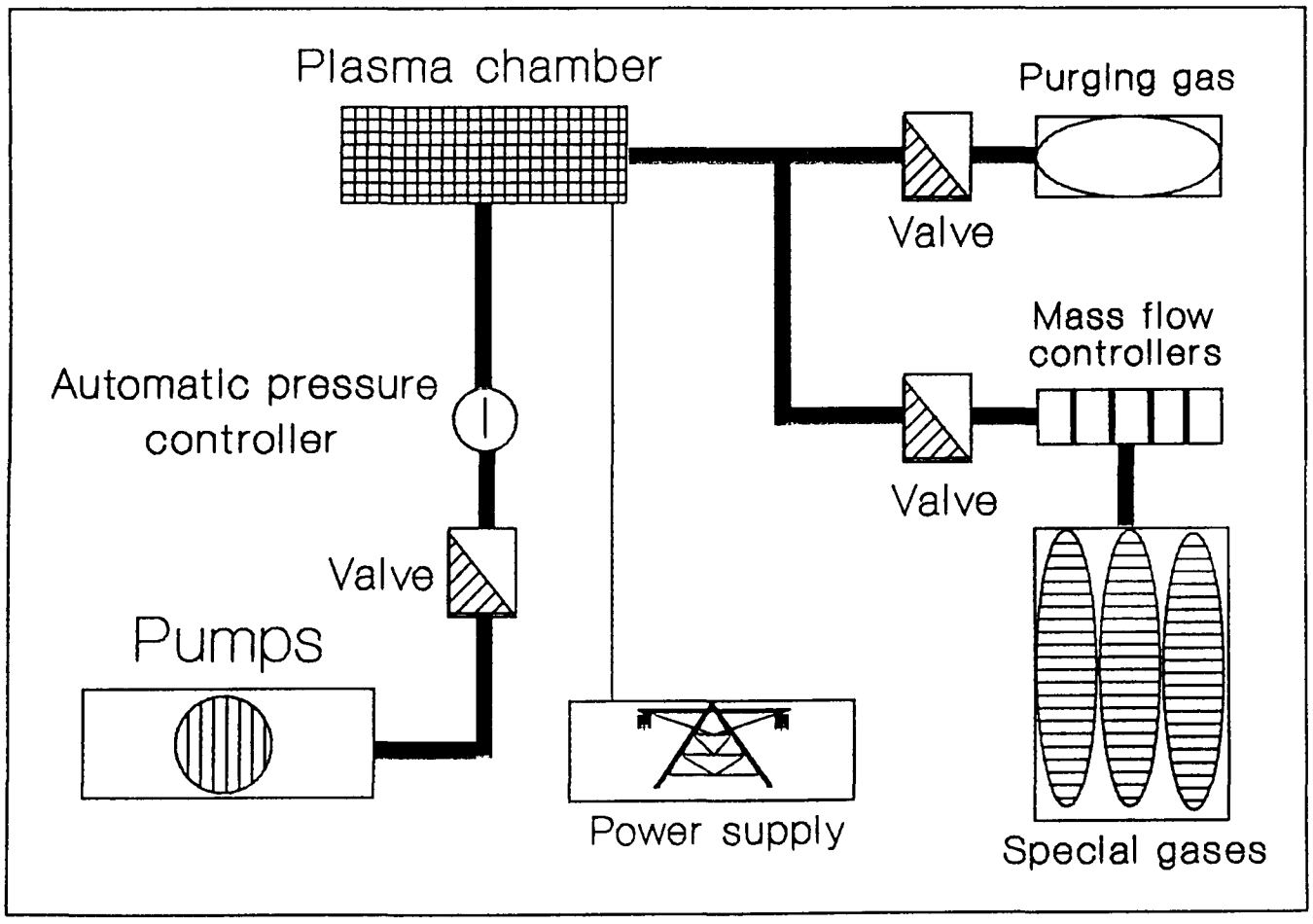

Figure 1.3. Diagram of a dry etching vacuum system.

Generally dry etching systems are relatively complex. Vacuum pumps are necessary to reduce pressure and mass flow controllers are needed to control the introduction of special gases. A power supply is required to ionize the gases. A valve between the process chamber and the pumps can control the pressure by changing the effective pumping speed. This allows control of pressure at different flow rates (see Figure 1.3).

The dry etching systems and configurations will be discussed in the next section. It must be noted that the number of configurations for dry etching systems increases as technology advances. For example electron cyclotron resonance system can be used in many configurations.

1.3 Mechanisms and configurations

Dry etching can be classified according to the three etching mechanisms as follows:

1. The physical mechanism.
2. The chemical mechanism.
3. The physical and chemical mechanism.

1. In a physical mechanism, the semiconductor is bombarded with ions of an inert gas (Horwitz, 1983). A typical gas used for this purpose is argon (Ar). Argon is ionized by creating a plasma in the chamber which contains the semiconductor. The surface of the semiconductor is then ion bombarded and the atoms in the surface are sputtered by the ions. The etch rate is slow and is dependent on the mass of the bombarding ions and the semiconductor binding energy. The selectivity is poor as any substance can be sputtered. The profile of the etch is approximately anisotropic as the ion direction at the surface is vertical.

2. A chemical mechanism uses gases which may be non-reactive normally,

but when ionized the molecules break down into reactive species (Flamm et al., 1983). These react chemically with the surface of the semiconductor to produce volatile species which escape from the surface. The selectivity is potentially good as the reactive species may not react with anything but the desired surface. The etch rate is fast and depends on the density of the reactive species, but the profile is isotropic as the active species will react with the semiconductor surface in all directions but not necessarily with equal rates.

3. The combined physical and chemical mechanism can be classified into two sub-mechanisms (Flamm and Donnelly, 1981). They are as follows:

(A). Energy-driven ion-enhanced mechanism.
(B). Inhibitor-driven ion-assisted mechanism.

In case (A), ions damage the surface causing bond damage and dislocations which allow reactions with reactive radicals to produce volatile products on the surface. These products will then escape from the surface.

In case (B), the reactive radicals are absorbed by the surface, creating an inhibitor thin film. The ions then supply energy to these radicals so that they react with the surface to produce the volatile products as above.

This process can provide an anisotropic profile, good selectivity and good etch rate. Table 1.2 indicates the characteristic of the above mentioned mechanisms.

There are at least 14 different configurations for dry etching (Fonash[a], 1985). These are listed in the table 1.3. Configurations 1 and 6 are of importance as they were used for the present study.

Table 1.2. Characteristics of dry etching mechanisms.

	PHYSICAL	CHEMICAL	PHYSICAL/CHEMICAL
PROFILE	Anisotropic	Isotropic and *Crystallographic	Isotropic, Anisotropic and *Crystallographic
ETCH RATE	Poor	Good	Good
SELECTIVITY	Poor	Very Good	*Good-Very Good
SUBMICRON PATTERNS	Very Good	Difficult	Very Good

*- Depending on the etching gas, etching parameters and material.

A barrel etcher (BE) using oxygen gas was generally used in the experiments to be described to remove negative photoresists and carbon and polymer films from the surface of the semiconductor. The etching mechanism of this configuration is chemical because the wafer stands at right angles to the electrodes so there is little ion bombardment of the surface. Only the radical species created in the plasma attack the surface of the semiconductor.

A reactive ion etching (RIE) system was used to etch the semiconductor surface . The mechanism is combined physical and chemical, as wafers were placed flat on the lower electrode (the cathode) which was connected to the power supply. Both the ions and the radical species attacked the surface of the semiconductor. The RIE system which was used here will be discussed later in detail.

1.4 Reactive ion etching process parameters

During RIE the process engineers require the following parameters to be under their control (Sze, 1985): power density, pressure, gas composition, flow rate, wafer area and temperature.

Table 1.3. Dry etching configurations.

	CONFIGURATIONS	MECHANISM	POWER DRIVE
1	Barrel etching	Chemical	RF
2	Downstream plasma etching	Chemical	RF
3	High pressure etching	Physical/chemical	RF
4	Plasma etching	Physical/chemical	RF
5	Ion etching	Physical	RF
6	Reactive ion etching	Physical/chemical	RF
7	Magnetic confinement ion etching	Physical	RF
8	Magnetic confinement reactive ion etching	Physical/chemical	RF
9	Triode etching	Physical/chemical	RF or DC
10	Ion beam etching	Physical	DC
11	Reactive ion beam etching	Physical/chemical	DC
12	Chemically assisted ion beam etching	Physical/chemical	DC
13	Photon assisted chemical etching	Physical/chemical	DC to drive photon source
14	+Electron cyclotron resonance etching	physical/chemical	MW or RF and MW

+- There are many configurations of electron cyclotron resonance system.
RF, DC and MW stand for radio frequency, direct current and microwave respectively.

Power density causes a breakdown of the gas molecules into reactive species. Increase in power density increases the etch rate non-linearly. Generally, high power density can cause substrate heating and can damage the semiconductor and photoresist.

Pressure can also affect the etch rate. An increase in pressure may increase the density of the molecular species in the etching chamber, but it causes a decrease in the ion bombardment intensity. Etch rate suffers when the etching mechanism is ion dependent. Mechanisms which are dependent on chemical species only will proceed faster (i.e. chemical mechanisms).

Gas composition is generally important for selectivity etching. A material may etch faster in one gas plasma than another because of the relative reaction rate of the radical species produced. Mixtures are also important as selectivity or surface roughness can improve by their use.

Gas flow rate determines the supply of reactants to the chamber. The residence time of the reactants in the chamber decreases as the flow rate increases. The relation between the flow rate Q and residence time τ_r is given by equation (1.1).

$$\tau_r = V_P \frac{p}{Q}, \qquad (1.1)$$

Where V_P is the plasma volume which can be taken as constant, and p is the chamber pressure. There are two flow regions, the high and low. At low flow rates, the etch rate may suffer because of inadequate supply of reactants. At high flow rates, the reactants are pumped away before they can react with the surface of the semiconductor. To achieve optimum etch rate, there is a need to choose a flow rate which can provide enough reactants, and allows enough time for the reaction at the surface of the semiconductor (Chapman and Minkiewicz, 1978).

The wafer area of the semiconductor may cause loading effect problems. This is because the species with long lifetimes react rapidly with the semiconductor surface. The species are consumed by the material and as the generation rate of the reactive species is fixed by parameters such as power density, pressure and flow rate, the concentration of the reactive species decreases as the etchable area of the semiconductor increases.

Temperature can also affect the etch rate of the material (Schwartz and Schaible, 1980). The etch rate changes at elevated temperatures also the roughness and uniformity may improve if the temperature of the substrate is controlled. The relation between etch rate R and temperature T is given

by equation (1.2).

$$R \sim \exp(-\frac{\xi}{KT}), \qquad (1.2)$$

where ξ is the activation energy for the reaction, T is the temperature and K is Boltzmann's constant.

1.5 Process variables

Process variables for dry etching can be divided into three broad categories and at the start of the present work the investigations were carried out on these process variables:

1. Etch rate.
2. Uniformity and reproducibility.
3. Selectivity and profile.

The etch rate which is generally important depends on the material to be etched and the process parameters such as power density, pressure, flow rate and gas composition (Carter, 1988).

Uniformity and reproducibility are dependent on (1) the length of exposure of the sample to the room ambient, (2) the electric field distribution, (3) the loading effect and (4) the gas distribution (Broydo, 1983). Selectivity and profile depend on the etching mechanism. When the mechanism is biased towards chemical etching, a strong loading effect is observed and the profile may not show a good anisotropic pattern. Choice of gas is important if selectivity is desired (Ibbotson[b] and Flamm, 1988).

1.6 Damage and deposition

Damage and deposition are inevitable side effects of dry etching. To

minimize these side effects they must first be identified. They can be separated into three groups (Fonash[b], 1985).

1. Film deposition.
2. Ion impregnation.
3. Intrinsic bond damage.

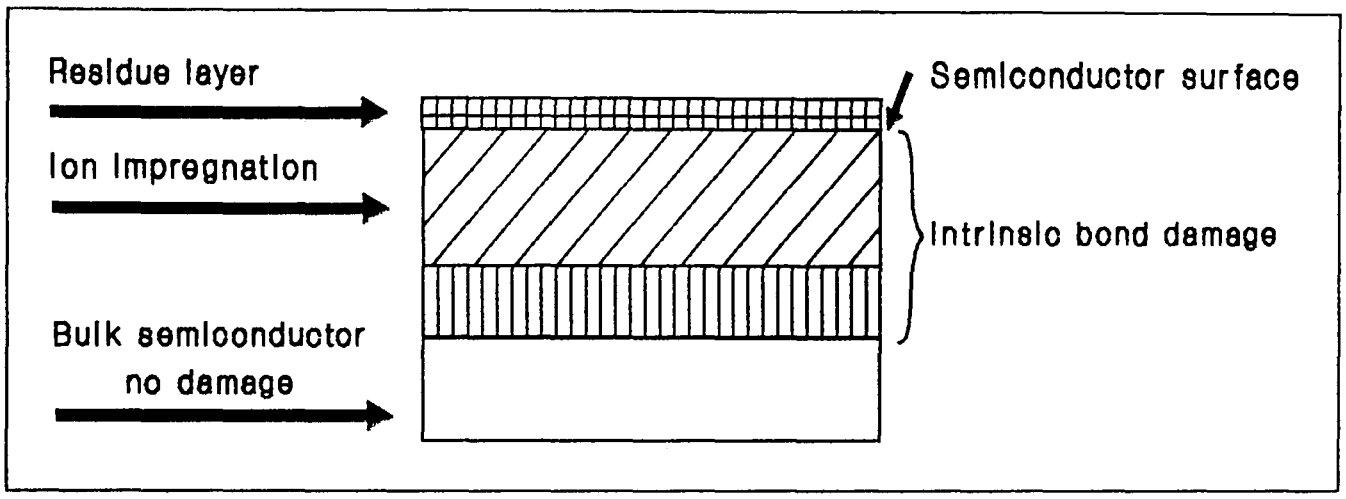

Figure 1.4. Macroscopic diagram of damage regions in semiconductors.

Figure 1.4 shows a schematic diagram of the damage regions with their identification. The top layer is the deposited or residual layer on the surface of the semiconductor. This layer may be present after chemical or combined physical and chemical dry etching. Its existence depends on the etching gas used and the etching chemistry.

Next is the ion impregnation region. This region is present after physical or combined physical and chemical etching. It contains the etching species or impurities which were implanted in the semiconductor during etching. This is because the high energy ions impregnate the semiconductor.

Last is the intrinsic bond damage. This region can extend further into the material than the ion impregnation region. This kind of damage is present in physical or combined physical and chemical etched samples. If the etched material is a compound, the stoichiometry may be disturbed. Dislocations, vacancies and interstitials will be present in this region.

CHAPTER 2
A REVIEW OF DRY ETCHING OF III-V COMPOUNDS

In this chapter the dry etching of III-V semiconductors is reviewed. There are many articles and papers published on this subject but only the most useful have been cited. The use of halogenated gases and mixtures, pure hydrogen and mixtures of hydrogen and hydrocarbon gases are reviewed for etching III-V semiconductors.

Numerical values of semiconductor etch rates are not discussed here as they are dependent on the dry etching equipment. There is no standard equipment which can be used to compare etch rates.

2.1 Dry etching with chlorinated gases

To etch III-V semiconductors it is important to etch both the semiconductor and the surface oxide layer because the oxide layer can act as an etch stop. It has been reported that gases such as Cl_2, CCl_4, CCl_2F_2, PCl_3 and HCl can be used for GaAs etching. With the exception of Cl_2 these gases can also remove the surface oxides, (Smolinsky, et al., 1981).

For InP etching, although chlorinated gases were used, the etch rate was low and the etched surface was discovered to be very rough at ambient temperatures. When etched at elevated temperatures, smoother surfaces were produced (Donnelly, et al., 1982). It has been also discovered that in a chlorinated plasma without fluorine gases, the etched surfaces were Ga or In rich for GaAs and InP respectively.

Hydrogen chloride (HCl) and carbon tetrachloride (CCl_4) were compared for etching GaAs, (Smolinsky, et al., 1983). HCl did not show a high etch rate

but no carbon deposition occurred on the sample compared with CCl_4. It has been suggested that HCl gas without plasma could not etch GaAs below 250°C, (Akita, et al., 1991). Nonetheless GaAs was etched in HCl gas when the surface of the semiconductor was irradiated with an electron beam. It has been found that the lower the wafer temperature, the faster the etch rate. It has been even suggested that an enhanced etch rate was possible if the wafer temperature was reduced below 0°C. The reasoning given for this suggestion was an assumption that the absorption of HCl molecules on the surface decreases with increase in temperature and so the lower the temperature of the semiconductor sample, the higher the absorption of the molecules. This would result in a higher etch rate. The electron beam enhanced the dissociation and excitation of HCl molecules such that the hydrogen and chlorine atoms could then react with the surface.

CCl_4 showed a high etch rate compared with HCl but the problem was the deposition of a poly-chloro-carbon film on the surface of the semiconductor. Addition of oxygen to CCl_4 increased the etch rate further and reduced the formation of the poly-chloro-carbon film. Analysis of the plasma during InP etching in CCl_4 showed the existence of $InCl_x$ species. Both GaAs and InP displayed non-Arrhenius behaviour and a loading effect. However, at elevated temperatures the loading effect was reduced, (Gottscho, et al., 1982).

The use of CCl_4 for patterning III-V compounds offered good reproducibility although it had many undesirable effects such as rough etched surfaces and deposition of poly-chloro-carbon films, (Semura, et al., 1984). When GaAs was etched in pure CCl_4, the surface looked either grey due to roughness or black due to film deposition. The profile of the etched pattern also showed non-anisotropy. To improve the etching quality, CCl_4 was diluted with oxygen (O_2) and then hydrogen (H_2) to etch GaAs.

At low concentrations of O_2, etch rate improved, but the etched surface

quality was poor. As the concentration of O_2 increased, the surface quality improved slightly but trenches were formed at the base of the etched walls. The addition of H_2 to the working gas instead of O_2 improved the quality of the etched surface. The etch rate decreased slightly but the etched profile was anisotropic with smooth surface and side walls.

The analysis of the CCl_4/H_2 etched GaAs surface showed traces of oxide and C. It was presumed that the oxygen contamination was due to the exposure of the sample to the atmosphere. The larger amount of C detected was thought to be due to contamination during etching. Raman spectroscopy showed no additional damage compared with a wet etched sample.

Boron trichloride (BCl_3) has also been used for GaAs etching. The GaAs etch rates obtained were rather low compared to other chlorinated processes, (Sonek and Ballantyne, 1984). The reason for this was that the process chamber together with the electrode was made of aluminium (Al). It is thought that this may have caused the reduction in etch rate of the semiconductor as the etching gas attacked the whole of the chamber. This may have caused a loading effect.

Generally the etched profiles were anisotropic at optimum conditions and the etched surface was smooth but the surface of the side walls was very rough. Increase in power density and pressure increased the etch rate slightly at first and then it decreased. This increase might have been much larger if the chamber were not made of aluminium. At high power density the anisotropic pattern was lost due to ion bombardment scattering from the surface. Analysis of the surface of the GaAs after etching in optimum conditions showed no chlorine or boron contamination.

Addition of chlorine to BCl_3 caused a loss of anisotropy but increased the etch rate. The surface was also very rough. Addition of argon reduced the surface roughness and improved the anisotropy for both GaAs and AlGaAs,

(Scherer, et al., 1987). The authors have suggested a model for the etching of GaAs and AlGaAs at different power densities, pressures and Ar volume concentration. This model was machine dependent which meant that it could not be used for all RIE systems.

During RIE of GaAs and AlGaAs in BCl_3/Ar mixtures, four problems were identified by the authors. They were;

(1) under-cutting at the high pressure caused a loss of directionality of etching.

(2) inclined side wall profiles (shadowing), due to low pressure which allowed too high a sputtering rate.

(3) surface roughness due to high power density and low chamber pressure.

(4) re-deposition of materials, mainly on the mask, due to etching at low power densities and pressures during very short etching periods.

To etch GaAs together with AlGaAs with a high degree of selectivity, it is best to use fluorine and chlorine based gases. One of the common gases used for selective etching of GaAs and AlGaAs is dichlorodifluoromethane (CCl_2F_2), which was also used in a mixture with an inert gas, (Hikosaka, et al., 1981).

In pure CCl_2F_2 the GaAs etch rate increased as the pressure increased but in the case of AlGaAs the etch rate decreased. It was demonstrated that the DC self bias voltage (See chapter four and appendix XI for a discussion of DC self bias voltage), decreased as pressure increased which indicated that the etching of AlGaAs was mainly dependent on ion bombardment. The low etch rate for AlGaAs was considered to be due to the formation of aluminium fluoride AlF_3 on the surface of the sample. The etching of the sample also started after a small delay due to the surface oxides which first had to be sputtered. This has been reduced by adding helium to CCl_2F_2.

Generally GaAs which was etched in pure CCl_2F_2 was covered with a thin film of contaminant which may have been a fluoro-chloro-carbon polymer. This could be eliminated by adding He to the etching gas. When He was used as a mixing gas, the GaAs etch rate decreased but the AlGaAs etch rate increased. This was due to an increase in the DC self bias voltage which indicated an intensification of ion bombardment and reduction of etchant species. At high pressures and high CCl_2F_2 to He ratio, the selectivity of GaAs to AlGaAs was very high with AlGaAs hardly showing any etching tendencies.

When the plasma chemical species were analyzed, (Chaplart, et al., 1983), Cl, Cl_2, CCl, CF, CF_2 and CF_3 species were detected. Increase in flow rate increased the etch rate due to increase in the supply of reactive species to the chamber. Increase in power density also increased the etch rate due to breakdown of the gas molecules which caused the supply of more reactive species and also intensification of ion bombardment. The etch rate however increased when Ar was let into the chamber. Large increases in Ar concentration caused a reduction in etch rate. It was established that the etching was primarily caused by Cl species reacting with GaAs to form $GaCl_x$ and $AsCl_x$, but F also reacted with the surface to form GaF_x and AsF_x. In this case the GaF_x species would not etch due to low volatility of these species. Addition of Ar to the gas caused the sputtering of these non-volatile species from the surface and hence increased the etch rate.

Further work on plasma diagnostics indicated the presence of other species in the chamber, (Seaward, et al., 1987). These were F, C_2F_2, HF, HCl and CO. H and O were also observed but it was thought that their presence may have been due to the presence of water vapour in the chamber. The volatile species were thought to be the same as above with the addition of $AsCl_xF_y$ and in the case of aluminium, $AlCl_x$. The non-volatile species detected were $GaCl_xF_y$ and AlF_3.

Further work on selective etching of GaAs and AlGaAs proved the case presented by Hikosaka, et al., (Knoedler and Kuech, 1986). The experiments were performed using different AlGaAs compositions. It has been found that the higher the Al content the lower the etch rate of the sample etched. Selectivity between GaAs and AlGaAs increased as the Al composition increased. Selectivity decreased as the DC self bias voltage increased.

However no delay in etching was observed when the samples were being etched, (i.e. no initiation time of etching was observed). This may have been due to removal of the surface oxides before etching.

Very good anisotropic pattern transfer was achieved using CCl_2F_2, (Hilton and Woodward, 1988). The profile of the pattern was controlled by addition of He to the etching gas, (Hirano and Asai, 1991). By controlling the He volume concentration the angle of the etched wall together with the degree of undercutting could also be controlled. Devices were fabricated using CCl_2F_2. An exotic optical device was the micro-lens array, (Darbyshire and Pitt, 1990). The fabrication was performed using a chemically assisted ion beam etching system, (CAIBE). In this case an Ar beam was used and CCl_2F_2 was introduced into the chamber as the working gas. The photoresist was overheated so that it took a hemispherical shape. Non-selective etching had to take place so that the photoresist and the GaAs substrate etched at the same rate. Other devices such as FETs were also fabricated to test the current-voltage (I-V) and capacitance-voltage (C-V) characteristics of the etched semiconductors (Hilton, et al., 1989).

Another gas widely used in III-V semiconductor etching is silicon tetrachloride ($SiCl_4$). The advantage of this gas over other halocarbon gases is that it does not produce poly-chloro-fluoro-carbon films on the surface (Stern and Liao, 1983). Also it can etch Al efficiently. Like other processes using chlorinated gases, the etch rate of GaAs was higher than that of InP,

due to the non-volatility of the $InCl_x$ species as discussed above. Increase in power density increased DC self bias voltage and etch rate. Decrease in pressure also increased DC self bias voltage. The profiles of the etched GaAs and InP were not anisotropic at high pressures but then improved as the pressure was reduced. To improve anisotropy Ar was added to the $SiCl_4$.

Further work on GaAs etching in $SiCl_4$ demonstrated orientation-dependent etching, (ODE) or crystallographic etching, (Li, et al., 1984 and 1985). This was observed at low power densities and high pressures. Decrease in pressure caused a reduction in reactive species and increased the DC self bias voltage. In such conditions the crystallographic etching gave way to anisotropic etching. Addition of Ar to $SiCl_4$ also caused the loss of crystallographic etching.

The selectivity experiments performed on masks showed $SiCl_4$ to be suitable for non-organic masks. For optimum conditions pure $SiCl_4$ was very selective for GaAs etching when chromium (Cr), silicon nitride (Si_xN_y) and silicon oxide (SiO_x) were used as masking materials. The photoresists did not show good selectivity compared with non-organic masks. Addition of Ar to $SiCl_4$ reduced the selectivity in all cases.

$SiCl_4$ has also been used for selective etching of GaAs over AlGaAs. This was possible by mixing the chlorinated gas with sulphur hexafluoride (SF_6), (Salimian and Cooper,III, 1988). The reaction of fluorine with the surface of AlGaAs formed non-volatile AlF_3.

The etch rate of GaAs increased slightly as the SF_6 volume concentration increased. However it had the opposite effect on the AlGaAs. Its etch rate decreased by a large amount as the SF_6 volume concentration increased. The only way the etch rate could be increased was by increasing the ion bombardment intensity. This effect was observed also for AlGaAs etching

in CCl_2F_2. Increase in ion bombardment did not have an effect on GaAs etching. From this it was apparent that the AlGaAs etching in this mixture was largely dependent on a physical mechanism.

The selectivity of GaAs to AlGaAs increased as the SF_6 concentration increased. However, at high concentrations of this gas the selectivity did not change. Increase in ion bombardment decreased selectivity.

Elemental analysis of etched GaAs sample indicated no traces of Cl, F, Si and S contamination. C and O contaminations were present due to exposure to ambient air. The AlGaAs sample did show traces of F due to the non-volatile AlF_3 on the surface. The etched profile of the GaAs/AlGaAs showed a very good anisotropy.

The etched profiles of GaAs and InP have also been investigated at elevated temperatures, (Van Daele, et al., 1990). At low temperatures GaAs showed good anisotropic profiles but at elevated temperatures this was lost. For InP the effect was the opposite. At low temperature the etch rate was slow and the surface was smooth but the pattern was not anisotropic. As the temperature increased the etch rate increased and the profile became more anisotropic but the surface became rough.

The I-V characteristics of GaAs Schottky diodes did not show much difference between the reference and etched samples. However the C-V measurements indicated some passivation of carrier concentration by a factor of 10 near the surface of the sample.

Chlorine, (Cl_2) gas has also been widely used to etch III-V compounds. This was used for crystallographic, selective and non-selective etching of GaAs and AlGaAs. Crystallographic etching of GaAs and AlGaAs was investigated using a reactive ion beam etching system, (RIBE) with an ECR source, (ECR-RIBE), (Sugata and Asakawa, 1987). GaAs was reported to

be etched by Cl radicals (plasma excited) and Cl_2 (with no plasma excitation) without the presence of an ion beam. Cl radicals etched GaAs from about 190°C. In the case of Cl_2, the etching did not start until 290°C.

The rate limitation of the etching process at low temperature was considered to be due to the thermal desorption of $GaCl_x$ which is higher than that of $AsCl_x$. At high temperatures this was due to the low supply of Cl species. When both Cl radicals and ions were used to etch the samples, rapid etching started at much lower temperatures than 190°C. This is the region where Cl radicals or Cl_2 molecules could not etch.

Etching started at such low temperatures because the non-volatile products which were formed on the surface were desorbed by ion bombardment. Crystallographic etching of GaAs and AlGaAs was performed by using both Cl radicals and Cl_2 molecules. In all cases the process was temperature dependent.

Generally during RIE of GaAs/AlGaAs the selectivity is affected by the presence of O_2 or water vapour, in the chamber. The selectivity of GaAs over AlGaAs is thought to be due to the oxidation of Al on the surface. The oxide does not normally react with Cl radicals and must be sputtered away. It was found that to etch GaAs and AlGaAs non-selectively, the partial pressure of O_2 and H_2O in the chamber must be reduced, (Vawter, et al., 1987).

At low pressures (< 10 mtorr) the non-selective etching of GaAs/AlGaAs was possible. Below 1 mtorr, the etch rate of GaAs was found to be greater than that of AlGaAs. When the DC self bias voltage increased, non-selective etching was observed again. This behaviour was due to the high partial pressure of O_2 and H_2O at very low pressures. Higher DC self bias was needed to etch away the native oxides.

In order to remove the oxide and carbon contamination from the surfaces of III-V compounds, the samples could be exposed to certain radical species, (Asakawa, et al., 1987). To remove the carbon from the surface of the sample it could be exposed to O radicals to produce CO species which would then escape from the surface. To remove the oxide layer the sample could be exposed to H radicals at about 100°C to form H_2O vapour which would also leave the surface. When the surface of the process samples were analyzed before exposure to the atmosphere no traces of surface oxide or C were observed.

Cl_2 has been used to remove a monolayer of GaAs molecules from the surface, (Aoyagi, et al., 1992). This was possible because of the design of the etching system. The etching stopped automatically after one molecular layer was removed because of the synchronisation between the etchant feeding rate and incident energetic beam flux.

Electrical characteristics of n-GaAs etched in Cl_2 were also investigated, (Lee and Baratte, 1990). These were compared with the characteristics of the sample etched in Ar. The ideality factor and barrier height of the Cl_2 etched sample improved compared to the sample etched in argon.

Chlorinated gases were found to be flexible etchants for III-V compounds. GaAs, AlGaAs and InP could all be etched under different conditions. The problem with the chlorinated gases is that they are either corrosive, toxic or both, which is not healthy for the operator or the system. There is also the problem of general roughness of the surface of the III-V compounds etched and also the low etch rate of InP. For this reason it was important to search for other etchant gases which were not hazardous to the operator or the etching system. This may be possible by reducing the amount of the chlorinated gas entering the chamber.

2.2 Exotic halogenated mixtures

Cl_2 was mixed with other gases to etch III-V compounds. The reason for this was the fact that Indium and Gallium were generally hard to remove as they remained as $InCl_x$ and $GaCl_x$ on the surface. Addition of Ar removed some of these species by sputtering but the surface remained rough. Various mixtures of Cl_2 have been used to etch GaAs, (Vodjdani and Parrens, 1987). These mixtures were $Cl_2/CH_4/Ar$, $Cl_2/CH_4/H_2$ and $Cl_2/H_2/Ar$.

When CH_4 was used in the Cl_2/Ar mixture, at optimum conditions the surface became very smooth and an anisotropic profile was observed. When the volume concentration of Cl_2 increased, the etch rate also increased but the surface became very rough and the results were not reproducible. At very low concentrations of Cl_2 the surface was very rough mainly due to film deposition because of CH_4 reactions.

When a $Cl_2/CH_4/H_2$ mixture was used, the etch rate was small at low volume concentration of H_2 due to film polymerization on the surface. As the H_2 volume concentration increased, the etch rate increased also. When $Cl_2/H_2/Ar$ was used, the etch rate decreased as the H_2 volume concentration increased. At low concentrations of H_2 the surface was rough but at high H_2 concentrations the surface was smooth and the etched profile was anisotropic.

The analysis of the surface showed Cl, C, and O contamination on all dry etched samples. The O and C peaks were considered to be due to exposure to atmosphere. However certain samples displayed a larger amount of C on the surface than usual and they were the samples which were exposed to the mixtures which contained CH_4.

CH_4 could be used to remove the Ga from the Ga-rich surface with the help of ion bombardment because Cl_2/Ar mixtures alone could not remove all

the Ga and provide a smooth surface. The H_2 could be used whenever CH_4 was used in order to stop polymerization on the surface. It is therefore important to use all these gases together, that is to use a mixture of $Cl_2/CH_4/H_2/Ar$. Mirror facets for InP/InGaAsP lasers have been etched using this mixture, (Van Gurp, et al., 1989). In order to produce a smooth surface the sample was heated to 200°C.

The damage on the surface of the etched InP was investigated using such a mixture. This was because InP is the hardest semiconductor to etch in chlorinated gases, (Van Roijen, et al., 1991). The analyzed surface of the etched InP showed large amounts of phosphorus (P). This was important because the surface of the InP etched in a gas mixture containing Cl_2 is In or $InCl_x$-rich due to the low volatility of these species. The amount of P detected on the surface was much larger when a higher power density was used. Generally no Cl species were detected on the surface and minimal Ar penetration was observed. The surface of the etched InP sample was very smooth and no trenching was visible at the base of the etched wall. The profile of the etched wall was highly anisotropic. High resolution transmission electron microscopy (HRTEM) confirmed the surface analysis results when the P-rich layer was observed. The thickness of this layer was shown to be greater when greater power densities were used to etch the surface.

The use of CH_4 and H_2 at 200°C meant that the C and H species could react easily with the In which was not generally volatile. This reaction could have generated In metal-organic compounds which are extremely volatile at this temperature.

It was suggested by the authors that the damage did not penetrate more than a few nanometres from the surface. Hydrogen could diffuse deep in the semiconductor at 200°C. Also the effect of ion bombardment could damage the crystal lattice up to a depth depending on ion energy. The

carrier concentration at different depths from the surface could have been determined if the authors had shown some C-V measurements.

A mixture of phosphorus trichloride (PCl_3) and Ar was also used to etch III-V compounds. A quantum-well laser structure with many layers of GaAs, AlGaAs and InGaAs was etched using an ECR-RIE system, (Pearton and Hobson, 1991). It was shown that the etched depth increased as the microwave power increased. However the anisotropy of the etched pattern was poor. Trenching was visible at the base of the etched wall and residues were formed on the surface of the semiconductor.

Chloromethane ($ClCH_3$) mixed with H_2 has been used to etch both GaAs and InP, (Law and Jones, 1992). Other admix gases were also used instead of H_2. They were helium (He), neon (Ne), argon (Ar) and oxygen (O_2). In order to vary the concentration of the mixture, the H_2 flow rate was kept constant but the $ClCH_3$ flow rate was varied. The etch rate of GaAs increased as the concentration of $ClCH_3$ was increased until it reached a maximum. Further increases of the concentration of $ClCH_3$ reduced etch rate due to the deposition of polymers on the surface of the sample until etching stopped all together. At low flow rates of H_2 the optimum etch rate was also low.

The etch rate of InP was much higher than the GaAs under the same conditions. Increase in power density increased the etch rate of GaAs linearly, but the InP etch rate appeared to increase exponentially. The etched GaAs displayed a very smooth surface and side wall but the anisotropy was poor. InP displayed good anisotropy and a smooth surface but the side walls were rough. The use of oxygen as the admix gas reduced etch rate.

When H_2 was replaced with other admix gases, the profile of the concentration graph was the same as when H_2 was used but the maximum

etch rate occurred at different concentrations of $ClCH_3$. The maximum etch rate was also much lower than when H_2 was used. When other admix gases were used instead of H_2, the mechanism of etching may be different.

Iodomethane (ICH_3) was one of the non-chlorinated halogen gases which was used to etch InP, (Doughty, et al., 1986). The etch rate was slow and the etched surface was rough. This was due to the deposition of a polymer film on the surface. The formation of the polymer film was reduced when Ar was added to the ICH_3. When O_2 was added to the ICH_3 instead of Ar, the etch rate improved and the polymer film was removed from the surface. The etched side wall was very rough and the anisotropy was not good.

Iodine (I_2) was used with Ar in an ion beam-assisted etching system, (IBAE) to etch InP. At the optimum conditions the etch rate was low but the surface was very smooth. The profile anisotropy was poor.

InP was also etched in hydrogen iodide (HI). HI was mixed with H_2 and Ar. The etching was performed in a ECR-RIE system. on both n and p type InP, (Pearton, et al., 1992). The etch rate of InP increased as the DC self bias voltage increased. The etch rate of both types of InP was the same for the same conditions within the limits of experimental errors. The profile of the etched samples showed a very good anisotropic pattern and the etched surface and side walls were very smooth but trenches were formed at the base of the etched walls. Removal of H_2 from the mixture increased the etch rate but the surface of the etched sample became very rough. Addition of the CH_4 to the mixture instead of H_2 decreased the etch rate by a large amount due to a CH_x and I reaction. The surface analysis of the etched surfaces indicated traces of C and O but no traces of I were found. The O and C found on the surface were due to surface oxidation and carbon contamination because of exposure of the sample to the atmosphere.

The etching of InP was considered to be due to the formation of volatile

species such as InI_x, PI_x and PH_x. Other III-V compounds could be etched if similar volatile compounds were to be formed.

2.3 Hydrogen plasma

Generally nearly all halogenated gases used for dry etching of III-V compounds are toxic and/or corrosive. Thus there is interest in gases which are not so hazardous to the operator or the etching system.

Hydrogen (H_2) was thought to be useful, (Chang[a & b], et al., 1982). It was thought that atomic hydrogen could be formed from dissociating hydrogen molecules by electron or photon collisions. The atomic hydrogen would then react with the surface to produce volatile hydrides. Also it could react with the surface oxides and remove them. For H_2 etching of III-V compounds, the required etching temperature was found to be higher for GaAs than InP. Micrographs of the sample showed undercutting of the etched surface.

It was found that atomic hydrogen can etch GaAs without the help of a plasma at atmospheric pressure but at high temperatures. The GaAs was heated to about 850°C in an H_2 or H_2/He atmosphere. A tungsten filament was heated to about 2000 °C above the sample, (Kobayashi, et al., 1991). At these conditions the GaAs could be etched at a reasonable rate. Reduction in the temperature of the filament resulted in pit formation which was Ga-rich. This was due to the difference in the vapour pressure of Ga and As. When the filament was heated again, the pit formation disappeared. The etch rate increased as the substrate temperature increased. The etch rate of GaAs in these conditions followed an Arrhenius model.

The RIE of n-GaAs was performed in hydrogen to measure the degree of damage caused by hydrogen ions, (Pang, 1986). The degree of damage during RIE was dependent on the extent of ion bombardment. Also in the

case of H_2, the higher the substrate temperature, the higher the possibility of H diffusion into the substrate. I-V characteristics of the hydrogen etched sample indicated a large divergence from the original ideality factor and the barrier potential.

Damage due to hydrogenation of GaAs was further studied by C-V measurements of the carrier concentration from the surface through the material, (Dautremont-Smith, 1988 and Pearton, et al., 1987). To permit H to diffuse in the GaAs the temperature had to be in the range 150°C to 300°C. For Si- doped n-GaAs hydrogenated at 250°C, the carrier concentration decreased by about a factor of 100 near the surface, compared to the control sample. The passivation of donors extended deep in the semiconductor in some cases greater than 10 μm.

The diffusion of hydrogen was assessed for Si doped n-GaAs and Zn doped p-GaAs of equal carrier concentrations etched under the same conditions. It was found that;

(1) the diffusion depth of H in p-GaAs was much greater than that in n-GaAs,

(2) in the case of low frequency plasma (10-30 kHz), the diffusion depth of H in n-GaAs increases with decreasing donor concentration and in p-GaAs it increases with increasing acceptor concentration,

(3) low frequency exposure of GaAs produced about an order of magnitude greater depth and greater peak concentration for the same conditions than did high frequency, (2.45 GHz).

After annealing, full recovery of carriers was reported. It was established that only a fraction of the hydrogen had diffused out of the GaAs. The complete recovery may have been due to the repair of defects within the crystal.

2.4 Non-chlorinated gases

The RIE of InP in chlorinated gases suffered from low etch rate and surface roughness due to low volatility of $InCl_x$ products. For this reason alternative etching gases were investigated. One mixture was discovered to etch InP at a high rate in room temperature. This was a mixture of methane and hydrogen, (CH_4/H_2), (Niggebrügge, et al., 1985).

When InP samples were etched in CH_4/H_2 mixtures, the etch rate was high and the etched surface was smooth with good anisotropy of etched walls. When CH_4 was replaced with Ar and the sample was etched under the same conditions, the surface became rough and etch rate decreased. This was claimed to be a characteristic of physical etching. In pure H_2, InP was hardly etched at all. As CH_4 was introduced into the chamber the etch rate increased. This continued with increase in volume concentration of CH_4 until the etch rate reached a maximum. Any further increases in CH_4 concentration decreased the etch rate until carbon polymerization occurred on the surface of the sample. This carbon polymerization also occurred at very low power density. The etching was also weakly dependent on temperature.

The deposited film was thought to be of hydrocarbon polymeric species. This polymeric film was deposited on the mask material for both photoresist and inorganic types. One good feature of this was the fact that the mask material was reinforced because of the polymer film on its surface. This allowed the etching to continue for a long time. This film could be removed in O_2 plasma.

The etch rates of other III-V semiconductors were also investigated using this mixture. It was discovered that the etch rate was reduced as the Ga content increased in the compound. The highest etch rate was achieved for InP, InGaAsP, InGaAs and GaAs respectively.

The electrical characteristics of the CH_4/H_2 etched GaAs were also investigated, (Cheung, et al., 1987). The I-V and photoluminesence, (PL) analysis indicated very low damage at different power densities. The etch rate of GaAs in H_2 was very low but as CH_4 was added the etch rate increased. The etch rate of GaAs followed the same pattern as for InP discussed above. This continued with increase in volume concentration of CH_4 until the etch rate reached a maximum and then it decreased with any further increases in concentration of CH_4 until deposition occurred on the surface of the sample.

It is thought that the RIE of III-V compounds in CH_4/H_2 mixtures is the reverse of metal-organic chemical vapour deposition, (MOCVD), Therefore this process is now called metal-organic reactive ion etching, (MORIE). Ar has been added to the CH_4/H_2 mixture to etch InP. It was claimed that the surface of InP was rough when Ar was not used in the mixture. However after etching in a $CH_4/H_2/Ar$ mixture the surface was smoother but trenches were visible at the base of the etched walls. It was also found that AlGaAs etched more slowly than GaAs. (Henry, et al., 1987 and Lecrosnier, et al., 1987). The possible volatile species of III-V compounds that were thought to be produced during etching are shown in Table 2.1.

It is thought that H and CH_x species created in the plasma react with the surface to produce the volatile species which then escape from the surface. At low concentrations of CH_4, the concentrations of CH_x species generated in the plasma are also low and so the etch rate was low. As the CH_4 concentration increased, the CH_x generation also increased which resulted in higher etch rates. At very high concentration of CH_4, the CH_x species polymerized at the surface and deposition occurred. The heat of formation may be useful for prediction of formation of above species, (Tirtowidjojo and Pollard, 1986).

Table 2.1. Possible volatile products during RIE of III-V compounds.

III-V semiconductors before etching	Possible volatile compounds after etching	
	Metal organic	Hydrides
GaAs	$Ga(CH_3)_3$	AsH_3
AlGaAs	$Ga(CH_3)_3$, $Al(CH_3)_3$	AsH_3
InGaAs	$Ga(CH_3)_3$, $In(CH_3)_3$	AsH_3
InGaAsP	$Ga(CH_3)_3$, $In(CH_3)_3$	AsH_3, PH_3
InP	$In(CH_3)_3$	PH_3

The generation of In and Ga metal-organic compounds was the reverse of that reported for the dissociation of such compounds, (Jacko and Price, 1963 and 1964). Therefore the generation of such compounds could be as follows for In

$$\begin{aligned} In + CH_3 &\rightarrow In(CH_3) \\ In(CH_3) + CH_3 &\rightarrow In(CH_3)_2 \\ In(CH_3)_2 + CH_3 &\rightarrow In(CH_3)_3 \end{aligned} \qquad \text{(C2.1)}$$

for Ga

$$\begin{aligned} Ga + CH_3 &\rightarrow Ga(CH_3) \\ Ga(CH_3) + CH_3 &\rightarrow Ga(CH_3)_2 \\ Ga(CH_3)_2 + CH_3 &\rightarrow Ga(CH_3)_3 \end{aligned} \qquad \text{(C2.2)}$$

The above formulae show the possible formation of trimethylindium and trimethylgallium. Generally it is thought that the reaction between the plasma species and the InP is of the form,

$$a\,CH_4 + b\,H_2 + c\,InP \rightarrow y\,In(CH_3)_3 + z\,PH_3 \qquad \text{(C2.3)}$$

and for GaAs,

$$a\,CH_4 + b\,H_2 + c\,GaAs \rightarrow y\,Ga(CH_3)_3 + z\,AsH_3 \qquad \text{(C2.4)}$$

The CH_4/H_2 etched GaAs and InP showed a very smooth surface and good anisotropy but GaAs suffered from rather low etch rates, (Thoms, et al., 1988). This may have been an advantage as chlorinated gases yield a high etch rate and short etching time and may not be controllable and reproducible. Also etching small dimensions for quantum-well structures may cause a problem due to possible dimension loss. The degree of damage of n-GaAs was further investigated by I-V and C-V techniques. (Cheung, et al. 1988). The I-V measurements indicated some damage. C-V measurements enabled the carrier passivation to be measured from near the surface into the bulk of the sample. However after annealing at 380°C the carriers were totally recovered.

The damage to the etched side walls was investigated by measuring the conductance of quantum wires. The side walls were damaged to a considerable depth when etched with CH_4/H_2 mixture compared to the $SiCl_4$-etched and wet-etched samples. After annealing, the damage was reduced to about 20nm depth on the etched walls.

I-V characteristics such as the ideality factor n and barrier height ϕ of etched n-GaAs at different depths has been determined, (Collot and Gaonach, 1990). After RIE with CH_4/H_2, Schottky diodes were fabricated, and n and ϕ were calculated from the I-V measurements. The n and ϕ values of the etched sample diverged from those of the control values up to a certain depth. Annealing at elevated temperatures improved the values up to 400°C where the best values of n and ϕ were obtained compared with those of the control sample. The C-V measurements indicated the passivation of carriers. Partial recovery of carriers was achieved at different annealing temperatures until at 360°C full recovery was accomplished. At lower temperatures full recovery was possible if the time of annealing increased.

Damage to InP after CH_4/H_2 etching due to hydrogen was different from that for GaAs, (Hayes[a], et al., 1989 and Singh, 1991). H penetrated further into n-InP and its concentration was slightly higher near the surface. p-InP did show passivation of carriers but n-InP indicated a slight increase in the carrier density. The carrier concentrations returned to normal after annealing.

The etch rate was found to be dependent on the masking material when InP and GaAs were etched in a CH_4/H_2 mixture with photoresist as the masking material. InP obeyed the Arrhenius relationship but GaAs did not (Carter, et al., 1989). When a Si_xN_y mask was used for GaAs its etch rate also obeyed the Arrhenius relationship. This was confirmed when samples were etched with different masks, (i.e. photoresist and Si_xN_y), (Law[b], et al., 1990). This was more evident at higher CH_4 flow rates, (higher CH_4 concentrations). This was attributed to the reaction of the photoresist with the active species.

The etch rate of GaAs in pure H_2 increased as the temperature increased. When CH_4 was added, the same occurred but the dependence on the temperature was not as sensitive as before. The sensitivity to temperature was reduced as the CH_4, concentration increased. At high concentrations of CH_4 no dependence on temperature was observed. This was claimed to be due to polymerization on the surface, (Law[a], et al., 1990).

The etch rate of GaAs decreased as the exposed GaAs area increased. This was confirmed at different CH_4 concentrations. However the etch rate also decreased when the area of the photoresist covering the sample increased. This confirmed the assumption that the CH_x species may react with the photoresist. It has been also discovered that the anisotropy of the etched patterns was poor as the etch-able area increased.

Investigation of the etch selectivity between GaAs and AlGaAs indicated

that the etch rate decreased as the Al content in Ga increased, (Law and Jones, 1989). To etch samples of high Al content, the power density had to be increased. The rate of AlGaAs etching was dependent on the CH_4 concentration. When the Al content in Ga was higher, the volume concentration of CH_4 in H_2 had to decrease. At various pressures or flow rates, the peak etch rate of the sample was found to be at different CH_4 volume concentrations, (Law, et al., 1989).

The plasma species were analyzed in order to detect the species responsible for etching III-V compounds. InP was used for etching and optical emission spectroscopy was employed to analyze the plasma, (Field, et al., 1990). When spectra of pure CH_4 were analyzed with no InP sample in the chamber, the species detected were H and CH. For a pure H_2 plasma H was detected. When CH_4/H_2 mixtures were used with 10% CH_4 the H and CH peaks were visible but the CH peak displayed much smaller intensity than that for H. When InP was etched in the CH_4/H_2 mixture, the CH peaks disappeared. No metal-organic compounds were detected.

Further studies of the plasma and InP surface also failed to detect any metal organic-compounds, (Hayes[b], et al., 1989). On the InP, species such as P, P_2, P_3, PH, PH_2, PH_3, PCH_2, PCH_3, In, InO, InP, and InP_2 were detected. In order to detect the species before the reaction with InP, it was best to identify the species deposited on the inorganic mask, as these species did not react with the mask. These species were identified as C_2H, C_3H, C_4H, $C_5..C_9$, $C_{10}H$, C_{11} and C_{12}. The deposited species were mainly carbon, and the hydrocarbon species had an abundance of carbon in them.

Surface analysis of the sample indicated large quantities of In rather than P. Therefore the rate limiting factor during etching of InP in a CH_4/H_2 mixture is the erosion of the In. The mechanism of etching was attributed to two species. First, H was said to react with P primarily to produce PH_x. Next the CH_x species were considered to be responsible for reaction with

In to produce volatile methyl radicals. Neither CH_x nor $In(CH_x)_y$ were detected, although CH species were detected in the plasma as reported before.

Ion bombardment plays an important part in CH_4/H_2 etching of III-V compounds. For this reason an ECR-RIE system was employed using a mixture of $CH_4/H_2/Ar$ to investigate the effect of low ion bombardment intensity on the sample by reducing the DC self bias voltage, (Law[b], et al., 1991). The etch rate of GaAs was much lower at optimum conditions for low DC self bias voltages.

The use of O_2 as an extra admix gas to CH_4/H_2, improved the etch rate above a certain concentration of O_2 but generally the etched surface was not as smooth as when no O_2 was used, (McNabb, et al., 1991). The authors devised an empirical model from which they could calculate the etch rate, polymer deposition rate and DC self bias voltage. This model however was machine dependent and could not estimate the above mentioned process variables on different systems.

It was recently argued that H_2 may not be necessary in the mixture to etch GaAs, (Law[a], et al., 1991). The reaction was thought to be of the form,

$$a\,(CH_3 - H) + b\,GaAs \rightarrow y\,Ga(CH_3)_3 + z\,AsH_3 \qquad \text{(C2.5)}$$

To establish the above relation, helium (He), neon (Ne) and argon (Ar) were used. When etch rate was plotted against admix gas concentration or flow rate both He and Ne displayed similar etching characteristics to those of H_2. The etch rates at optimum concentration of Ne and He were not as high as when H_2 was used, with He showing the lowest etch rate. The authors argued that MORIE did occur on the surface. Side wall roughness has also been investigated after etching InP in $CH_4/H_2/Ar$, (Chakrabarti and Pearton, 1991). It was claimed that the problem was related to the photoresist formed on the surface of InP.

Other non-halogenated gases have been used to etch III-V compounds. A mixture of ethane (C_2H_6) and H_2 was first used to etch InP, GaAs, and InGaAs, (Matsui, et al., 1988). The etched surfaces of InGaAs and InP were very smooth. The etching of AlGaAs was also studied, (Pearton, et al., 1989 and Pearton and Hobson, 1989).

Ref.	Etching gas	Etch rate nm/min	Front metal	Carrier cons. cm^{-3}	GaAs type	I-V		C-V	
						Barrier V	Ideality	Barrier V	Carrier cm^{-3}
Hilton et al 1989	CCl_2F_2	43	Ti/Au	---	n	0.72	1.10	0.85	2.6×10^{17}
Van Daele et al 1990	$SiCl_4$	160#	Au	1.5×10^{17}	n	0.79	1.14	---	---
				4×10^{17}	p	0.47	1.20	---	---
Lee & Baratte 1990	Cl_2	150	Ti/Au	---	n	0.71	1.14	0.91	---
	Ar	12#	Ti/Au	---	n	0.55	1.25	0.91	---
Pang 1986	H_2	6@	Ti/Au	---	n	0.58	1.26	---	---
	O_2	---	Ti/Au	---	n	0.47	1.20	---	---
Cheung 1988	CH_4/H_2	20	Ti/Au	2×10^{17}	n	0.99	1.06	---	2×10^{17}

From Pang 1986

@ From Cheung et al 1987

Table 2.1. Some quantitative values for GaAs etching.

Generally etching in this mixture was similar to that of CH_4/H_2 etching, except that optimum etching occurred at lower concentrations of C_2H_6. Temperature had no effect for AlGaAs etching but the etch rate of GaAs was affected. Propane (C_3H_8) was also used to etch GaAs, (Law[c], et al., 1990). Table 2.1 shows some quantitative values for GaAs etching in different gases.

2.5 Objectives of present work

GaAs is an important material for microelectronics industry because of its high electron mobility and photonic capabilities. It is widely used for

communication and defence, therefore any research involving the processing of this material will be beneficial to mankind and will enrich knowledge which could then be used for commercial reasons.

The industry uses chlorinated gases for etching GaAs because of its high etch rate at room temperatures compared to the low etch rate of CH_4/H_2 mixtures. The primary objective of this research is therefore to explore the advantages of using mixtures of CH_4/H_2 plasma for etching GaAs in RIE mode by taking into account its low etch rate. A method is considered such that the final etched product would yield repeatable results with improved etched characteristics such as etch rate, anisotropy and smoother etched side walls and surfaces.

A CH_4/H_2 mixture is used for etching GaAs because it does not damage the etching system and is not hazardous to the human operator. It is not a destroyer of ozone and therefore can be considered more environmentally friendly than the chlorinated gases. Its advantages will be considered for etching GaAs, in particular its effect on the inorganic mask erosion used on GaAs.

The effect of using mixtures of CH_4/H_2 for etching p-GaAs and the degree of damage induced in the semiconductor is also of interest as p-GaAs is not generally used as much as n-GaAs for fabrication of devices due to its low mobility of carriers. However there are new devices which do need p-GaAs layers and these surfaces may get exposed to plasmas such as CH_4/H_2 mixtures. The advantage of using such mixtures for p-GaAs etching is therefore of importance.

The advantages of selective deposition of carbon polymeric film on the inorganic mask and its passivation during etching of GaAs in CH_4/H_2 plasma is also of importance and is investigated here.

CHAPTER 3
EXPERIMENTAL PROCEDURES

The experimental procedures are considered in two parts. The first part is the dry etching of GaAs, and the second part is the electrical testing of etched samples. The etching experiments took place in the Microelectronics Centre clean room. The test and measurements and electron microscopy laboratories were used for electrical testing and surface analyses. Metallisation of certain samples took place outside the clean room in a vacuum deposition laboratory at Kings College University of London. Figure 3.1 is a flow chart showing the route taken for RIE experiments.

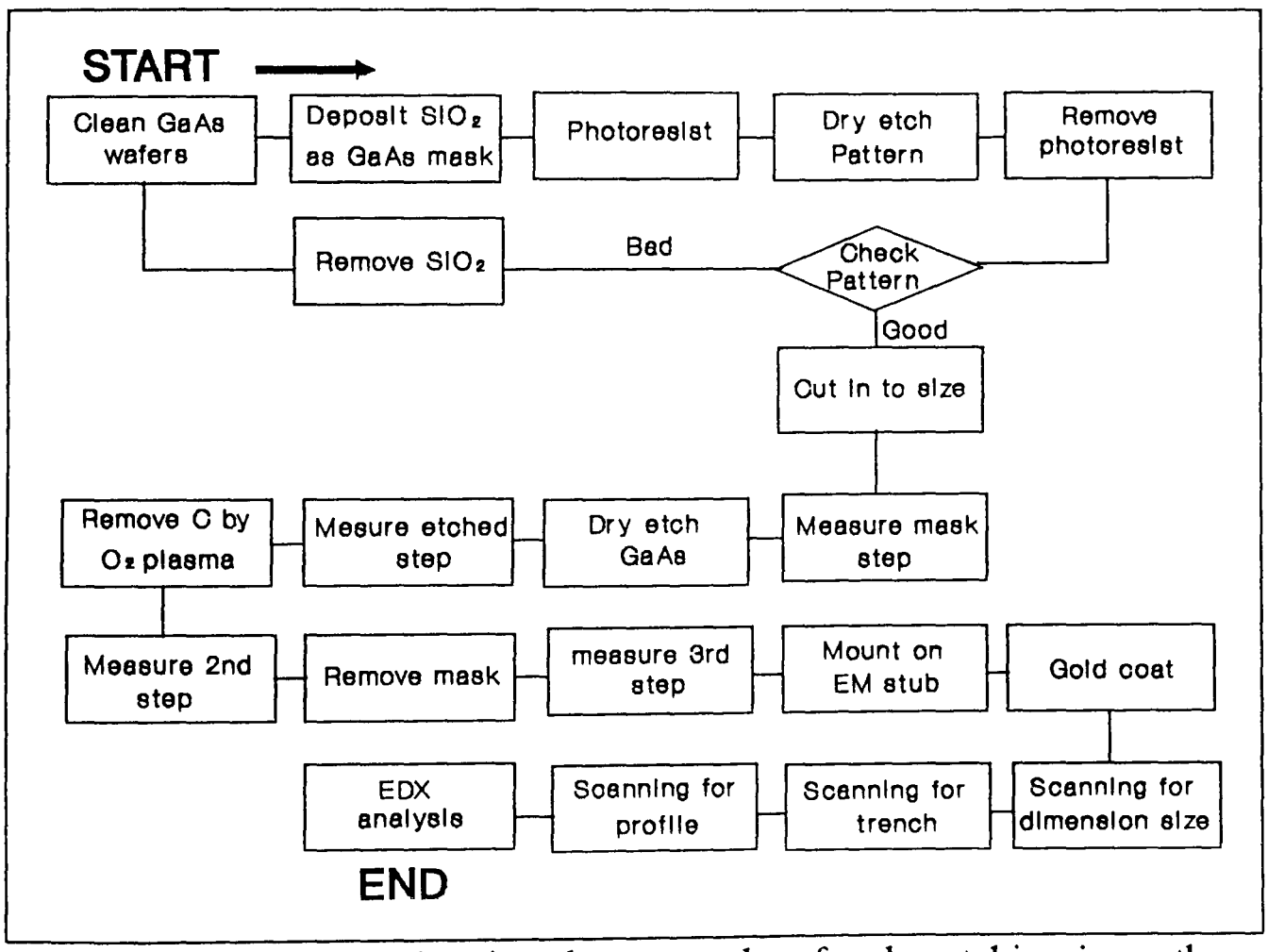

Figure 3.1. Flow chart showing the steps taken for dry etching in methane and hydrogen mixtures.

For the first part of the experiment two inch <100> GaAs semi-insulating substrate wafers were used. The AlGaAs layers of various Al content were

grown on some GaAs semi-insulators by Metal Organic Chemical Vapour Deposition (MOCVD), to a thickness of 1μm (The semi-insulating wafers and the wafers with AlGaAs epi-layers were supplied by Plessey Research, Caswell). For the second part, two inch <100> p-type GaAs wafers were used. The semiconductor was Zn doped with a dopant concentration of about 2 X 10^{18} cm^{-3}. (p-type wafers were supplied by the University of Sheffield Department of Electrical and Electronics Engineering).

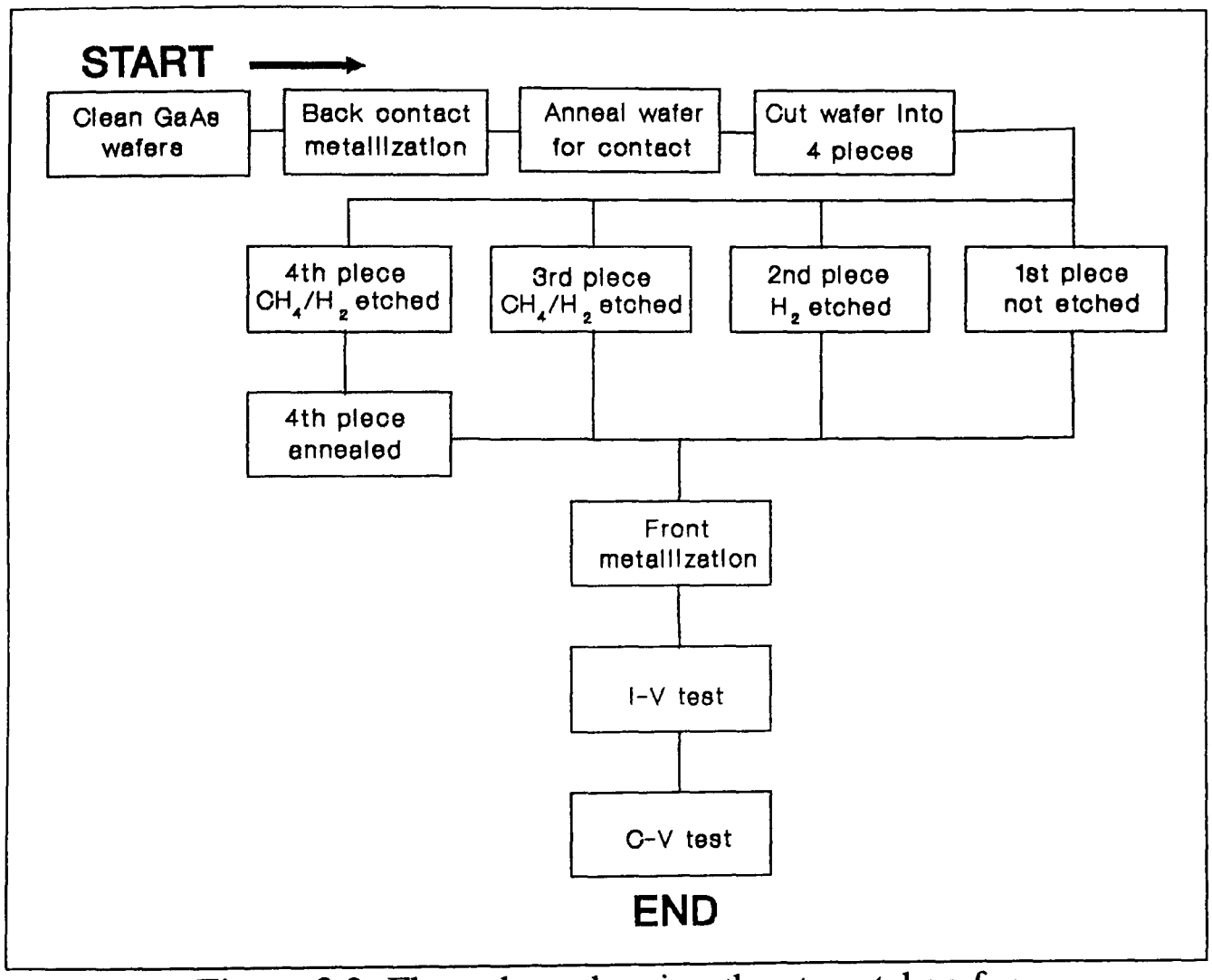

Figure 3.2. Flow chart showing the steps taken for electrical testing of etched samples.

All wafers in parts one and two of the experiment were grown by the Liquid Encapsulated Czochralski method (LEC). Figure 3.2 describes the procedures for preparation and electrical testing of the etched samples.

3.1 Preprocessing procedures

Before dry etching, the GaAs samples were cleaned and masked. The cleaning procedure was as follows:

The GaAs wafers were first immersed in a bath of acetone and then iso-propyl alcohol (IPA), to remove possible organic contamination on the surface. Next, the wafers were placed in a bath of 10% hydrochloric acid and 90% deionised, (DI) water, (1 HCl : 9 H_2O), for general cleaning and removal of the surface oxides of Ga and As. Finally a bath of 10% ammonium hydroxide and 90% DI water (1 NH_4OH : 9 H_2O) was needed to remove any remaining oxide and carbon at the surface. Each bath took 30 minutes.

The wafers which were selected for the dry etching experiments were then dipped in DI water and then in IPA and left to dry in air. The p-type wafer selected for electrical testing after dry etching was dried by blowing N_2 gas over the surface in order to minimise the surface oxidation (Miers, 1982). In all cases contact with water was minimised so that the surface oxidation would be reduced.

Inorganic compounds were chosen for masking of GaAs instead of the usual organic photoresists due to possible reaction of CH_x species with the organic masks. Another reason for using inorganic mask was because of the heating of the electrodes in the RIE system. The driven electrode (the cathode) was not cooled because no cooling system was available. It was discovered that long term exposure to the plasma caused heating of the electrode which caused the photoresist surface to degrade. A SiO_2 mask was used for the majority of the experiments. A Si_3N_4 mask was also used on certain experiments involving AlGaAs.

For deposition of SiO_2 an Electro Gas Systems SILOX EG 8/2 reactor was

used. This is a atmospheric pressure chemical vapour deposition system (APCVD). For deposition of Si_3N_4, a Plasma-Therm PK 2430 PD system was used. This is a plasma enhanced chemical vapour deposition (PECVD) system. The process conditions are stated in appendix II.

3.2 Masking of gallium arsenide

After the deposition of the inorganic layer on top of the semi-insulating GaAs wafers, they were masked with Merck N-45 negative photoresist. The N-45 was then patterned with a Cobilt CA 800 contact aligner which illuminated the surface of the mask with ultra violet light from a mercury vapour lamp. The procedure is detailed in appendix III.

The pattern was then transferred to the epi-layer by dry etching the wafers in trifluoromethane plasma (CHF_3) also known as Freon 23 or Halocarbon 23, using the Electrotech Plasmafab 340. The semi-insulating wafers were then transferred to a Nanotech Plasma Prep 100 barrel etcher in which the N-45 negative photoresist was removed in oxygen (O_2) plasma, (see appendix II for the operation procedures).The wafer was cut to size, (5mm X 5mm, unless stated otherwise), and was then ready to be etched in methane and hydrogen mixtures with the epi-layer masking the GaAs.

Picture 3.1 shows the micrographs of the edge of masking patterns. The edge of N-45 mask is smoother than the rest. The edge of the SiO_2 mask is not as well defined as the edge of the Si_3N_4 mask.

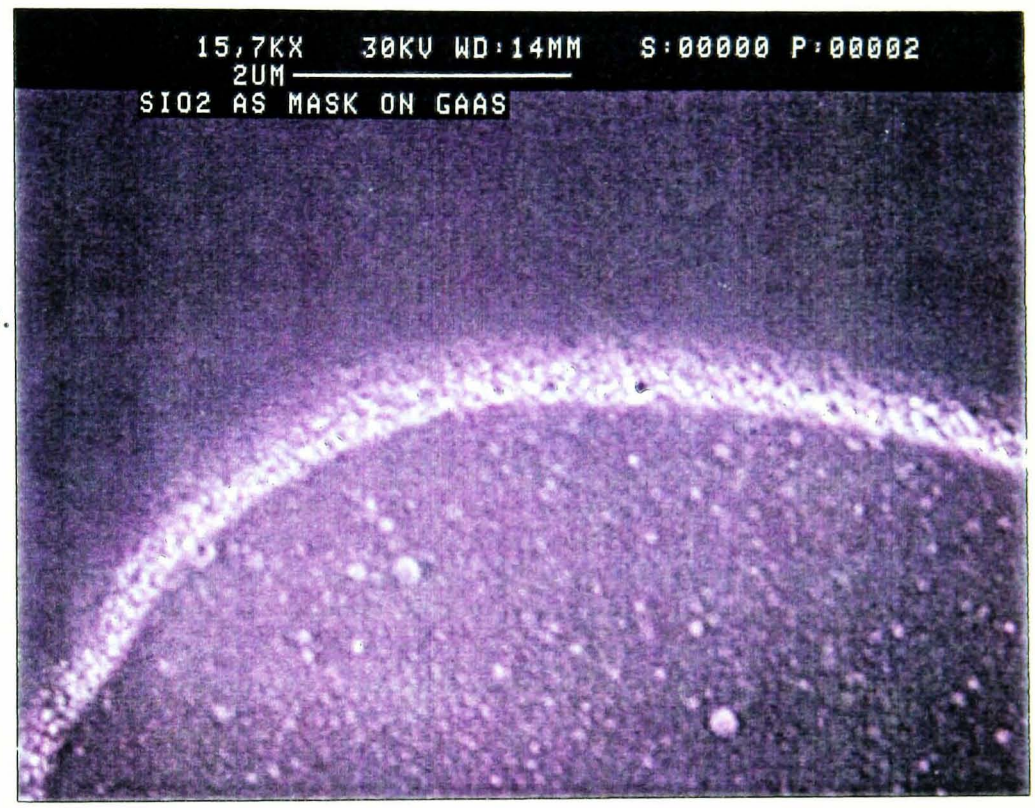

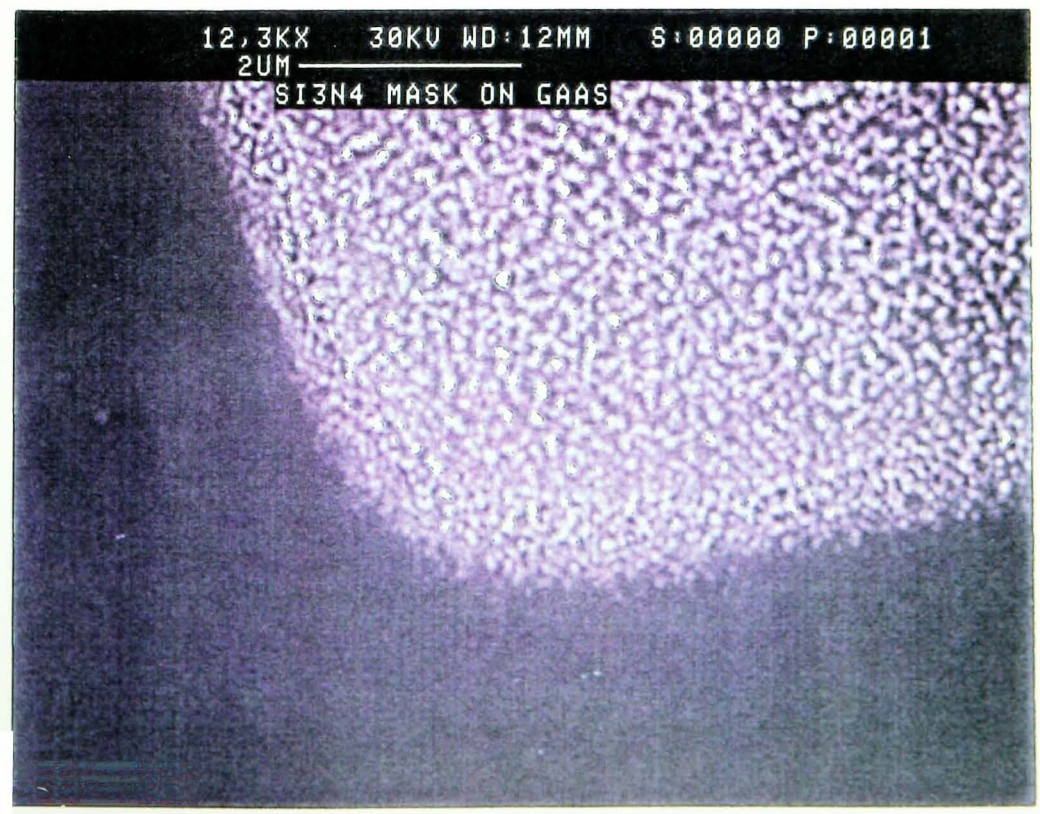

Picture 3.1. Micrographs of masks.
(Top) Merck N-45,
(middle) SiO_2 epi-layer and
(bottom) Si_3N_4 epi-layer.

3.3 Reactive ion etching of GaAs and analysis

The GaAs samples were etched in methane and hydrogen for 30 minutes. Test etching was carried out with mixtures of argon, hydrogen and methane. This was important as the gas which might have caused the combined chemical and physical etching had to be identified. The experiment was performed using the methane/hydrogen, methane/argon and hydrogen/argon mixtures (see appendix IV for information on gases), and the etch rate for each mixture was compared with regards to the variation of the DC self bias voltage.

Different process parameters were used which will be discussed in the results chapter. The procedures before and after etching were as follows:

Before etching, the depth t_1 of the SiO_2 layer was measured using a Tencor model 200 profiler. This was performed by measuring the depth of 10 different patterns and taking a mean. The sample was then etched in methane and hydrogen mixtures for the specified time.

After etching, it was observed that an unknown layer was deposited on the SiO_2 masking layer but not on the GaAs surface. The depth t_2 was measured with the profiler a second time and then the sample was exposed to an O_2 plasma in the barrel etcher for 5 minutes. The etched depth t_3 was measured a third time from which it was obvious that the unknown deposited layer had been removed. This suggested that the layer was carbon (C) or a hydrocarbon polymeric film. Finally the GaAs was dipped in a hydrofluoric solution (5% HF in DI water). The SiO_2 layer on the GaAs was then dissolved in the HF solution. The sample was then washed in DI water and dried by blowing nitrogen (N_2) over its surface. The profiler was used for a final time to measure the dept t_4 of GaAs etched.

3.3.1 Measurements and calculations

From the profiler measurements it follows that,

$$t_1 = t_{mask}, \tag{3.1}$$

and,

$$t_4 = t_{GaAs}, \tag{3.2}$$

where t_{mask} was the depth of mask before etching and t_{GaAs} was the depth of etched GaAs.

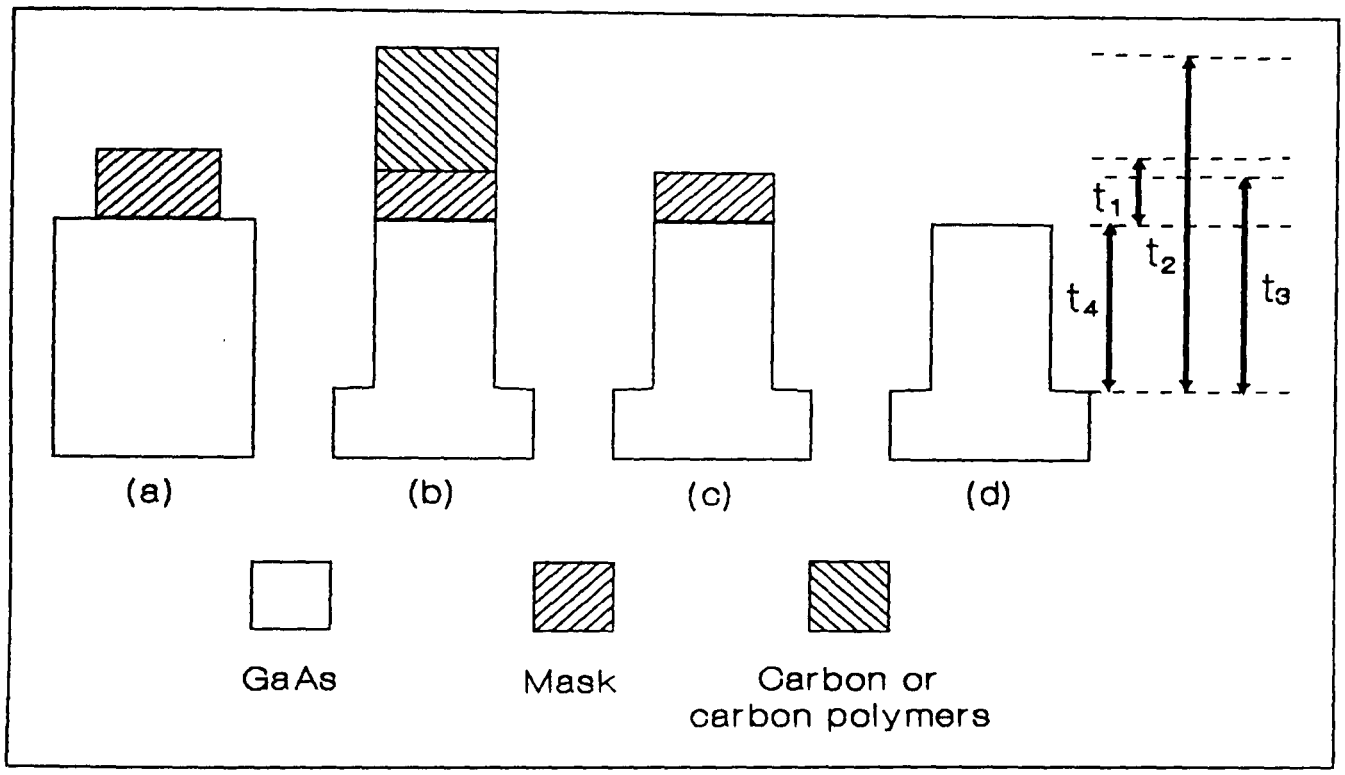

Figure 3.3. Diagram of the GaAs. (a) before etch, (b) after etch, (c)after carbon polymer removal, (d) GaAs etched step.

Depth t_{carbon} of the deposited carbon was given by,

$$t_{carbon} = t_2 - t_3, \tag{3.3}$$

The depth of the etched mask $t_{E\text{-}mask}$ was,

$$t_{E\text{-}mask} = t_{mask} - (t_3 - t_4), \tag{3.4}$$

The etch rate R was given by,

$$R = \frac{t}{\tau}, \tag{3.5}$$

where τ is the time of etching and t is the depth measured by profiler. The deposition rate D of unknown layer can also be calculated from equation (3.1). If D is the deposition rate with t as the deposited height and τ as the deposition time, than $D=t/\tau$. Figure 3.3 shows the depth of the sample measured at different stages using the profiler.

3.3.2 Pressure and gas flow

The pressure was measured in units of mtorr using a Baratron gauge. The lowest base pressure achieved was 10 mtorr. The international systems unit (SI unit) for pressure is the Pascal (Pa). The units in this work are therefore converted to SI units. Since 1 Pa = 7.5 mtorr, pressure in mtorr can be converted to Pa by dividing the pressure in mtorr by 7.5.

The flow of gas was measured by mass flow controllers. The units of flow were given as standard cubic centimetres per minute, (sccm). This also needs conversion to SI units which measure flow in Pa m^3/ sec. 1 sccm is therefore 1 cubic centimetres per minutes at atmospheric pressure, (i.e 101333.33 Pa). To convert into Pa m^3/ sec, multiply the value in sccm by 1.69×10^{-3}, (see appendix V).

The total flow Q of gases entering the system is given by,

$$Q = \sum Q_x, \tag{3.6}$$

where Q_x is the flow of each gas entering the system (x = Gas). If two

types of gases were admitted to the chamber, the total flow is given by,

$$Q = Q_1 + Q_2, \tag{3.7}$$

The percent volume concentration $V_{\%1}$ of gas 1 is given by,

$$V_{\%1} = \frac{Q_1}{Q} 100, \tag{3.8}$$

In case of methane and hydrogen mixtures the total flow of gas can be set by three methods. First, the flow of hydrogen $Q_{hydrogen}$ can be kept constant but the flow of methane $Q_{methane}$ can vary. In this case the flow of methane and therefore the total flow Q are varied which indicates that the residence time of the gas mixture is changing.

The second method is to keep the methane flow $Q_{methane}$ constant and vary the flow of hydrogen $Q_{hydrogen}$. The problem will be as before, the total flow Q will vary which causes the variation of the residence time.

The third method is to keep the total flow Q constant. This indicates that the flow of methane and hydrogen can vary. When the total flow is constant the residence time of the gas mixture will remain constant also.

After considering these methods of flow control, the third option appears more attractive. This is because in the first and second case there are three variables, (i.e. methane flow or the hydrogen flow, total flow and the residence time of the gas mixture in the chamber). In the third case only two variables exist, (methane and hydrogen flow).

3.4 Surface analysis

After dry etching and measurements the surface of the GaAs was scanned using a Cambridge Stereoscan 240 electron microscope (SEM), with Energy Dispersive X-ray system, (EDX). The GaAs samples were mounted on an

electron microscope stub using conductive carbon cement. The samples were then coated with about 10-20 nm of gold using a Polaron E5100 coating unit. This was performed so that the incident electron beam would not diverge from the GaAs surface.

After coating, the stub was then placed in the electron microscope chamber and the surface was analyzed. The dimensions of the etched surface were measured to find evidence of any change in linewidth. The profile was examined for anisotropy and trench formation. This was performed by looking at the surface from different angles.

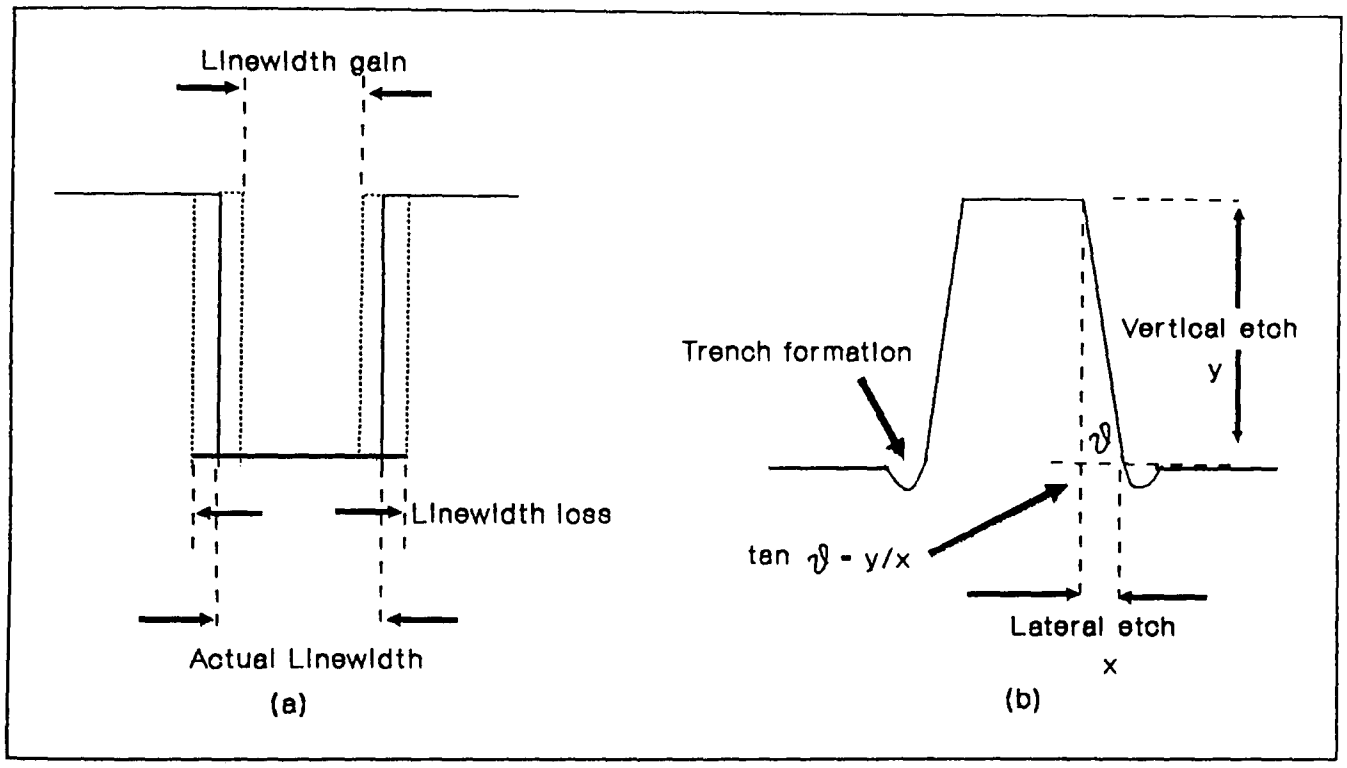

Figure 3.4. Profile of etched surface. (a) Linewidth. (b) Profile.

Figure 3.4 shows the general profile of the etched surface. The profiles were at times complex as curvatures sometimes occurred at the top and bottom of the etched step.

The surface of semiconductor was analyzed for any chemical thin film that may have been deposited during etching. This was possible in the SEM system because when a sample is bombarded with electrons, X-rays are generated which are characteristic of the material which is analyzed (Sze,

1985). The intensity of X-ray emitted by the material can then be plotted against the X-ray energy which identifies the material. This was performed using the EDX system.

The anisotropy A_f of the etched pattern was then calculated by measuring the lateral x and vertical y etch rates using the cursors on the SEM.

The degree of anisotropy is given by,

$$A_f = 1 - \frac{x}{y}, \tag{3.9}$$

or the angle of anisotropy θ is given by,

$$\theta = \arctan \frac{y}{x}, \tag{3.10}$$

3.5 Metallization and electrical testing

P-type GaAs wafers were used for electrical testing. After cleaning, the back contact metal was deposited on the back of the wafer using an Edwards E306 thermal evaporation system.

The base pressure was 5 X 10^{-7} torr. The metals evaporated were: nickel (Ni) 5 nm, gold/germanium (Au/Ge) with 12% Ge 100 nm, nickel (Ni) 30 nm and gold (Au) 100 nm (Howes and Morgan, 1986). The wafer was then annealed in nitrogen (N_2) gas and atmospheric pressure for 20 minutes at 405 °C and cut into four equal pieces. The first piece was kept as a control reference. The second was etched in H_2 plasma and the third and fourth piece were etched in methane and hydrogen plasma separately. The fourth piece was then annealed at 400 °C in a N_2 gas and atmospheric pressure for 20 minutes. Figure 3.5 shows the metallization layers.

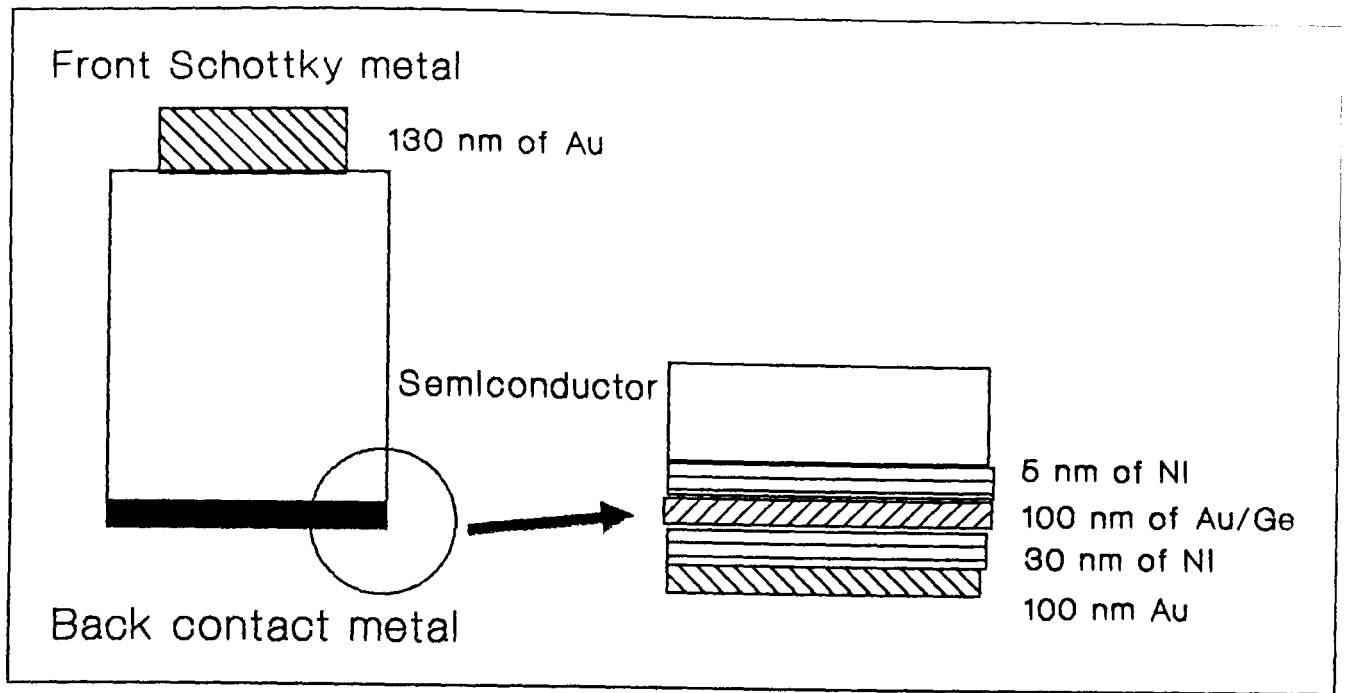

Figure 3.5. Metallization layers for GaAs.

Picture 3.2 shows the pattern of the masks for etching experiments and the front Schottky metal layer. A complex pattern was used for the etching mask so that the effect of etching could be observed for different sizes and geometry. The shape of the front Schottky metal contact for electrical testing was a simple hexagon.

The fronts of the samples were then metallized with gold using the Edwards E306 system. The thickness of this gold Schottky barrier metal was about 130 nm.

The electrical testing was in two parts. First the current-voltage (I-V) and then the capacitance-voltage (C-V) characterization were carried out. For both cases 10 Schottky diodes were examined on each of the four samples and mean of the 10 was calculated. The samples were placed on a wafer probe station in a dark box so no photo-emission occurred. For current-voltage (I-V) measurements a Hewlett-Packard 4145A Semiconductor Parameter Analyzer was used. The thermionic-emission theory was used to calculate the ideality factor n and barrier height ϕ, (see appendix VII and VIII for the derivation of the equations). Figure 3.6 shows the profile of the graphs of the I-V measurements.

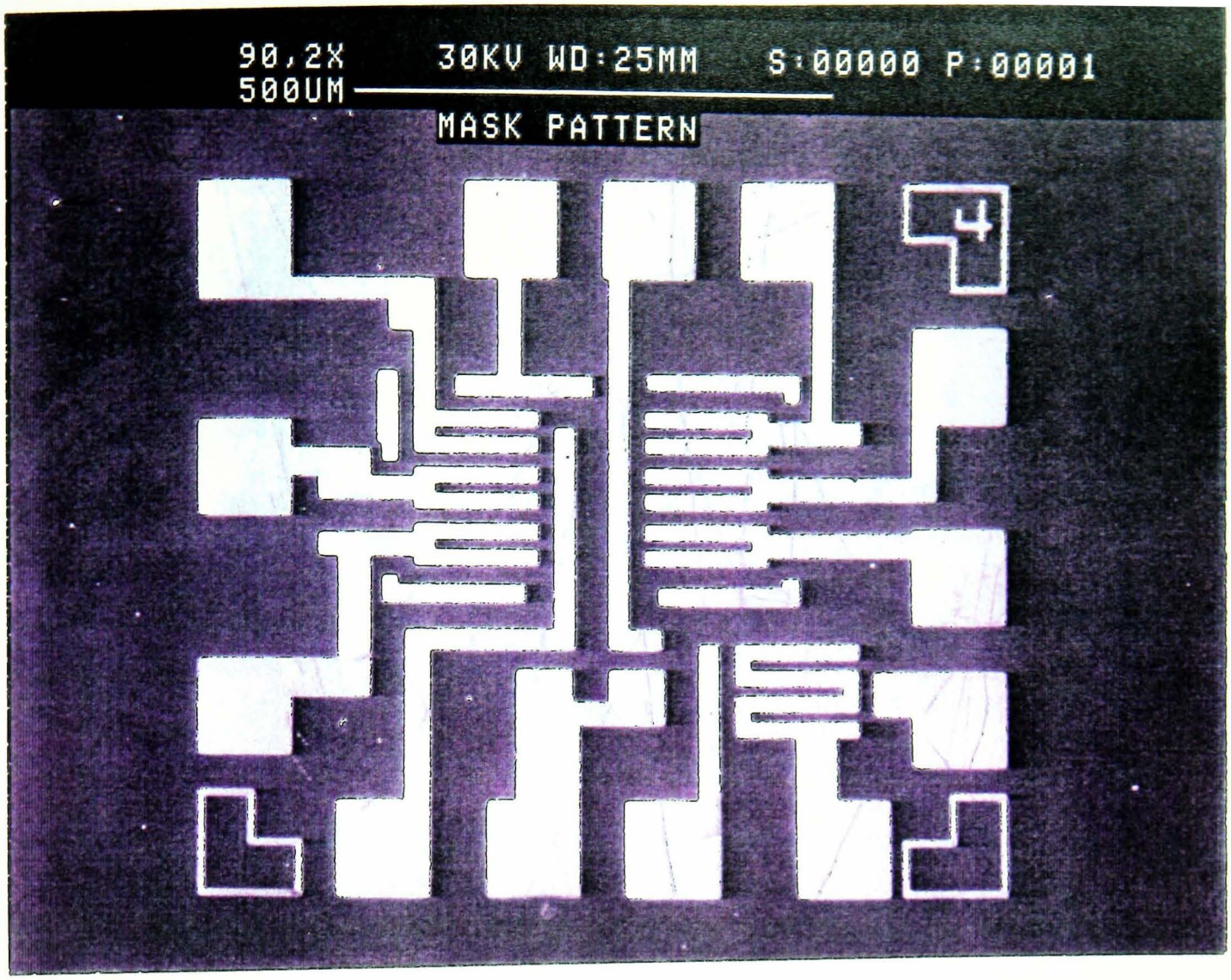

Picture 3.2. Micrographs of, (top) SiO_2 mask pattern and (bottom) front Schottky metal.

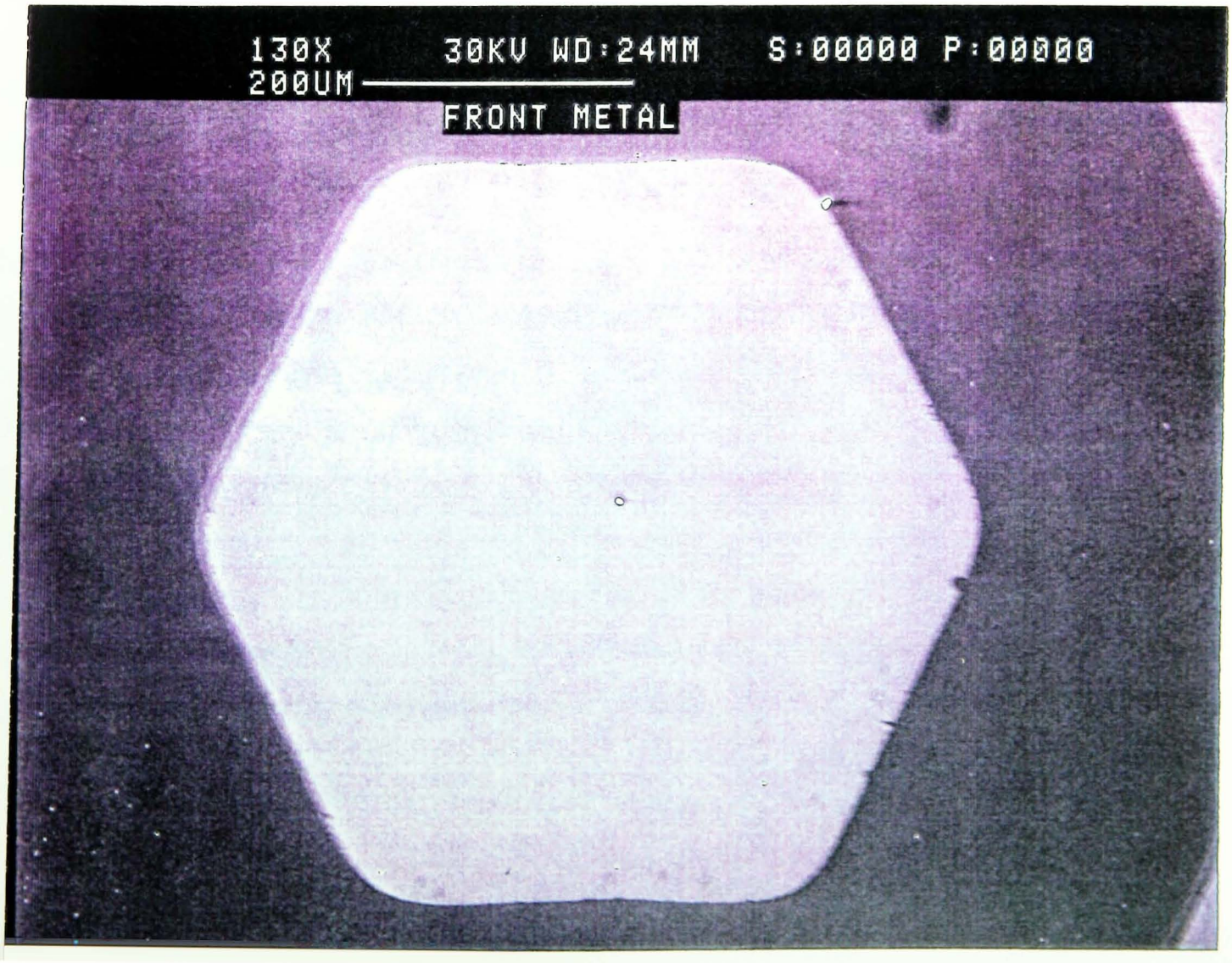

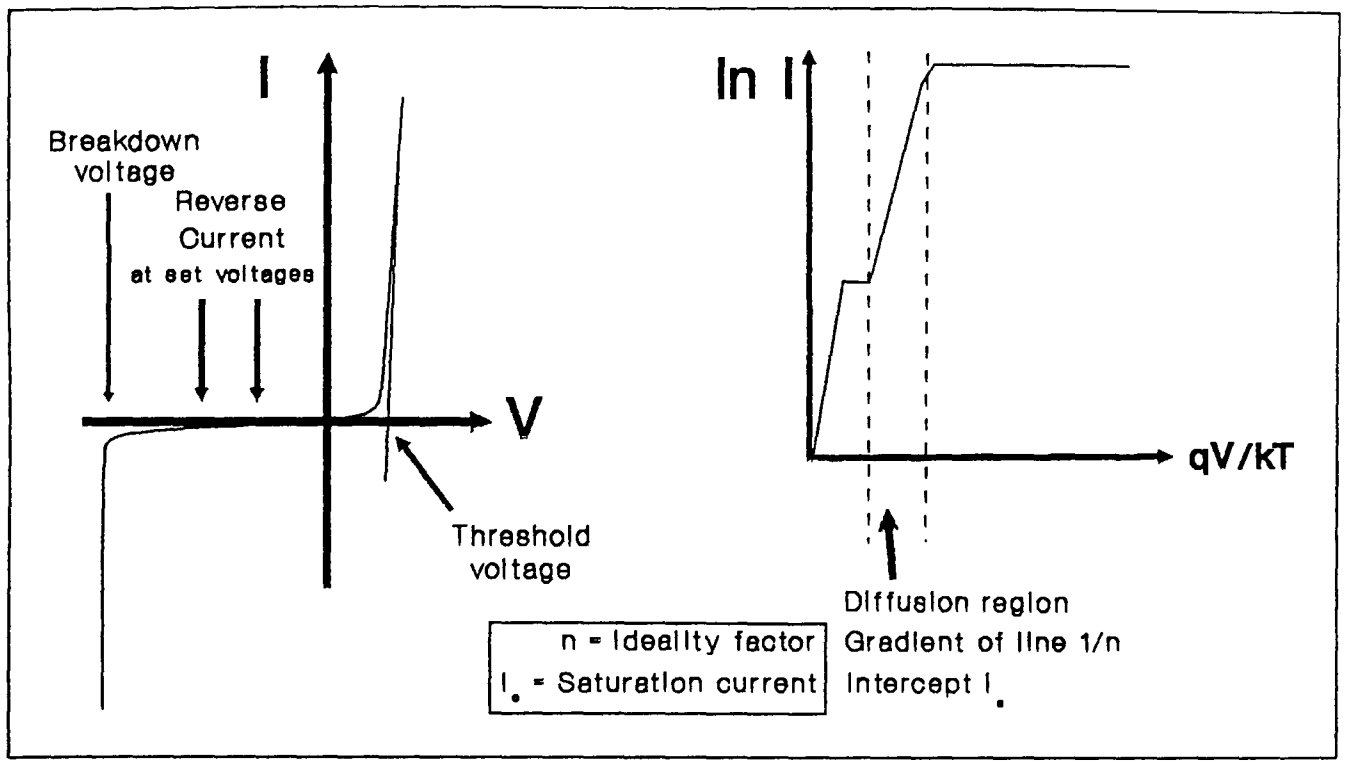

Figure 3.6. The diagram of the I-V characteristic graphs.

From the graph of I against V, the threshold voltage, breakdown voltage and reverse current at pre-selected voltages was measured. When lnI was plotted against qV/kT, the gradient of the curve in the diffusion region yielded 1/n from which ideality factor was calculated. The saturation current was found from the intercept of the graph from which the barrier height was computed. The voltage for this experiment was set from 3 V in the reverse range, to -2 V in the forward range for the p-GaAs sample, (except for when the breakdown voltage was measured for which reverse voltage exceeded 3 V).

In the case of (C-V) measurements a Hewlett-Packard 4275A Multi-Frequency LCR meter set to high frequency, (1 MHz) was used. The reverse voltage range was set from 3 V to 0 V for p-GaAs sample. Figure 3.7 shows some of the possible information from C-V measurements. Figure 3.7 (a) shows a curve for C against V. $1/C^2$ against V shown by figure 3.7 (b) yields a straight line if the carrier concentration through the bulk is uniform. For non-uniform carrier concentration this would be a curve as shown in figure 3.7 (c), and in this case carrier concentration N could be plotted against the depletion width W_d as shown in figure 3.7 (d).

This was the case for this work as RIE caused non-uniformity of carriers. (see appendix IX for C-V derivations).

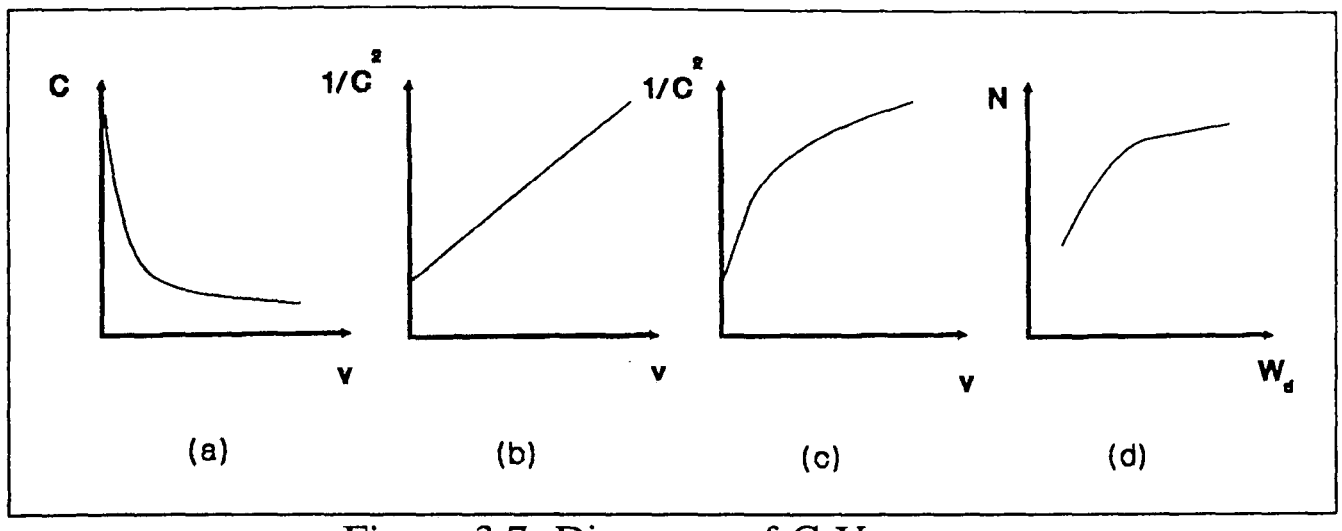

Figure 3.7. Diagrams of C-V curves.

CHAPTER 4
CHARACTERIZATION OF THE REACTIVE ION ETCHING SYSTEM

Before dry etching experiments on GaAs commenced, the reactive ion etching system was characterized. This was important in order to specify the exact conditions in which methane and hydrogen would be used for etching of GaAs.

The chamber condition is of importance in dry etching. Results for a chamber which was dirty differ from those with a cleaned chamber. Other process parameters such as pressure, applied power density and flow rate in the chamber affect the results more obviously.

These quantities can specially effect the DC self bias voltage V_{self} which is related to the physical mechanism (ion bombardment) and the reflected power which is the power not dissipated in the chamber. In this chapter the characterization of the Electrotech Plasmafab 340 is described.

4.1 Reactive ion etching system

The dry etching system was a Special Research Systems (SRS), (now Surface Technology Systems (STS)), Electrotech Plasmafab 340 dual system (McQuarrie, 1988), with a combination of a two stage rotary and a Roots blower pump (Picture 4.1). The dual chamber system was designed such that both corrosive and non-corrosive gases could be used for semiconductor dry etching. The RIE equipment was also called a master/slave system. The slave system was used for non-corrosive gases, in this case gases such as methane and hydrogen mixtures for GaAs etching and Freon 23 for SiO_2 and Si_3N_4 etching.

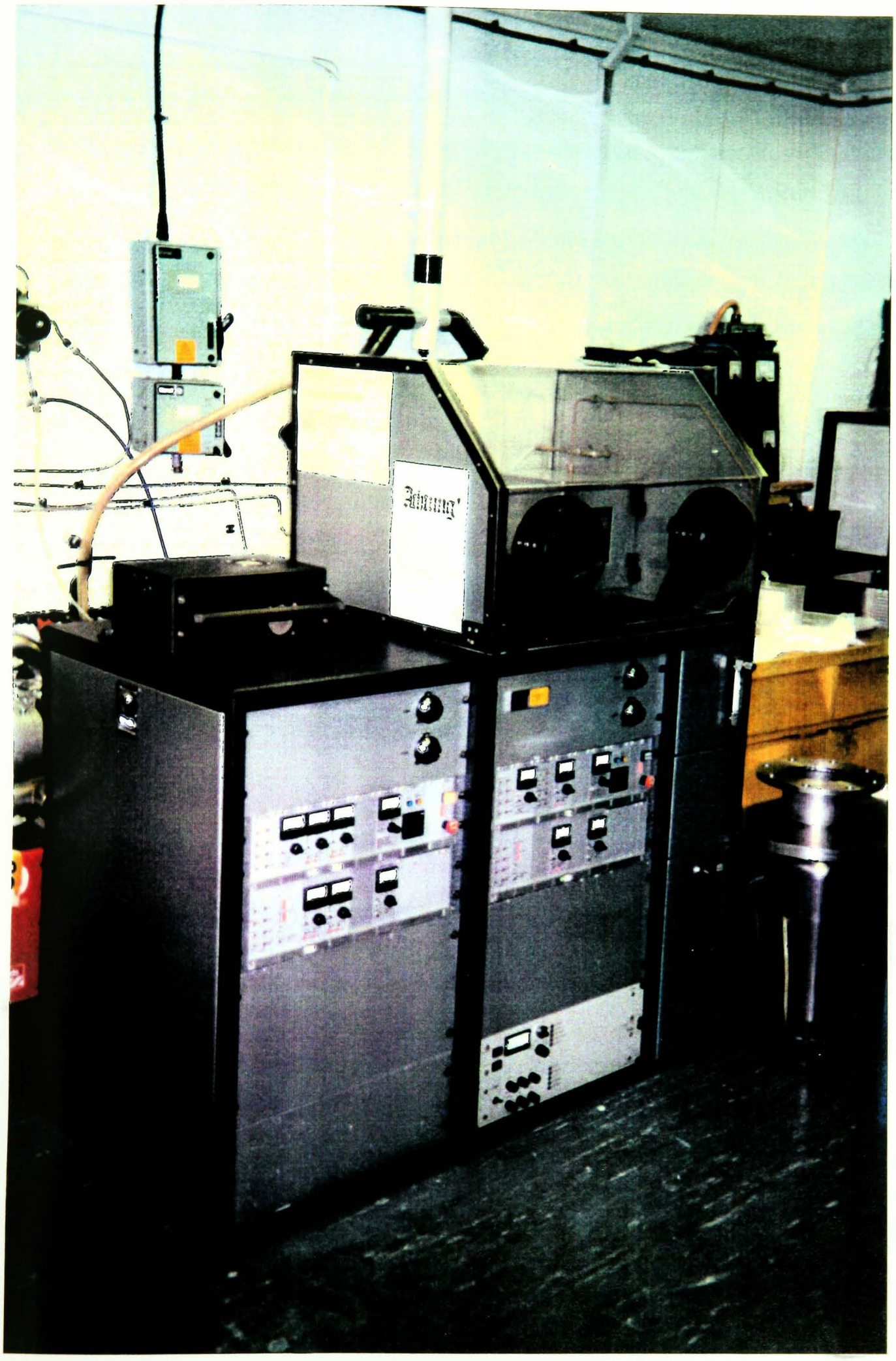

Picture 4.1. Photograph of the SRS Electrotech Plasmafab 340 dual system.

The master system was fitted with a glove box that contained a nitrogen atmosphere to isolate the chamber from the outside air environment to enable the use of corrosive gases.

The master/slave system was connected to the vacuum pumps and to the RF power supply with an RF matching system as shown in Figure 4.1. The slave and the master system could not be used together. A switch changed the pump/power supply from one chamber to another via a network of pneumatic valves for the pumps and relays for the RF power supply.

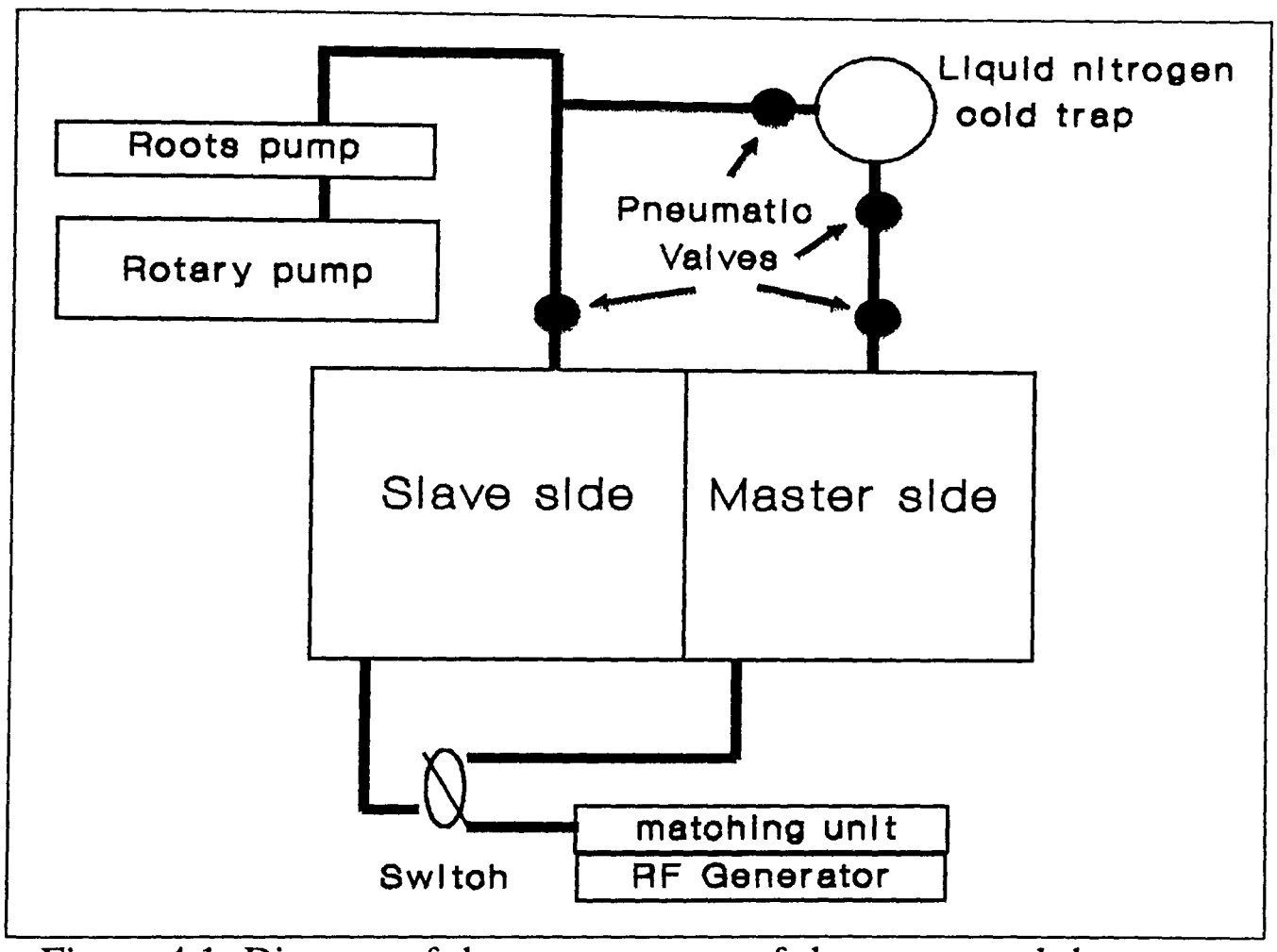

Figure 4.1. Diagram of the arrangements of the pumps and the power supply of the master/slave system.

In order to use the master system the cold trap had to be filled with liquid nitrogen before the system was fully operational. The pneumatic valves on the traps could be operated automatically only if the trap was full of liquid nitrogen.

The pneumatic valves on the Plasmafab 340 needed a minimum of 4.2 X 10^5 Pa, (60 psi) air pressure to operate. Below this limit the whole system would shut down. The RF power supply also needed pressurised water for cooling.

The pumps were a combination of a two-stage rotary pump, (E2M40) capable of sweeping 42.5 m^3/h and a Roots blower pump, (EH250) capable of sweeping 310 m^3/h. It was claimed that this pump combination was capable of an ultimate pressure of 1.5 mtorr. However the best base pressure achieved was 10 mtorr. The reason maybe due to the reduction in pump efficiency because of excessive use of chlorinated gases in the master side before this project started, (leak rate < 1 mtorr/min).

The lubricants used for the pumps were Edwards 15 for the rotary pump and Edwards 16 for the Roots blower pump. These are both hydrocarbon based and therefore not inert to oxygen. For cleaning deposited films such as hydrocarbons from the chamber walls, cathode and pipeline components, oxygen plasma could not be used. The system was cleaned by wiping the cathode and the chamber walls by a clean cloth soaked in acetone. Scrubbing the dirty components using a nylon scourer soaked in acetone resulted in a cleaner chamber.

The master/slave system was arranged in reactive ion etching mode, with the lower electrode connected to the RF power supply. This indicates that if inert gases such as argon are used the configuration can also be called sputter or ion etching.

The lower electrode (cathode) was made of aluminium and was coated with titanium oxide. The chamber hatch acted as the upper electrode (anode) and was connected to earth. The ratio of the areas of cathode and anode was 1:3. The cathode diameter was approximately 17.4 cm with an area of about 237.7 cm^2.

A diagram of the chamber is shown in Figure 4.2 (a). The gas was admitted to the chamber radially. The volume of the chamber in which the plasma was struck was about 2100 cc. This volume would be used as the plasma volume for this system which is of importance for the calculation of residence time of the gas in the chamber, (see equation 1.1).

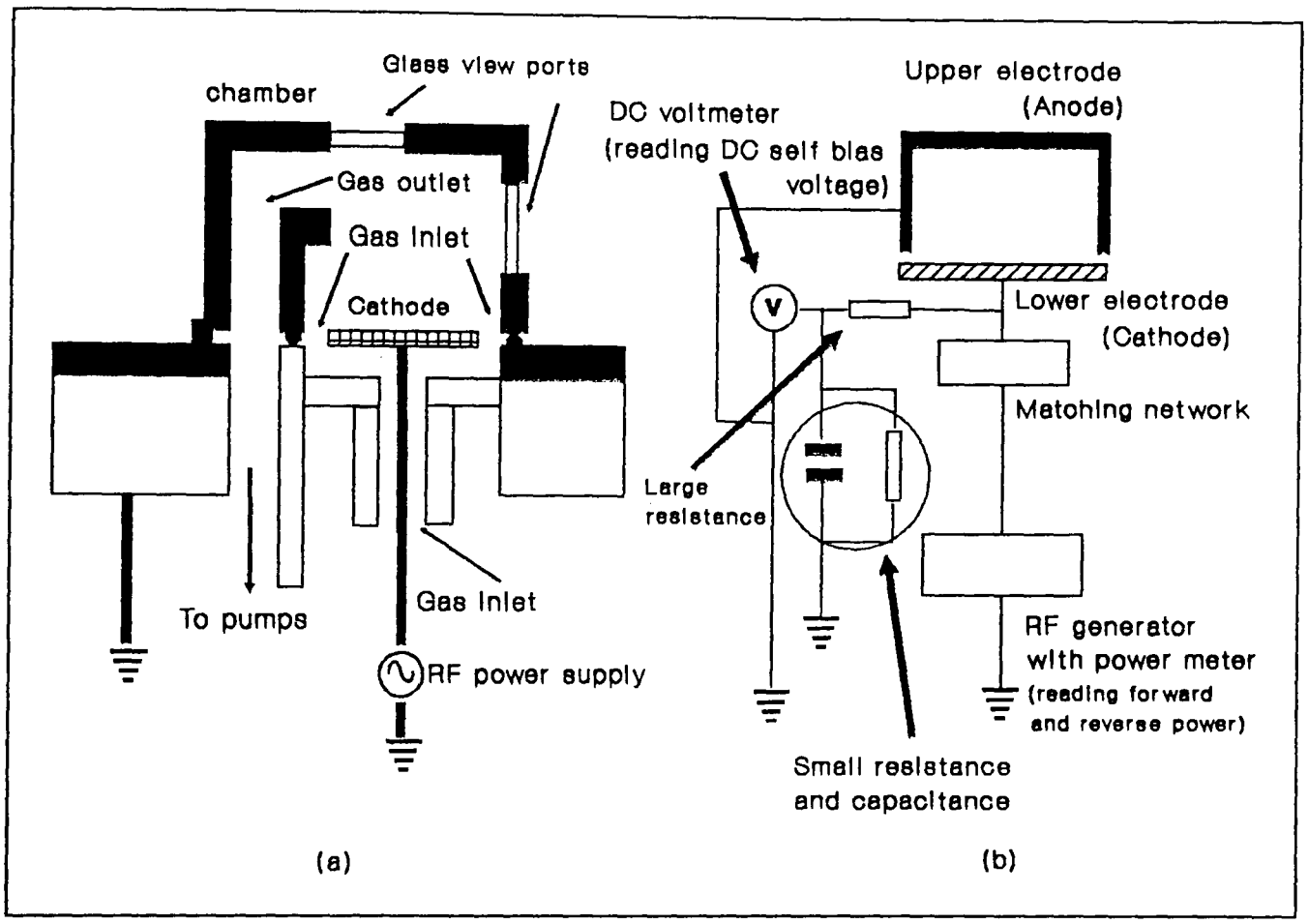

Figure 4.2. Chamber diagram of the Plasmafab 340. (a) General view. (b) Electrical diagram.

Figure 4.2 (b) is the simplified electrical diagram for the measurement of DC self bias voltage V_{self}, on the cathode. The small resistance and capacitance is required to filter the high frequency signal. The large resistance is needed to act as a potential divider to scale down the voltage by 100 times so that a voltage of -1000 V can be measured on the DC meter as a maximum of -10 V. The RF power supply was able to provide up to 300 W at 13.56 MHz. The impedance matching unit on this system was manually controlled.

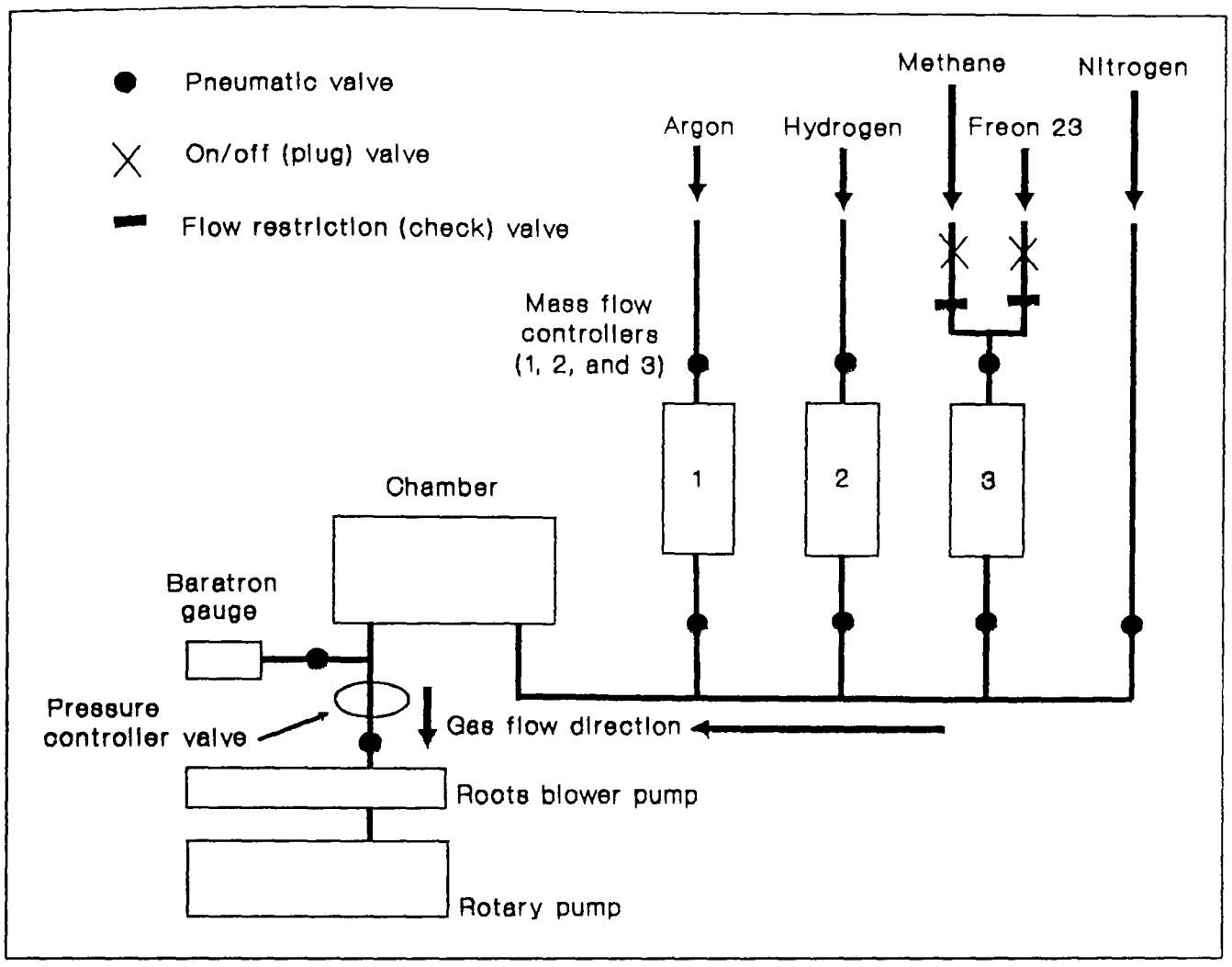

Figure 4.3. Diagram of gas controllers in Plasmafab 340.

The process was controlled from the front panel on the slave system. These were the system controller, the pressure controller, the mass flow controllers, the RF power controller and the process timer modules. The operating pressure and gas flow were pre-adjusted on the relevant controller modules and the process duration was set on the timer before the process began. When the chamber pressure reached the base pressure, the gas pressure and flow controllers were activated. Figure 4.3 shows the diagram of gas controllers.

Argon was admitted by mass controller 1 which was calibrated for nitrogen and could admit gas in to the chamber at a maximum flow of 200 sccm. Mass flow controller 2 was calibrated for hydrogen and could admit gas to the chamber at a maximum flow of 200 sccm. Mass flow controller 3 was

calibrated for nitrogen and admitted gas to the chamber at a maximum flow of 100 sccm. Methane or Freon 23 were admitted in the chamber by this mass controller. The gases were led to the mass controllers by a series of on/off (plug) valves and flow restriction (check) valves. The flow of gas Q_{gas} through mass flow controllers 1 and 3 was calculated by equation 4.1.

$$Q_{Gas} = Q_N C, \tag{4.1}$$

Where Q_N is the flow of gas indicated on the mass flow controller calibrated for nitrogen and C is the conversion factor.

Nitrogen was used for purging the system when the chamber hatch had been opened. The pressure of the chamber was measured by a Baratron gauge which could be separated from the chamber by a pneumatic valve. The pressure was controlled by a pressure controller valve which varied the pumping speed of the system.

4.2 DC self bias voltage

DC self bias voltage V_{self} is caused by the accumulation of negative charge on the cathode, (the electrode which is connected to the RF generator). This is due to the high mobility of the electrons in the plasma, (Chapman, 1980. Also see appendix X). Generally increase in V_{self} indicates an increase in the intensity of ion bombardment. This is because the higher the negative charge on the cathode the higher the acceleration of positive ions will be towards the cathode.

The behaviour of V_{self} for the Electrotech Plasmafab 340 is described here. Experiments were carried out with mixtures of methane and hydrogen. The plasma was struck when no GaAs was present in the chamber and the value of V_{self} was measured at different process parameters. Figure 4.4 shows the graphs of V_{self} against process parameters. The measurements were taken for power density, pressure, total flow rate and volume concentration of

methane in hydrogen.

Figure 4.4 (a) shows the variation of V_{self} against power density. The total flow rate was set at 4.4 X 10^{-2} Pa m^3/sec (26 sccm), with methane concentration of 10% volume in hydrogen. At 4 Pa (30 mtorr) V_{self} increased as the power density increased. This behaviour was observed at different pressures between 6 Pa to 10 Pa (45 mtorr to 75 mtorr). The increase in V_{self} because of the increase in power density was due to the increase in the ionization of the species in the chamber. The higher the power density the higher the degree of ionization, hence the higher the negative charge on the cathode.

Increase in pressure caused a decrease in V_{self} as shown in figure 4.4 (b). At 6, 8 and 10 Pa (45, 60 and 75 mtorr), the profiles of the curves are similar. The total flow rate and the methane concentration in hydrogen was as before but the graph shows the trend of the curves for different power densities between 0.21 to 0.84 W/cm^2 (50 to 200 W of power). The trends for all curves are the same between 4 to 10 Pa (30 to 75 mtorr). The decrease in V_{self} because of increase in pressure was due to the decrease of the mean free path of the species in the chamber, indicating more collisions between the species and hence less probability of electrons and ions reaching the electrodes in any one cycle.

Figure 4.4 (c) shows V_{self} against total flow rate of methane and hydrogen. The measurements were taken for different power densities, pressure and methane concentration in hydrogen. V_{self} was measured for total flow rates from 4.4 X 10^{-2} to 9.4 X 10^{-2} Pa m^3/sec (26 to 56 sccm). The general trend of the graph indicates a slight decrease in V_{self} as the total flow increases.

This also shows that an increase in pressure and/or methane concentration in hydrogen decreased V_{self}. This may have been due to the decrease in the residence time of the gas mixture in the chamber as the total flow rate

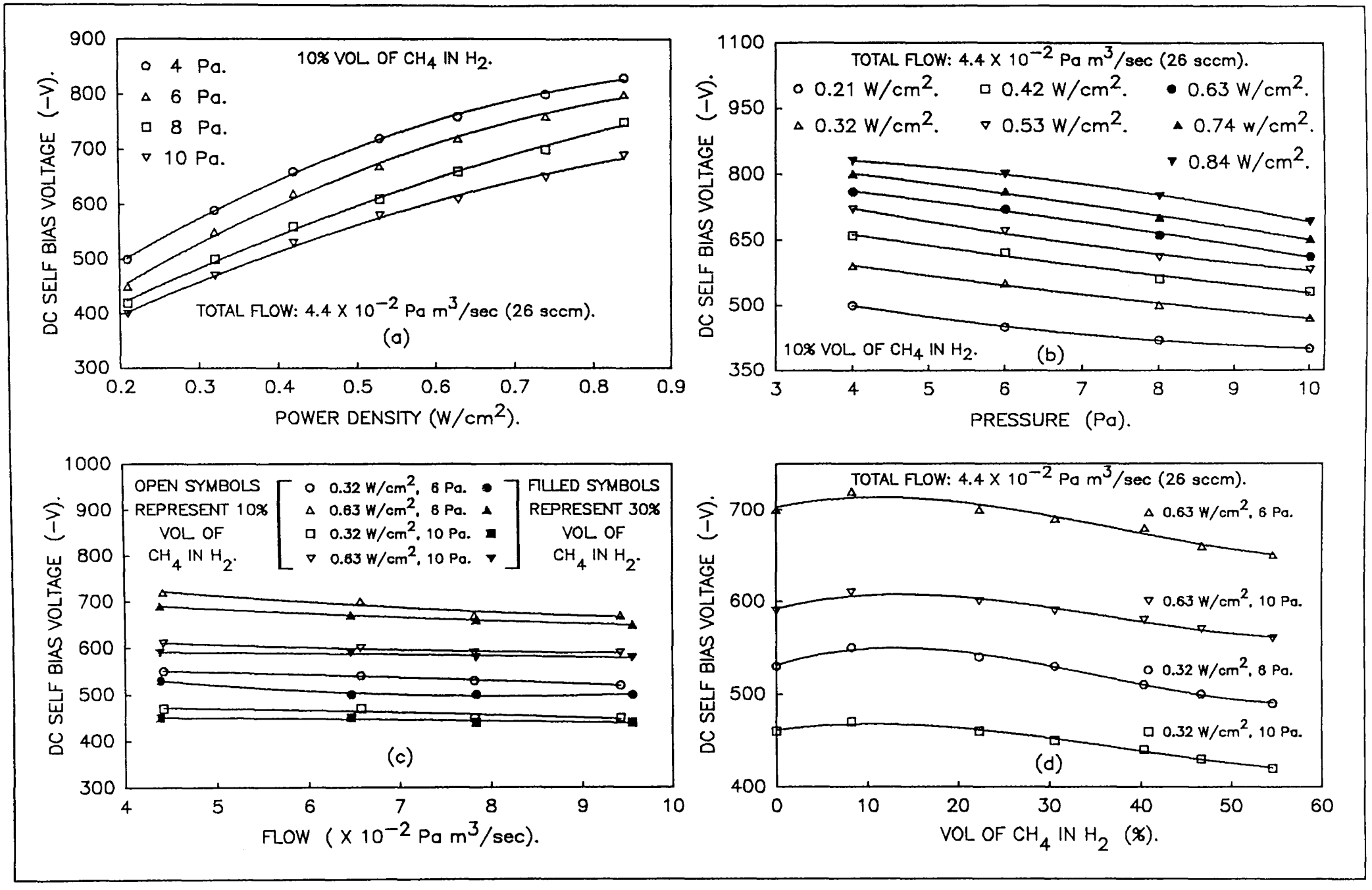

Figure 4.4. DC self bias voltage against process parameters.

increased. The species were passing so quickly through the chamber that they may not have had enough time to charge the cathode.

Figure 4.4 (d) shows the behaviour of V_{self} against volume methane concentration in hydrogen from 0 to about 55%. The experiment was performed at different power densities and pressures. Generally V_{self} increased until 10% volume of methane in hydrogen and then it decreased. However at high power densities and low pressures the magnitude of V_{self} increased.

This slight increase in V_{self} after the introduction of CH_4 (up to 10% volume concentration) to the chamber may have been due to the production of electrons by ionization following the breakdown of molecules. As a result of this the cathode was charged to a higher negative value. When CH_4 volume concentration increased beyond 10% most of the energy was spent in breaking down the molecules rather than ionization. this resulted in reduction of negative charge on the cathode and hence decrease in V_{self}.

4.3 Reflected power

When a RF generator supplies power to a load, some of this power is reflected back to the RF generator. This is called the reflected power and its magnitude depends on the matchings of the impedances of the system, (Duffin, 1980. Also see appendix XI).

Figure 4.5 shows the graph of minimum reflected power against forward power of the system. The measurements were taken at different pressures from 4 to 7 Pa (30 to 52.5 mtorr), for forward power between 25 to 150 W. The total flow rate was set at 8.1 X 10^{-2} Pa m^3/sec (48 sccm), and the volume concentration of methane in hydrogen was at 25%.

The reflected power increased as the forward power increased. This was

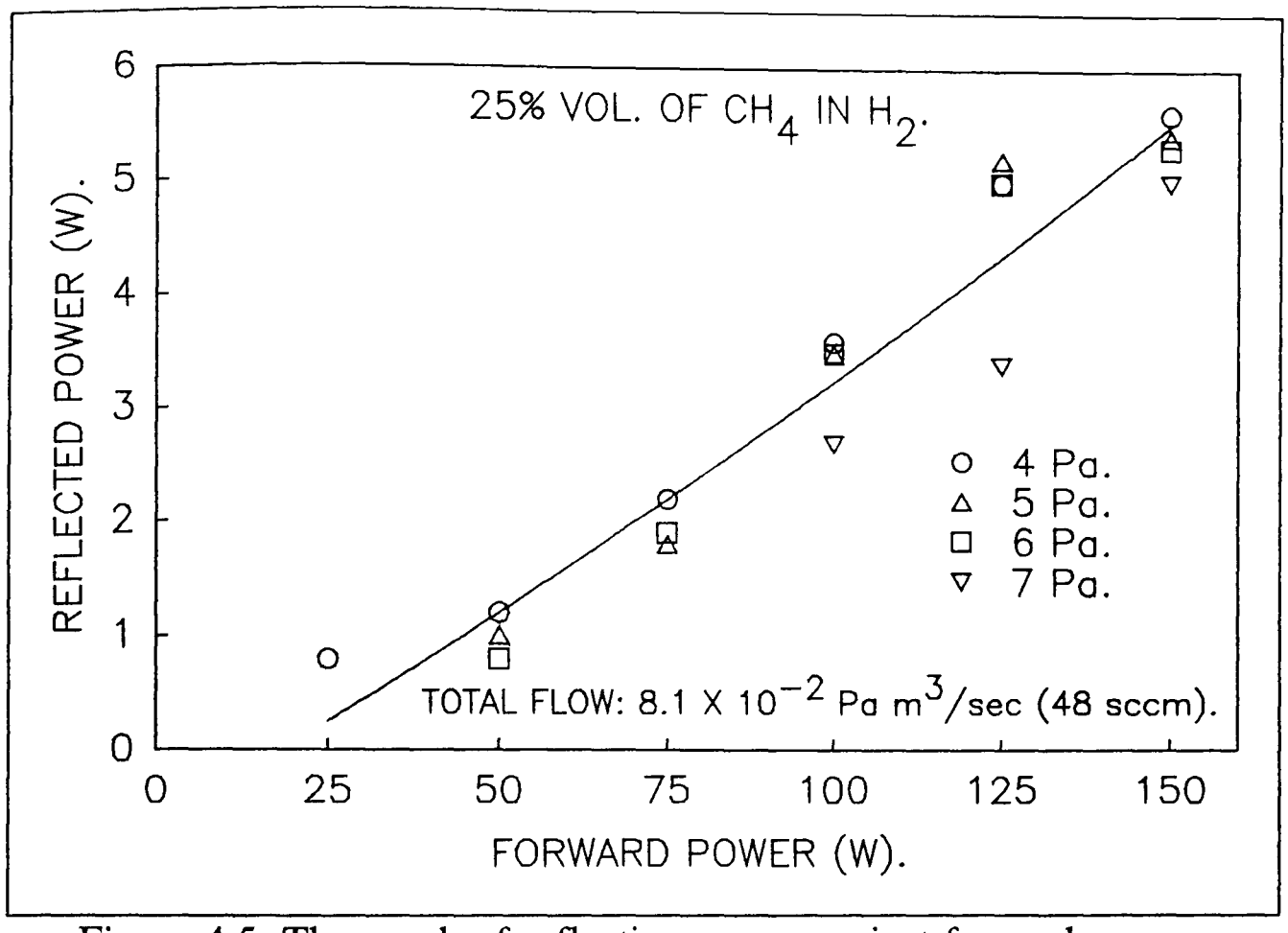

Figure 4.5. The graph of reflection power against forward power.

tuned to a minimum value manually. For all cases the minimum value of reflected power was less than 5% of the forward power.

4.4 Condition of the chamber

The condition of the chamber is very important for dry etching. Figure 4.6 also shows the behaviour of V_{self} against volume concentration of methane in hydrogen. The measurements were taken for clean, and dirty chamber (dirty chamber walls and cathode), and also clean cathode with dirty chamber walls (dirty is defined here as condition of chamber after 10 usage in CH_4/H_2 mixtures). The results were similar within the limits of experimental errors for a clean chamber and clean cathode only, with dirty chamber walls. The trend of the graphs of V_{self} was the same as that shown in figure 4.4 (d) but the quantity of V_{self} decreased for dirty chamber compared with other conditions. The etch rate of the GaAs sample at 40% volume concentration of CH_4 was the same for the clean chamber and clean

cathode which was about 50 nm/min. However for dirty chamber deposition occurred at 30% volume concentration of CH_4.

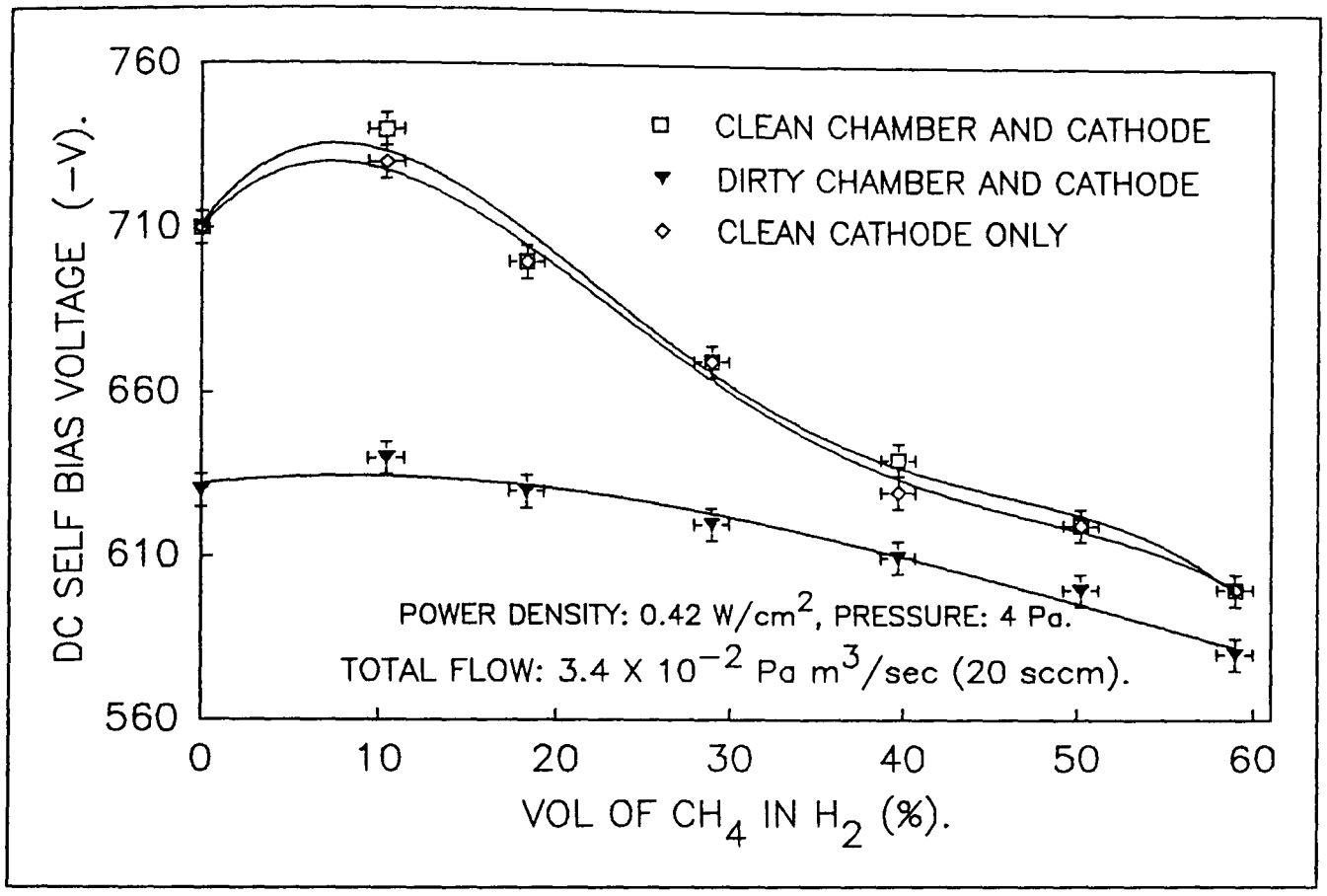

Figure 4.6. Graph of DC self bias voltage against volume methane concentration in hydrogen for different conditions of the vacuum chamber.

One of the problems of this Electrotech Plasmafab 340 was the inability to control the cathode temperature. Figure 4.7 shows the graph of temperature of the cathode, as it cooled after opening the chamber hatch.

After processing for 30 minutes at power density of 0.42 W/cm^2, pressure of 4 Pa (30 mtorr), flow of 3.4 X 10^{-2} Pa m^3/sec (20 sccm) and 100% hydrogen, 30 seconds elapsed until the chamber hatch opened. It must also be noted that for the chamber hatch to open after the pumps were isolated, the chamber had to be purged with nitrogen gas so that the pressure inside and outside of the chamber would equalise. The purging gas was let in the chamber from the base of the cathode and then radially from the side. This gas also cooled the cathode.

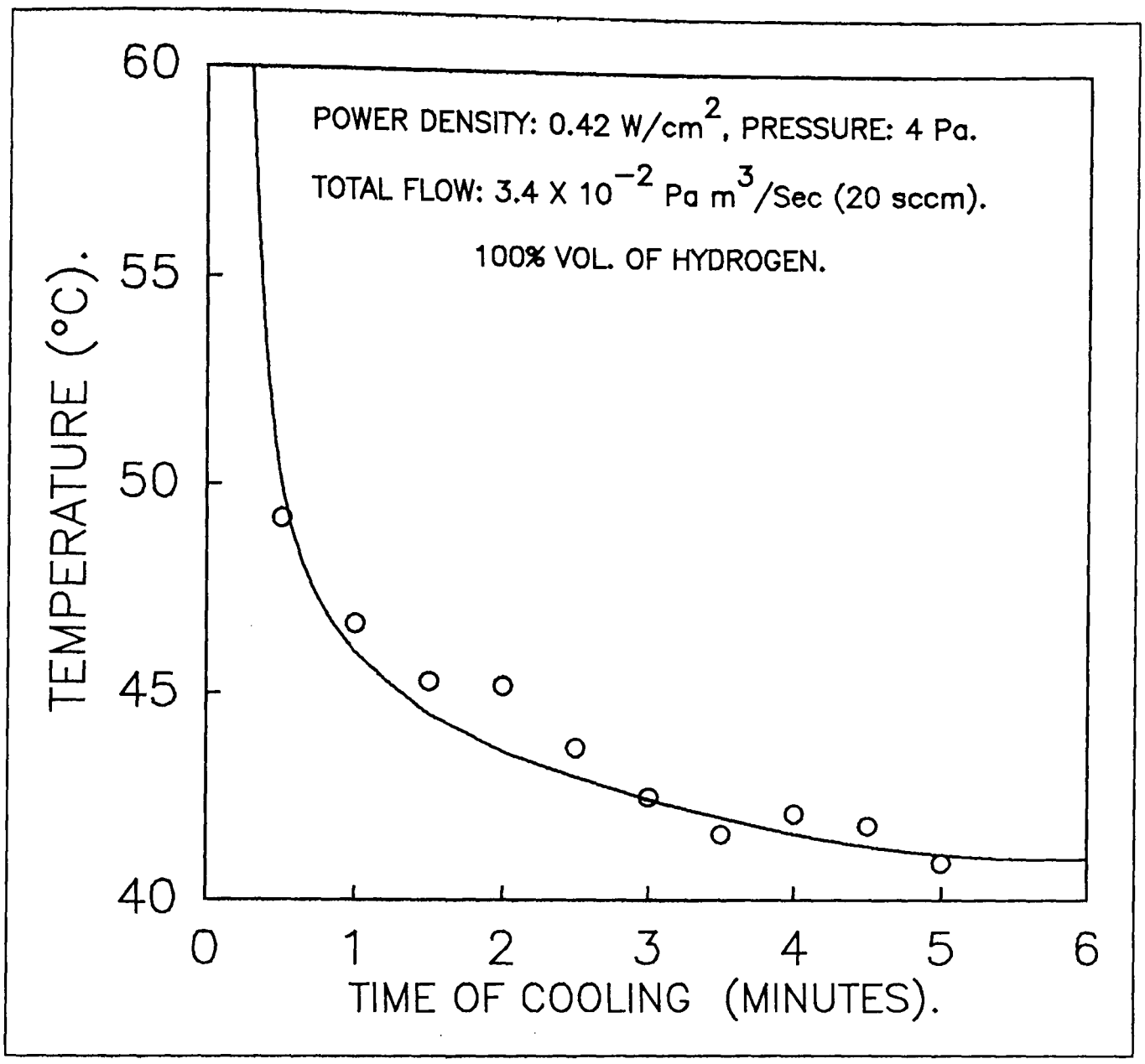

Figure 4.7. The graph of the cooling temperature of cathode against time.

The temperature was measured by immediately placing a thermocouple on the surface of the cathode when the hatch was opened. Temperature decreased as time advanced.

The 30 second elapsed time to open the chamber hatch was not the only cooling factor. The nitrogen used for purging also presented an important influence on cooling the cathode and thus it is difficult to estimate the original temperature at time t=0.

The position of the semiconductor samples on the cathode does not appear to effect the etching process. Figure 4.8 shows the variation of etch rate of

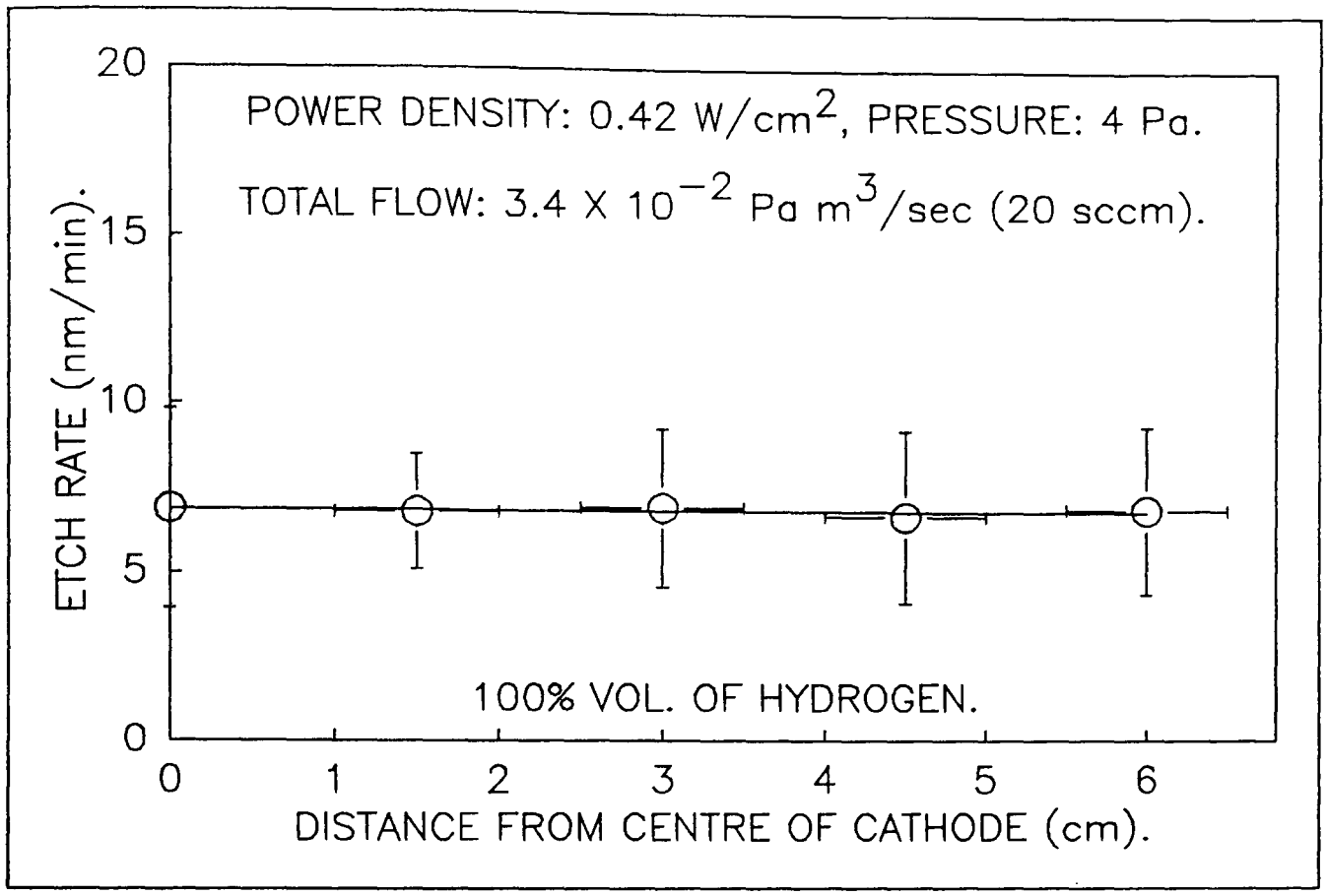

Figure 4.8. The graph of etch rate against the position of the sample.

GaAs against the distance from the centre of the cathode. The samples were etched at the same time at different positions on the cathode. The power density and pressure were set at 0.42 W/cm^2 and 4 Pa (30 mtorr), with flow rate set at 3.4 X 10^{-2} Pa m^3/sec (20 sccm). The GaAs samples were etched in 100% hydrogen. The etch rate was constant for all samples within the limits of experimental errors which indicated uniform etching at different positions of the cathode. As the physical mechanism is dominant under these conditions, the electric field is considered to be uniform across the cathode.

The plasma can affect the pressure set by the operator. Figure 4.9 shows this effect. The set pressure p_s is plotted against the difference Δp between the set pressure and plasma pressure p_p which is the pressure in the process chamber after the plasma is struck, ($\Delta p = p_p - p_s$).

The experiment was performed at different power densities from 0.21 to 0.63 W/cm^2. The pressure was set from 30 to 52.5 mtorr. Note that SI unit

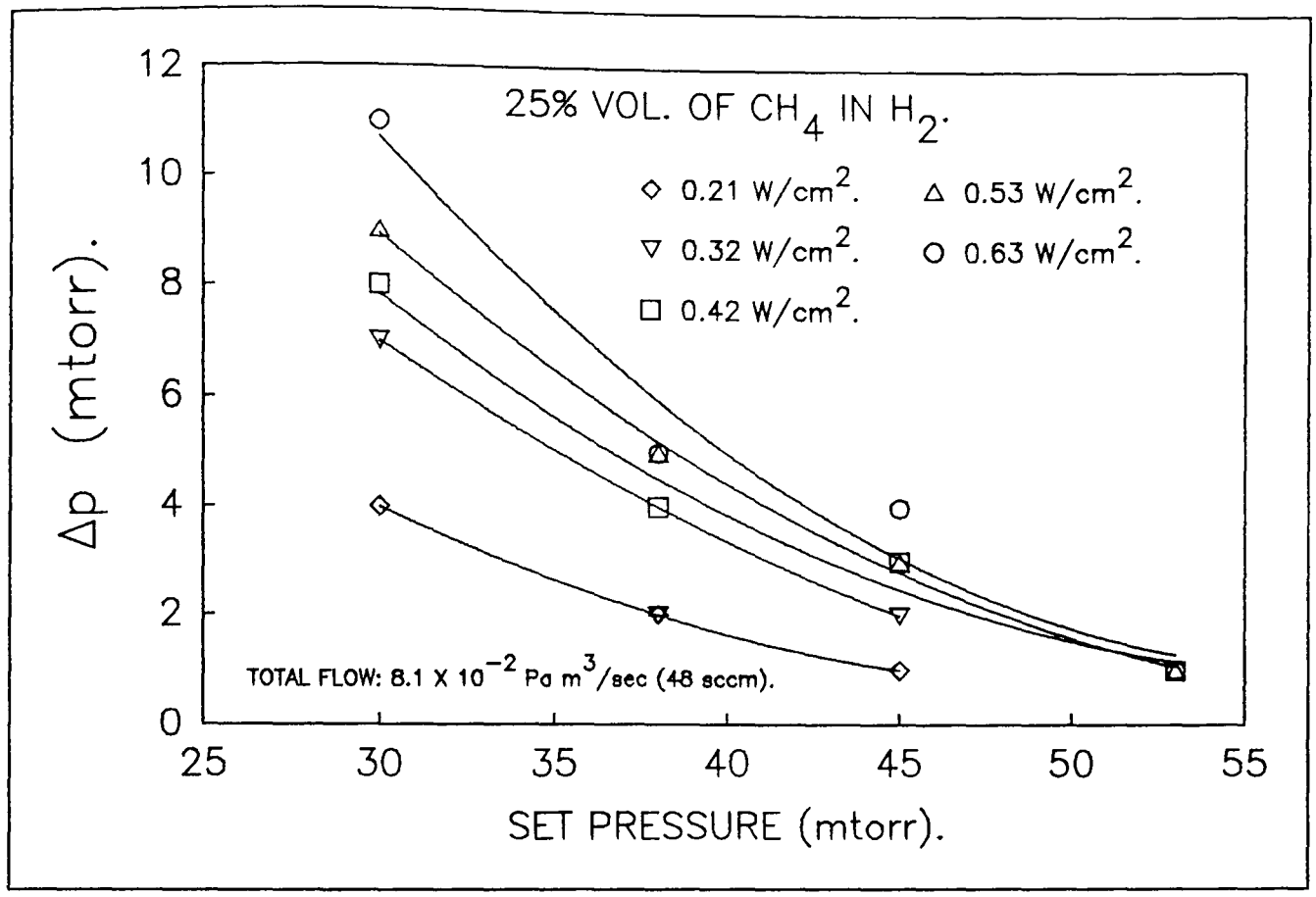

Figure 4.9. The graph of Δp against the set pressure.

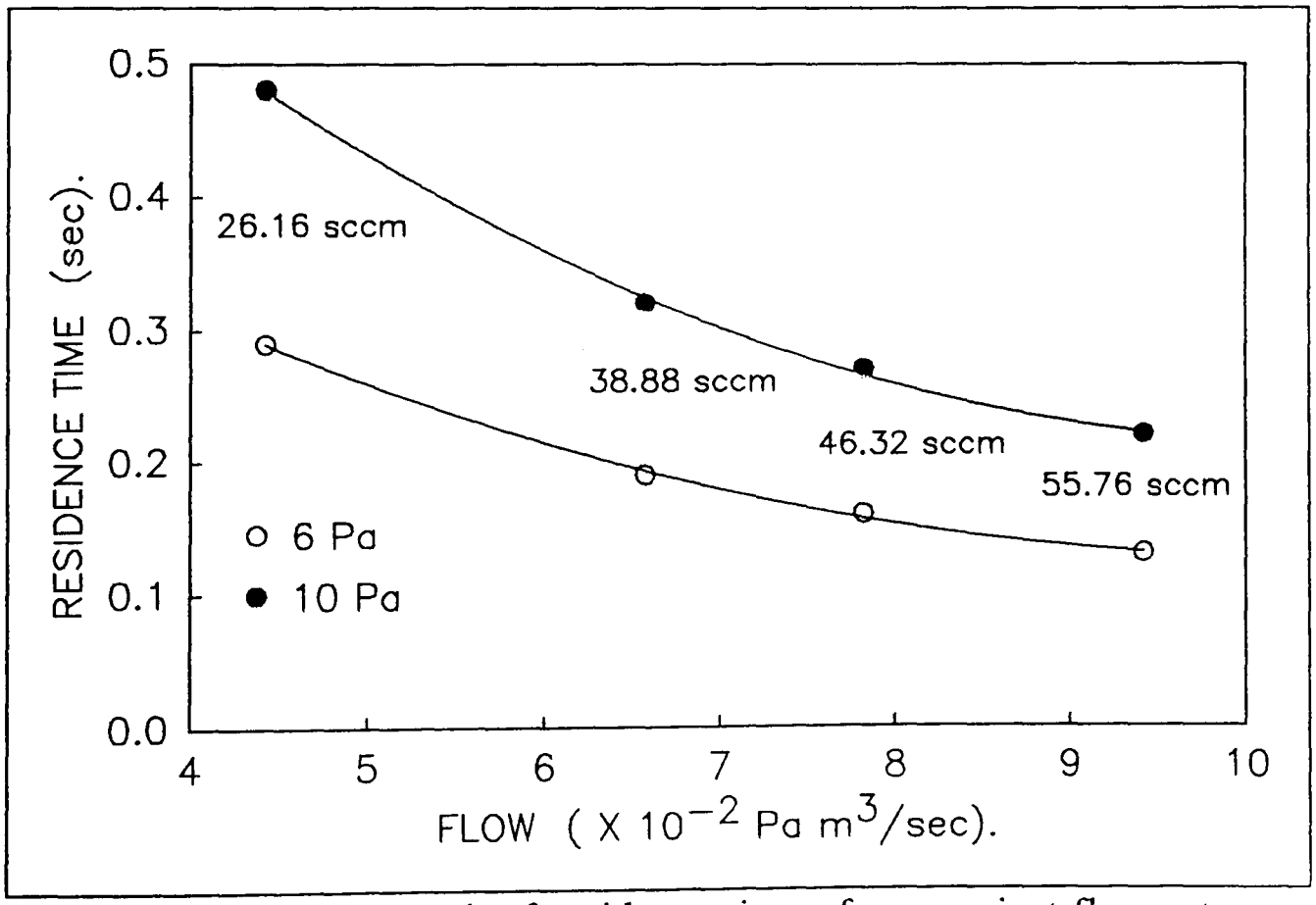

Figure 4.10. The graph of residence time of gas against flow rate.

for pressure was not used for this case as Pa (pascal) is not a sensible unit at these pressures for small changes. The total flow rate was set to 8.1 X 10^{-2} Pa m^3/sec (48 sccm), and the methane concentration was 25% volume in hydrogen. The general trend of the graph shows an increase in Δp as the set pressure is decreased.

Figure 4.10 is shows the graph of residence time of the gas in the chamber against the flow rate. The residence time was calculated for the stated flow rates at two different arbitrary pressures, from equation 1.1. The residence time of the gas in the chamber decreases as the flow rate increases. At high pressures the residence time of the gas is higher than at low flow rates.

CHAPTER 5
REACTIVE ION ETCHING RESULTS

In this chapter results of experiments on reactive ion etching of gallium arsenide in mixtures of methane and hydrogen are presented. Etch rate and anisotropy were compared for various values of the process parameters. The deposition of carbon polymers was also investigated together with erosion of the masking pattern.

5.1 Non-chlorinated gas mixtures

Three different configurations of gas mixture were used to etch GaAs. The mixtures used were methane/hydrogen (CH_4/H_2), methane/argon (CH_4/Ar) and hydrogen/argon (H_2/Ar). The reason for using these gas mixtures was to investigate the basic mechanisms of the etching process.

The power density and pressure chosen for the experiment were 0.42 W/cm^2, (power 100 W) and 4 Pa (30 mtorr) respectively. The area of the GaAs samples used for this experiment was 100 mm^2. The total gas flow rate was set to about 3.4 X 10^{-2} Pa m^3/sec (20 sccm).

Figure 5.1 shows the graphs of etch rate R and DC self bias voltage V_{self} against volume concentration of admixed gases. Figure 5.1 (a) shows the variation of R and V_{self} for mixtures of methane and hydrogen. R was a minimum for 100% hydrogen. As methane was added to hydrogen R increased until it reached a maximum of about 28 nm/min at about 50% volume of methane in hydrogen. At 50% concentration of methane although the etch rate was at maximum, carbon pellets were deposited on the surface of the GaAs sample.

In order to produce a good GaAs surface the best volume concentration of methane in hydrogen at the set conditions was considered to be about

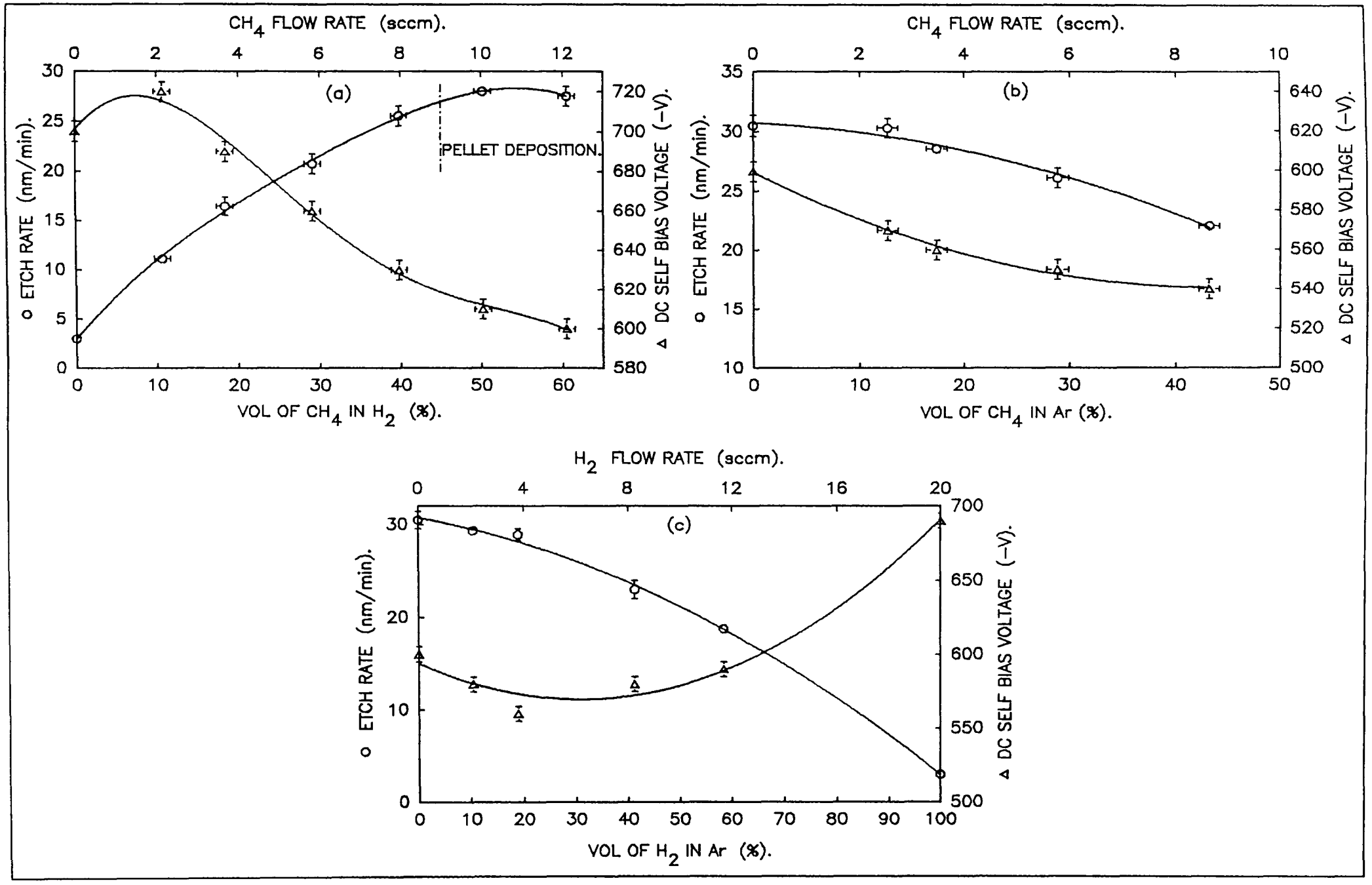

Figure 5.1. Graphs of etch rate and DC self bias voltage against volume concentration of admix gases, (a) CH_4/H_2, (b) CH_4/Ar and (c) H_2/Ar at 0.42 W/cm^2, 4 Pa and 3.4 X 10^{-2} Pa m^3/sec.

40% which yielded an etch rate of about 26 nm/min. The value of V_{self} increased to about -720 V at 10% volume of CH_4 in H_2. Then it started to decrease until at about 60% volume of CH_4 in H_2 it reached to its lowest value. The value of V_{self} was about -630 V at 40% volume of CH_4. This indicated that the etch rate increased as the DC self bias voltage decreased. A decrease in DC self bias voltage indicates a reduction in the intensity of ion bombardment. This suggests that the chemical component of etching (reactive species), was becoming intense and the physical component of etching (ion bombardment), was slightly decreasing.

Figure 5.1 (b) shows the variation of R and V_{self} for mixtures of methane and argon. As methane was added to argon, R decreased. The value of V_{self} also decreased. The maximum R of 31 nm/min, occurred at maximum V_{self} of -600 V at 100% argon. The mechanism of etching was mainly physical as a reduction in ion bombardment intensity caused a reduction in etch rate.

Figure 5.1 (c) shows the variation of R and V_{self} for mixtures of hydrogen and argon. R decreased from 31 nm/min at 100% Ar to a minimum of 4 nm/min at 100% hydrogen. V_{self} however did not show the trends of figure 5.1 (a) or (b). It decreased at first from -600 V at 100% Ar to a minimum of -570 V at about 30% volume of H_2 in Ar, then increased to its maximum value of -690 V at 100% H_2. At 100% H_2 ion bombardment was intense but R was low because of the low mass of the hydrogen bombarding ions. The mechanism of etching in this case was also mainly physical.

The methane and hydrogen experiment showed a strong tendency to combined physical and chemical etching mechanism. The rest of the experiments were carried out in methane and hydrogen mixtures.

5.2 Effect of flow on RIE of GaAs

The RIE of GaAs was repeated in methane and hydrogen mixtures at a power density and pressure of 0.42 W/cm^2 (power 100 W), and 4 Pa (30 mtorr), respectively. The methane concentration experiments discussed here were carried out at different total flow rates of 3.4 X 10^{-2}, 5.1 X 10^{-2}, 6.8 X 10^{-2} and 8.1 X 10^{-2} Pa m^3/sec (20, 30, 40 and 48 sccm). The area of GaAs samples for etching was reduced from 100 mm^2 to 25 mm^2. Figure 5.2 shows the results of the experiments performed at different total flow rates.

Figure 5.2 (a) shows the variation of etch rate R and DC self bias voltage V_{self} against volume of CH_4 concentration in H_2 at 3.1 X 10^{-2} Pa m^3/sec (20 sccm). R increased as the volume of methane in hydrogen increased up to about 45% volume where R was about 50 nm/min. It then decreased as the methane concentration increased further until at 60% volume of CH_4 where R was zero. The etch rate fell after 45% volume concentration of CH_4 until the whole of GaAs surface was covered with deposited carbon at 60% volume of CH_4. V_{self} increased from about -710 V to -730 V from 0 to about 10% volume of CH_4 in H_2. It then decreased as the CH_4 volume increased. at optimum R, V_{self} was at about -630 V.

Figure 5.2 (b) also shows the variation of R and V_{self} with respect to CH_4 concentration, but in this case the total flow rate was set to 5.1 X 10^{-2} Pa m^3/sec (30 sccm). R increased as the CH_4 concentration increased until at about 29% the maximum R of about 50 nm/min was achieved. As before, a further increase in CH_4 caused carbon polymerization which inhibited the etching process. V_{self} also increased until 10% volume of CH_4 where the maximum V_{self} was -710 V. It then decreased to about -660 V at 29% concentration of CH_4.

Figure 5.2 (c) shows the variation of R and V_{self} at a constant total flow of

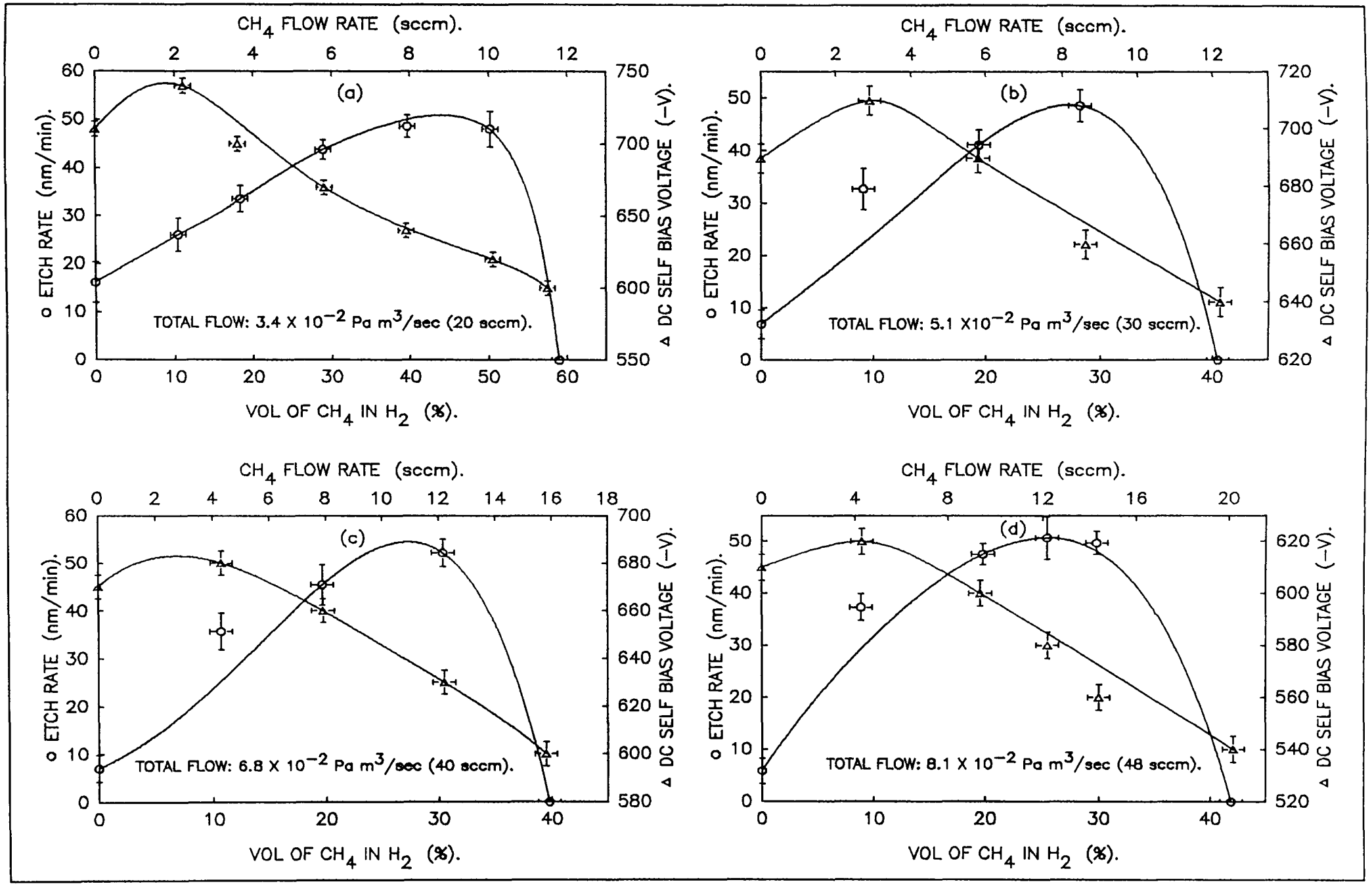

Figure 5.2. Graphs of etch rate and DC self bias voltage against volume CH_4 concentration in H_2 at different total flow rates at 0.42 W/cm^2 and 4 Pa. (a) 3.4 X 10^{-2}, (b) 5.1 X 10^{-2}, (c) 6.8 X 10^{-2} and (d) 8.1 X 10^{-2} Pa m^3/sec.

6.8 X 10^{-2} Pa m^3/sec (40 sccm). Again, the trend of the graph was the same as before for both R and V_{self}. R increased until at 27% volume of CH_4 where R was at maximum of about 50 nm/min and V_{self} was about -630 V.

A similar trend can be observed in Figure 5.2 (d) where the total flow rate was kept constant at 8.1 X 10^{-2} Pa m^3/sec (48 sccm). Maximum R was achieved at 25% volume of CH_4 which was about 50 nm/min, as before. The value of V_{self} at optimum CH_4 concentration was about -580 V. The flow rate was not increased above 8.1 X 10^{-2} Pa m^3/sec, because the pressure could not be kept at a constant 4 Pa when total flow rate was increased further.

Figure 5.3 shows the effect of the total flow rate from 3.4 X 10^{-2} to 8.1 X 10^{-2} Pa m^3/sec (20 to 48 sccm). Figure 5.3 (a) shows The etch rate R and the optimum volume of CH_4 against total flow rate. R remained constant within the limits of experimental error but the optimum volume of CH_4 decreased from about 45% at 3.4 X 10^{-2} Pa m^3/sec to 25% at 8.1 X 10^{-2} Pa m^3/sec.

Figure 5.3 (b) shows the variation of carbon deposition rate on mask and DC self bias voltage V_{self} against total flow rate. The carbon deposition decreased as the total flow rate increased. At 8.1 X 10^{-2} Pa m^3/sec the carbon deposition rate was at about 7 nm/min. V_{self} increased slightly at the beginning but then it decreased as the total flow rate increased.

Picture 5.1 shows the micrographs of the etched surface. Picture 5.1 (top) shows the profile of the surface etched at total flow rate of 3.4 X 10^{-2} Pa m^3/sec and 45% methane concentration. The side wall was rough and curvatures were present at the top and bottom of the wall. Picture 5.1 (bottom) shows the profile of the sample etched at total flow rate of 8.1 X 10^{-2} Pa m^3/sec and 25% methane concentration. There are no curvatures present at the top and bottom of the etched wall. Anisotropy was very good.

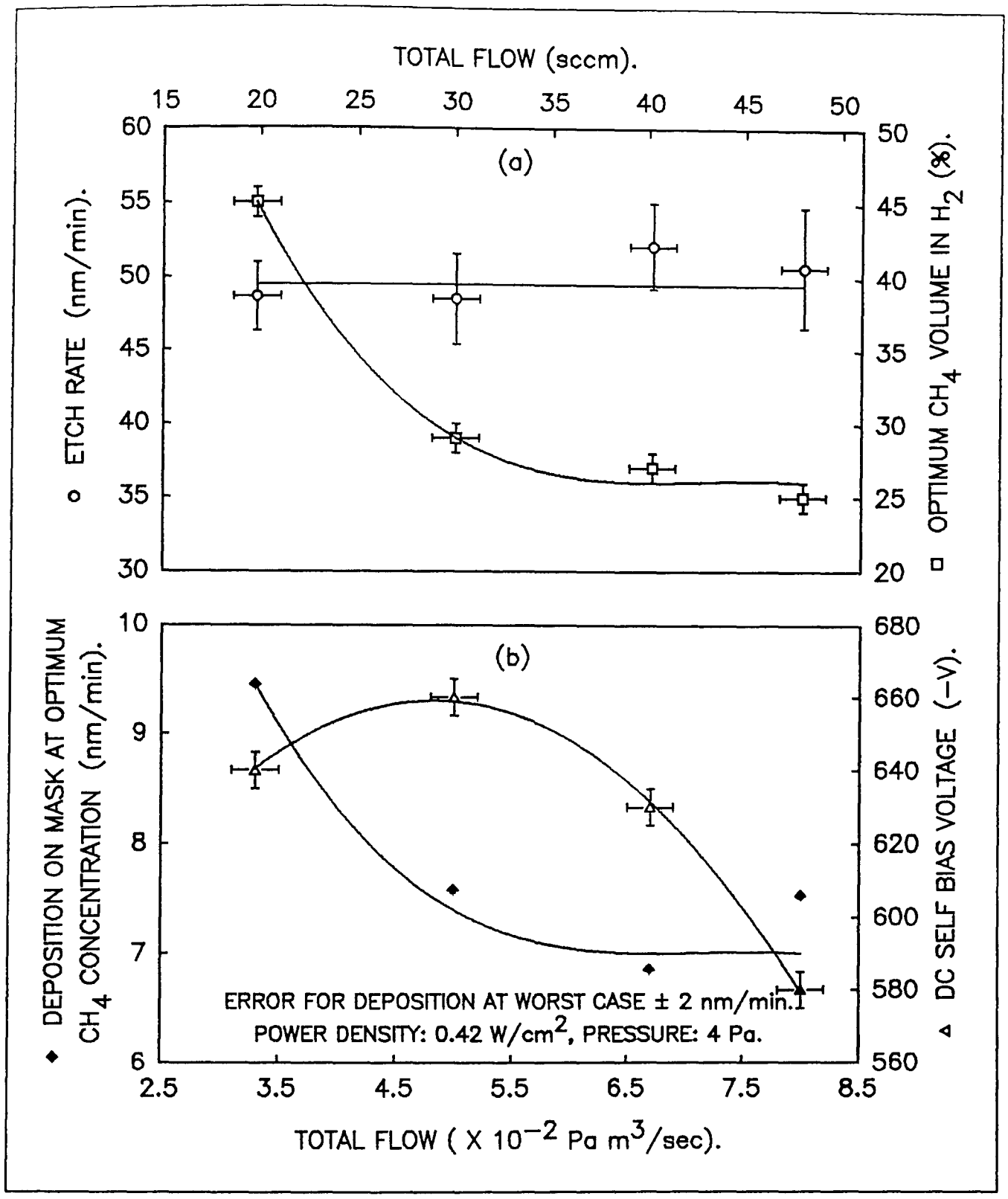

Figure 5.3. Graph of (a) etch rate and optimum methane concentration, (b) carbon deposition and DC self bias voltage against total flow rate.

Figure 5.4 shows the graph of etch rate R and DC self bias voltage V_{self} against total flow rate at an arbitrary methane concentration of 20%. R increased as the total flow rate increased but V_{self} decreased.

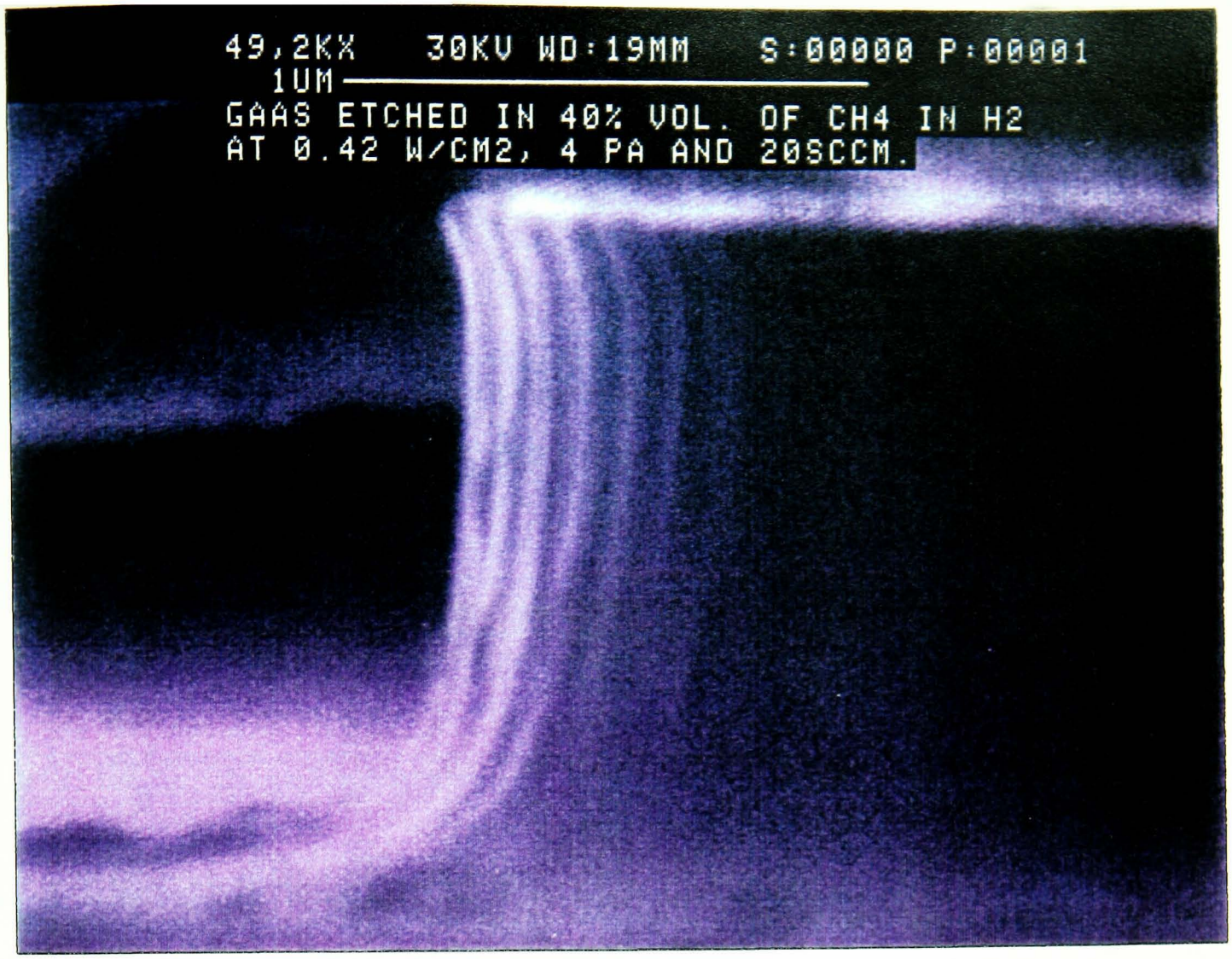

Picture 5.1. Micrographs of the etched surface. (Top) etched at 3.4 $X10^{-2}$ and (bottom) etched at 8.1 $X\ 10^{-2}$ Pa m^3/sec.

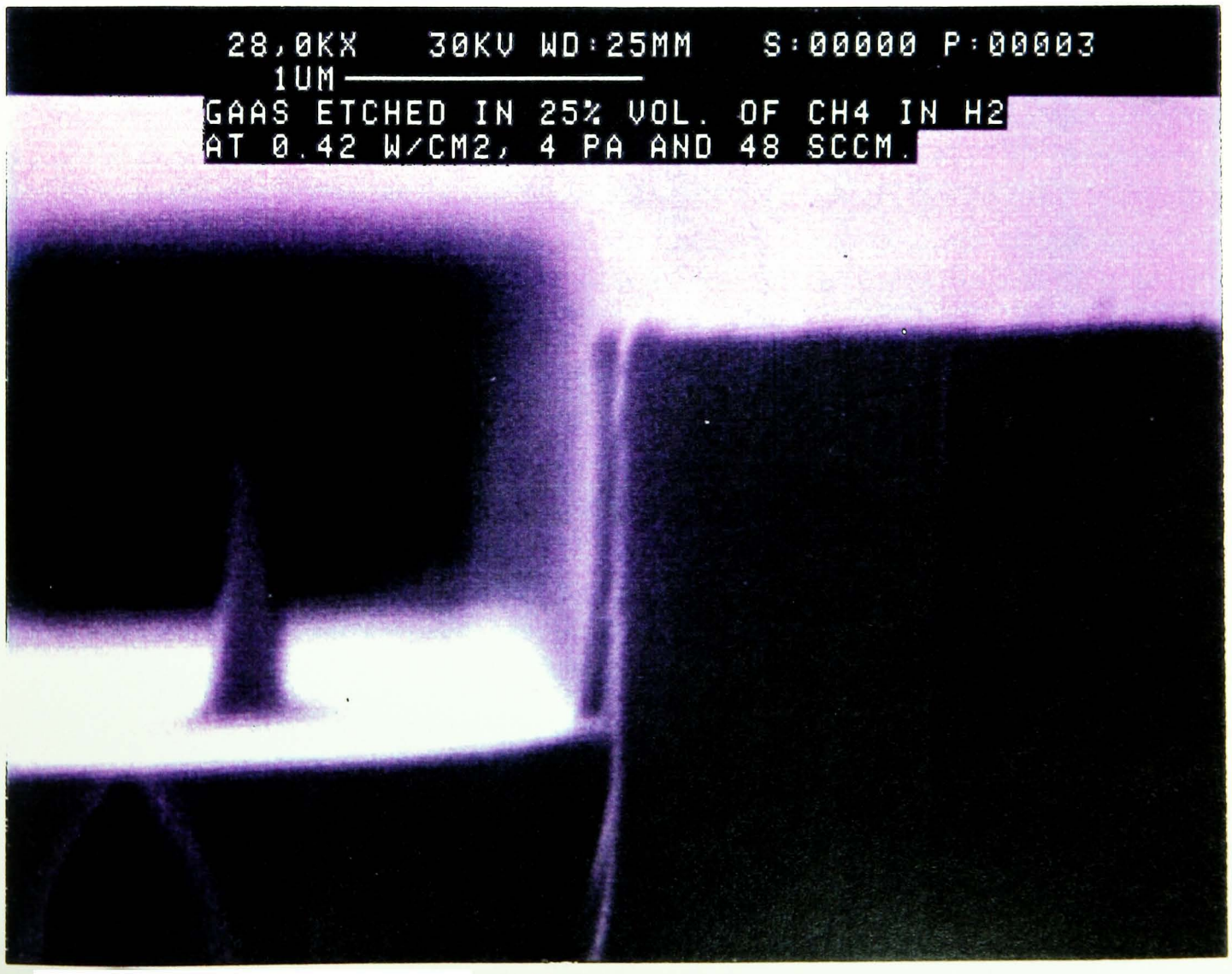

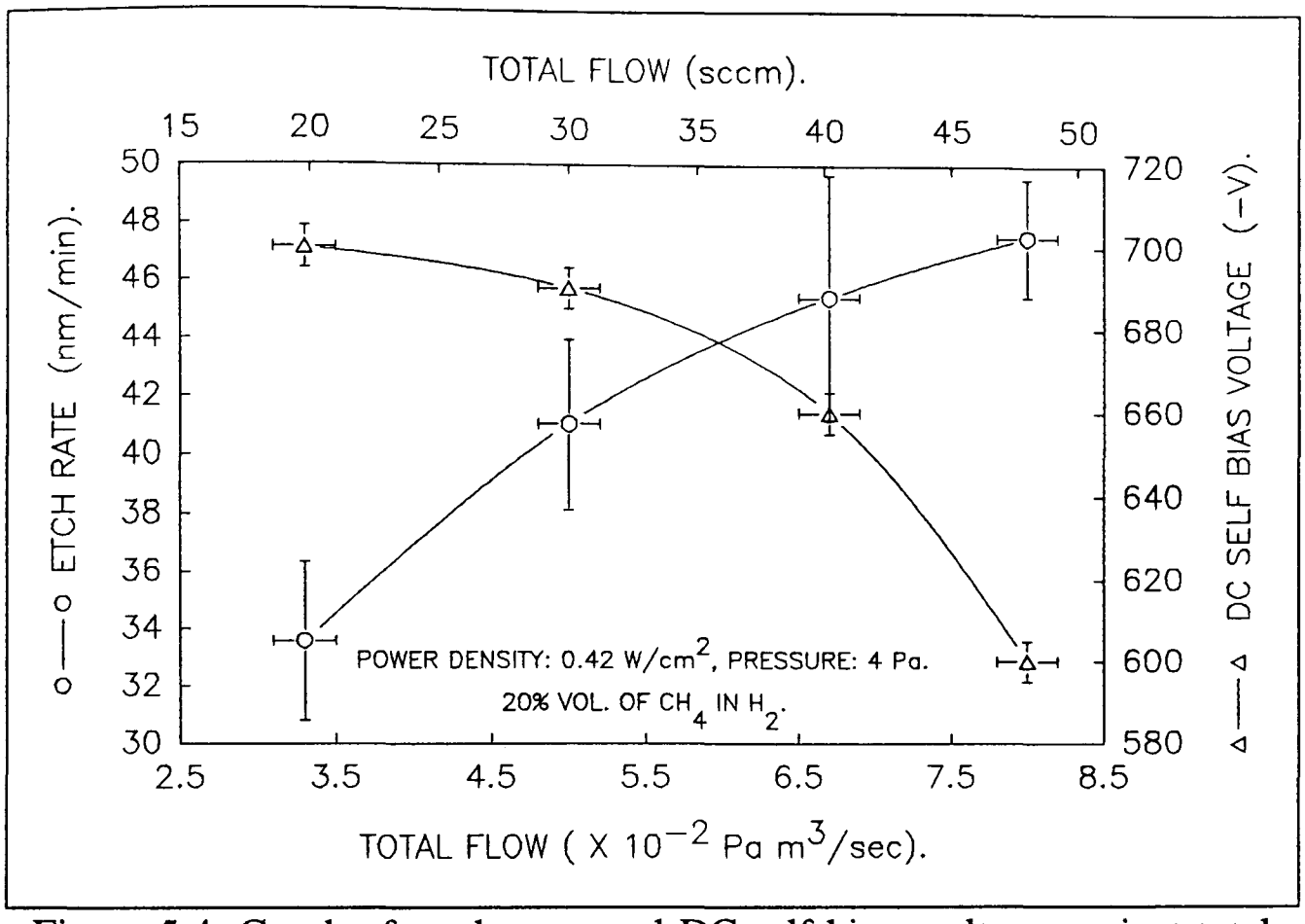

Figure 5.4. Graph of etch rate and DC self bias voltage against total flow rate at an arbitrary 20% methane concentration.

Picture 5.2 shows the micrograph of the profiles of the etched surfaces at 8.1 X 10^{-2} Pa m^3/sec. Picture 5.2 (top) shows the surface of the sample etched in 20% CH_4 concentration. The surface of the wall was very smooth but trenching occurred at the base of the wall. At about 25% CH_4 concentration, the surface of the wall was also smooth but there was minimum trenching at the base of the wall, (picture 5.2 (bottom)).

Fine adjustment of DC self bias voltage V_{self} was possible because the total flow rate of the gas could be controlled. V_{self} decreased from -600 V to -580 V between 20% and 25% volume CH_4 concentration, a change of about 3%. Through fine adjustment of V_{self} by varying the total flow rate, smooth walls of high anisotropy were etched with minimum trenching at the base of the walls and smooth etched surfaces.

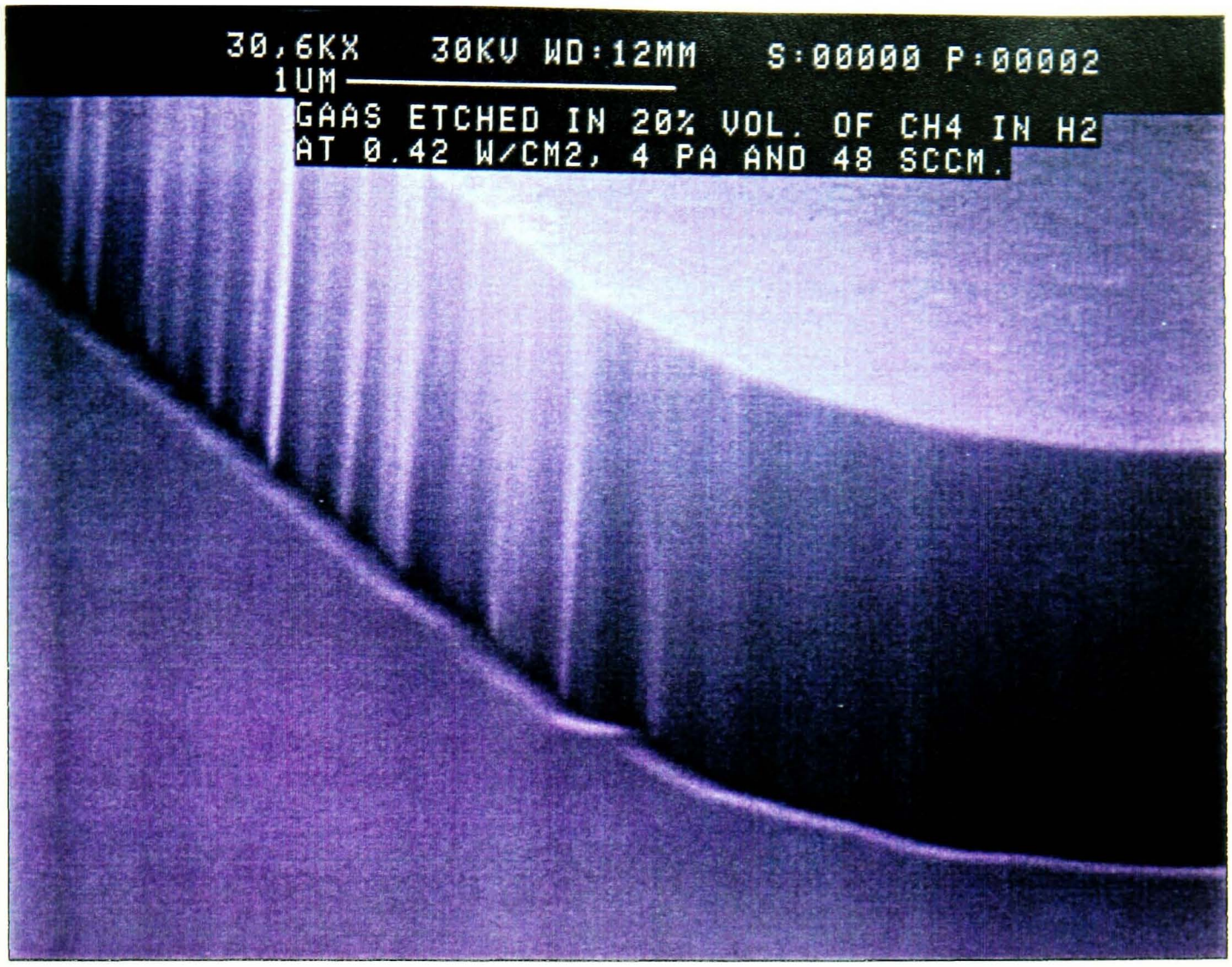

Picture 5.2. Micrographs of etched surfaces at total flow rate of 8.1 X 10^{-2} Pa m^3/sec. (Top) 20%, (bottom) 25% volume CH_4 concentration in H_2.

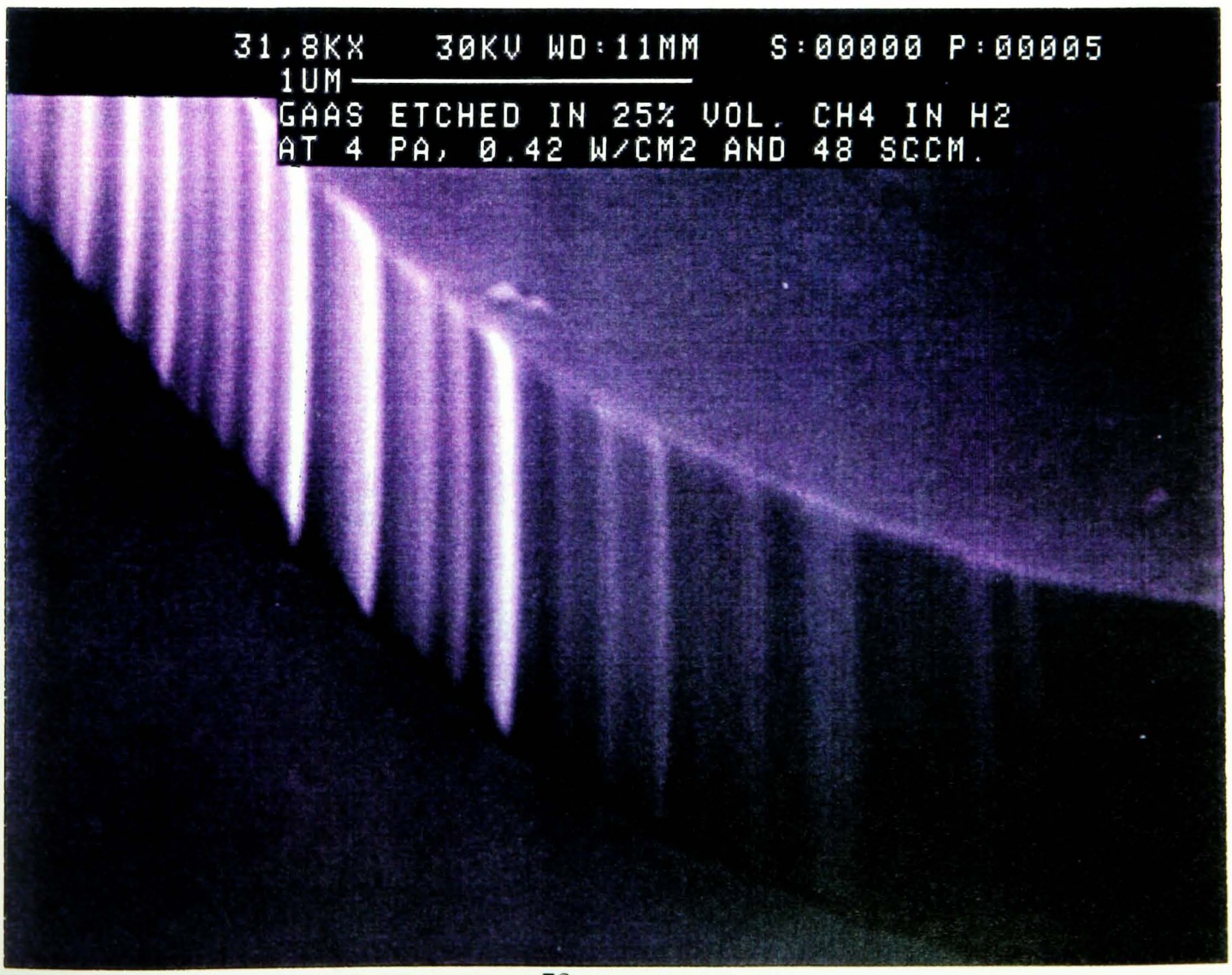

Figure 5.5 shows the graph of anisotropy against total flow rate. The anisotropy improved as the flow rate of the gas mixture increased to a limit determined by the pumping speed of the system. (See appendix I for the definition of x and y).

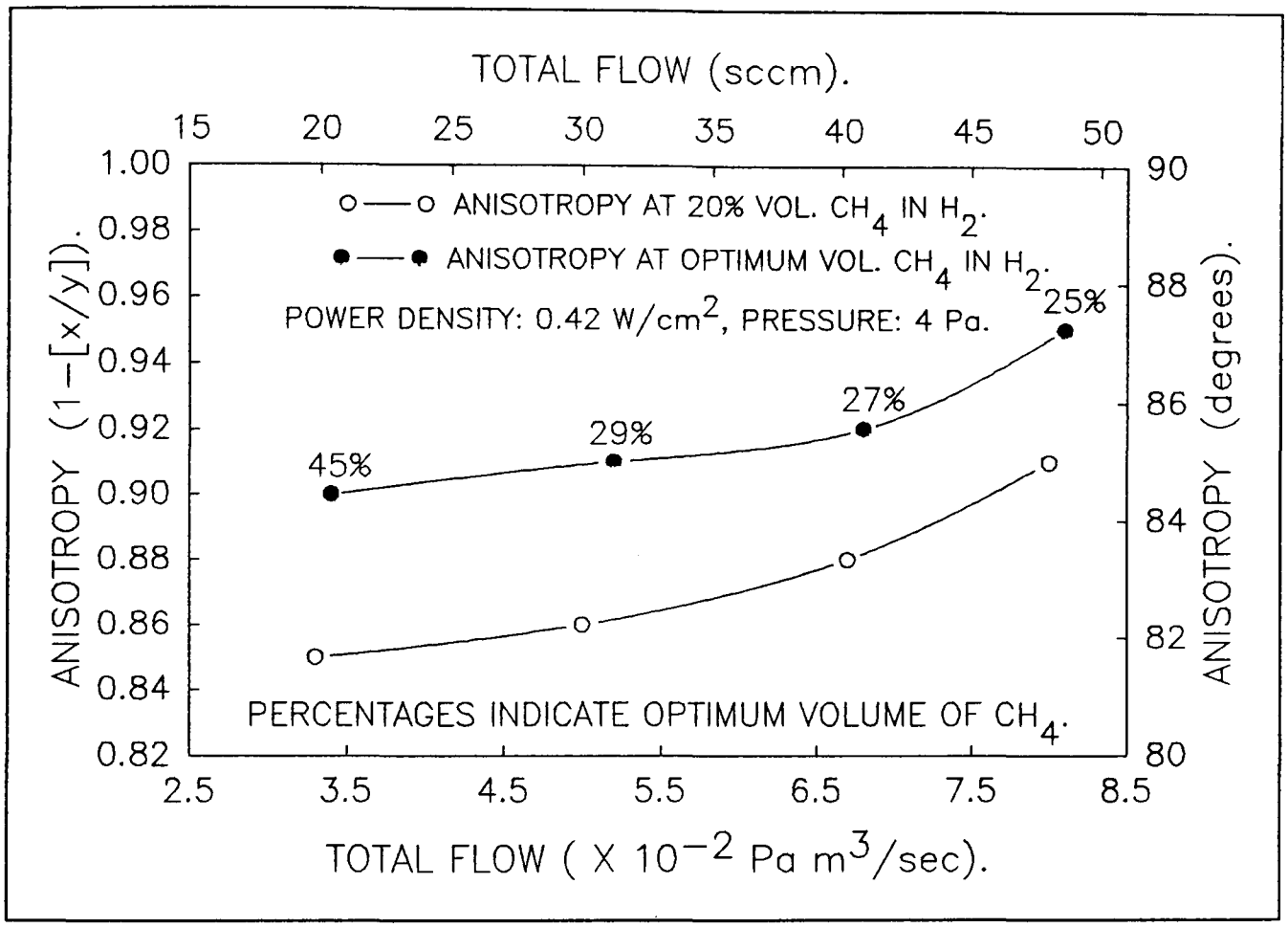

Figure 5.5. Graph of anisotropy against total flow rate.

5.3 Effect of power density and pressure

Experiments have also been performed at varying power densities and pressures. The total flow rate was kept constant at 8.1 X 10^{-2} Pa m^3/sec (48 sccm) and the volume of CH_4 concentration in H_2 was kept at 25%.

Figure 5.6 shows the graph of variation of etch rate against power density and pressure. Figure 5.6 (a) shows the variation of etch rate against power density at different pressures.

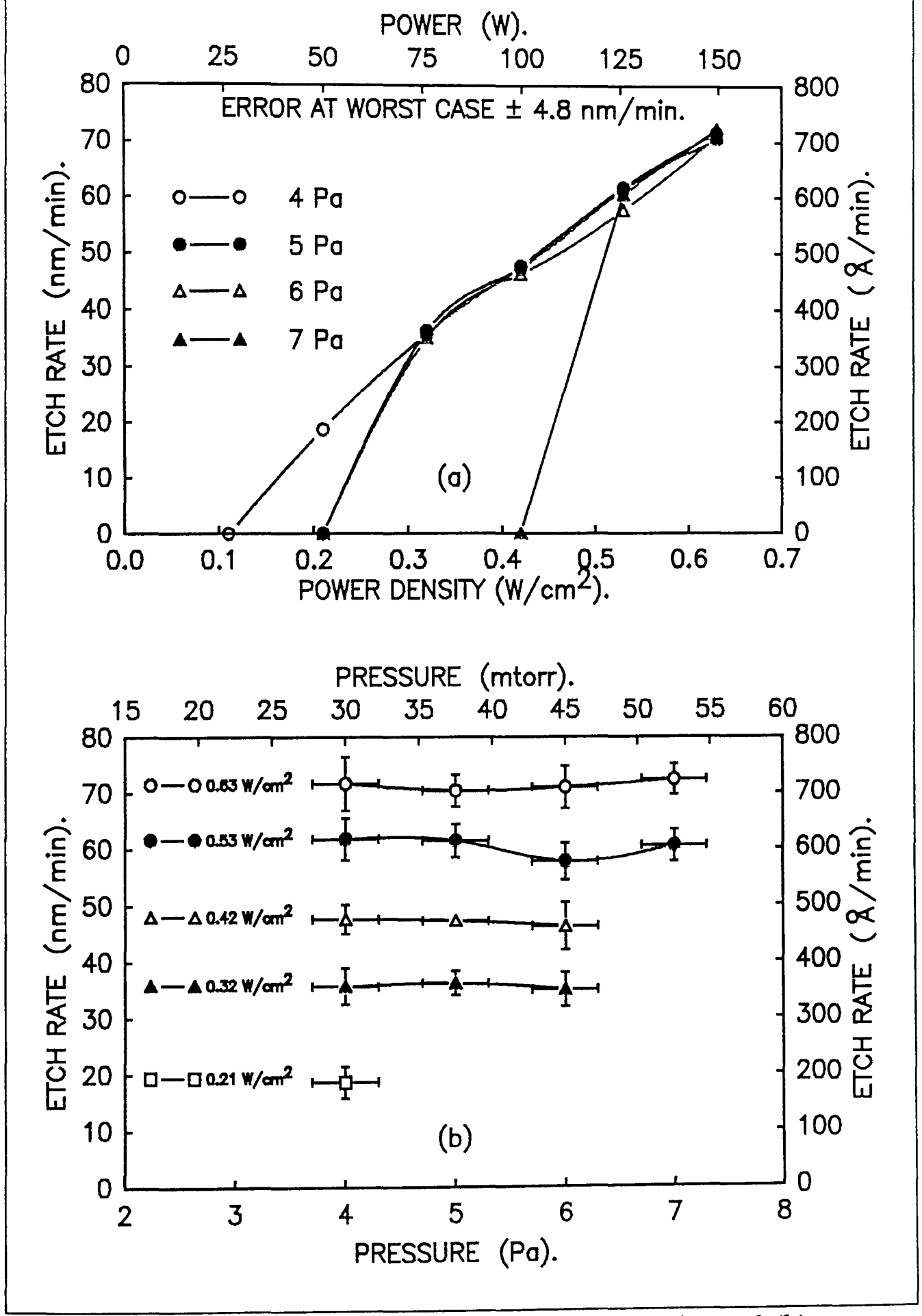

Figure 5.6. Graphs of etch rate against (a) power density and (b) pressure at a total flow rate of 8.1 X 10^{-2} Pa m^3/sec and 25% CH_4 concentration.

At 4 Pa (30 mtorr), carbon polymerization occurred at about 0.11 W/cm^2 which resulted in zero etching. As the power density was increased etching was initiated. The power density was increased to about 0.63 W/cm^2. The trend of the graph shows an increase in etch rate as the power density increased.

At 5 and 6 Pa (38 and 45 mtorr) carbon polymerization occurred at power densities of up to 0.21 W/cm^2. When the power density was increased further, etching commenced. At 7 Pa (53 mtorr) polymerization occurred up to about 0.42 W/cm^2. At higher power densities etching was initiated.

Figure 5.6 (b) shows the variation of etch rate against pressure. It can be seen that when etching occurred, increasing the pressure had no effect on etch rate. The etch rate remained constant within the limits of experimental errors. This was true for all operated power densities. A further increase in pressure (not shown in figure 5.6 (b)) caused carbon deposition.

Picture 5.3 shows the micrographs taken for the sample which was etched at low pressure of 4 Pa (30 mtorr) and high power density of 0.63 W/cm^2. The top picture shows the etched wall from one side. The good anisotropy achieved at about 0.42 W/cm^2 was lost at this power density. This was because of very strong ion back scattering from the surface of the sample. The bottom picture shows the base of the wall where a large trench is visible. This was caused by ions scattering from the side walls to the surface at the base of the wall (see figure 5.7).

Picture 5.4 shows the micrograph of the sample which was etched at the same power density as before but at the higher pressure of 7 Pa (53 mtorr). The same effects as before can be observed but generally there was a better anisotropy and less trenching at the base of the wall. This was because of a decrease in the intensity of ion bombardment due to increase in pressure.

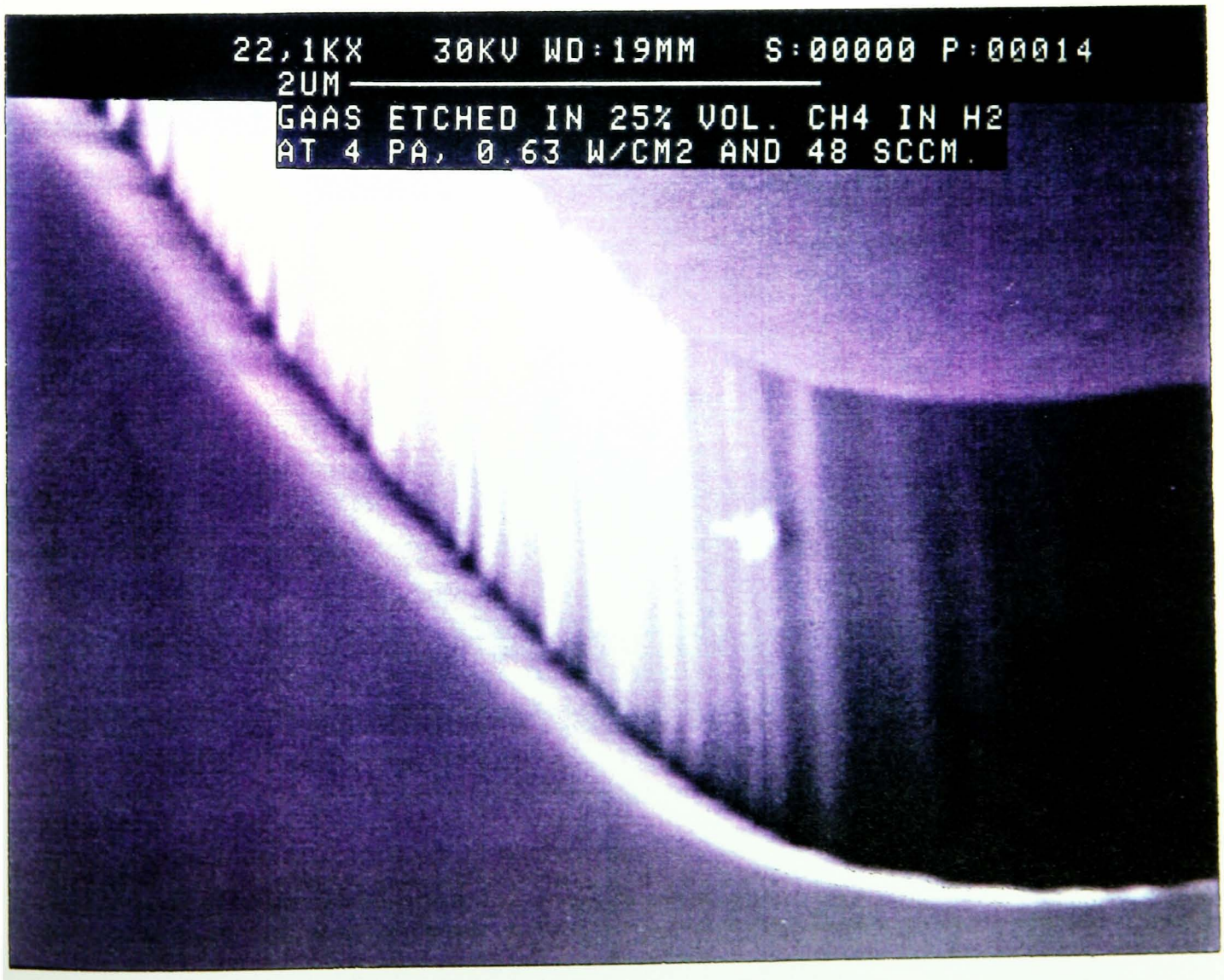

Picture 5.3. Micrographs of GaAs sample etched at low pressure and high power density. (Top) side view, (bottom) elevated view.

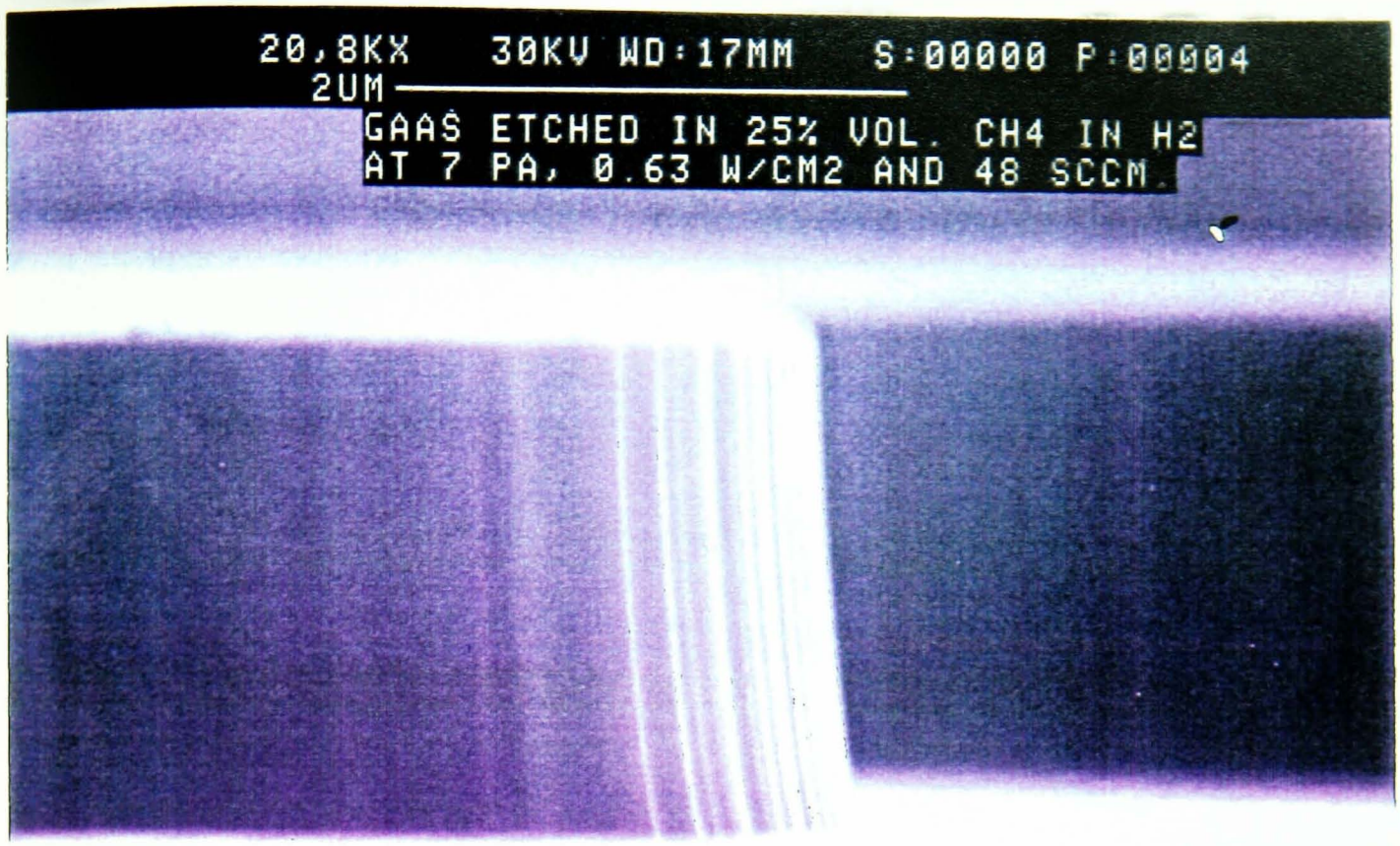

Picture 5.4. Micrographs of GaAs sample etched at high pressure and high power density. (Top) side view, (bottom) elevated view.

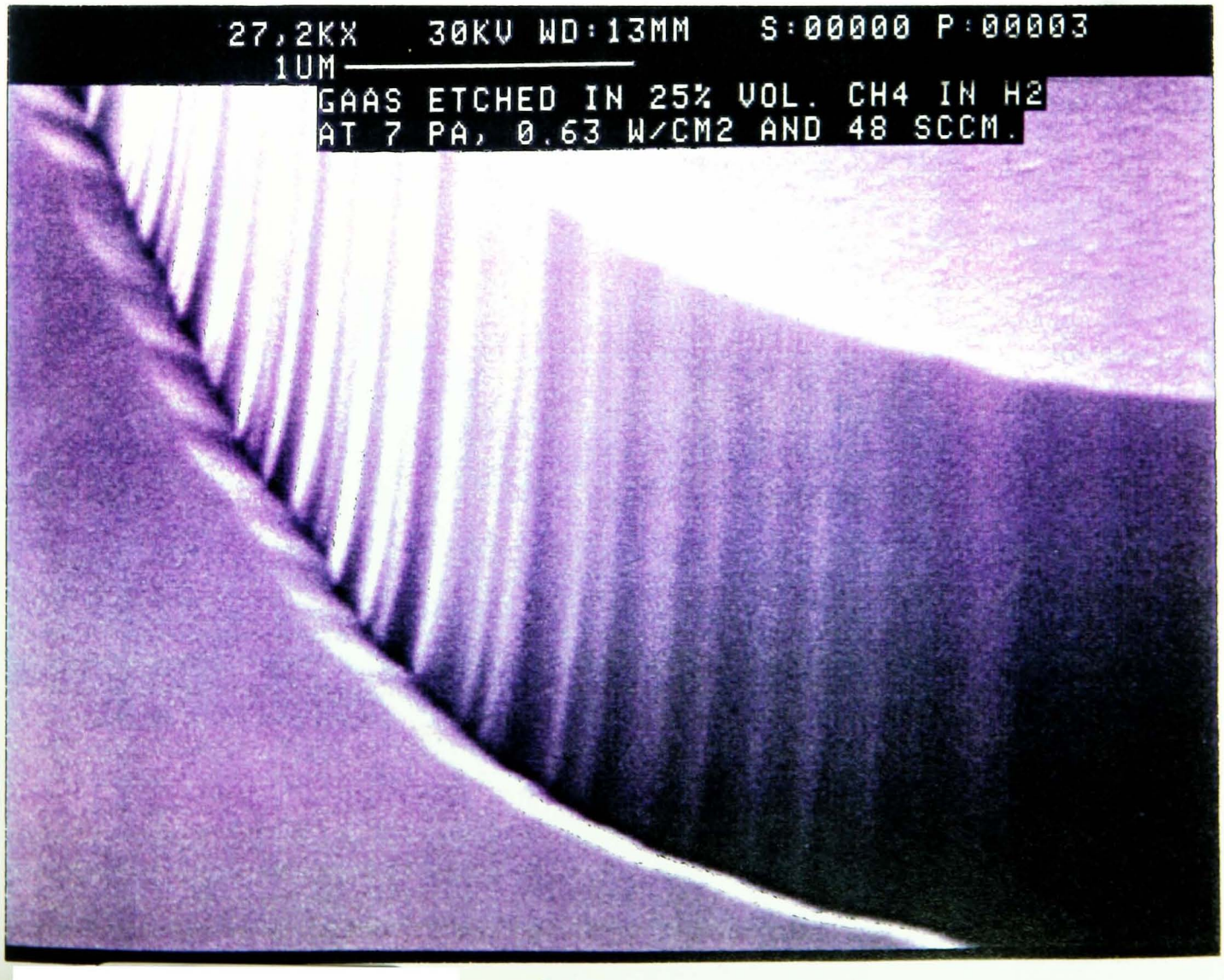

Picture 5.5. Micrographs of GaAs etched at low pressure and low power density. (Top) side view, (bottom) elevated view.

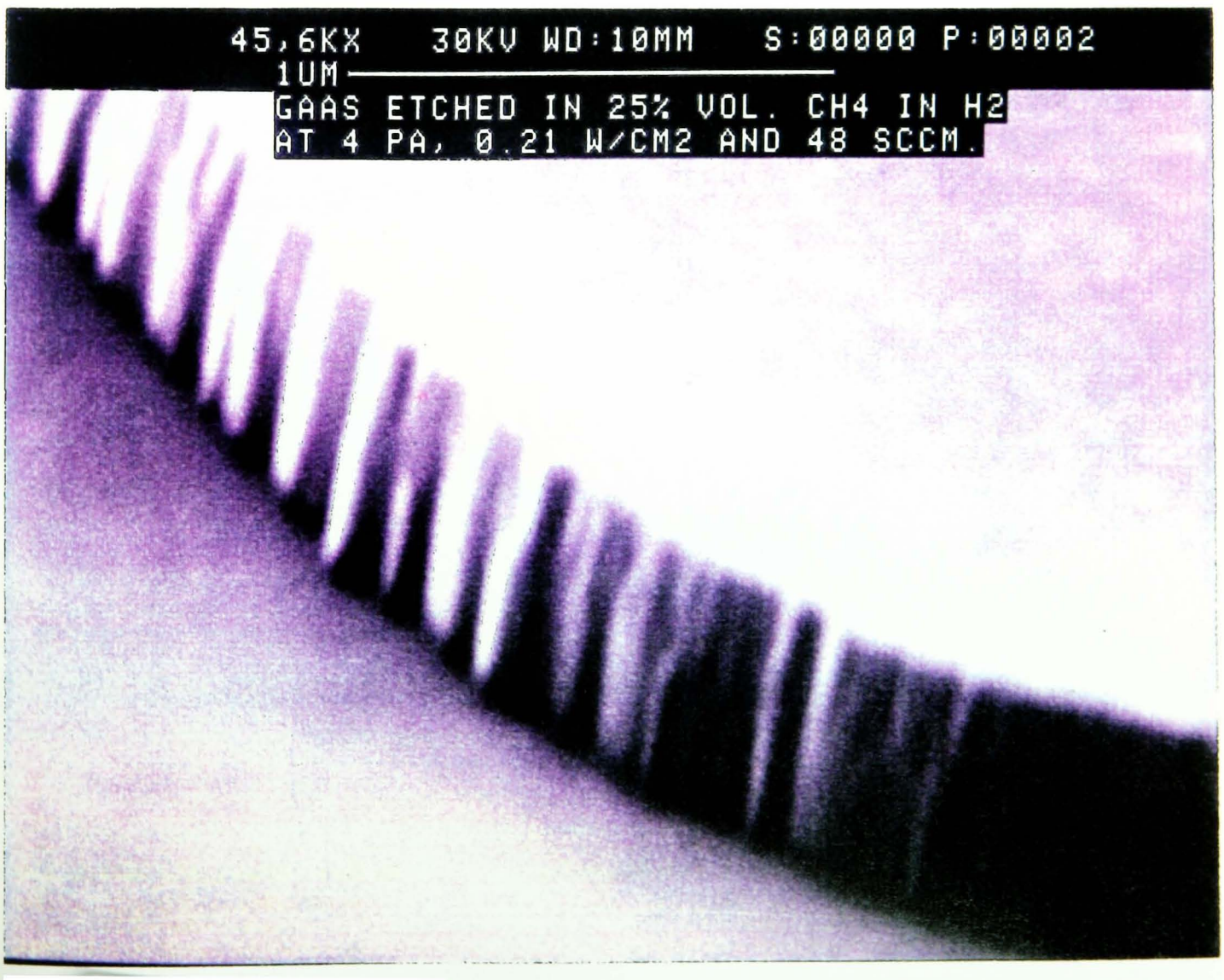

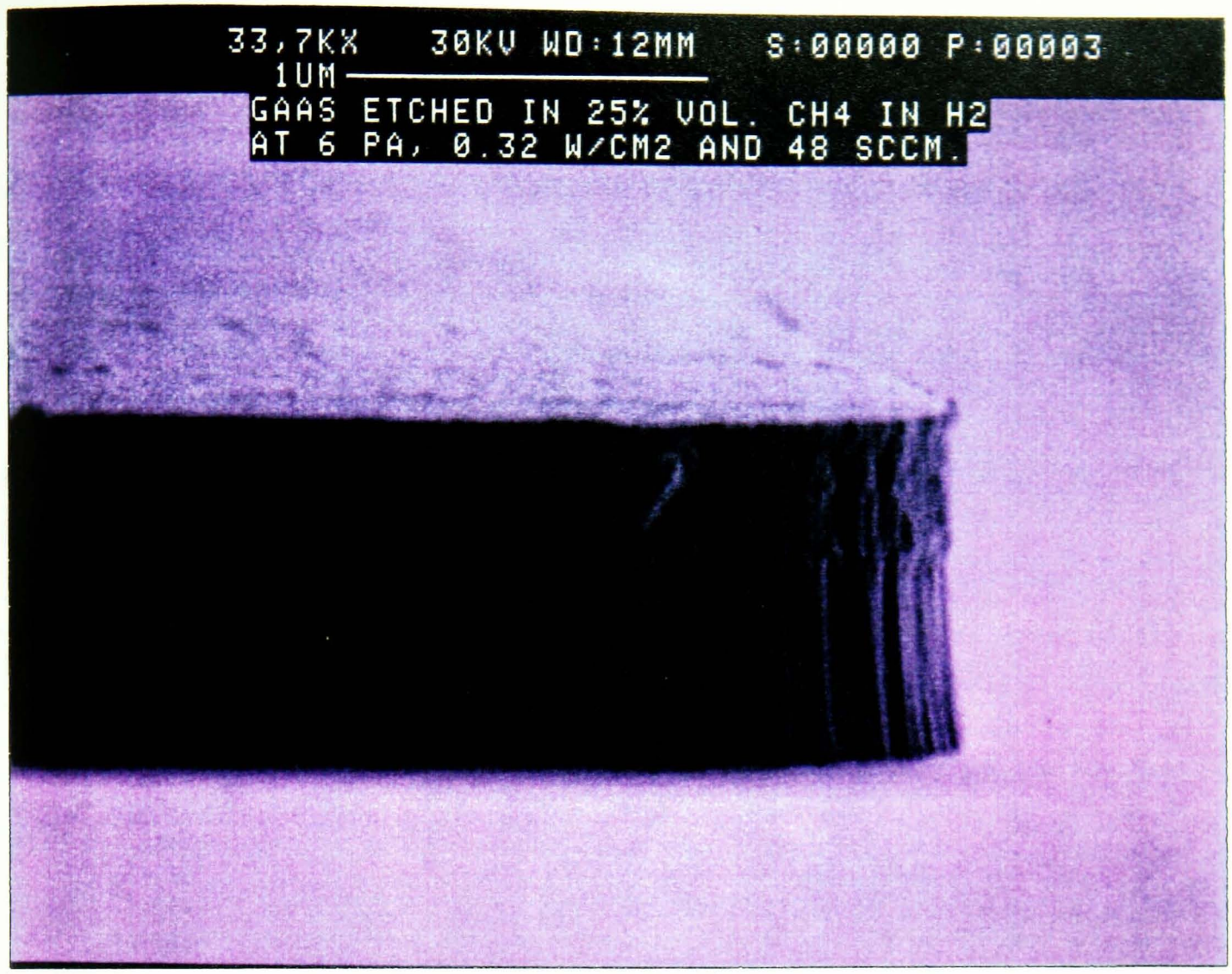

Picture 5.6. Micrographs of GaAs etched at high pressure and low power density. (Top) side view, (bottom) elevated view.

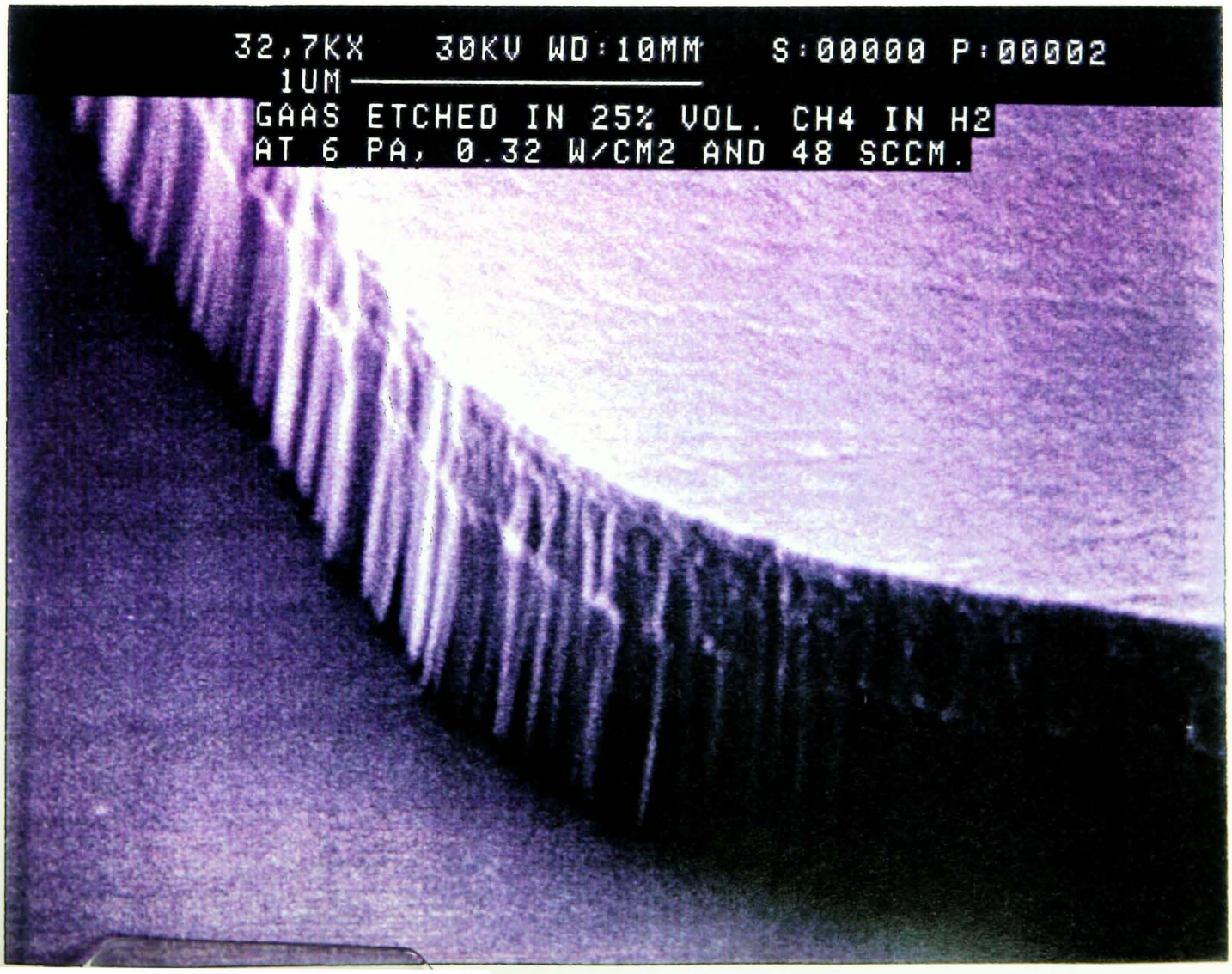

Picture 5.5 shows the micrographs of the samples etched at low pressure of 4 Pa (30 mtorr) and low power density of 0.21 W/cm^2. The wall shows reverse slope and a very high degree of roughness. This was due to a very low ion bombardment.

Picture 5.6 shows the micrographs of sample etched at high pressure of 6 Pa (45 mtorr) and low power density of 0.32 W/cm^2. Although there is no trenching present, there seems to be some re-deposition on the side walls at the top.

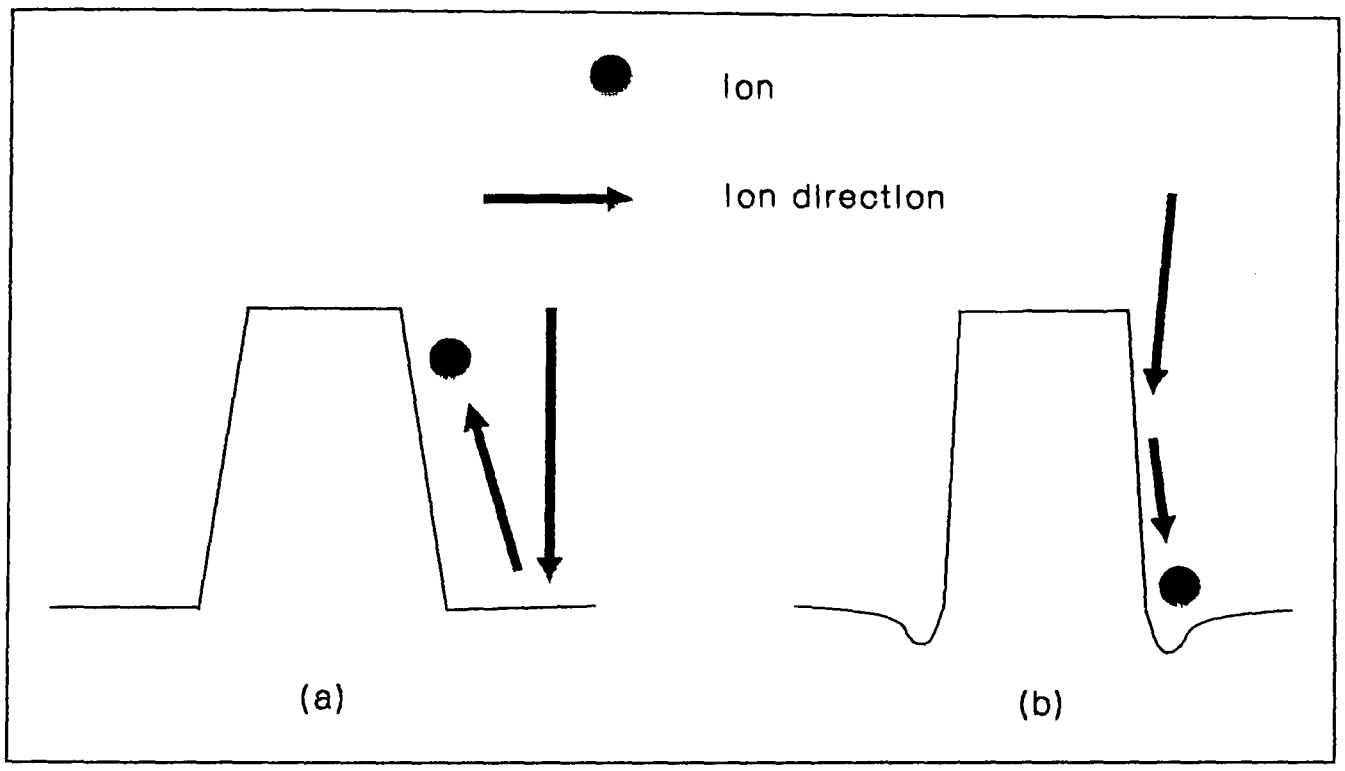

Figure 5.7. Diagram of ion bombardment. (a) Back scattering, (b) wall to surface scattering.

Figure 5.8 shows the variation of etch rate R and DC self bias voltage V_{self} as a function of power density and pressure. In figure 5.8 (a), The pressure and total flow rate were set to 4 Pa (30 mtorr) and 8.1 X 10^{-2} Pa m^3/sec respectively with 25% volume of CH_4 in H_2. R increased as the power density increased. At the same time V_{self} also increased. This indicates that ion bombardment was intensified when R increased. However it also indicates that at low power density of about 0.11 W/cm^2 where V_{self} was also at a low of -320 V, etching stopped and polymerization occurred.

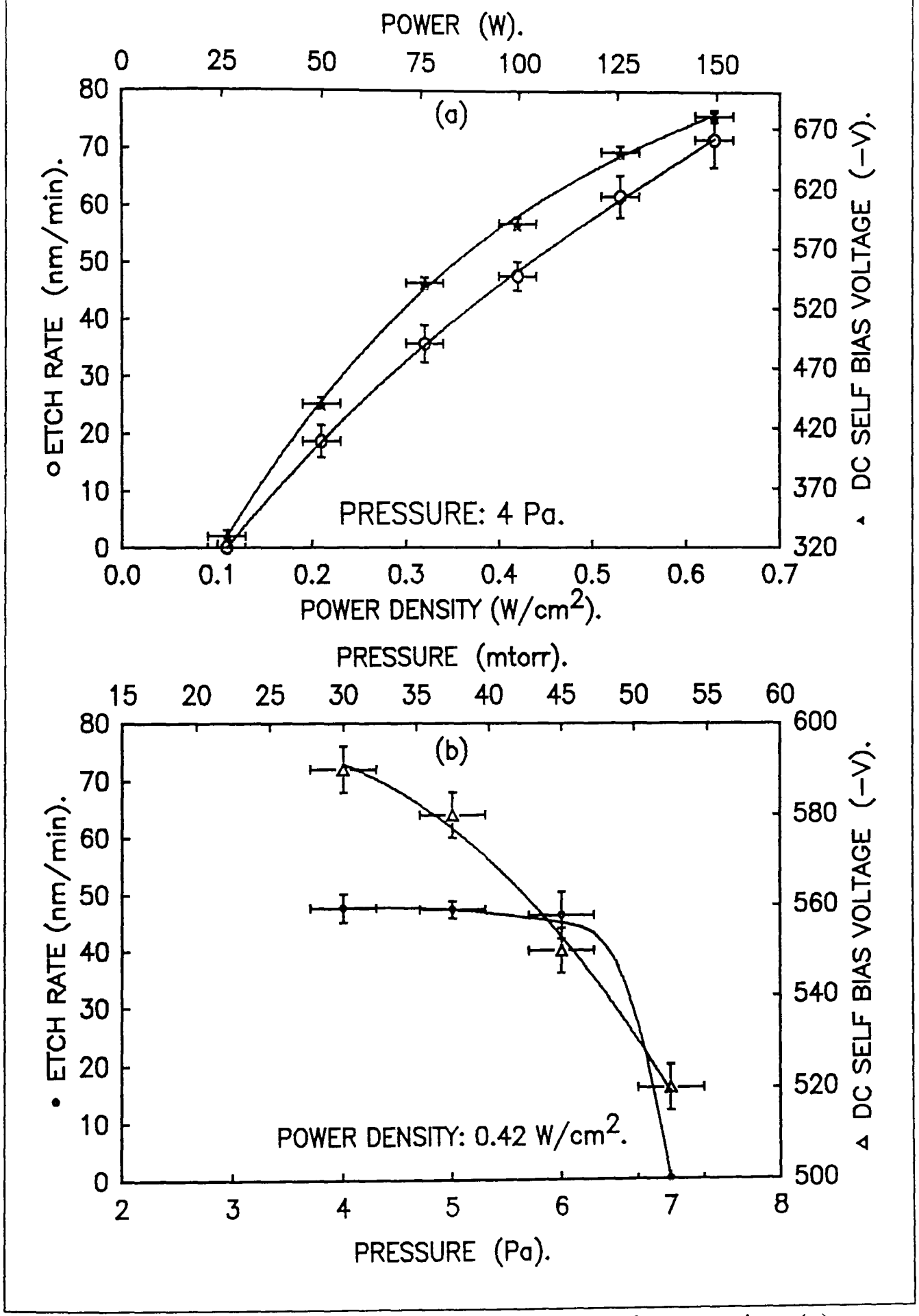

Figure 5.8. Graph of etch rate and DC self bias voltage against (a) power density and (b) pressure.

Figure 5.8 (b) shows the variation of R and V_{self} against pressure. The total flow rate and CH_4 concentration were set as before. The power density was set to 0.42 W/cm^2. The etch rate was constant with in the limits of experimental errors, between 4 to 6 Pa, (30 to 45 mtorr), but at 7 Pa (53 mtorr), carbon deposition occurred. Taking V_{self} into consideration, it is clear that as pressure increases V_{self} decreases and in this case at about -520 V deposition had occurred.

Figure 5.9 shows the graph of anisotropy against power density and pressure. Figure 5.9 (a) shows the anisotropy against power density. At about 0.42 W/cm^2 the best anisotropy was achieved for all set pressures between 4 to 7 Pa (30 to 53 mtorr).

At 4 pa (30 mtorr), anisotropy was at its worst at 0.21 W/cm^2. As the power density increased anisotropy also improved until at 0.42 W/cm^2 it was at an optimum value of about 0.95, or more than about 87°. However after the power density was further increased to 0.63 W/cm^2, the degree of anisotropy was reduced. The trend of the graphs at other pressures was similar except at 7 Pa where the anisotropy just decreased as power density increased. Figure 5.9 (b) shows the anisotropy against pressure. It shows the anisotropy was at its best at 0.42 W/cm^2. The anisotropy was poor at other power densities.

The linewidth of the etched surface was also measured. The linewidth of the SiO_2 mask on GaAs was measured to be about 9.2 μm before the CH_4/H_2 etching. Figure 5.10 shows the measured linewidth of the etched surface against power density and pressure. Figure 5.10 (a) shows the measured linewidth against power density. After etching at 4 Pa (30 mtorr) and 0.21 W/cm^2, the linewidth was less than that of the mask. As the power density increased the linewidth measured increased until at 0.42 W/cm^2 the linewidth was about the same as the mask. Further increases of the power density increased the linewidth further. Figure 5.10 (b) shows the linewidth

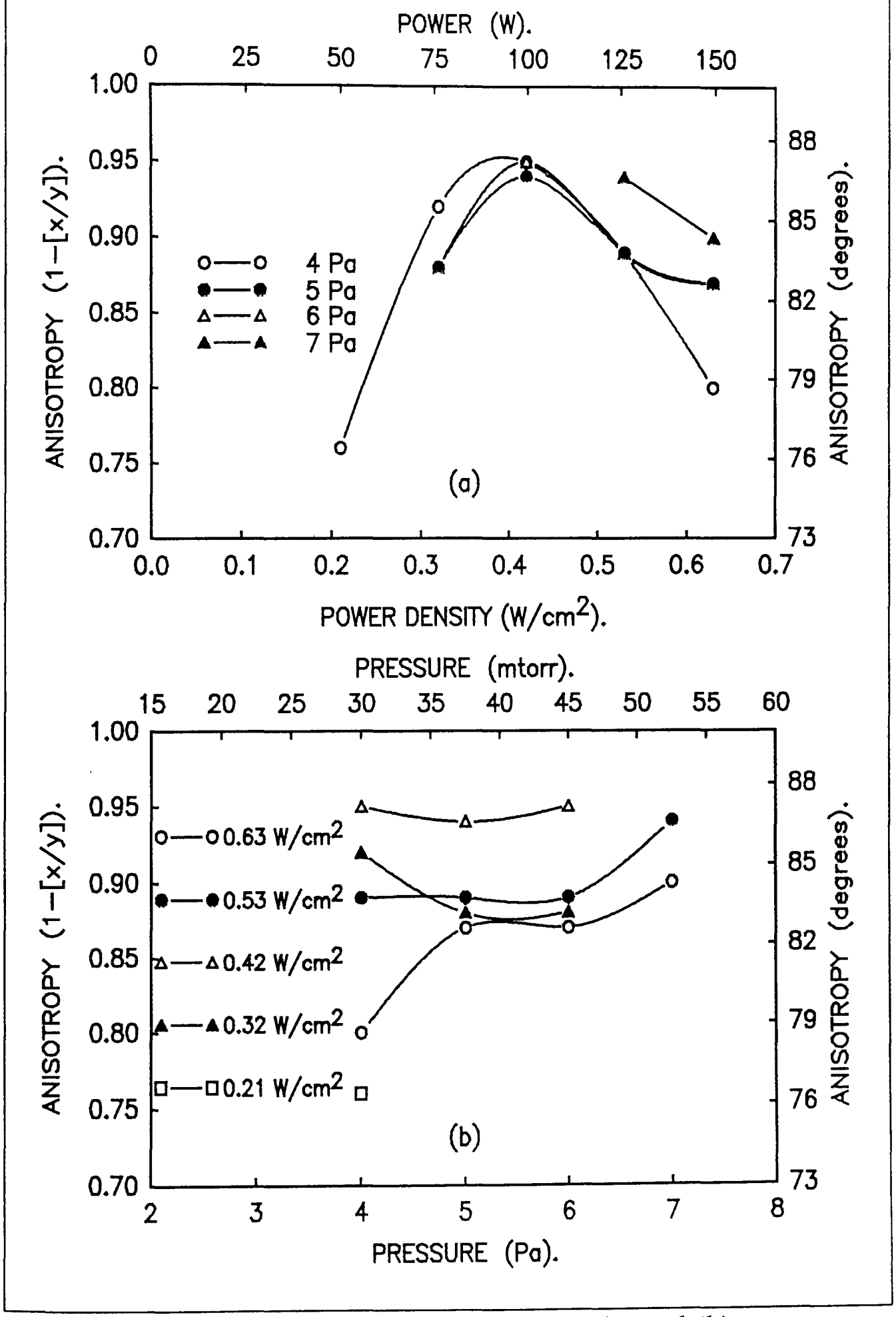

Figure 5.9. Anisotropy against (a) power density and (b) pressure.

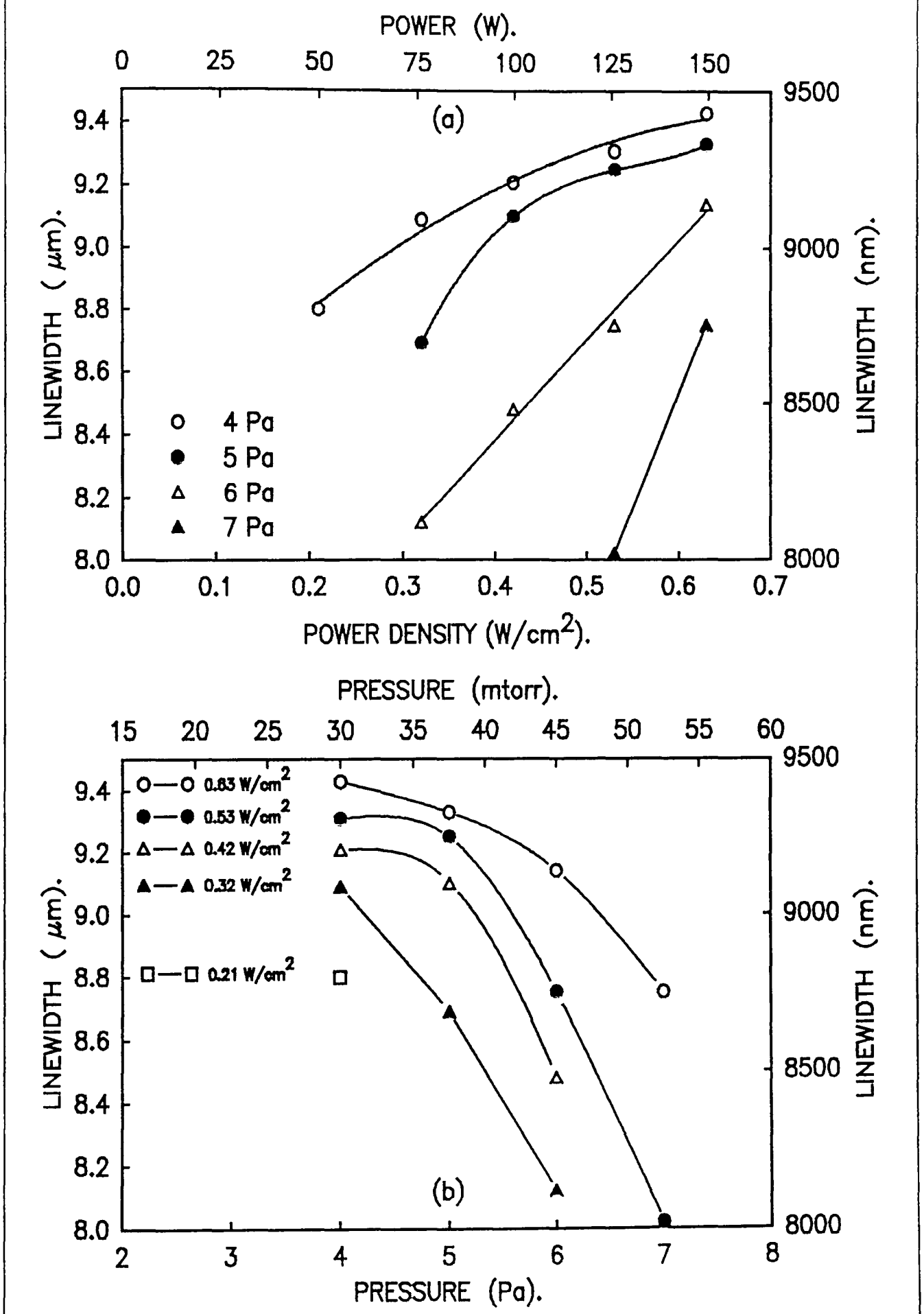

Figure 5.10. Linewidth against (a) power density and (b) pressure.

against pressure. Increase in pressure caused a decrease in the linewidth dimension of the etched sample. Only at 4 and 5 Pa (30 and 38 mtorr) and between 0.42 and 0.53 W/cm^2 was the linewidth dimension produced at the pre-etched mask dimension.

5.4 Carbon polymer deposition

One effect of using methane and hydrogen mixtures was the deposition of carbon polymers on the surface of mask and side walls, as discussed in chapter 2. The deposition of carbon polymers on the mask can protect it against further etching no matter how long the process continued. The greater the time of etching, the thicker the protective carbon polymer layer deposited on the mask.

In this section the deposition rate of the carbon polymers on the surface of the mask is shown. First the effect of the volume concentration of methane in hydrogen and total flow rate of the gas mixture is presented. Next the consequence of power density and pressure is demonstrated and finally the proof of deposition of carbon polymers on the surface of mask is confirmed.

The carbon polymer deposition rate on the mask was measured for different CH_4 concentrations at different total flow rates. The process variables such as power density and pressure were set to 0.42 W/cm^2 and 4 Pa (30 mtorr) respectively.

Figure 5.11 shows the graphs of carbon deposition rate D, and thickness of mask removed when etched $t_{E\text{-}mask}$, against the volume CH_4 concentration in H_2 at different total flow rates. The mask etch rate was not represented because the etching of mask took place for a short time at the beginning of the process. This is due to the carbon polymerization of the surface, which protected the mask. Therefore etching of the mask did not take place for the

whole 30 minutes of the process.

Figure 5.11 (a) is shows the variation of D and $t_{E\text{-}mask}$ against CH_4 concentration at a total flow rate of 3.4 X 10^{-2} Pa m^3/sec, (20 sccm). As the volume of methane concentration increased, The carbon deposition rate also increased. At 50% volume of CH_4, D was about 10 nm/min but $t_{E\text{-}mask}$ was about 15 nm.

The trends of figure 5.11 (b), (c) and (d) were similar to those of (a). At the optimum total flow rate for etching GaAs, (8.1 X 10^{-2} Pa m^3/sec, [48 sccm]), at 30% volume concentration of CH_4, D was about 8 nm/min. but $t_{E\text{-}mask}$ was about 5 nm. At the optimum concentration of 25% volume of CH_4, D was over 7 nm/min and $t_{E\text{-}mask}$ was just under 10 nm.

In terms of solving engineering problems of etching III-V compounds, this shows a very good potential for mask protection. The results showed that at optimum conditions only a very small depth of mask was etched away because of carbon polymerization. Also RIE of III-V compound semiconductors could continue for a very long time.

For the next set of experiments the total flow was set to 8.1 X 10^{-2} Pa m^3/sec, (48 sccm), with 25% volume of CH_4 in H_2. Figure 5.12 shows the variation of carbon deposition against power density and pressure.

Figure 5.12 (a) shows the change in deposition rate D against power density. As the power density was increased the value of D decreased. This was repeated through out the set pressure from 4 to 7 Pa, (30 to 53 mtorr). Figure 5.12 (b) shows the change in D against pressure. As the pressure increased D also increased.

The variation of the mask thickness etched $t_{E\text{-}mask}$ against power density and pressure is presented in figure 5.13. The change in $t_{E\text{-}mask}$ against power

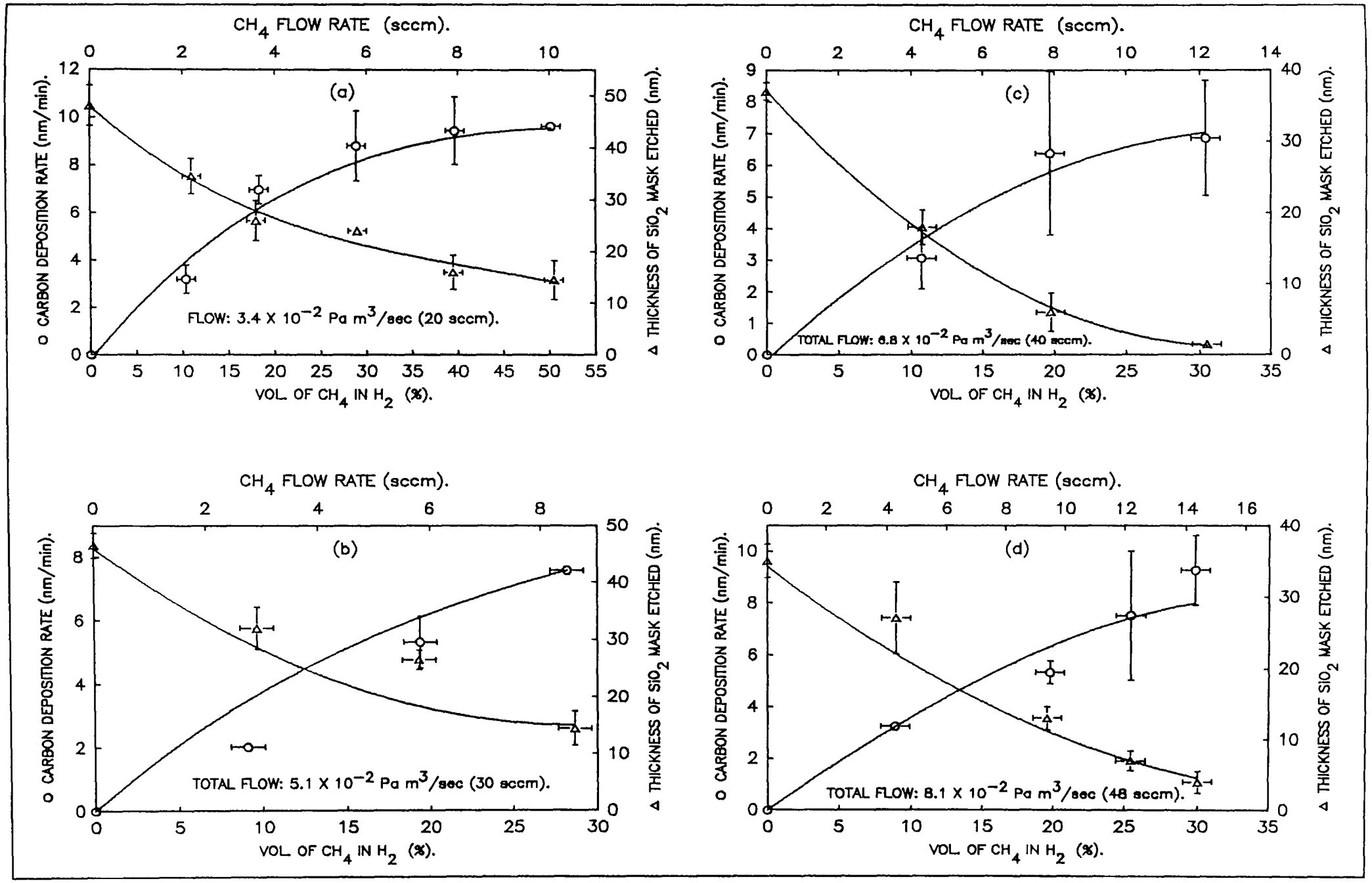

Figure 5.11. Graphs of carbon deposition rate and mask thickness etched against volume CH_4 concentration in H_2 at different total flow rates at 0.42 W/cm^2 and 4 Pa. (a) 3.4 X 10^{-2}, (b) 5.1 X 10^{-2}, (c) 6.8 X 10^{-2} and (d) 8.1 X 10^{-2} Pa m^3/sec.

density is presented in figure 5.13 (a). When the power density increased the $t_{E\text{-}mask}$ increased. This was because of the intense ion bombardment which removed some of the SiO_2 mask which was vulnerable before carbon polymer protection layers were deposited on the surface. The higher the set power density, the faster the mask was removed from the surface at the beginning of the process. Figure 5.13 (b) shows the effect of pressure on $t_{E\text{-}mask}$. As the pressure increased $t_{E\text{-}mask}$ decreases. This is because of the fast polymerization of the surface as the density of carbon species in the chamber increases. The higher the pressure, the higher the carbon polymerization on the surface.

Figures 5.14 and 5.15 show the EDX analysis of the surface of the GaAs samples. The electron accelerating voltage was set to a minimum of 6 KV. Figure 5.14 represents the analysis of the GaAs samples etched at power density, pressure and total flow rate of 0.42 W/cm^2, 4 Pa (30 mtorr) and 3.4 X 10^{-2} Pa m^3/sec, (20 sccm) respectively.

In all the graphs of figure 5.14, the peaks of gallium Ga, arsenic As and gold Au were expected. The Ga and As peaks existed because of the GaAs sample which was etched and Au peak existed because the sample was coated with gold so the electron beam would not charge and ultimately diverge from the surface.

Figure 5.14 (a) shows the unetched GaAs sample used as standard. Figure 5.14 (b) and (C) and (d) were the samples for which etching at 20%, 40% and 60% CH_4 volume concentration in H_2 was attempted. The samples represented in figures 5.14 (b) and (c) were etched successfully but polymerization occurred on the sample represented in figure 5.14 (d).

The surfaces of samples presented in figure 5.14 (b) and (c) were exposed to O_2 plasma after CH_4/H_2 RIE to remove the film from the mask but sample (d) was not exposed to the O_2 plasma because polymerization

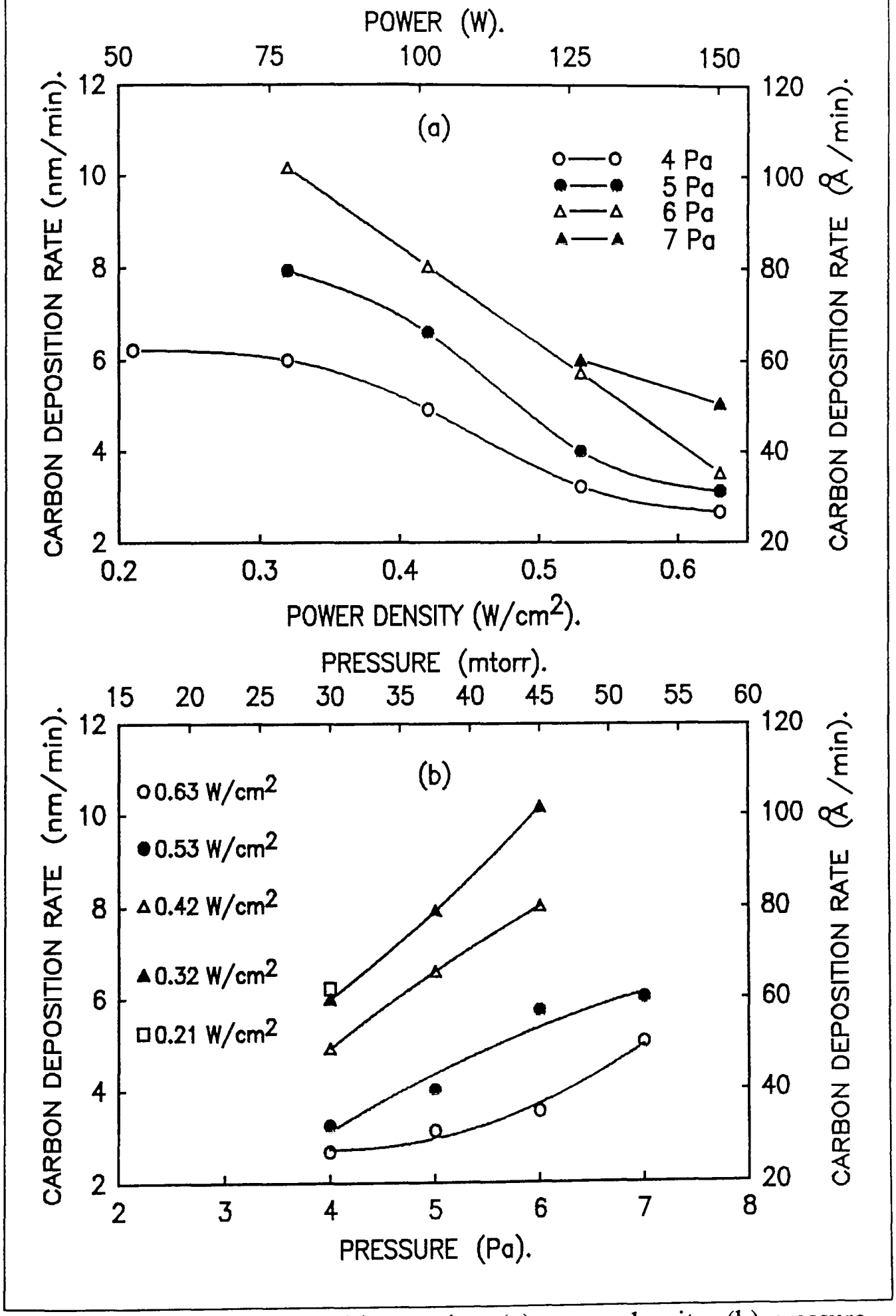

Figure 5.12. Carbon deposition against (a) power density, (b) pressure.

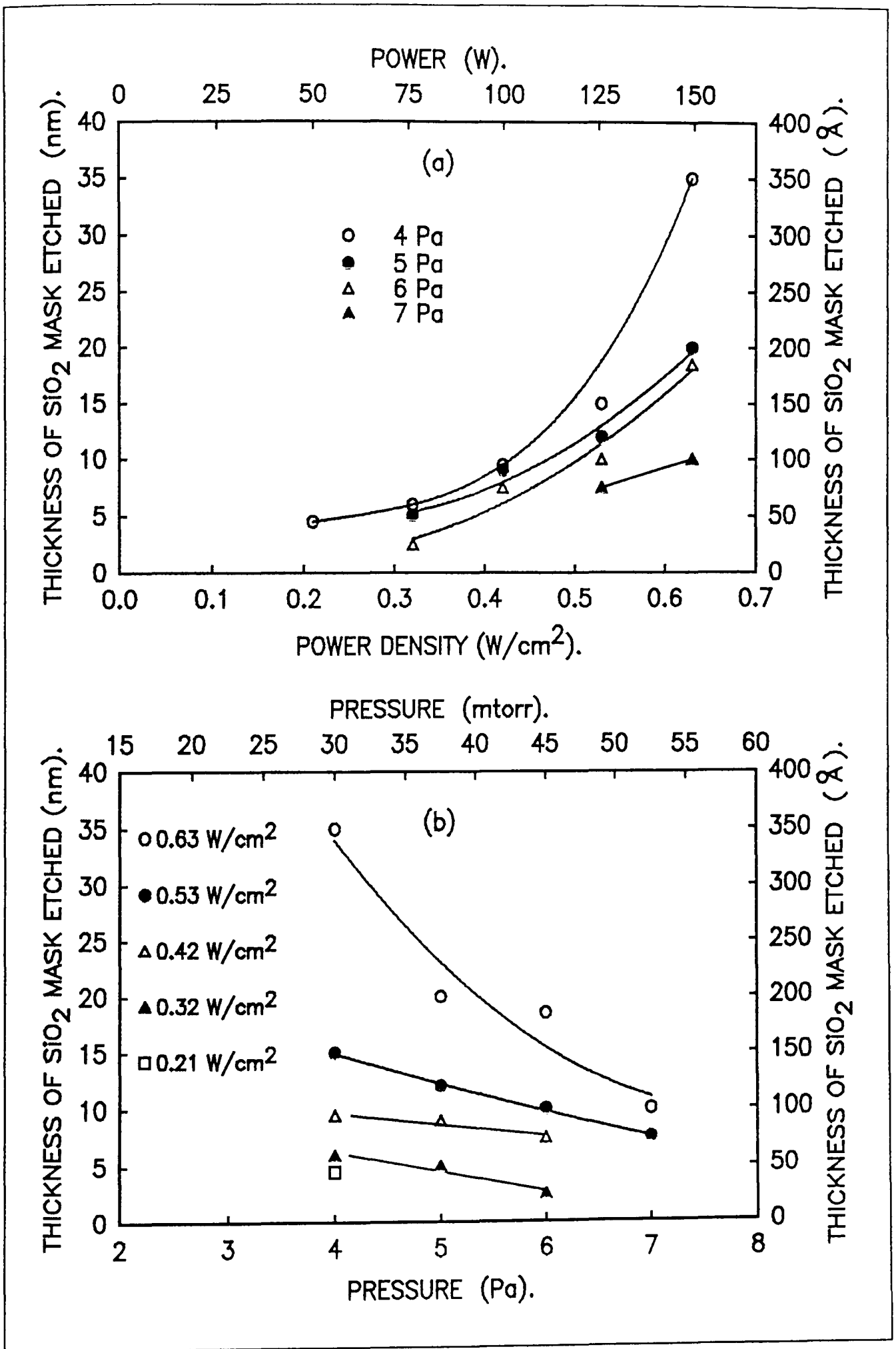

Figure 5.13. Mask etched against (a) power density, (b) pressure.

occurred not only on the mask but also on the surface of GaAs. Furthermore samples presented in figure 5.14 (b) and (c) were bathed in 5% HF solution to remove the SiO_2 mask.

In all graphs there were two unexpected peaks. They were carbon C and oxygen O. The standard represented by figure 5.14 (a) was exposed only to air and so this could be due to exposure to ambient atmosphere. The processed samples which are represented by figure 5.14 (b) and (c) show the same peaks as the standard and they have the same intensity. Figure 5.14 (d) shows a very intense carbon peak which dominates the graph. It indicates that the film which was deposited was carbon based.

The EDX system could not detect any element lighter than boron B, so the existence of hydrogen in the polymer film could not be confirmed. The literature has been consulted for exact diagnostics of the deposited film on the surface, and is discussed in chapter 7.

Figure 5.15 shows the EDX analysis of a GaAs standard and a sample etched at the same conditions as before but at optimum flow of 8.1 X 10^{-2} Pa m^3/sec, (48 sccm) and 25% volume CH_4 in H_2. Figure 5.15 (a) shows the EDX characteristics of the standard. Figures 5.15 (b) and (c) show the characteristics of the etched surface and the mask respectively. The etched GaAs sample was not exposed to the O_2 plasma or 5% HF solution. The EDX conditions were the same as before.

Figure 5.15 (b) shows the surface of the etched GaAs sample. The peaks are the same as before except for an extra peak between As and Au which is silicon Si. This should not be present for the etched surface analysis. The reason for presence of this small peak is the fact that the RIE system was used for Si, SiO_2 and Si_3N_4,etching as well. It was then possible for the GaAs sample to have been contaminated. The Si peak which is present is therefore judged to be due to contamination from the RIE chamber.

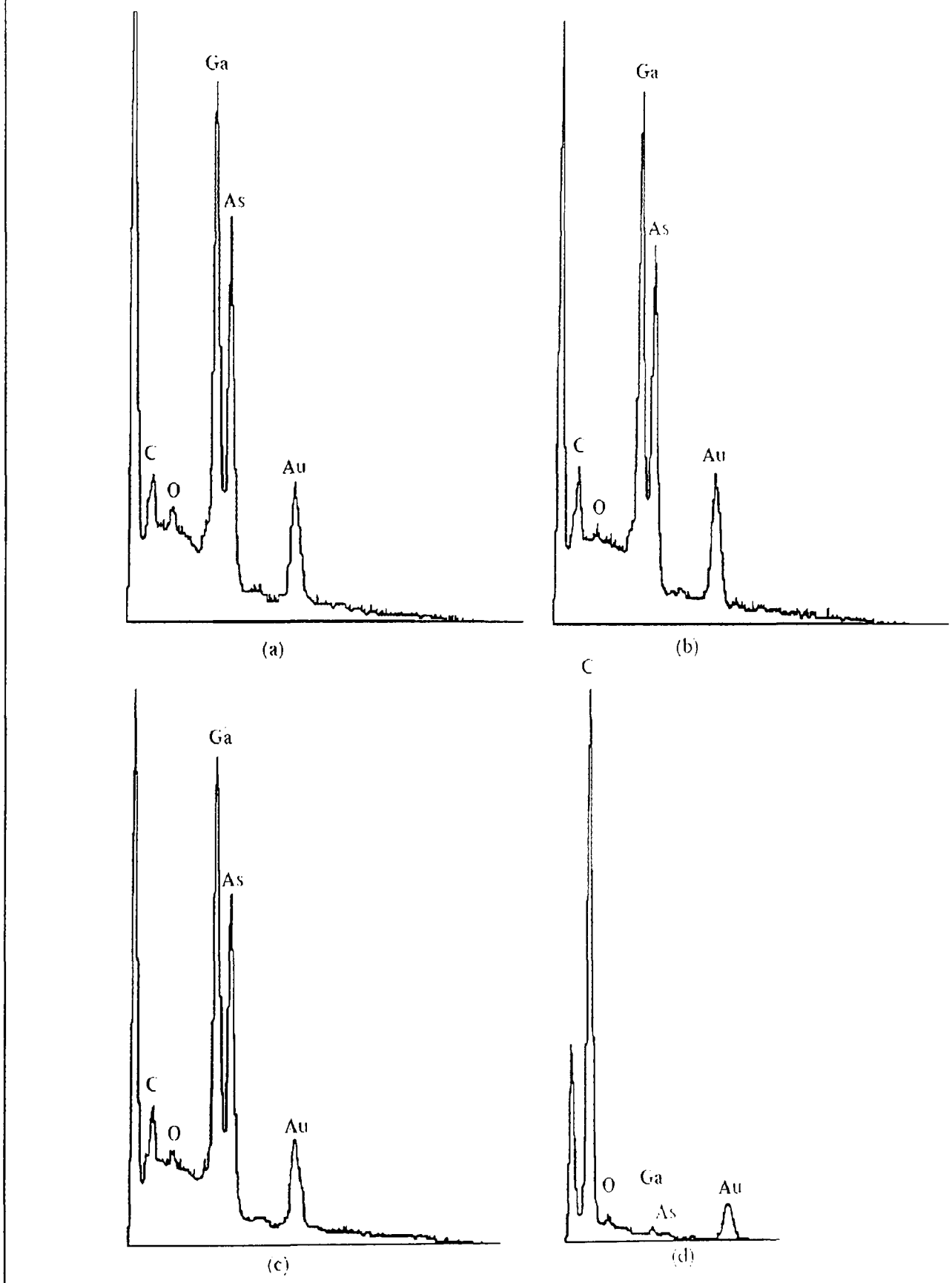

Figure 5.14. EDX analysis of GaAs samples. (a) Standard, (b) 20% CH_4, (c) 40% CH_4 and (d) 60% CH_4 volume concentration.

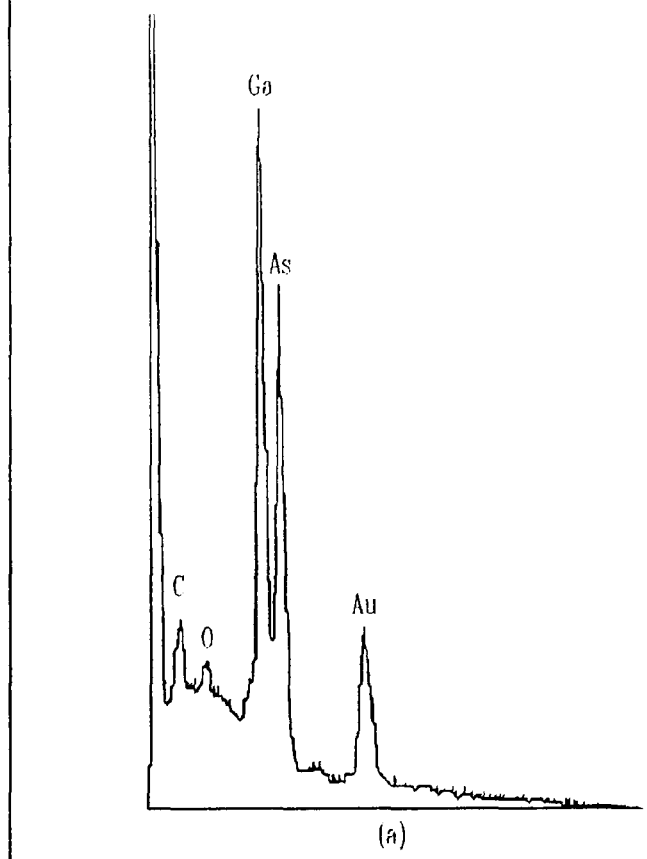

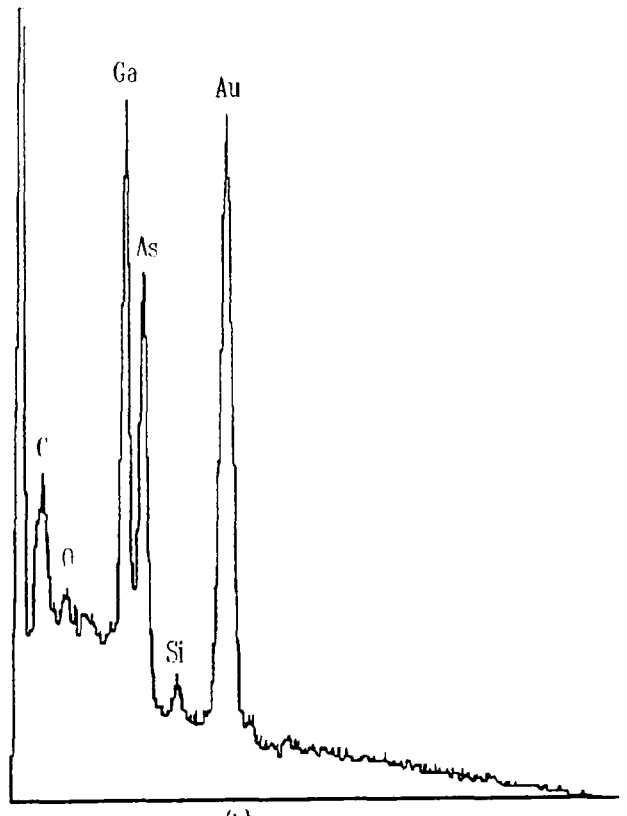

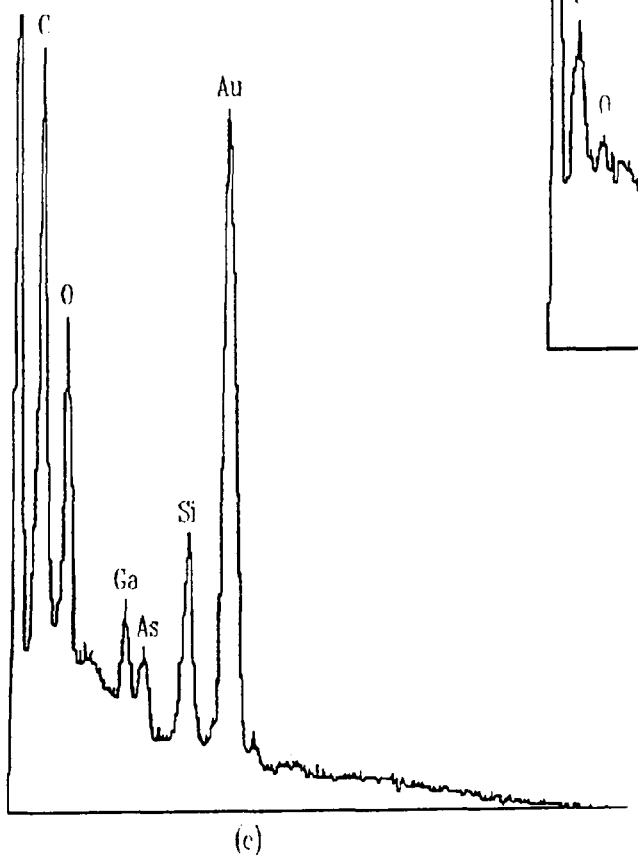

Figure 5.15. EDX analysis of GaAs samples. (a) Standard, (b) etched surface, (c) SiO_2 mask.

The carbon peak also looks larger compared to that of the standard. This was perhaps due to the carbon monolayer present on the sample just before the production of the volatile species. The difference between this and the standard was the fact that this sample was not exposed to O_2 plasma.

Figure 5.15 (c) shows the EDX analysis of the top of the mask which was not etched. There are large C, O and Si peaks. Si and O peaks are present due to the SiO_2 mask. The C peak is large because of the deposition of carbon polymers on the surface of the mask. The Au peaks on figure 5.15 (b) and (c) are larger than that shown in the figure 5.14 because a thicker gold coat was deposited on the surfaces of these samples.

5.5 AlGaAs etching

The optimum conditions to etch 25 mm^2 GaAs samples were found to be at power density, pressure, total flow rate and CH_4 volume concentration of 0.42 W/cm^2, 4 Pa (30 mtorr), 8.1 X 10^{-2} Pa m^3/sec (48 sccm) and 25% CH_4 volume concentration in H_2, respectively. These parameters represented the optimum residence time and DC self bias voltage. All further experiments were conducted at these values unless otherwise mentioned.

The effect of aluminum content in GaAs is discussed here. The experiment was performed on samples of $Al_xGa_{1-x}As$, where the Al contents were x= 0.1, 0.2, 0.3 and 0.5. For this experiment each wafer was cut into two 25 mm^2 samples. One was masked with SiO_2 and the other with Si_3N_4. The procedures were explained in chapter three. The samples were then etched together. This was performed in order to find the AlGaAs etch rate and also to investigate the effect of the different mask materials on AlGaAs during processing. It was claimed that the AlGaAs samples which were masked with Si_3N_4 etched more quickly*.

---

* - Private communication with Dr. Alan Webb, GEC-Marconi, Caswell.

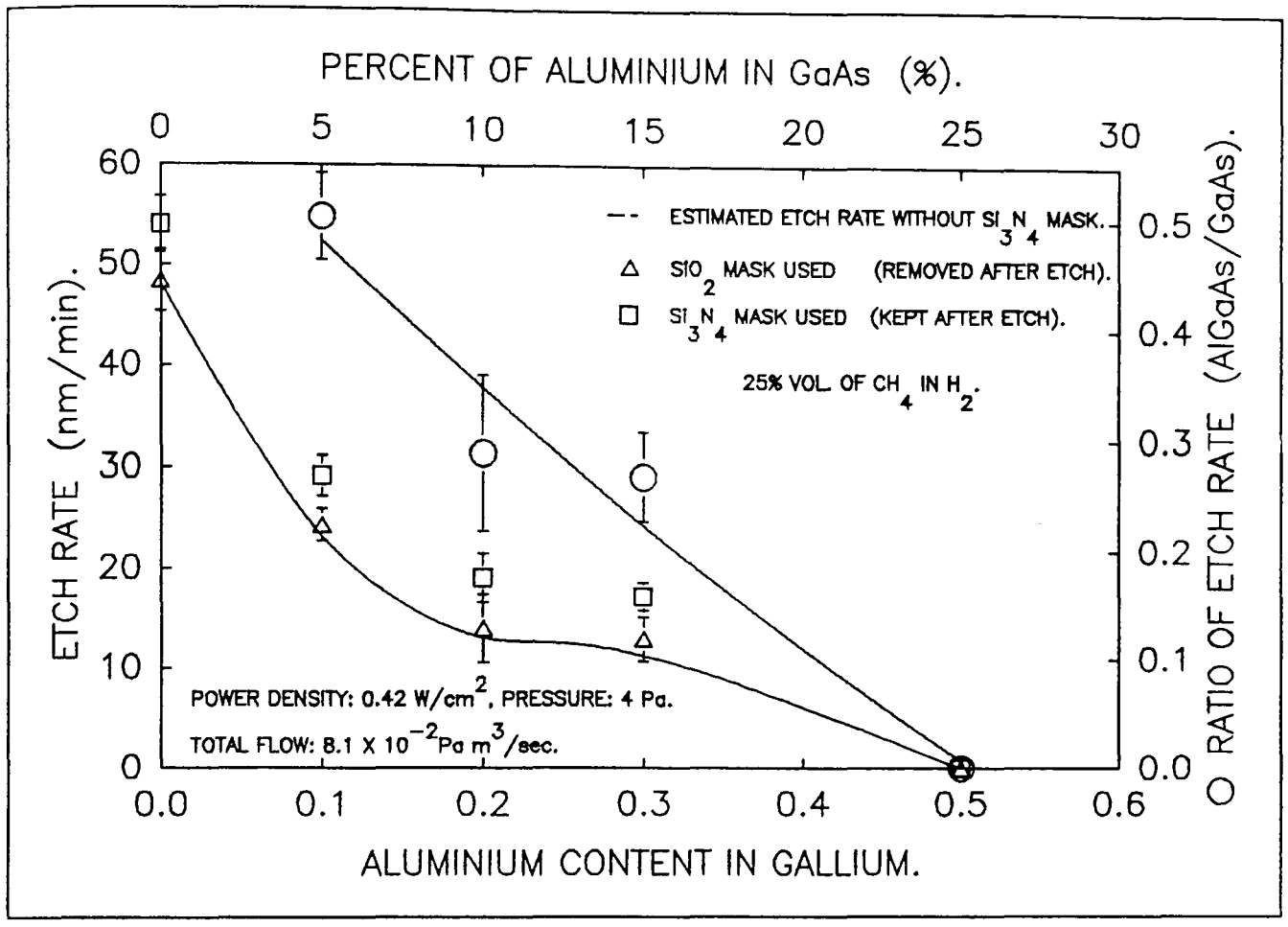

Figure 5.16. Graph of etch rate and etch ratio of AlGaAs against Al content in Ga.

Figure 5.16 shows the graph of etch rate R and ratio of etch rate of GaAs to AlGaAs (AlGaAs/GaAs) against the aluminum content in gallium. The depth of the samples etched with SiO_2 mask was measured after exposure to O_2 plasma to remove the carbon polymers from the surface and removal of the mask in 5% HF solution.

The samples etched with the Si_3N_4 mask were also exposed to O_2 plasma to remove the carbon polymers but the Si_3N_4 mask was not removed. Wet etching of Si_3N_4 in phosphoric acid at elevated temperatures or HF solution would also have dissolved the Al content of the GaAs.

The actual etch rate of the AlGaAs samples with the Si_3N_4 mask was estimated from the results found for the SiO_2 mask removal. The trend of the graph shows a reduction in etch rate as the Al content x increased. This was true for both SiO_2 and Si_3N_4 masks.

At x=0 (i.e. GaAs only), the etch rate was about 50 nm/min. At x=0.1 (i.e. 5% Al in GaAs), the etch rate had dropped by about 50% to 25 nm/min. At x=0.5 (i.e. 25% Al in GaAs) the etch rate was zero and carbon polymerization occurred on the surface of the samples.

The results for etched samples which were masked with Si_3N_4 were similar to the samples which were masked with SiO_2. The difference was the thickness of the Si_3N_4 mask which was not removed. The line through open triangle symbol in figure 5.16 shows the estimated etch rate of AlGaAs with Si_3N_4 mask and the etch rate is the same for SiO_2 mask. The ratio of etch rate of AlGaAs to GaAs (AlGaAs/GaAs) is presented in figure 5.16 also. As the x value increased the ratio of etch rate decreased.

Thus at these operating conditions, AlGaAs was etchable in CH_4/H_2 mixtures up to an Al content x of 0.4. above which AlGaAs was not etchable. It might have been possible to etch AlGaAs with larger x value if the methane concentration had been reduced.

5.6 Loading effect and uniformity

The effect of increase in area of GaAs sample for RIE in CH_4/H_2 was also investigated. The area which was masked on the GaAs sample was about 2 mm^2. This masked area remained constant as the total sample area increased.

Figure 5.17 shows the etch rate R and carbon polymer deposition rate D against the GaAs sample area. The trend of the graph shows a decrease in R as the wafer area increased. The maximum R was about 50 nm/min for a 25 mm^2 sample. It then decreased to about 35 nm/min for a 2000 mm^2 GaAs sample, (2 inch GaAs wafer). R remained the same for both the 25 and 100 mm^2 samples. This is higher than the R value found for the 100 mm^2 sample shown in figure 5.1 (a). The high value is due to the increase

in total flow rate which in this case supplied enough species to the chamber to react with the surface of the GaAs samples. The deposition rate of carbon polymer D seems to be constant as area increased.

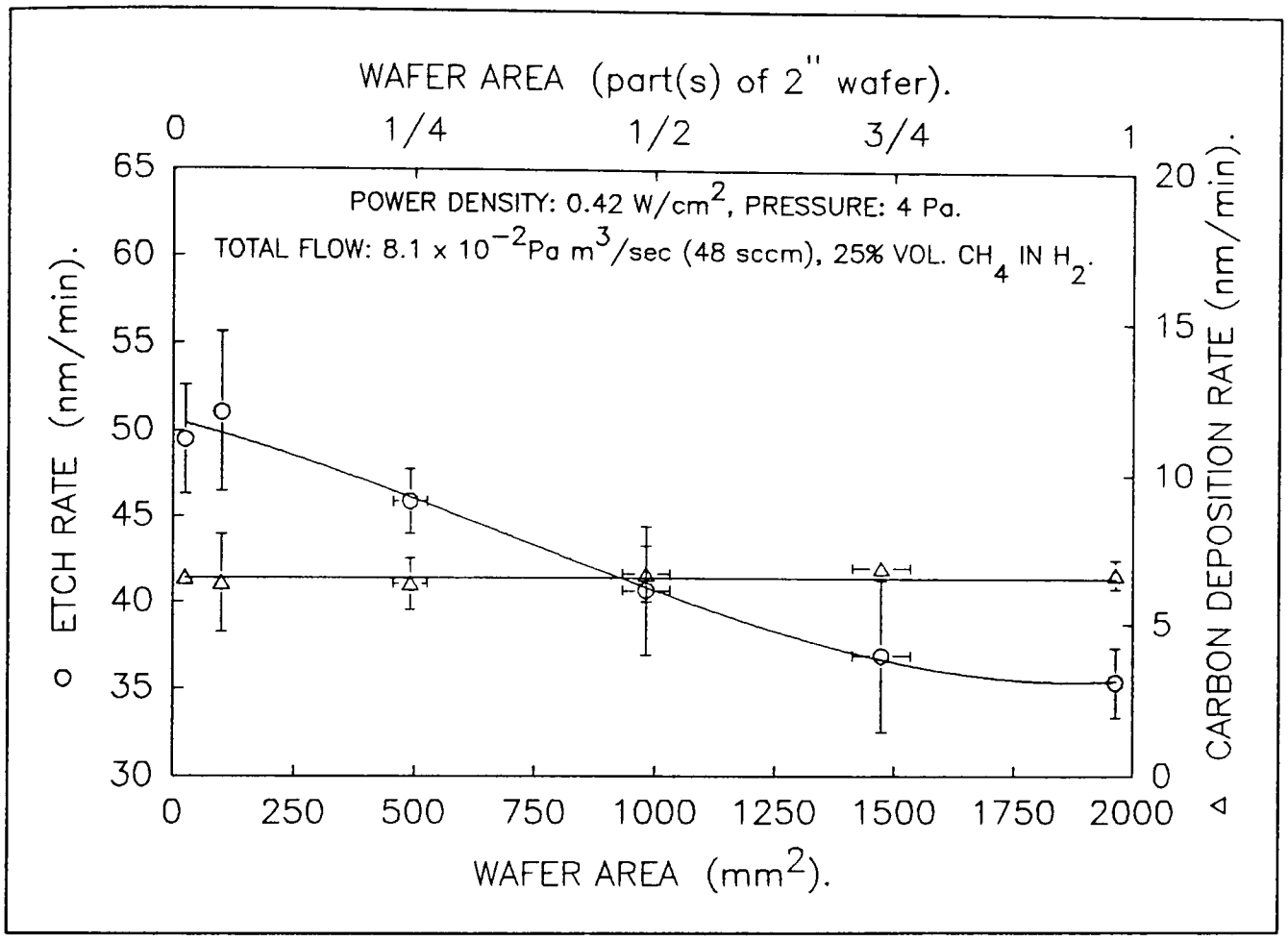

Figure 5.17. Graph of etch rate and carbon deposition against wafer area.

Picture 5.7 shows the micrographs of the profile of the etched 2 inch GaAs sample. The top picture is a side view of an etched wall. It is very clear that the wall does not show good anisotropy as found for smaller GaAs samples. The bottom picture shows the wall from another angle. There is clearly trench formation at the base of the wall and the side wall roughness appears to have increased. This indicates an imbalance between the chemical mechanism (C_xH_y species) and the physical mechanism (ion bombardment). This problem may be solved by repeating the experiment for different CH_4 volume concentrations to find a new value for the optimum methane concentration.

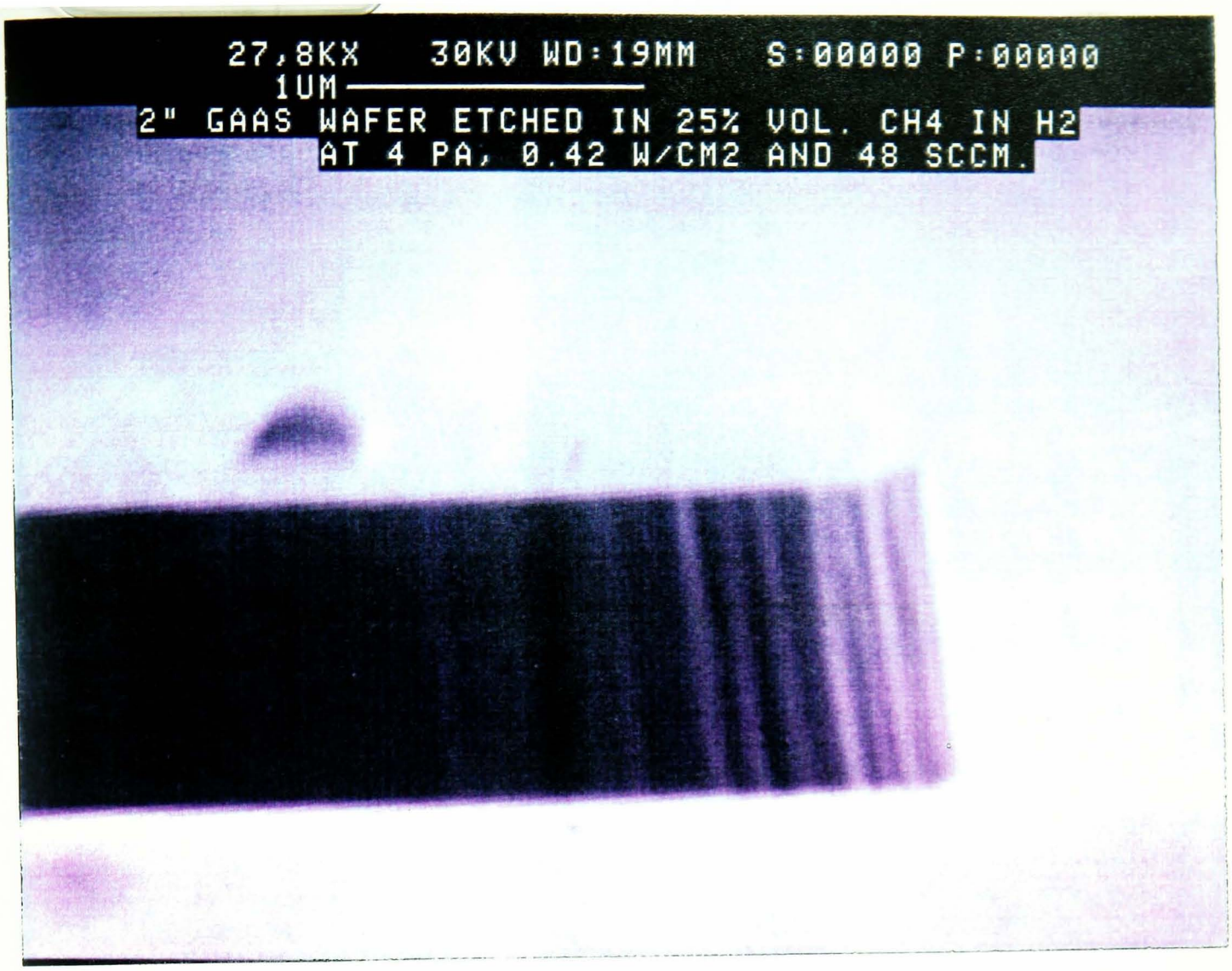

Picture 5.7. Micrographs of etched 2 inch GaAs wafer.
(Top) side view and (bottom) elevated view.

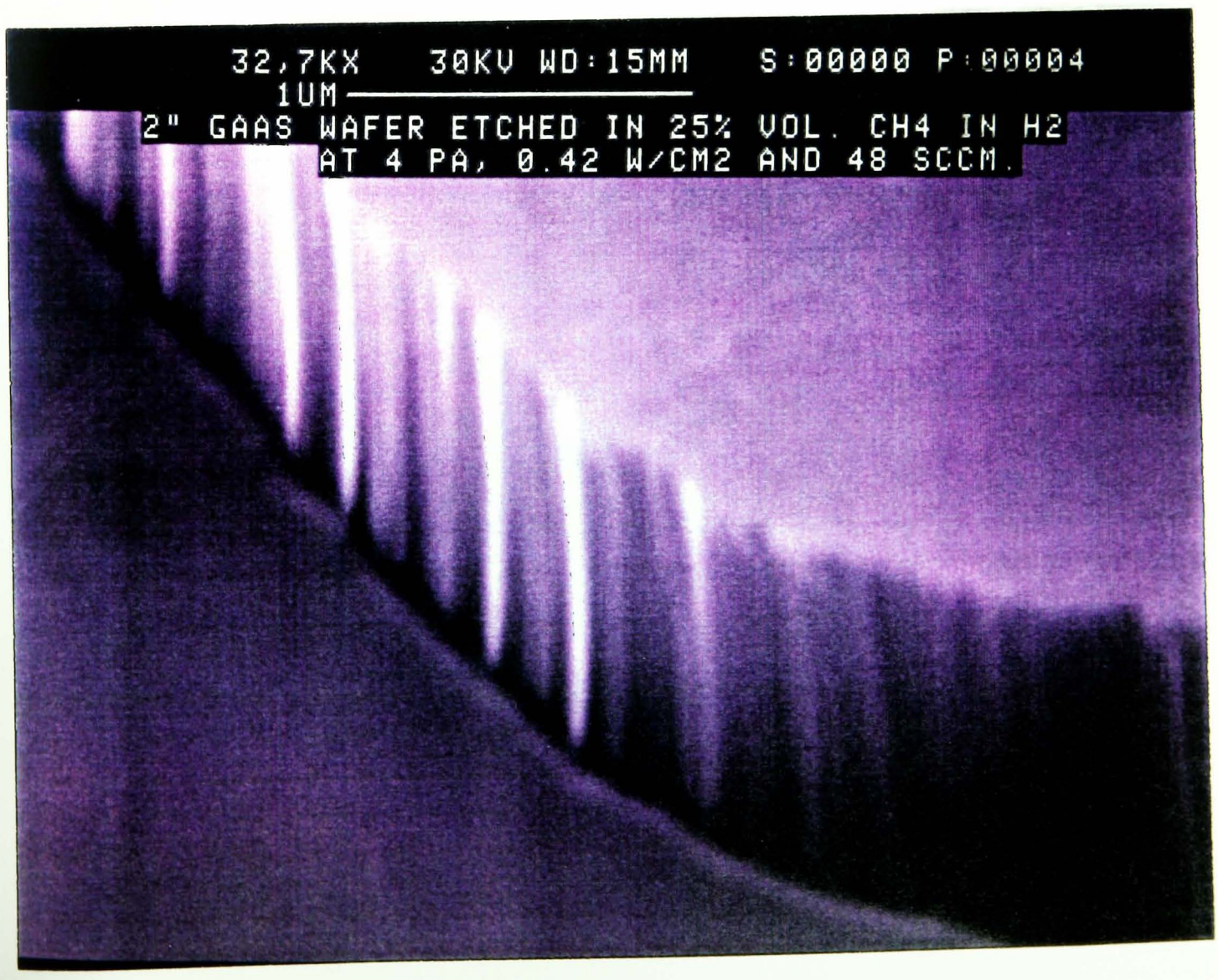

Figure 5.18 shows the etch rate R against edge to edge distance of a 2 inch GaAs wafer. The measurements were taken from north to south and west to east. In both cases the trend of the graphs were identical with maximum etch rate R_{max} of about 37 nm/min and minimum etch rate R_{min} of about 32 nm/min. R_{max} occurred at the edges of the wafer whereas R_{min} occurred at the centre. The uniformity U of the etched depth is given by (Carter, 1988),

$$U \simeq \pm \frac{R_{max} - R_{min}}{2R_{mean}} X\, 100\%, \qquad (5.1)$$

where R_{mean} is the mean. North-south and east-west uniformities were ± 7.6% and ± 9.1% respectively.

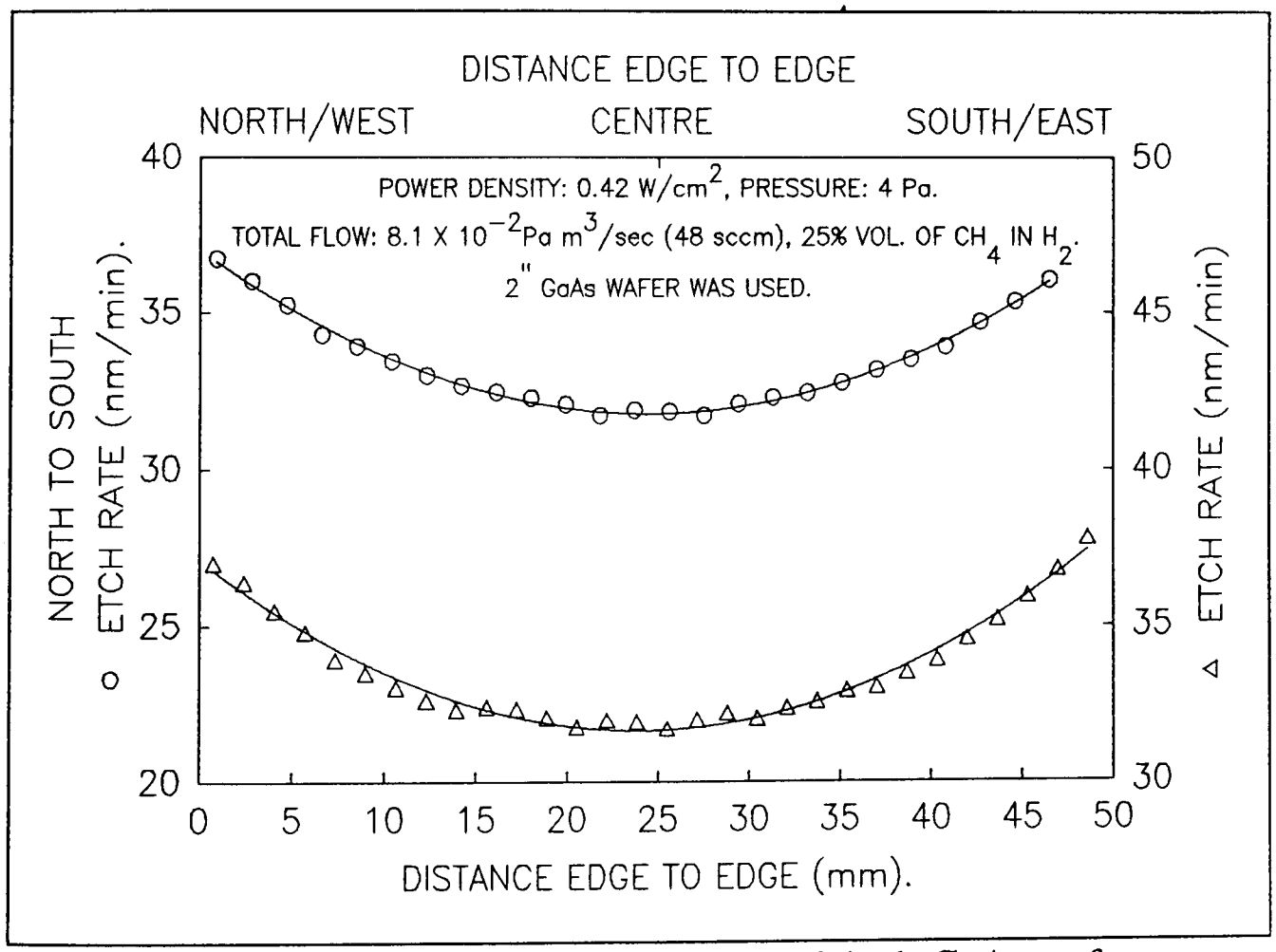

Figure 5.18. Etch uniformity graph for 2 inch GaAs wafer.

This is very different from the results obtained for the chamber conditions presented in chapter 4, where figure 4.8 showed that the etch rate was constant against distance from the centre of the cathode.

An explanation for the difference between the two cases is simple. For the characterization of the system, 100% hydrogen was used, (chapter 4). At the set conditions, hydrogen etched the surface of the GaAs largely by a physical mechanism (i.e. ion bombardment). In the case of the present experiment, a mixture of methane and hydrogen was used in which the methane volume concentration was 25%. The mechanism of the etching was therefore combined physical and chemical.

The gas mixture was let in to the chamber radially from the surroundings of the cathode. As a result of this the active species reached the edges of the wafer before the centre and therefore etching occurred more rapidly at the edges of the wafer.

5.7 Heating effect and reproducibility

As mentioned in chapter 4, The Electrotech Plasmafab 340 had no cathode cooling system. As a result the cathode was heating up as the time of etching progressed. Figure 5.19 shows the graph of etch rate R and temperature T of the cathode against the set etching time.

R increases as the set time of dry etching increases. R should have remained constant as set time increased, i.e. time should not have effected R. The only reason for this increase in R was the increase in T which was measured after the process had ended. The graph of T shows an increase as set time increased.

Reproducibility was also investigated. Figure 5.20 shows the graph of etch rate R and DC self bias voltage V_{self} as a function of time period. The graph of R against reproducibility was constant with in the limits of experimental errors. The graph of V_{self} shows a trend with a minimum at about the 75th day. The drop in the DC self bias voltage was caused because the chamber may have been dirty during this period. The

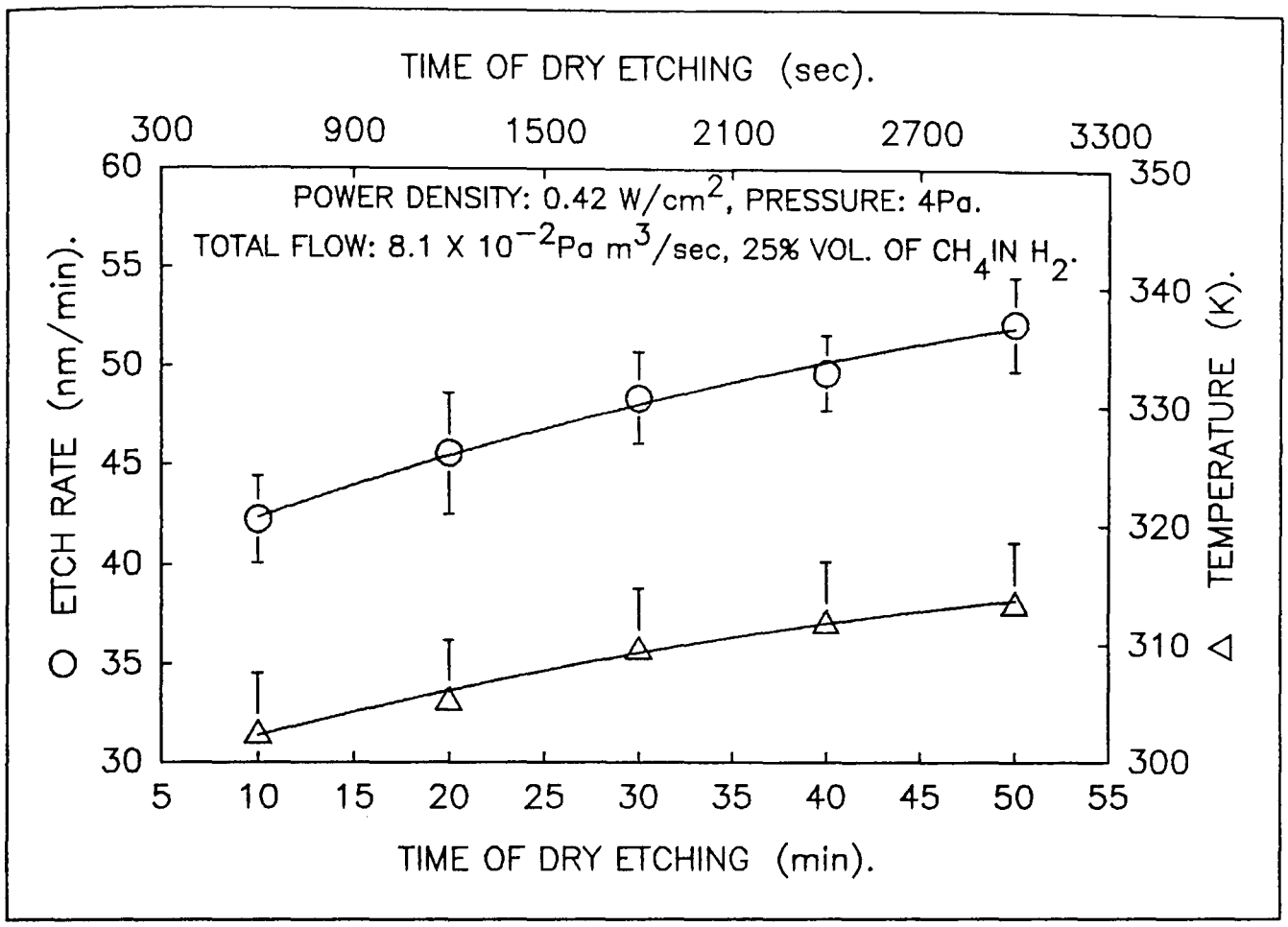

Figure 5.19. Etch rate and cathode temperature against time of etching.

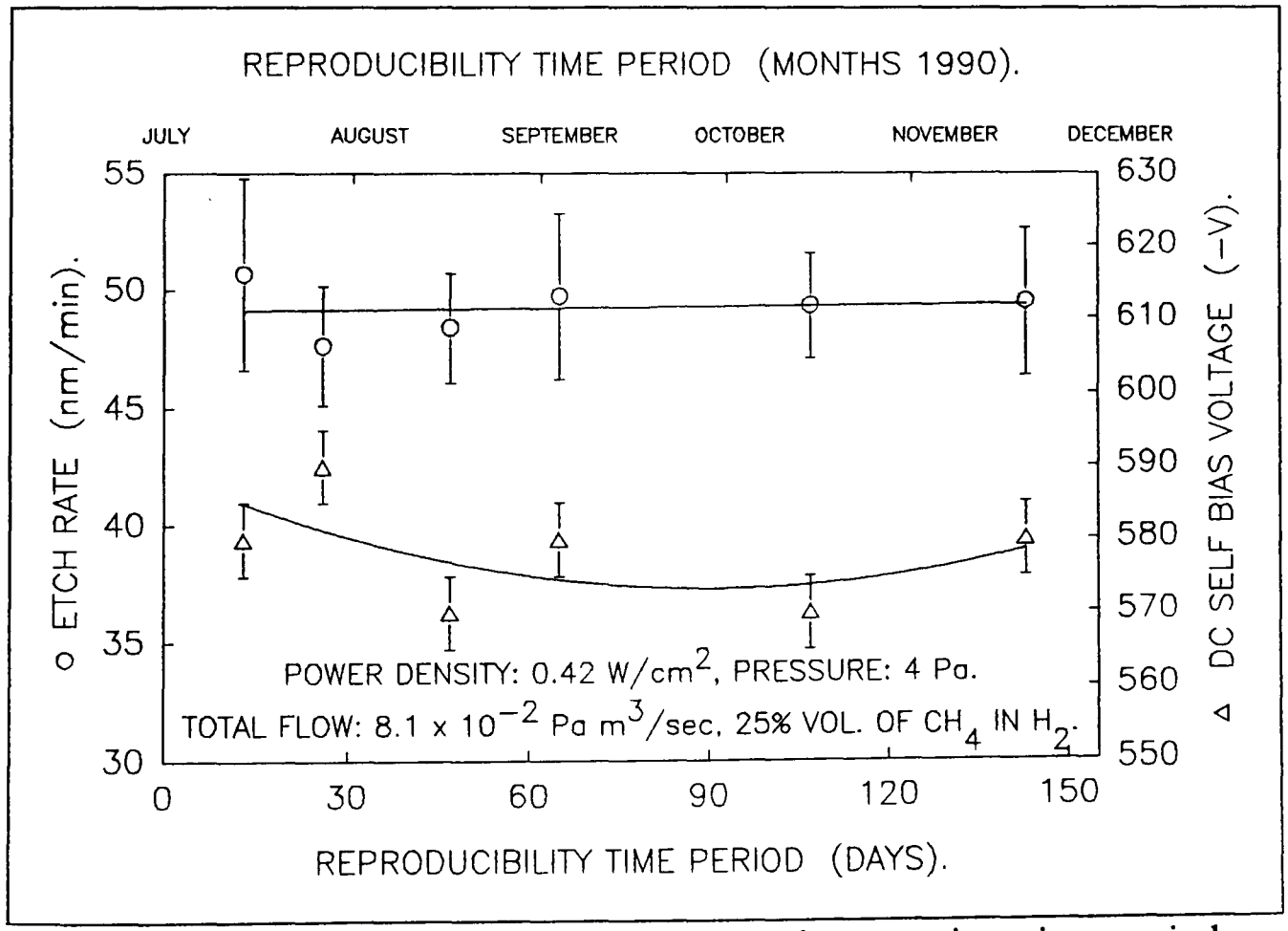

Figure 5.20. Etch rate and DC self bias voltage against time period.

chamber was then cleaned and as a result the value of V_{self} recovered. The small decrease in V_{self} did not affect the etch rate but it could have affected the profile of the etched walls and the etched surfaces. A large drop in the etch rate could cause carbon polymerization of the surface.

5.8 A method for RIE of GaAs in CH_4/H_2 mixture

The etching was controlled through the adjustment of power density, pressure and total flow rate. At the high pressures allowed by RIE, carbon polymerization occurred. The method of etching was then altered so that etching was possible at higher pressures.

When the pressure increased and the total flow rate of the gas mixture was kept constant, the residence time of the gas mixture increased (equation 1.1). From experiments performed it was evident that the DC self bias voltage decreased as the pressure increased because of the decrease in mean free path of the electrons. In order to etch at high pressure it is therefore necessary to keep the residence time and DC self bias voltage constant and to alter total flow rate and power density.

The best conditions for etching at 0.42 W/cm^2 and 4 Pa, (30 mtorr), were found to be 8.1 X 10^{-2} Pa m^3/sec, (48 sccm) and 25% volume CH_4 in H_2. The residence time τ_r of the gas mixture was 0.1 sec and the DC self bias voltage was -580 V.

The experiments were then performed at pressures between 7 and 12 Pa, (53 to 90 mtorr), keeping the residence time at 0.1 sec and DC self bias voltage at -580 V by varying the total flow rate and power density with the CH_4 concentration at 25%.

Figure 5.21 shows the results obtained with the first method. Figure 5.21 (a) shows the etch rate R and cathode temperature T against pressure. As

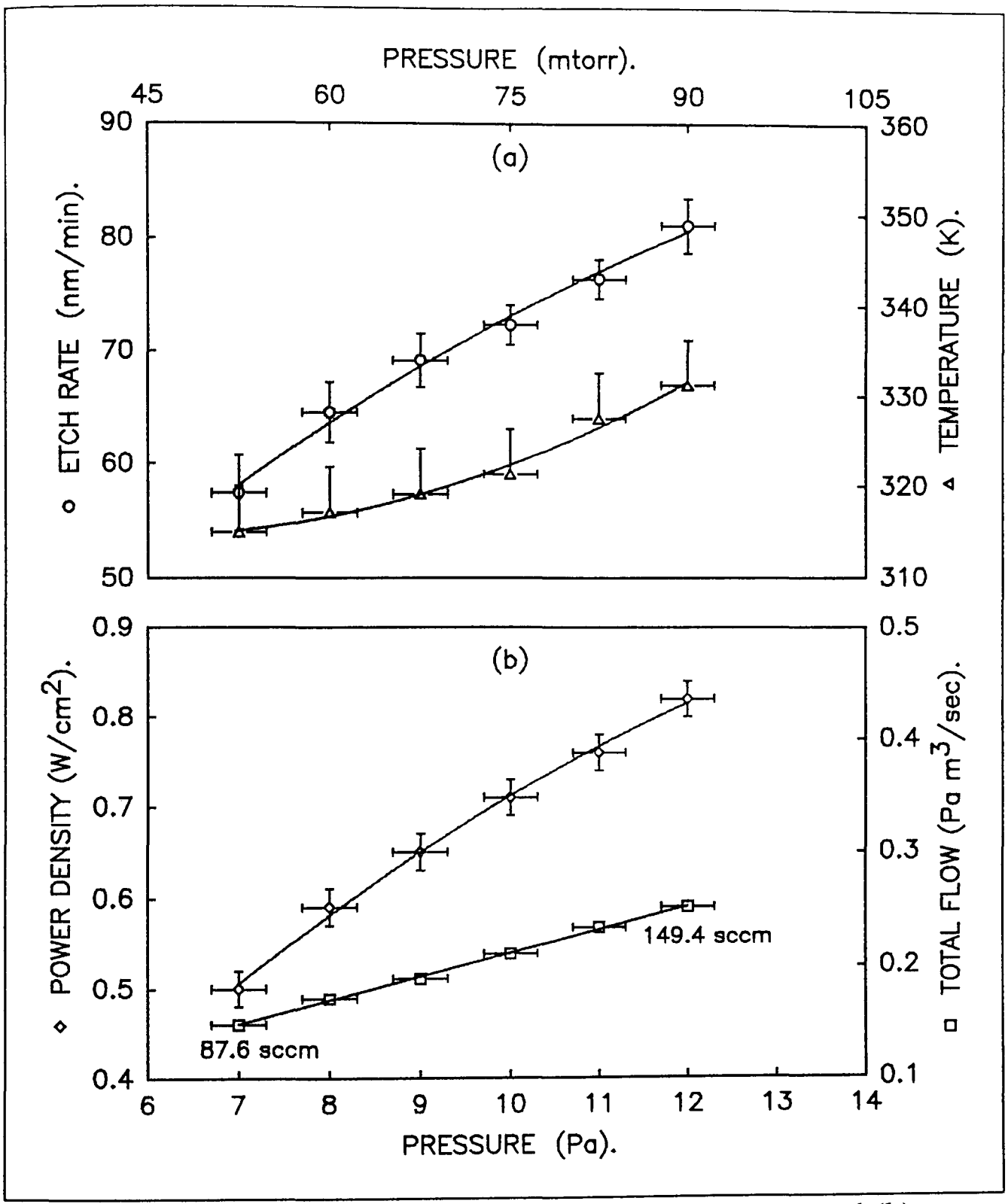

Figure 5.21. Graph of (a) etch rate and cathode temperature and (b) power density and total flow rate against pressure.

the pressure increased, R also increased. This was not expected, as R should have remained constant at about 50 nm/min. The explanation for this was related to the cathode temperature. As pressure increased, the power density was increased in order to keep the DC self bias voltage constant at -580 V. This increase in power density caused an increase in cathode temperature

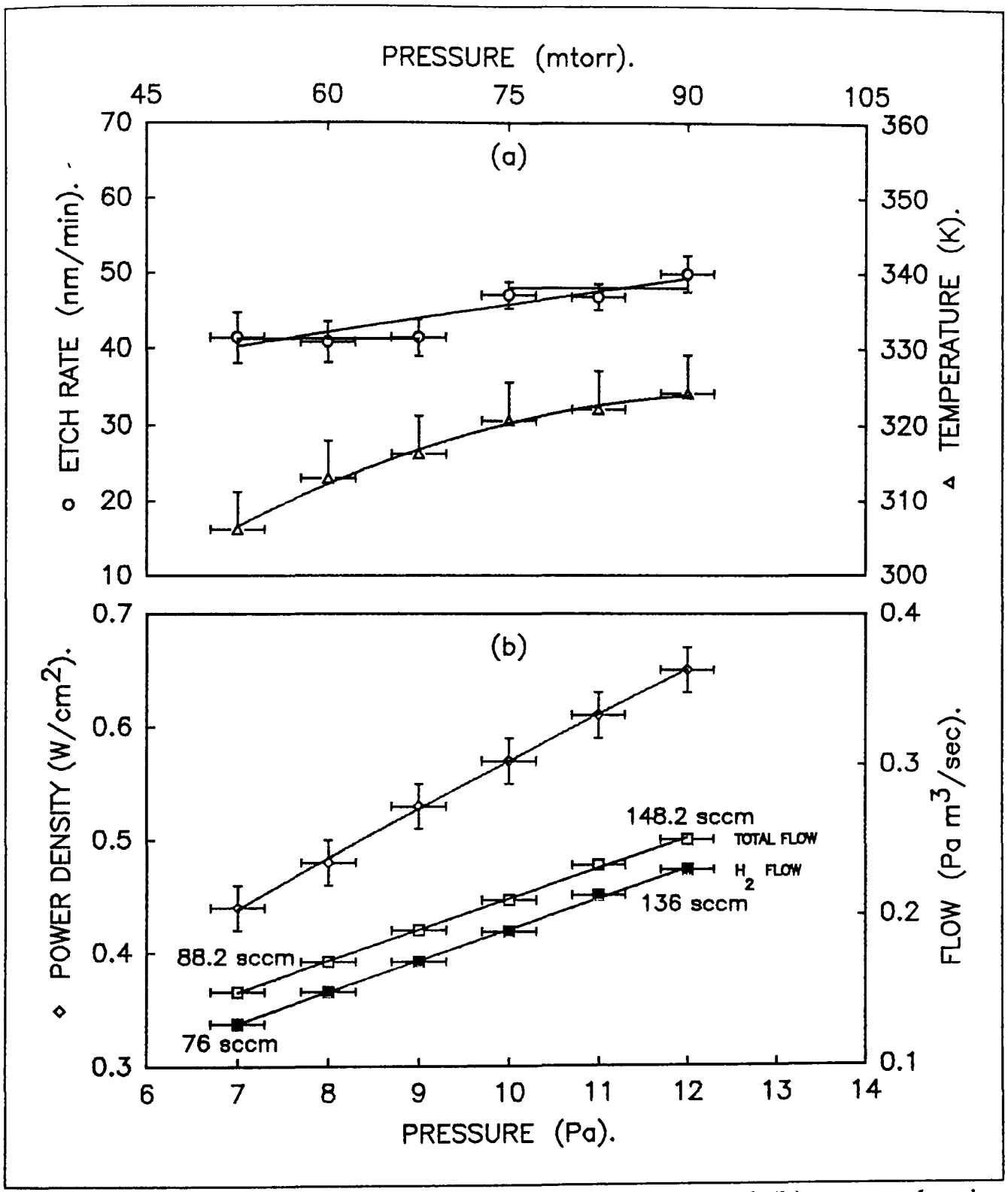

Figure 5.22. Graph of (a) etch rate and temperature and (b) power density and flow rate against pressure.

which is also shown in Figure 5.21 (a). As the temperature of the cathode was not controllable, an increase in temperature was inevitable with an increase in power density. Figure 5.21 (b) shows the variation of power density and total flow rate against pressure to keep the DC self bias voltage and residence time of the gas mixture constant.

In order to reduce the effect of temperature on the etch rate and prove that the first explanation was correct, a second method was devised. To keep the DC self bias voltage constant at -580 V, the total flow was increased but the methane flow was kept constant. This allowed the volume concentration of hydrogen to increase, which gave a more effective way to increase DC self bias voltage without large increases of power density.

Figure 5.22 shows the graphs of results obtained for the second method. Figure 5.22 (a) shows the variation of etch rate R and cathode temperature T against pressure. The etch rate increased but the rate of increase was lower than that shown in figure 5.21 (a). T also increased as pressure increased because of the increase in the power density, but the rise was not as much as with the first method. Figure 5.22 (b) shows the variation of power density and flow rate with pressure to keep the DC self bias voltage and residence time of the gas mixture constant.

The Arrhenius plot was thought to be unreliable as the temperature could not be controlled. The process variables for etching GaAs in mixtures of methane and hydrogen were therefore:

$$<P_d, p, Q, V_{\%methane}>, \tag{5.2}$$

where P_d, p, Q, and $V_{\%methane}$ are power density, pressure, total flow rate and volume concentration of methane in hydrogen respectively. In order to etch with reproducible results it is best to set the following parameters:

$$<V_{self}, p, \tau_r, V_{\%methane}>, \tag{5.3}$$

where V_{self} and τ_r are DC self bias voltage and residence time of the gas mixture in the chamber respectively.

CHAPTER 6
ELECTRICAL CHARACTERIZATION RESULTS

In order to evaluate the damage caused to the GaAs samples due to ion bombardment and hydrogen in-diffusion, the electrical characteristics of p-GaAs semiconductor samples exposed to pure hydrogen and a mixture of methane/hydrogen plasma were investigated.

Although electrical behaviour of n-GaAs due to RIE damage in mixtures of CH_4/H_2 plasma has been reported in the literature, very little information exists for p-GaAs. This may be due to the unpopularity of p-GaAs because of its low mobility. However p-GaAs is used for hetrojunction bipolar transistors (HBT's), (Ashburn and Rezazadeh, 1988 and Herbst, 1992), and the complementary high electron mobility transistors (Ali et al., 1989).

To evaluate the degree of damage due to ion bombardment and hydrogenation, two methods were employed. They were current-voltage (I-V) and capacitance-voltage (C-V) techniques and to employ these techniques gold Schottky diodes were fabricated on the p-GaAs samples.

6.1 RIE of p-type GaAs and electrical measurements

As described in chapter three, a two inch p-GaAs was cut into four equal quarters and processed. However before front Schottky metallization, three pieces were exposed to the plasma. The process parameters such as power density, pressure and total flow rate were set to the best conditions found which were 0.42 W/cm^2 (100 W power), 4 Pa (30 mtorr) and 8.1 X 10^{-2} Pa m^3/sec (48 sccm) respectively and the time of etching was set to 30 minutes. The temperature of the cathode after etching was less than 60°C.

One of the three pieces was exposed to pure hydrogen plasma. The DC self-bias voltage was -680 V which was higher than before. This was due

to extensive cleaning of the chamber and the cathode. The other two pieces were exposed to methane and hydrogen plasma individually with 25% volume concentration of CH_4. The DC self-bias voltage was -580 V. In the first and second case about 150 nm and 1400 nm were removed from the semiconductors respectively. One of the samples which was etched in methane and hydrogen was then annealed in N_2 gas at 400°C and atmospheric pressure. Front barrier metal was then deposited on all samples.

The I-V method was performed to test the ideality factor of the Schottky diodes for both the processed and unprocessed samples. The saturation current I_o was measured so the barrier height of the diode ϕ could be calculated. The reverse current at 2 V and 3 V, the threshold voltage and the break-down voltage of the diodes were also measured. The I-V relation and the derivation of the ideality factor n and barrier height ϕ is shown in appendix VII.

The C-V method was performed primarily to measure the carrier concentration N of the processed and control samples. The ion bombardment of the surface however caused N to become non-uniform in the etched samples and so N was therefore measured against the depletion width W_d. Both N and W_d were measured at zero volts also. The C-V relation is shown in appendix IX.

6.2 Current-voltage measurements

Figure 6.1 shows the ideality factor n and the barrier height ϕ of the Schottky diodes for the control and the processed samples respectively. In figure 6.1 (a), the control sample displayed an n value of about 1.33. This may be due to the high carrier concentration. Semiconductors with large carrier concentrations may yield high n values, (Madams et al., 1975 and Sze, 1981). The samples used for this experiment had a carrier concentration of about 2 X 10^{18} cm^{-3}. The sample which was etched in a

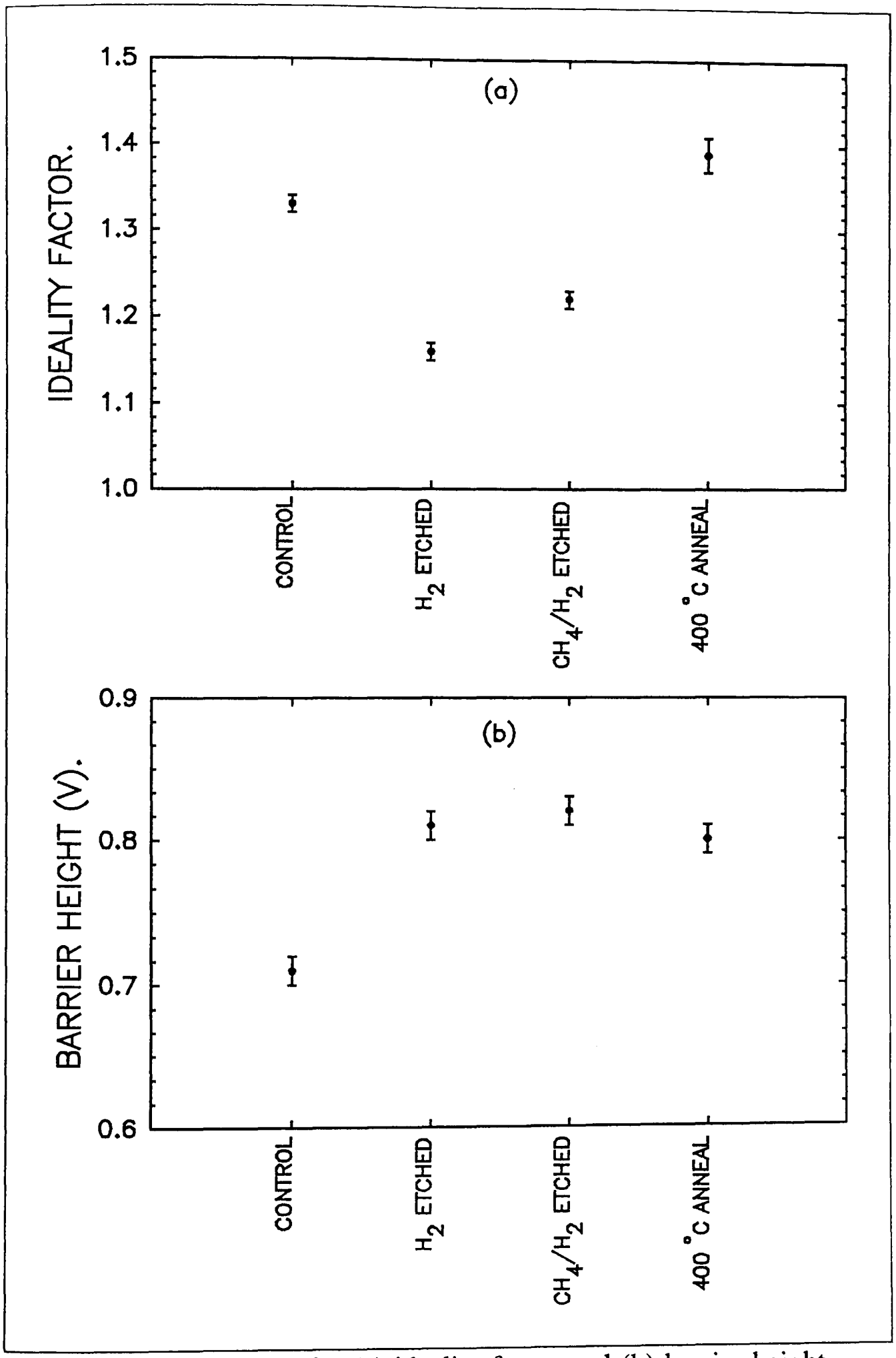

Figure 6.1. I-V test for (a) ideality factor and (b) barrier height.

hydrogen plasma indicated a much lower value for n which was about 1.16. The sample which was etched in the mixture of CH_4/H_2 plasma, displayed a slightly higher n value of 1.22 compared to that etched in pure H_2. Finally the sample which was etched in CH_4/H_2 plasma and subsequently annealed at 400°C in N_2 atmosphere displayed a n value of about 1.39. This shows some recovery.

Figure 6.1 (b) shows the behaviour of the barrier height ϕ. The control sample displayed a barrier hight of about 0.71 V, which is high for a gold front metal Schottky diode. This may be due to pinning of the Fermi level, (Spicer et al., 1980 and 1982). The sample which was etched in H_2 plasma displayed a ϕ value of about 0.81 V while the sample which was exposed to CH_4/H_2 plasma indicated a ϕ value of 0.82 V. The annealed sample displayed very little improvement with a ϕ value of 0.80 V.

Figure 6.2 shows the saturation current I_o and the threshold voltage of the control and processed Schottky diodes. In figure 6.2 (a), the control sample displayed an I_o value of about 10^{-8} A. This decreased to 3 X 10^{-10} A for the H_2 etched sample and 10^{-10} A for the CH_4/H_2 etched sample. The annealed sample displayed an I_o value of 3 X 10^{-10} A which was only a negligible recovery.

The threshold voltage is represented in figure 6.2 (b). The control sample showed a threshold voltage of about 0.5 V. This increased to 0.9 V for the H_2 etched sample and 0.65 V for the CH_4/H_2 etched sample. The annealed sample showed no further improvement from 0.65 V. In cases of ϕ, I_o and threshold voltage, the annealed sample did not recover its original value.

Figure 6.3 shows the reverse current and breakdown voltage of the control and the processed samples. Figure 6.3 (a) represents the reverse current of the samples. The control sample presented values of 0.2 mA and 2 mA at 2 V and 3 V respectively, which were very leaky. The sample which was

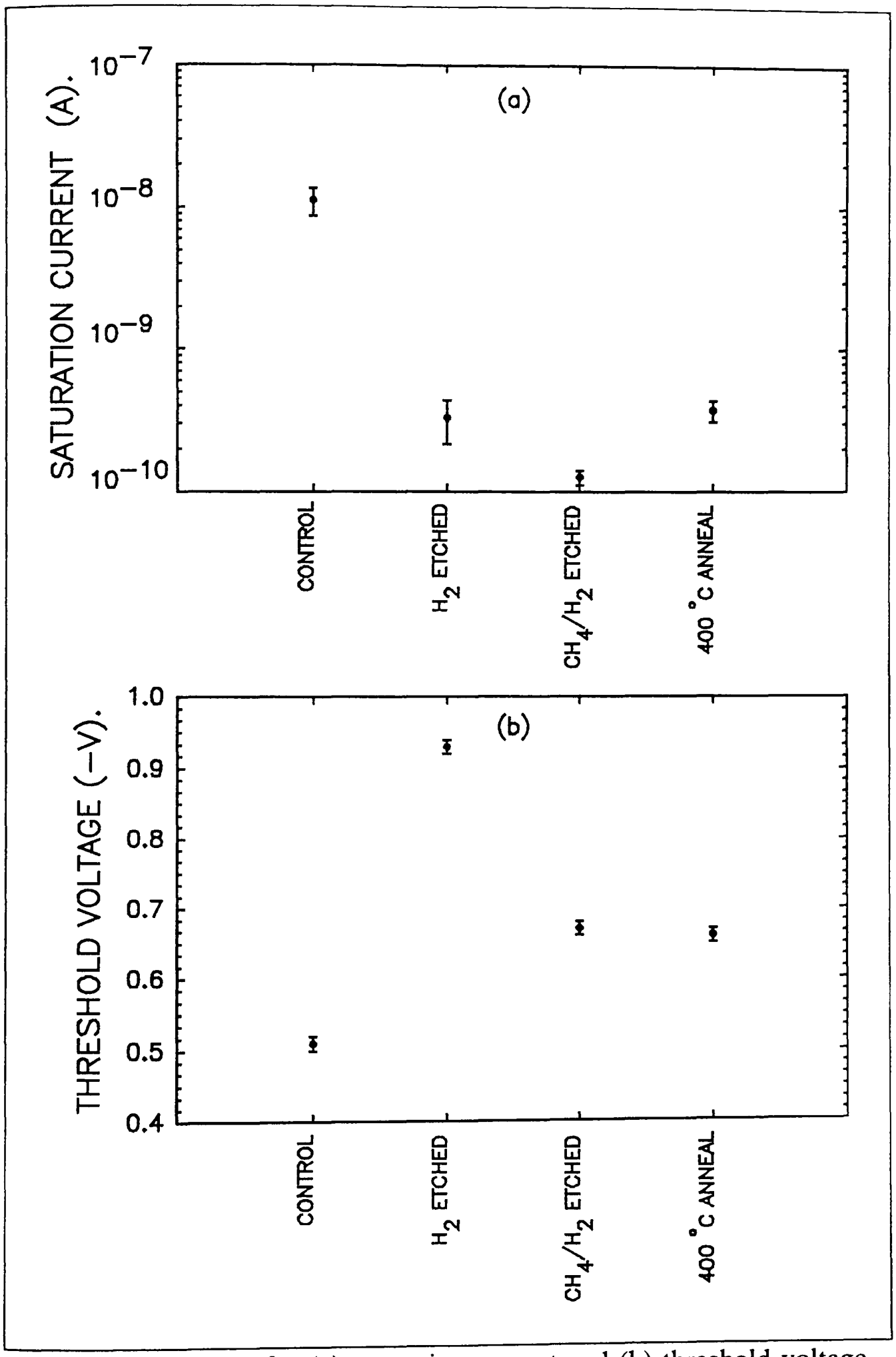

Figure 6.2. I-V test for (a) saturation current and (b) threshold voltage.

etched in H_2 plasma displayed an improved value of about 30 nA and 0.2 μA at 2 V and 3 V respectively. These values improved further for the sample which was etched in CH_4/H_2 plasma. The reverse current at 2 V and 3 V was about 6 nA and 30 nA respectively. After annealing, the reverse current decreased to its lowest values which were 2 nA and 20 nA at 2 V and 3 V respectively.

Figure 6.3 (b) shows the behaviour of the breakdown voltage. The control diodes displayed a very low value of 3.2 V which was due to the high carrier concentration. The sample which was hydrogenated in pure H_2 plasma, presented a much higher value of about 9 V for breakdown voltage. The CH_4/H_2 etched sample presented a lower value of about 7 V and the annealed sample partially recovered the original breakdown voltage which was about 5 V.

The results show distinct changes in the I-V characteristics of the processed samples to the control. This behaviour is explained by using C-V characterization.

6.3 Capacitance-voltage measurements

The C-V measurements were performed on the same samples which were used for I-V measurements. The ion bombardment may have caused a non-uniformity of carrier concentration N across the depth of the processed samples, therefore N was measured against depletion width W_d of the GaAs to examine the profile of the carrier concentration in the depth of the material.

Figure 6.4 shows the carrier concentration N_o and depletion width W_{do} at zero volts. Figure 6.4 (a) which represents the carrier concentration N_o, clearly indicates the N_o value of the control sample to be at about 2×10^{18} cm^{-3}. The sample which was etched in pure H_2 displayed a decrease in the

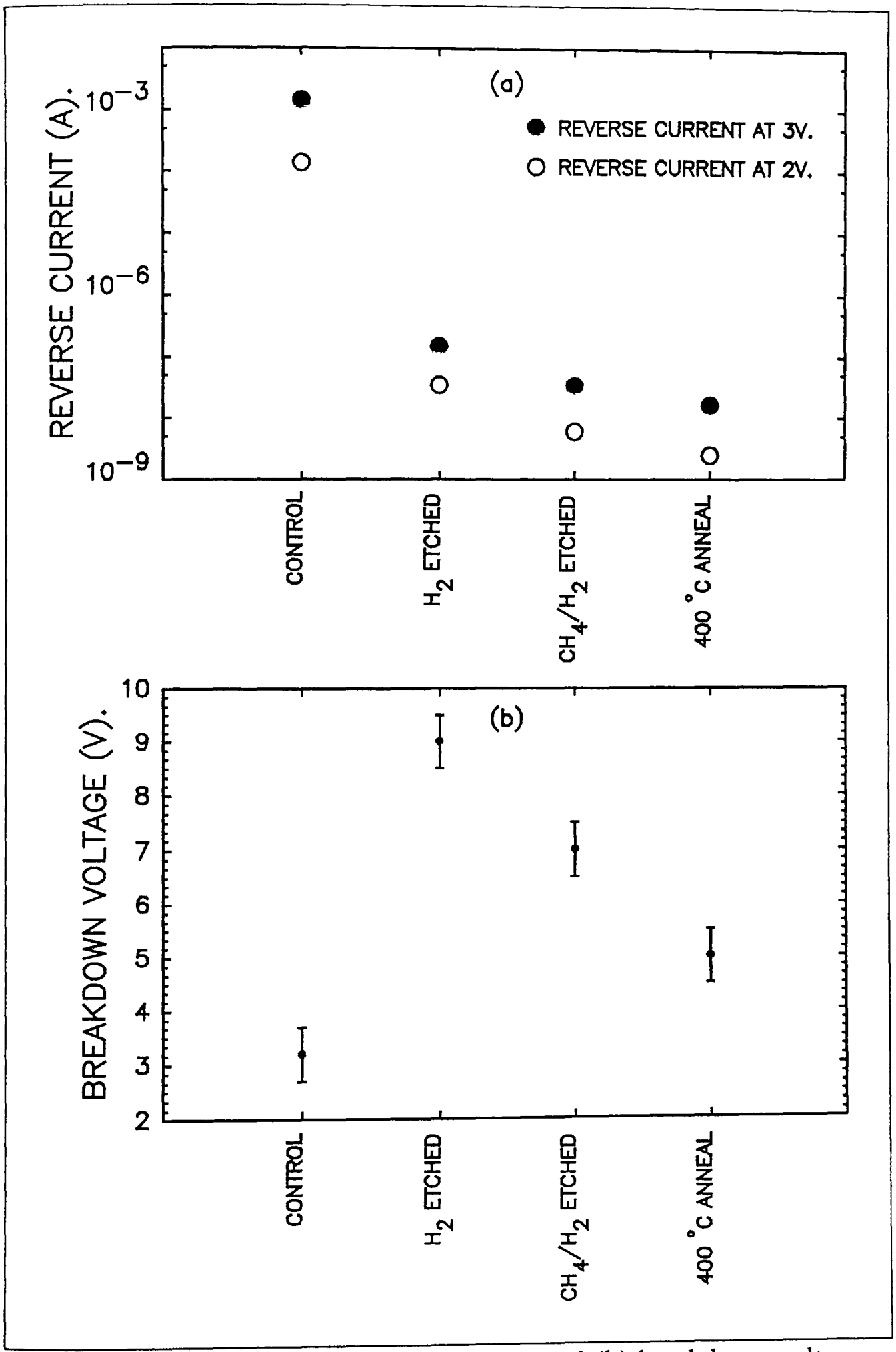

Figure 6.3. I-V test for (a) reverse current and (b) breakdown voltage.

N_o value by a factor of 100 to about 2 X 10^{16} cm^{-3}. The sample which was etched in a mixture of CH_4/H_2 plasma displayed a higher N_o value of 6 X 10^{16} cm^{-3}. Finally the sample which was etched in CH_4/H_2 plasma and annealed displayed a complete recovery of N_o to about 2 X 10^{18} cm^{-3}.

Figure 6.4 (b) which represents the depletion width W_{do} at zero volts also indicates a large change between the control and the processed samples. The control sample displayed a W_{do} of about 0.024 μm. The sample which was etched in H_2 plasma displayed an increase in W_{do} of about a factor of 8, to 0.2 μm. The CH_4/H_2 treated sample displayed a W_{do} of 0.1 μm. The annealed sample indicated a value of 0.036 μm for W_{do}.

Figure 6.5 shows the carrier concentration N against the depletion width W_d. The control sample displayed a W_{do} of about 0.024 μm and a N_o value of about 2 X 10^{18} cm^{-3}. As the depletion width increased the carrier concentration increased slightly but remained in the 10^{18} cm^{-3} region. For comparison the original value of N is considered to be 2 X 10^{18} cm^{-3}.

The sample etched in H_2 plasma indicated a drop in N_o by a factor of 100 to about 2 X 10^{16} cm^{-3} and W_{do} of 0.2 μm. As W_d increased N increased. The solid tail line shows the interpolation of this plot from which the extent of the passivation of carriers could be estimated. In this case the passivation continued until 0.5 μm where N reached its original value.

The sample which was etched in the mixture of CH_4/H_2 plasma also indicated a large decrease in N_o value but not as much as the H_2 treated sample. The W_{do} value was about 0.1 μm. As W_d increased the N value increased. The solid tail line also shows the interpolation of this plot. The acceptor passivation extends 0.3 μm into the semiconductor.

The sample which was etched in a mixture of CH_4/H_2 plasma and annealed shows a complete recovery as far as the N_o value was concerned. However

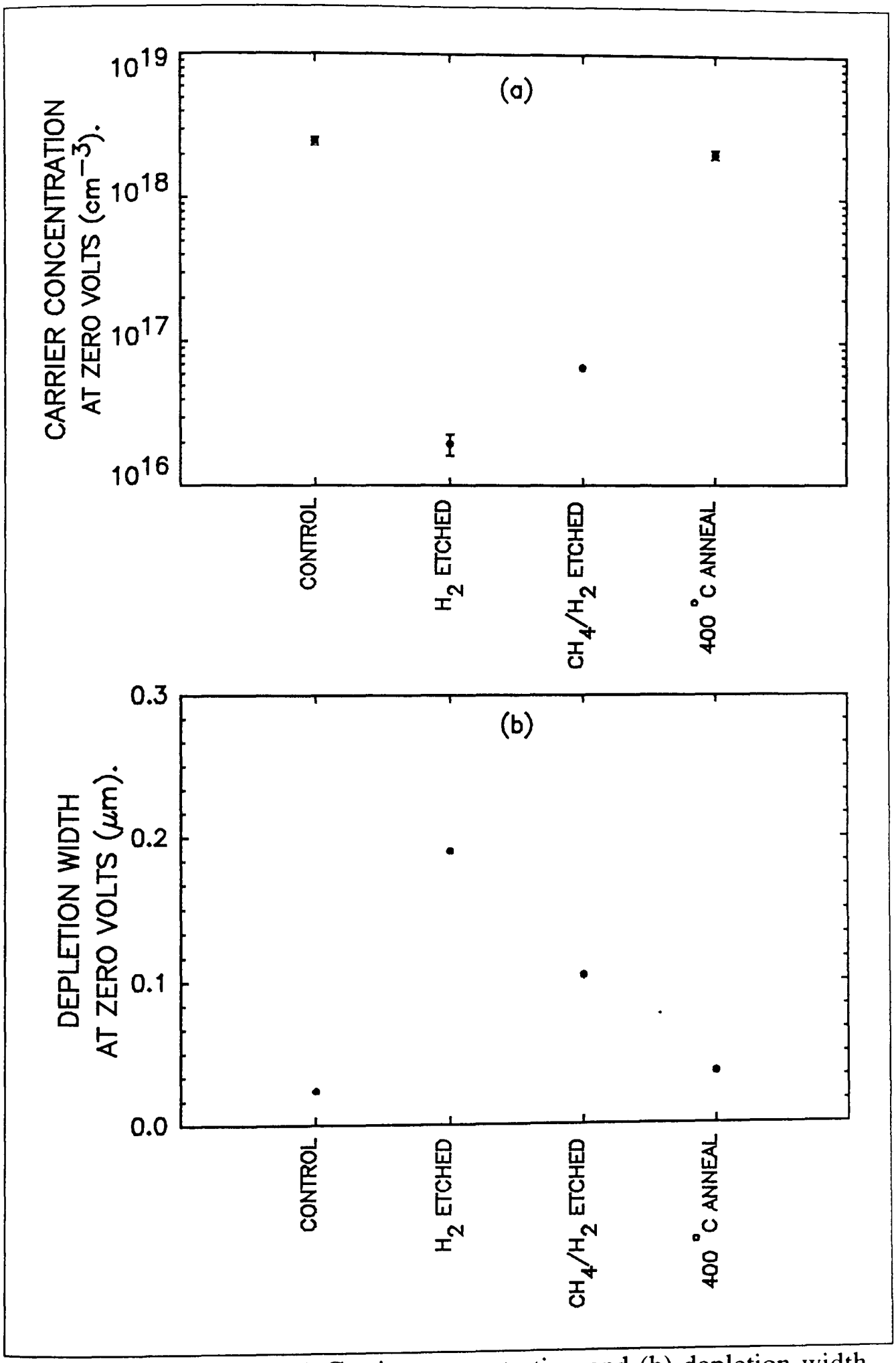

Figure 6.4. C-V test. (a) Carrier concentration and (b) depletion width.

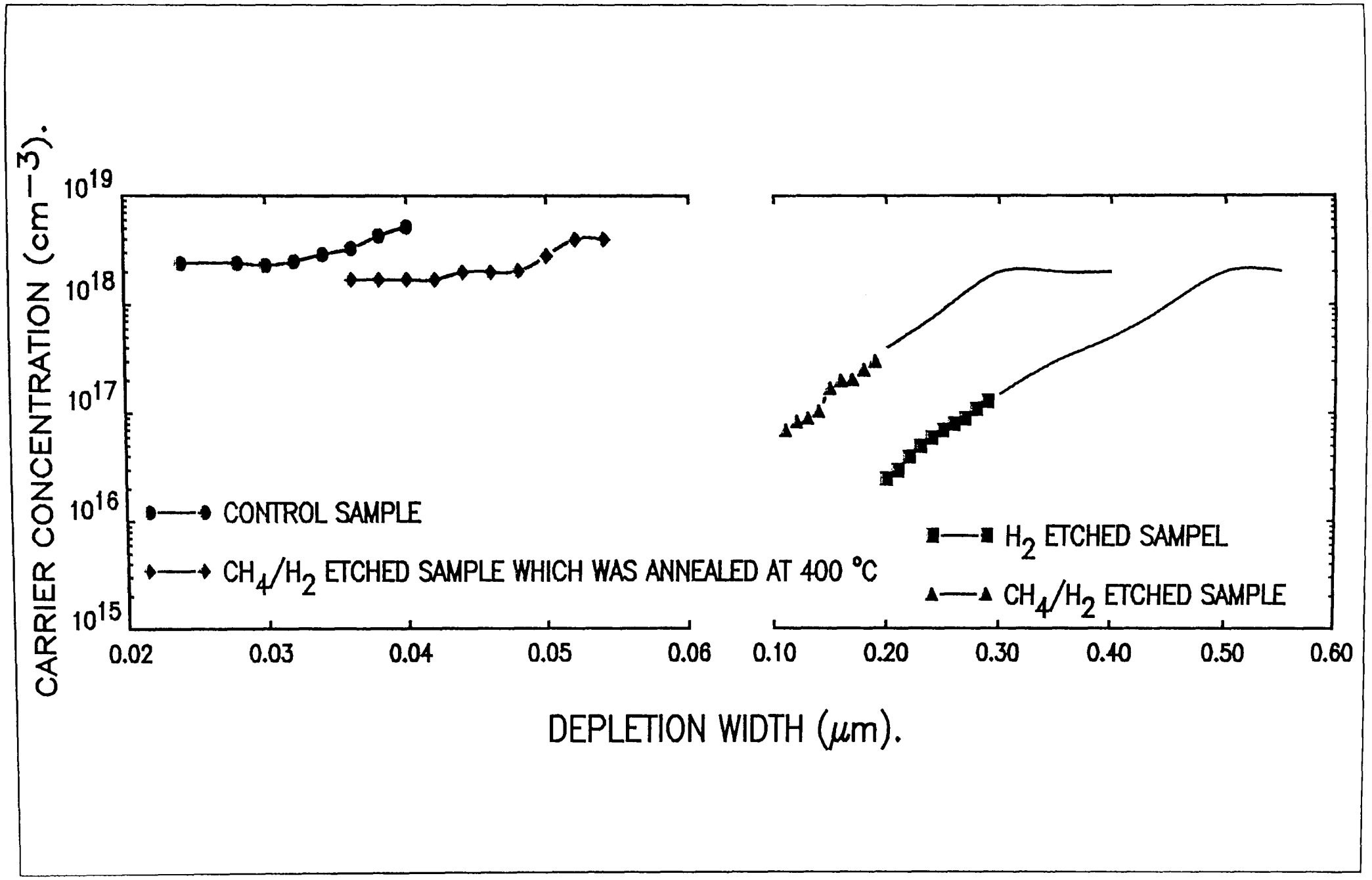

Figure 6.5. C-V profile of carrier concentration against depletion width.

W_{do} did not recover totally. A difference of about 12 nm remained between the control and annealed samples. This may be due to the surface modification caused by the etching procedure which will be discussed in the next chapter.

CHAPTER 7
DISCUSSIONS

In this chapter the results of reactive ion etching and electrical characterization of GaAs will be discussed and a possible model for the mechanism of etching GaAs in mixtures of methane and hydrogen (CH_4/H_2), will be presented.

The influence of H_2 and CH_4 on etching of GaAs, together with the effect of the process parameters and the deposition of carbon polymers on the surface of the samples are considered here. Finally the current-voltage and capacitance-voltage results are assessed.

7.1 Non-chlorinated gas mixtures

The effectiveness of H_2 in the CH_4/H_2 mixture is argued here. When CH_4/H_2 was used to etch GaAs, the etch rate R increased as the CH_4 volume concentration increased (figure 5.1 (a)). At the same time the DC self bias voltage V_{self} decreased. This indicated that the ion bombardment intensity was decreasing and therefore the increase in R was due to reactive species which reacted with the surface to produce volatile species which escaped from the surface. In other words, the increase in R was due to the chemical mechanism as the influence of the physical mechanism decreased.

When argon Ar was used instead of H_2, R decreased as CH_4 volume concentration increased (figure 5.1 (b)). The reduction in R may be due to many factors. First was the reduction of ion bombardment intensity which is indicated by V_{self}. This value decreased which indicated that the ion bombardment intensity was reduced and so R was reduced also. This occurred because overall, more energy may have been needed to break the CH_4 bonds and to ionize the atomic and molecular remains than for ionizing an Ar atom. The second reason is the polymeric deposition of the surface

which could make the sputtering of the surface of GaAs difficult as ions had to remove two items, the GaAs and the deposited polymer film. Finally reduction of the molecular mass of the admixed gas (in this case CH_4) could reduce the sputtering yield.

When Ar was used instead of CH_4 The same behaviour was observed for R as when H_2 was added (figure 5.1 (c)). That is, R was reduced as the H_2 volume concentration increased. However, V_{self} decreased at the beginning and then increased until at 100% H_2, V_{self} was at its highest value. Although the ion bombardment was more severe the R value decreased. This was due to the small mass of H or H_2 ions. Increase of V_{self} was due to increased H_2 concentration. H_2 molecules could dissociate into two H atoms and then these could be ionized. The ionization energy of H_2 molecules and H atoms is lower than that of Ar atoms. This could explain the higher V_{self} value when pure H_2 was used compared with that when pure Ar was used.

Usually Ar, being an inert gas, does not react with anything. When Ar is ionised however, the outer shell configuration will resemble that of chlorine and becomes similarly reactive. In the presence of H_2 or H, reactions may take place to produce a complex ion such as ArH^+, (Chapman, 1980).

Experiments involving CH_4 and other inert gases have been reported, (Law[a], et al., May 1991). These were neon and helium. The authors argued that it was possible to achieve MORIE without using H_2. They also argued that the damage to the semiconductor would be much lower if H_2 is not used. They did not show any evidence for their argument on damage. However the graphical information showed similar profiles for the CH_4/H_2, CH_4/Ne and CH_4/He curves, although the optimum etch rate for the inert admix gases were much lower than for H_2.

In both cases when inert admix gases were used, etch rate increased as the methane concentration increased. The etch rate reached a maximum and

then polymerization occurred. This is similar to when CH_4/H_2 is used and so because of this, MORIE has been diagnosed. However this can be explained in another way. For both cases, the ionisation energy of Ne and He is much higher than that of CH_4 and so methane will ionise more easily than He or Ne and so the surface will be sputtered primarily by the CH_4 ionised species rather than by He or Ne. At high concentrations of CH_4 polymerization occurred. In the case of He there is an additional explanation. As CH_4 is a heavier molecule than He, a higher sputter yield is observed when it is mixed with He.

There is a possibility that MORIE may have taken place but at a very low rate. Generally etching could have occurred primarily by the physical mechanism, (i.e. ion sputter etching was performed). In order to achieve reactive ion etching it is necessary to use CH_4/H_2 mixtures.

7.2 The effect of CH_4 concentration and flow rate

Figure 5.2 (a) to (d) shows the graphs of etch rate and DC self bias voltage against volume concentration of CH_4 in H_2. In all cases the etch rate R increased initially as the CH_4 volume concentration increased. After R reached an optimum level, increases of CH_4 volume concentration caused a decrease in R until finally carbon polymers were deposited all over the GaAs sample and etching stopped.

This is explained by suggesting that the CH_x and H_y radicals may have reacted with the surface of the GaAs to produce metal organic and hydride compounds. Therefore the reactive component of etching is dependent on the supply of CH_4 because as the CH_4 supply to the chamber increases R increases. The reactive species are absorbed on the surface and the incident ions supply kinetic energy to the surface so that volatile compounds are formed because of the reaction between the GaAs and the polymeric film and then they escape from the surface. After the etching process the

polymeric film cannot be detected on the surface of GaAs with the naked eye but as this film does not react with the inorganic mask material (in this case SiO_2), it can be noticed on the mask.

The reduction in R and deposition of the polymeric film all over the sample at high concentrations of CH_4 can be interpreted by suggesting that as the CH_4 volume concentration increases, the carbon polymeric deposition rate D increases. The incident ions are unable to supply enough kinetic energy to the surface to continue with the optimum condition of etching the sample and at the same time remove the extra amount of deposited film. Eventually as the CH_4 concentration increases, the deposition rate of the carbon polymeric film would be so high that the ions would not be able to continue to etch the surface of the sample and deposition occurs on all GaAs surfaces.

In all cases in figure 5.2 the profile of the DC self bias voltage V_{self} was the same. V_{self} increased slightly as the CH_4 volume concentration in H_2 increased by a small amount. This may have been due to the production of electrons by ionisation following the breakdown of the molecules, (i.e. if the CH_4 molecule dissociates completely five atoms can be ionised compared with two atoms when a H_2 molecule breaks down). As a result of this the cathode was charged to a higher negative value. When the CH_4 volume concentration increased further, most of the energy was spent in breaking CH_4 molecules rather than in ionisation. This resulted in reduction of negative charge on the cathode and hence a decrease in the value of V_{self}.

The effect of flow rate is presented in figures 5.2 and 5.3. It is clearly seen from figure 5.2 that the optimum etch rate was shifting as the total flow rate was increasing. In fact the increase in flow rate caused the optimum R to occur at a lower CH_4 volume concentration. Figure 5.3 (a) and (b) shows the variation of etch rate, optimum CH_4 volume concentration in H_2, deposition rate of polymer film at optimum CH_4 concentration, and the DC

self dias voltage at different flow rates.

Usually when a reactive gas is used to etch a surface the etch rate changes as the flow rate is varied (as mentioned in chapter 1). At low flow rates the etch rate is low because although the residence time of the gas is high, enough species are not supplied to the chamber. When the flow rate increases the supply of species to the chamber will increase until at an optimum flow rate the residence time and the supply of the gas is balanced and a maximum etch rate will occur. When the flow rate is increased further the etch rate will fall again because the residence time of the gas is so low that the species will not have enough time to react with the surface.

It is accepted that the reactive gas in this case was CH_4. At low total flow rate of the gas mixture the residence time of the mixture was high but the total supply of the species to the chamber was low. In order to overcome this deficiency so that the etch rate could remain high, the partial flow rate of the reactive gas then had to be high or in other words the volume concentration of CH_4 had to be high. When the total flow rate increased, the supply of the species to the chamber increased also such that the partial flow rate for optimum etching decreased.

It is obvious from figure 5.3 (a) that the optimum etch rate remained constant as the flow rate increased and the CH_4 volume concentration decreased. In this case further increases of the total flow rate were avoided or the pressure would have changed due to the limits of the pumping speed of the system. The deposition rate of the carbon polymeric film was also reduced as the flow rate increased, (figure 5.3 (b)), because of the reduction in CH_4 volume concentration and residence time of the gas.

The behaviour of the DC self bias voltage V_{self} for varying total flow rate was similar to its behaviour for varying CH_4 volume concentration. The initial rise in V_{self} because of the increase in total flow rate was due to a

reduction in CH_4 volume concentration so that most of the input energy was not wasted on breaking down CH_4 molecules. However further increases in total flow rate caused a decrease in V_{self}. This was due to the decrease in the residence time of the species in the chamber.

This behaviour was shown clearly when etch rate R and DC self bias voltage V_{self} were investigated for varying the total flow rate of the gas mixture at an arbitrary CH_4 volume concentration of 20% as shown in figure 5.4. R increased because as the total flow rate increases, the supply of active species increases. V_{self} decreased because the residence time of the species in the chamber decreased.

Figure 5.5 shows the variation of anisotropy as a function of total flow rate. The anisotropy for both the arbitrary 20% and optimum volume concentration of CH_4 improved when total flow rate was increased. The DC self bias voltage decreased as the total flow rate increased. This indicated a reduction in ion bombardment intensity and as a result a possible lowering of the bombardment of the side walls by the back scattered ions. In the case of the samples which were etched at optimum volume concentration of CH_4, the variation of the DC self bias voltage was in conjunction with the reduction in the volume concentration of the reactive species. There seems to be a ratio between the physical and chemical components of the process which has to be satisfied in order to etch a pattern with good anisotropy. This ratio is obviously dependent on the process parameters chosen.

The quality of the etched walls also improved as shown in picture 5.1 and 5.2. Picture 5.1 (top) shows the effect of high ion bombardment. The sample was etched at low total flow rate and high CH_4 concentration. There is a lip formation at the top and at the bottom the etched wall is not perpendicular to the etched surface.

The pattern shows a curvature on the etched wall and it is generally very rough. This is thought to be due to the bombardment of the wall by back scattering ions. In contrast the sample which was etched at a higher total flow rate and therefore lower optimum CH_4 concentration showed a much better anisotropy and surface roughness (picture 5.1 (bottom)). Picture 5.2 shows the smoothness of the etched side walls for 20% (picture 5.2 (top)), and optimum concentrations of CH_4 (picture 5.2 (bottom)).

At low CH_4 concentrations, when the ion bombardment intensity was high, trenching occurred at the base of the etched walls. This is visible in picture 5.2 (top) and was due to the ions which were scattered from the side wall to the base, as shown in figure 5.7. This problem was removed when the CH_4 concentration was at its optimum. The trenching at the base of the etched wall is at a minimum. This was achieved by varying the total flow rate and the CH_4 volume concentration which affected the ion bombardment intensity as indicated by the change in DC self bias voltage. At optimum CH_4 volume concentration a change of about 10% was noted for V_{self} between the lowest and the highest set total flow rates. At highest total flow rate a change of about 3% was noted for V_{self} between the 20% and optimum CH_4 volume concentration.

7.3 The effect of power density and pressure

The effect of power density and pressure was investigated by keeping the total flow rate and the CH_4 volume concentration in H_2 constant. Figures 5.6 and 5.8 show the behaviour of etch rate R and DC self bias voltage V_{self}. At low power densities deposition occurs but as the power density increases etching is triggered. Further increases in power density increased R. At higher pressures the same pattern of etching was repeated except that deposition occurred up to a higher power density (figure 5.6 (a)). In figure 5.6 (b), the variation of R is plotted against pressure. Increases in pressure had no effect on R which remained constant until suddenly deposition

occurred (not shown in this graph). The same occurred for all selected power densities. This may be explained better when figure 5.8 is discussed where V_{self} is shown alongside R.

When pressure is constant and power density is increasing, the intensity of ion bombardment is also increasing, causing an increase in the transfer of kinetic energy to the surface. The intensification of ion bombardment is indicated by the increase in V_{self} as shown in figure 5.7 (a). However an increase in power density causes also an increase in the cracking of the gas molecules which supply the reactive species. This in turn will cause an increase in R because of higher ion bombardment intensity and increase in reactive species concentration.

At low power density the bombarding ions are not energetic enough and so as a result the kinetic energy transferred to the surface will be small. No reaction will take place between the deposited polymer film and the GaAs surface and so no volatile species will be created to escape from the surface. At higher pressures, higher power density is required to transfer the kinetic energy to the surface because the ion bombardment intensity will be lower.

The effect of pressure on ion bombardment is indicated in figure 5.8 (b). Although R remained constant at lower pressures, V_{self} was decreasing. Deposition occurred when V_{self} was at its lowest. This confirms the fact that ion bombardment is necessary to etch GaAs in CH_4/H_2 mixtures and there is a minimum value of V_{self} above which etching occurs and below which deposition follows. This is the triggering value of V_{self} which is dependent on process parameters.

The etch rate was not the only process variable which was critical. Anisotropy and side wall roughness were also of importance. Although the etch rate was constant at varying pressures, the anisotropy and side wall

conditions were not the same. Pictures 5.3 to 5.6 show the micrographs of the etched patterns. At a constant high power density the profiles of the etched samples at high and low pressure are different. Although not at optimum, the anisotropy at high pressure is much better than at low pressure because of the reduction in the ion back scattering to the side walls from the surface. In addition the trenching formed at the base of the etched wall is a little smaller because of the reduction in ion scattering from the side walls to the base of the walls. Figure 7.1 indicates the etched profile observed.

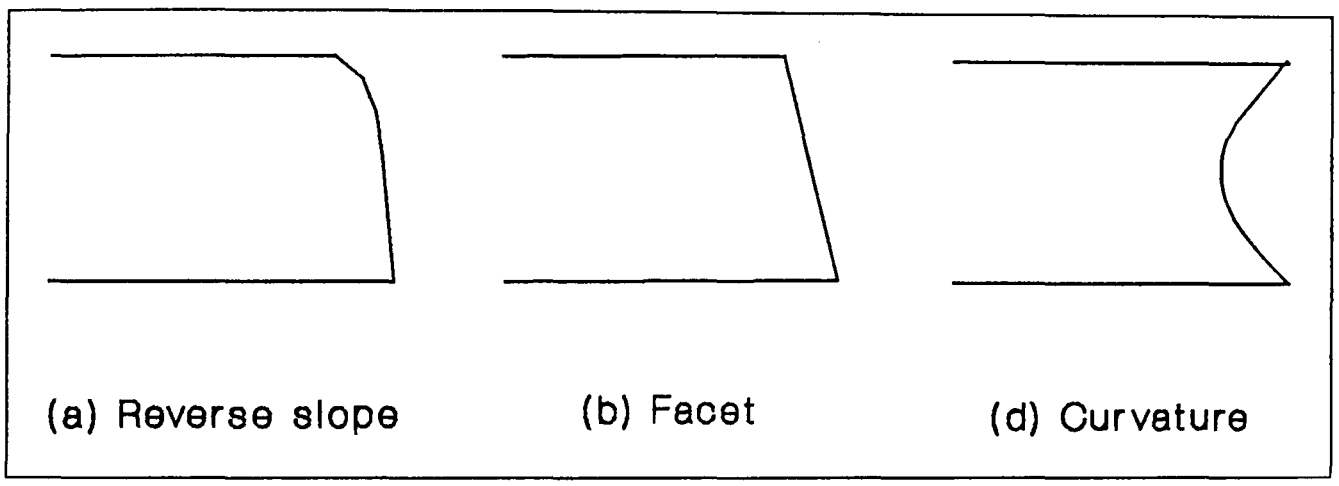

Figure 7.1. Selected etched patterns.

At low power density and low pressure the anisotropy showed reverse slope and the side wall was very rough. This is an indication of low intensity ion bombardment. At slightly higher power density and high pressure the anisotropic pattern transfer improved. However possible side wall deposition was observed.

The behaviour of the anisotropy is shown in figure 5.9 for varying power density and pressure. Generally anisotropy improves as the power density increases until it reaches an optimum and then further increase causes the deterioration of anisotropy as shown in figure 5.9 (a).

The behaviour of the etched anisotropy against pressure was a little more complex (figure 5.9 (b)). At very low power density and low pressure the

anisotropy was poor. However as power density increased slightly, anisotropy improved. Increase in pressure degraded anisotropy again. Further increases in power density improved anisotropy and increases in pressure did not effect anisotropy. At high power densities and pressures the anisotropy was poor but improved as pressure increased.

Generally high power density or low pressure causes high DC self bias voltage and hence high ion bombardment intensity. At a very low power density, because the ion bombardment intensity was low, the anisotropy was poor. When the power density increased the ion bombardment increased and so anisotropy improved. Increase in pressure caused a reduction in ion bombardment intensity and so caused poor anisotropy again. At optimum power density and pressure the best anisotropy was observed. Increases of pressure did not seem to have affected the anisotropy because although ion bombardment intensity decreased it was enough to keep the anisotropy the same. At high power density the anisotropy was poor when pressure was low because the ion bombardment intensity was so high that the ion back scattering from the surface caused etching of the wall and so facets were formed. Increase in pressure reduced ion bombardment back scattering and so anisotropy improved.

The linewidth of the etched sample for optimum conditions was about the same as the linewidth of the mask before etching. Increase in power density increased linewidth (linewidth loss, see chapter three). Increase in pressure caused a decrease in linewidth (linewidth gain, see chapter three). The loss of linewidth was due to the ion bombardment intensity which caused a back scattering from the surface and hence formation of facet side walls. The gain of linewidth was possibly caused because of the polymer formation over the edge of the mask.

7.4 Carbon polymerization

When III-V compounds are etched in CH_4/H_2 mixtures, a thin film layer is always deposited on the surface of the masking material. This layer is more apparent when an inorganic mask such as Si_3N_4 or SiO_2 is used. Generally it is best to achieve the highest etch rate with minimum deposition. The deposition rate against total flow rate was shown in figure 5.3 (b) for optimum CH_4 concentration. The deposition decreased as the total flow rate increased and this was due to the reduction of CH_4 volume concentration and reduction in residence time of the gas mixture.

Figure 5.11 (a) to (d) shows the graph of carbon polymer deposition rate and thickness of mask removed from the surface against the CH_4 volume concentration in H_2. In all cases the carbon deposition rate increases sub-linearly as the volume concentration of CH_4 increases. The carbon deposition rate was reduced due to the increase in total flow rate. The deposition rate of the carbon layer was about six to seven times lower than the etch rate.

The thickness of the mask removed was reduced as the CH_4 volume concentration increased. This was due to the protection provided by the deposited carbon film. At optimum concentration of CH_4 and total flow rate the thickness of the mask removed was a few nanometres. The rate of mask removal was not calculated because it is thought that the mask removal occurred only at the beginning of the etching process when no protective film was present on the mask.

The effects of power density and pressure are shown in figure 5.12 (a) and (b) respectively. It seems that as power density increased the deposition rate of the carbon polymeric film decreased. It is thought that the deposition rate of the polymeric film should increase as the power density increases. The cracking of the CH_4 species should cause a higher density of carbon based

polymeric species to deposit on the surface. In this case the intensity of ion bombardment is such that any increase in power density would cause a high value of DC self bias voltage which indicates a large increase in ion bombardment intensity. Therefore the actual deposition rate, based on the measured thickness of the carbon polymeric film, decreases due to sputtering of that film. However the effect of pressure on deposition of this polymeric film is as expected. The increase in pressure increased the deposition rate because first, the density of polymeric species increased in the chamber and second, the DC self bias voltage reduced which indicated a reduction in ion bombardment intensity. Therefore reduction in the sputtering of the deposited carbon polymeric film was observed.

The effect of ion bombardment is more apparent when the influence of power density and pressure is examined for the thickness of mask removed, (figure 5.13 (a) and (b) respectively). The polymeric film does not seem to react with the mask and as a result there is only a deposition of the polymeric film rather than a reaction producing volatile species which would result in etching. As protection of the mask material by the polymeric film is not instantaneous, the removal of mask at the beginning of the process will be by sputtering only. The amount of mask sputtered will show the severity of the ion bombardment. This is another way of looking at intensity of ion bombardment which will confirm the evidence of DC self bias voltage. The etched mask thickness increases as the power density increases indicating an increase in sputtering. This is the same at all pressures. However the increase in pressure has the opposite effect. This is as indicated by the DC self bias voltage behaviour discussed in chapter four.

The polymeric film was analyzed using an energy dispersive x-ray system (EDX). The surface of the etched sample after exposure to oxygen plasma did not show any extensive carbon contamination compared with the standard sample. The sample which had a polymer film deposited all over

the surface and was not exposed to oxygen plasma did show extensive carbon polymerization (figure 5.14 (a) to (d)).

When the surface of a GaAs sample was compared with its mask before exposure to oxygen plasma, the GaAs surface did show a very small increase in carbon compared with that of the standard. This may have been due to the inhibitor film on the surface which was not yet removed. The surface of the mask however showed a very large carbon peak compared with the standard sample (figure 5.15 (a) to (c)).

A carbon polymeric film forms on all surfaces during the process, but the effect on the mask surface is different from that on the exposed horizontal semiconductor surface. The kinetic energy of the ions and the reactive species from the plasma combine to react with and etch the semiconductor surface. On the mask the chemical reaction does not take place. Hence the build-up of the carbon polymer and its identification after etching. A film may also form on the side walls as etching proceeds. This may protect the wall to provide good anisotropic pattern transfer.

The EDX analytical system could not detect hydrogen, as discussed in chapter five. When the polymer film was analyzed (Hayes[b] et al., 1989), the majority of the species were C_xH_y where x could be as high as 12 but y was either 0 or 1 (i.e. H_0 indicates no H exists). It was suggested that light elements such as CH to CH_3 could not perhaps be detected. However it was evident that there was an abundance of carbon in the polymer. This information will be used here in a later section of this chapter when a mechanism is suggested.

7.5 AlGaAs etching

The effect of variation of the relative aluminium (Al) content in aluminium gallium arsenide (AlGaAs) was investigated (figure 5.16). The etch rate

decreased as the Al content increased. The etching of AlGaAs was investigated for SiO_2 and Si_3N_4 masks and these masks gave similar results at the operating conditions.

The reason for using Si_3N_4 was the possibility that the Al in AlGaAs may react with the oxygen in SiO_2 and create Al_xO_y which is hard to etch. If this is the case it did not manifest itself for the conditions under which the experiments were carried out. Perhaps it may be possible to etch AlGaAs and GaAs non-selectively in a mixture of CH_4/H_2 but the conditions for this may require a reduction in partial pressure of oxygen and water vapour, as was discovered for etching in Cl_2 plasma (Vawter, et al., 1987).

Generally it was shown that as the content of Al in AlGaAs increases the etch rate decreases until deposition of polymer occurs instead of etching. The ion bombardment intensity remained the same as indicated by DC self bias voltage because the conditions remained fixed. It is therefore possible that for the conditions under which these experiments were carried out the Al was mainly removed physically.

7.6 Loading effect and uniformity of the process

The loading effect of the GaAs was investigated by increasing its area and yet keeping the masked area constant (figure 5.17). The etch rate decreased as the GaAs area increased but the carbon deposition rate remained constant. The decrease in etch rate was due to the loss of reactive species because of their reaction with the surface of the etchable material. As the generation rate of the reactive species was constant (set by the process parameters), when the area of the etchable material increased the concentration of available reactive species is reduced due to reaction and hence a decrease in etch rate occurs. The deposition rate on the mask material remained the same because this was not dependent on the rate of generation and loss of the reactive species.

Generally the micrograph of the two-inch etched sample showed poor anisotropy of the etched walls, the onset of trench formation at the base of the etched walls, and side wall roughness (Picture 5.7 (top) and (bottom)). These features are characteristic of etching in CH_4/H_2 plasma when there are low amounts of reactive species present (reduction in the chemical etching mechanism).

When a two-inch wafer was etched and the etch rate was measured across the diameter for uniformity variations (figure 5.18), the etch rate at the centre was seen to be lower than that at the edges. This was because the gas entered the chamber radially and hence the reactive species reached the edges of the GaAs wafer first. The reaction started at the edges of the wafer before the centre. This is mainly because of the chemical component of the etching mechanism. Figure 4.8 shows the etch rate against distance from the centre of the electrode when 100% H_2 was used. It is thought that the hydrogen etched GaAs largely by a physical mechanism at 13.56 MHz. The etch rate was uniform and hence the electric field was uniform across the electrode.

7.7 Heating effect and reproducibility of the process

The problem of cathode heating is very important because the temperature increase which was caused by the power density and ion bombardment affected the etch rate. The cathode did not have a cooling system and therefore its temperature was not controllable. Consequently the increase in the set time of the etching caused a gradual increase in temperature which caused an increase in etch rate, (figure 5.19).

The relation between the etch rate and temperature is shown by equation 1.2. The etch rate was not plotted against temperature in this case because the temperature could not be controlled. It was increasing with elapsed time.

The reproducibility of the etch rate was excellent. Etch rate remained constant at set process parameters for the period which was designated for the reproducibility test. The DC self bias voltage was reduced slightly. This was due to the condition of the process chamber. The processing of GaAs in CH_4/H_2 mixtures caused the deposition of carbon polymers on the chamber walls and the cathode.

The small decrease in DC self bias voltage during the middle of the reproducibility test was due to the dirtiness of the chamber. This value returned to normal when the chamber was cleaned. The condition of the chamber can affect the DC self bias voltage and in extreme cases a relatively large drop may result in deposition of carbon polymers on the GaAs sample rather than etching of the surface. This is due to the reduction in the kinetic energy transferred to the surface of the sample. The effect of contamination of the chamber on DC self bias voltage and hence reduction in ion bombardment intensity was discussed in chapter four for various conditions.

7.8 The technique for RIE of GaAs in CH_4/H_2 Plasma

The technique discussed here for RIE of GaAs in CH_4/H_2 mixtures may be used to etch at higher pressures allowed by RIE to yield the optimum results which were found for that at lower pressure. The reason was to indicate that the important parameters in etching in such mixtures are the DC self bias voltage and the residence time of the gas mixture.

Unfortunately the problem of uncontrollable cathode temperature caused the result to be rather different from that which was expected. To prove that the result was different because of temperature, another technique was demonstrated.

It is accepted that the set process parameters are generally power density

(P_d), pressure (p), total flow rate (Q) and percent volume concentration of CH_4 ($V_{\%methane}$). The sample area and the cathode temperature are also important. It was however shown that the pressure had no effect on etch rate until V_{self} decreased below the etch trigger value (figure 5.8). Only etch rate remained independent of pressure above the V_{self} trigger value. The profile of the etched pattern and the side wall smoothness did show some dependence on pressure. This was considered to be caused by the imbalance between the chemical and physical components of the etching mechanism.

The process parameters for optimum etching were established during the etching procedures. V_{self} and the residence time (τ) of the gas mixture were recorded. To keep the etch rate the same and the profile as anisotropic with smooth side walls as that achieved for optimum condition, it was considered that V_{self} should be kept constant when pressure increased, such that the ion bombardment intensity would remain the same as for optimum condition. $V_{\%methane}$ was also kept constant but the increase in pressure caused an increase in the number of molecular species. To keep the value of V_{self} constant for increasing p the value of P_d had to increase. This meant that there would be an increase in the cracking of the molecular species also. Increase in p also caused an increase in τ. The value of τ was also reduced by increasing the total flow rate, to the value found for the optimum condition such that the deposition of polymeric species and their reaction with the surface was kept at optimum.

Figure 5.21 (a) and (b) shows the etch rate and the measured cathode temperature with applied power density and total flow rate against pressure for keeping V_{self} and τ constant. The etch rate was expected to be constant but in this case it increased with the increasing pressure. The reason for this was that the temperature was increasing due to the necessity for increasing the power density to keep V_{self} constant. If the cathode temperature could have been controlled such that it was constant than constant etch rate would have been possible.

To prove that the increase in etch rate was due to temperature a second technique was devised to test the behaviour of the etch rate against pressure. Generally all conditions stated above were satisfied except that $V_{\%methane}$ was varied. To reduce τ, total flow rate was increased by increasing only the H_2 flow and keeping the CH_4 flow constant. This was necessary because as the P_d increased, V_{self} increased significantly when the H_2 concentration was high in the mixture, (see DC self bias voltage in chapter four).

Figure 5.22 (a) and (b) shows the variation of etch rate, temperature, applied power density and total flow rate against pressure for the conditions set above. The etch rate was lower than that expected in the beginning, but this was due to the fact that the CH_4 concentration was lower. The etch rate generally increased with increasing pressure as before but the rate of increase was much lower than that found for the first technique. The temperature was slightly lower than before because less power density was required to keep the value of V_{self} constant with increasing pressure.

It is therefore considered that the increase in etch rate was due to increase in cathode temperature and if this was kept constant the etch rate and anisotropy together with side wall smoothness may have been consistent with the optimum values. This is not dependent on the RIE etching system. The process parameters must first be used to find the optimum V_{self} and τ which can then be used to optimise etching at all pressures. This is thought to be possible only for RIE in CH_4/H_2 mixtures because of the independence of etch rate with pressure.

7.9 Electrical characteristics

The current-voltage relation of the diodes was dependent on the process characteristics used for etching. The ideality factor (n) and barrier height (ϕ) of the diodes are shown in figure 6.1. The high n value of the control

sample was due to its high carrier concentration (Madams et al., 1975 and Sze, 1981). The n value decreased when the sample was etched in pure H_2. This may have been due to the passivation effect near the surface.

The CH_4/H_2 etched sample also showed a decrease in the n value but not as much as when pure H_2 was used. The annealed sample recovered the original n value. In this case the carriers were recovered, possibly by repair of the crystal damage or out-diffusion of hydrogen. The difference of n value between the H_2 etched and CH_4/H_2 etched sample is not thought to be due to a reduction in H_2 volume concentration in CH_4 but to a reduction in the value of DC self bias voltage hence reduction in ion bombardment intensity and causing less damage.

The breakdown voltage increased to its highest value when the sample was etched in H_2 plasma and when etched in CH_4/H_2 mixture it also increased but not as much as for a H_2 plasma. The annealing reduced the value of breakdown voltage to its original value within the limits of experimental error (figure 6.3 (b)).

The ϕ value for the control sample was rather high for a gold front metal Schottky diode. This was considered to be due to Fermi level pinning (Spicer et al. 1980 and 1982). The H_2 and the CH_4/H_2 etched samples indicated a higher ϕ value but the annealed sample displayed no recovery. The reverse of this was observed for the saturation current (I_o) (figure 6.2 (a)), from which ϕ was calculated.

The threshold voltage also increased when etched in H_2. A large decrease in its value was observed when the sample was etched in a CH_4/H_2 mixture but this value was not as low as that found for the control sample. The annealed sample did not show any improvement compared with the sample which was etched in the mixture and not annealed.

In the case of the barrier height, the saturation current and the threshold voltage, the changes were due to the passivation of the carriers but the problem of non-recovery of the annealed sample may be connected with the surface modification of the sample after etching. After referring to the literature, it was found that when InP was etched in a mixture of CH_4/H_2, an indium rich layer was left on the surface after etching (Hayes[b] et al. 1989). The depth of this layer was found to be about 5 to 7.5 nm. In the present case it is possible that a gallium-rich layer was left on the surface causing the non-recovery of certain electrical characteristics. No degree of annealing could replace the arsenic which was lost from the gallium-rich layer.

The reverse current of the control sample was very high. However after RIE in a pure H_2 and CH_4/H_2 mixture, the reverse currents decreased with the latter showing a better improvement. The annealed sample showed the best improvement of all. It is likely that the annealing may have repaired the crystal damage caused by the RIE and, possibly, damage which was present before RIE.

The capacitance-voltage measurements revealed some of the reasons why the processed samples behaved in this way. The carrier concentration and depletion width at zero volts indicated large changes between the control and the processed samples. The carrier concentration decreased by about a factor of 100 for the sample etched in pure H_2. This was a little less for the sample etched in CH_4/H_2 mixture. Depletion width increased also for the samples etched in pure H_2 and a mixture of CH_4/H_2 with the latter showing a smaller increase. For the carrier concentration, the annealed sample showed a complete recovery. For depletion width there was not a total recovery. A very small difference was apparent between the annealed and the control sample (figure 6.4).

The graph of carrier concentration against depletion width revealed the

degree of damage in the semiconductor (figure 6.5). If the in-diffusion of the hydrogen ions was only a few nanometres due to the low etching temperature, then the extent of the damage to the semiconductor was due to large bond damage and dislocations. The difference between the depletion width of the annealed sample and the control was about 14 nm. This could be the result of a gallium- rich layer on the surface. The width is nearly twice that reported (Hayes[b] et al. 1989), but in this case the DC self bias value which indicates the severity of ion bombardment was more than twice as much.

7.10 A model for the mechanism of etching

It was discovered that when CH_4/H_2 mixtures are used for etching GaAs a carbon polymeric film is deposited on the masking material. This film is deposited everywhere on the semiconductor material but it probably reacts with the GaAs surface to produce volatile species which then escape the surface resulting in etching of the sample.

Through experimentation it was discovered also that the ion bombardment played an important role in etching the surface as indicated by DC self bias voltage. Ion bombardment not only caused etching to occur but the anisotropy of the etched sample together with its etched side wall roughness was dependent on the intensity of ion bombardment. For very low ion bombardment, deposition of a carbon polymeric film on the semiconductor was apparent. Therefore it is safe to assume that the kinetic energy from the ions was transferred to the polymeric film which then reacted with the surface of the GaAs to produce the volatile species.

There are other effects as well. The polymeric film could be depositing on the etched side walls so that it could protect the surface from the scattered ions. The polymeric film could act as a passive film helping anisotropic pattern transfer.

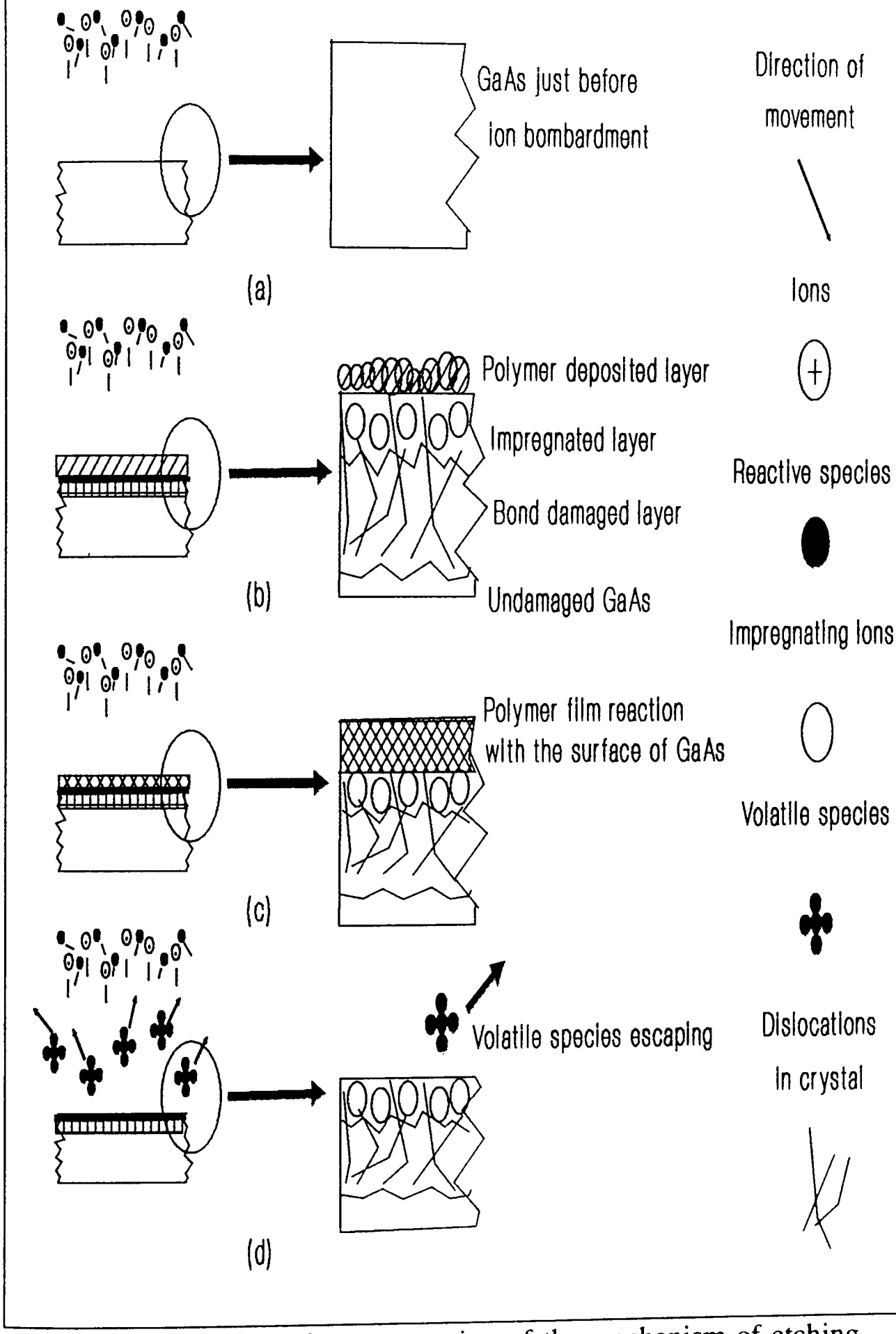

Figure 7.2. Pictorial representation of the mechanism of etching. (a) Just before start, (b) deposition, (c) reaction and (d) etching.

Figure 7.2 is a pictorial representation of the mechanism of etching. Figure 7.2 (a) represents the GaAs sample in the plasma chamber just before ion and radical attack. Figure 7.2 (b) shows the deposition of a polymeric film and ion impregnation with dislocations extending deep into the semiconductor. Figure 7.2 (c) indicates the reaction of the film with the surface and finally figure 7.2 (d) represents the escape of the volatile species formed.

Another important factor is the damage caused by the ion bombardment. This was discovered from the electrical measurements. It has been argued that the passivation of the Zn dopants in p-GaAs is due to trapping of hydrogen ions by these centres (Dautremont-Smith, 1988). The argument was true in their case because the sample temperature was kept at about 300°C. However in the present work the temperature was much lower (not exceeding 60°C). It is suggested that in this case the hydrogen impregnation would not extend more than 10 nm*, specially at low ion accelerating voltages, (DC self bias voltage of was less than -1000 V). If this is true the passivation of carriers in this case is caused by the dislocations and crystal bond damage due to collisions at the surface which extend into the bulk of the semiconductor. Therefore it is possible that in this case the ion bombardment of the surface produces bond damage extending deep into the semiconductor and that the broken bonds near the surface are hydrogenated causing the formation of some volatile species which will escape from the surface.

Therefore the mechanism of etching is a combined physical and chemical with both sub-mechanisms, inhibitor-driven ion-assisted etching, and energy-driven ion-enhanced etching working together. The carbon polymeric film would probably react with both gallium and arsenic to form methyl

---

* - Private communication with Dr. A. A. Rezazadeh, Department of Electronic and Electrical Engineering. King's College, London.

volatile species, after the ions supply enough kinetic energy to the surface whereas arsenic would react with hydrogen to form hydride volatile species after the surface lattice bonds were damaged by the ions.

Next the formation of species will be formalised. It will be divided into two parts. First, the possible species created in the plasma and then, the reaction on the surface which would create the possible volatile species.

In the chamber before the plasma was struck CH_4 and H_2 were present. When the plasma was struck the possible species were formed either from hydrogen or from methane. In case of hydrogen the species formed were,

$$H_2 + e \rightarrow H + H + e$$

$$H_2 + e \rightarrow H_2^+ + 2e$$

$$H + e \rightarrow H^+ + 2e$$

for methane the species formed were,

$$CH_4 + e \rightarrow CH_3 + H + e$$

$$CH_4 + e \rightarrow CH_4^+ + 2e$$

$$CH_3 + e \rightarrow CH_2 + H + e$$

$$CH_3 + e \rightarrow CH_3^+ + 2e$$

$$CH_2 + e \rightarrow CH + H + e$$

$$CH_2 + e \rightarrow CH^+ + 2e$$

$$CH + e \rightarrow C + H + e$$

$$CH + e \rightarrow CH^+ + 2e$$

$$C + e \rightarrow C^+ + 2e$$

$$H + e \rightarrow H^+ + 2e.$$

There are many other reactions such as excitation of the species and reaction between the radicals and the ions (Tachibana et al. 1984). Etching of GaAs occurs when carbon polymeric species deposit on the surface of the semiconductor. The analysis of the deposited species showed an

abundance of carbon rather than hydrogen (Hayes[b], et al., 1989).

The reaction on the surface may be as follows;

$$\left[a\sum_{\alpha=0}^{4} CH_{\alpha}+b\sum_{\beta=1}^{2} H_{\beta}\right]_{Gas} \rightarrow \left[a\sum_{\alpha=0}^{4} CH_{\alpha}+b\sum_{\beta=1}^{2} H_{\beta}\right]_{Surface} \qquad \text{(C7.1)}$$

where Σ implies that the sum is taken over all constituent species in the plasma playing a role in etching the GaAs. From here the kinetic energy of the bombarding ions is needed to cause reaction between the carbon polymeric film and the GaAs surface. Ion bombardment is also necessary to damage the bonds to make surface reaction of the GaAs easier. The most probable reaction on the surface may happen between the carbon polymeric species and it may be as follows:

$$\left[a\sum_{\alpha=0}^{4} CH_{\alpha}+b\sum_{\beta=1}^{2} H_{\beta}\right]_{surface} \rightarrow \qquad \text{(C7.2)}$$

$$\left[c\sum_{\sigma=1}^{m}\sum_{\eta=0}^{n} C_{\sigma}H_{\eta}\right]_{surface} + \left[d\sum_{\delta=1}^{2} H_{\delta}\right]_{\substack{implanted+\\ free\ radical}}$$

Next a reaction may occur between the GaAs and the polymeric film as follows;

$$\left[c\sum_{\sigma=1}^{m}\sum_{\eta=0}^{n} C_{\sigma}H_{\eta}\right]_{surface} + \left[d\sum_{\delta=1}^{2} H_{\delta}\right]_{\substack{implanted+\\ freeradical}} + x\,GaAs \rightarrow \qquad \text{(C7.3)}$$

$$\left[g\sum_{\gamma=1}^{3}\sum_{\psi=1}^{3} Ga\,(CH_{\psi})_{\gamma}+l\sum_{\lambda=1}^{3}\sum_{\pi=1}^{3} As\,(CH_{\pi})_{\lambda}+r\sum_{\rho=1}^{3} AsH_{\rho}\right]_{surface}$$

and then,

$$\left[g\sum_{\gamma=1}^{3}\sum_{\psi=1}^{3} Ga(CH_{\psi})_{\gamma} + l\sum_{\lambda=1}^{3}\sum_{\pi=1}^{3} As(CH_{\pi})_{\lambda} + r\sum_{\rho=1}^{3} AsH_{\rho}\right]_{surface} \rightarrow$$

$$\left[g\sum_{\gamma=1}^{3}\sum_{\psi=1}^{3} Ga(CH_{\psi})_{\gamma} + l\sum_{\lambda=1}^{3}\sum_{\pi=1}^{3} As(CH_{\pi})_{\lambda} + r\sum_{\rho=1}^{3} AsH_{\rho}\right]_{gas} \quad \text{(C7.4)}$$

and there may be a small reaction on the surface from the radicals presented in equation C7.1. This will be as follows;

$$\left[a\sum_{\alpha=0}^{4} CH_{\alpha} + b\sum_{\beta=1}^{2} H_{\beta}\right]_{surface} + z\,GaAs \rightarrow$$

$$\left[f\sum_{\phi=1}^{3}\sum_{\mu=1}^{3} Ga(CH_{\mu})_{\phi} + t\sum_{\tau=1}^{3}\sum_{\epsilon=1}^{3} As(CH_{\epsilon})_{\tau} + u\sum_{\omega=1}^{3} AsH_{\omega}\right]_{surface} \quad \text{(C7.5)}$$

The next step of the reaction is as C7.4.

$$\left[f\sum_{\phi=1}^{3}\sum_{\mu=1}^{3} Ga(CH_{\mu})_{\phi} + t\sum_{\tau=1}^{3}\sum_{\epsilon=1}^{3} As(CH_{\epsilon})_{\tau} + u\sum_{\omega=1}^{3} AsH_{\omega}\right]_{surface} \rightarrow$$

$$\left[f\sum_{\phi=1}^{3}\sum_{\mu=1}^{3} Ga(CH_{\mu})_{\phi} + t\sum_{\tau=1}^{3}\sum_{\epsilon=1}^{3} As(CH_{\epsilon})_{\tau} + u\sum_{\omega=1}^{3} AsH_{\omega}\right]_{gas} \quad \text{(C7.6)}$$

where all the Greek letters from α to ω and Latin lower case letters from a to z are integers with m>n. The above is the proposed model of the mechanism of etching for GaAs. In case of AlGaAs the Al content is removed by a physical mechanism (i.e. ion sputtering), hence the argument for deposition of a carbon polymeric film on the semiconductor when the Al content increases in the sample.

CHAPTER 8
CONCLUSIONS AND RECOMMENDATIONS

In this chapter conclusions to RIE of GaAs in methane/hydrogen plasma will be presented and recommendations for continuing this work will be suggested.

8.1 Conclusions

By monitoring the DC self bias voltage and using the method of total flow control described in previous chapters, CH_4/H_2 gas mixture was successfully used to etch GaAs surface. The final etched surface showed an anisotropy of better than 87° with smooth etched surface and side wall, and minimal or no trenching at the base of the etched walls. Deposition of a carbon polymeric film on the surface of the inorganic mask protected it from erosion. Some of the damage induced on the p-GaAs due to CH_4/H_2 RIE was repaired after annealing.

A combined physical and chemical mechanism of etching of GaAs was possible only when CH_4/H_2 mixtures were used. When Ar was substituted instead of H_2 or CH_4, the etching was dominated by a physical mechanism only. The etch rate increased as the volume concentration of CH_4 in H_2 increased.

When the etch rate reached an optimum level at a specific CH_4 volume concentration, further increases of volume concentration of this gas caused a decrease in etch rate accompanied by carbon polymer deposition over the GaAs surface. After an initial increase, the DC self bias voltage decreased when the volume concentration of CH_4 increased, indicating a reduction in ion bombardment intensity.

Carbon polymeric deposition occurred on all surfaces during the process, but the effect on the mask surface was different from that on the exposed GaAs surface. The kinetic energies of the bombarding ions and the reactive species formed in the plasma combine to etch the GaAs surface due to certain chemical reactions. The chemical reactions did not take place on the inorganic mask and hence the build up of polymeric film occurred on the mask.

The increase in the total flow rate of the gas mixture did not affect the etch rate of the GaAs at optimum CH_4 volume concentration. The deposition rate of the carbon polymeric film was reduced when the total flow rate of the gas mixture increases.

At an arbitrary CH_4 volume concentration lower than the optimum level, the etch rate increased with increasing total flow rate. If the pumping speed of the vacuum system allowed, as the total flow rate increased the etch rate would have reached a maximum and then any further increases in the total flow rate would have caused a decrease in etch rate. The DC self bias voltage decreased with increasing total flow rate.

The anisotropy improved with increasing total flow rate as long as the CH_4 volume concentration was not set above the optimum level. The roughness of the etched surface was very low in all cases. The etched side walls showed the best smoothness at the optimum volume concentration of CH_4 and high total flow rates. The trenching at the base of the etched walls was formed at high DC self bias voltage.

The etch rate increased with increasing power density. The DC self bias voltage also increased with increasing power density. The pressure had no effect on etch rate until polymerization of the GaAs surface occurred. The DC self bias voltage decreased with increasing pressure.

The best anisotropy was achieved at optimum power density and pressure, and any divergence from optimum conditions resulted in imperfect anisotropy. The linewidth of the etched patterns was conserved at optimum conditions. Any change in the power density and pressure caused a loss or gain in linewidth. Generally, an imbalance between the chemical component and physical component caused a divergence from optimum pattern transfer.

Increase in the volume concentration of CH_4 increased the carbon polymerization rate on the inorganic masking material. At the same time the rate of removal of the masking material decreased as the polymerization rate increased. Polymerization on the surface of the mask reinforced it such that continuous etching of the GaAs was possible for long periods.

Increase in power density decreased the carbon polymeric film deposition rate and increased the quantity of mask removed from the surface of the GaAs. Increase in pressure increased the carbon polymeric film deposition rate and decreased the quantity of mask removed.

On all GaAs samples there were minute traces of oxygen and carbon because of the exposure to atmosphere. However an abundance of carbon was detected on the inorganic mask after etching and on the entire surface of the samples which were deposited with the polymeric film.

An increase in the aluminium content in AlGaAs decreased etch rate until carbon polymeric film deposition occurred on the entire surface. Different inorganic masks such as SiO_2 and Si_3N_4 had no effect on etch rate for the same conditions of etching.

At the set conditions of etching a loading effect was observed for samples larger than 1 cm^2. Samples with area smaller than 1 cm^2 did not show any loading effect. Rough etched side walls, trenching and divergence from anisotropy were observed when a piece of GaAs larger than 1 cm^2 was

etched. The carbon deposition rate on the mask was constant as the area of etching increased.

The reproducibility of the etching procedure was excellent. The uniformity of etched patterns across the wafer and the temperature dependence of etching of the wafer were dependent on the system design and independent of CH_4/H_2 process performance.

As long as the substrate area and temperature were kept constant, the process variables such as etch rate and anisotropy were reproducible at different pressures as long as the DC self bias voltage, residence time and CH_4 volume concentration in H_2 were kept the same as those found at optimum conditions

The use of H_2 and CH_4/H_2 for etching GaAs has a profound effect on this semiconductor. This is mainly due to the presence of hydrogen in both H_2 and CH_4. The damage to GaAs however could be partially or completely repaired by annealing it in N_2 gas at 400°C and atmospheric pressures.

The ideality factor of highly doped p-GaAs Schottky diodes decreased when etched in H_2 or CH_4/H_2 plasmas. However it recovered after annealing.

The barrier height of the sample increased after etching in H_2 or CH_4/H_2 plasmas and annealing did not cause recovery.

The breakdown voltage of the samples increased after etching in H_2 or CH_4/H_2 plasmas. Annealing only partially recovered the original value.

The reverse current improved after etching in H_2. It further improved when etched in CH_4/H_2. After annealing, it reached its lowest best value.

The carrier concentration near the surface of GaAs after etching in H_2 and CH_4/H_2 plasmas was reduced because of the passivation of acceptors. The case of the H_2 etched sample was a little more severe than that of the CH_4/H_2 etched sample. Annealing caused a complete recovery of the carriers.

The depletion width at zero bias of the Schottky GaAs diode increased after etching in H_2 and CH_4/H_2 plasmas because of the passivation of acceptors. The case of the H_2 etched sample was more severe than that of the CH_4/H_2 etched sample. Annealing caused a partial recovery of the depletion width at zero bias.

The damage extended to about 0.3 μm in the p-GaAs after RIE in CH_4/H_2. The extent of damage was caused by dislocations to the crystal structure rather than H in-diffusion. The degree of this damage was dependent on the severity of ion bombardment.

The difference between the depletion width at zero bias of the etched-annealed sample and the control sample was probably caused by a gallium-rich layer at the surface of the CH_4/H_2 etched sample.

Combined physical and chemical mechanism of etching GaAs occurred. In this case both sub-mechanisms were at work. They were the inhibitor-driven ion-assisted etching and energy-driven ion-enhanced etching.

The carbon polymeric film deposited on the entire surface of the sample reacted with the GaAs due to the transfer of the kinetic energy of the bombarding ions to the surface (inhibitor-driven ion-assisted). The probable volatile species produced in this reaction were methyl gallium and methyl arsenic.

The ions also damaged the crystal lattice and the damaged bonds then reacted with the hydrogen radicals (energy-driven ion-enhanced). The probable volatile species involved were arsenic hydrides.

8.2 Recommendations for further work

The project can continue in at least four different paths. They are; (1), use of other carbon containing gases instead of methane and use of oxygen as an admix gas, (2), use of new etching systems, (3) further electrical characterization and (4), surface and bulk analysis.

8.2.1 Use of other non-chlorinated gases

There are three areas where this can be done. They are; (1), the use of CO or CO_2 instead of CH_4 in the gas mixture to observe if etching is possible, (2), the use of oxygen (O_2) in the mixture, to investigate if these gases help GaAs etching and (3), electrical characterization of samples etched in such conditions.

If combined physical and chemical etching with CO is possible it may be replaced by CO_2 which is not a flammable gas. It may show also that CH_x species formed from cracked CH_4 do not necessarily react with GaAs to etch the surface, and in fact CH_x will form on the surface after C deposition and then will react with the GaAs surface.

The use of O_2 in the mixture to observe if this gas will help the etching of GaAs. At the mtorr range of base pressures there is some oxygen and water vapour present. The partial pressure of both O_2 and H_2O could be high in the chamber during RIE and these may help etching. If there is a reaction and etch rate increases, there may be a different mechanism involved which should be investigated.

Electrical characterisation of a wafer etched in such plasmas can be useful. In this case a larger number of diodes can be fabricated on the processed wafer and therefore a larger statistical sample for current-voltage (I-V) and capacitance-voltage (C-V) measurements can be obtained.

8.2.2 Use of other etching systems

Other etching systems could be used for GaAs etching in CH_4/H_2 mixtures, such as electron cyclotron resonance-reactive ion etching system (ECR-RIE) and radio frequency-reactive ion beam etching system (RF-RIBE).

The ECR-RIE could be used to etch GaAs in CH_4/H_2 mixtures at very low DC self bias voltage (V_{self}). This is possible because in such systems V_{self} can be independently controlled. The microwave power can be increased so that more radicals can be produced, at the same time the RF power can be reduced such that the DC self bias voltage could be decreased to a minimum. The electrical characterization of GaAs samples etched in ECR-RIE system is important because damage to the crystal lattice due to ion bombardment can be shown at different DC self bias voltages and microwave power densities. The depth of passivation of carriers may be reduced by setting very low DC self bias voltages.

The RF-RIBE system could also be used for etching GaAs. This is important as the production of the species will be the same as that produced by the RIE system because the RF source used is the same, operating at 13.56 MHz. The use of RF-RIBE is necessary because an important objective of research in this field would be the identification of the volatile species after etching. No paper has been seen to date about the identification of possible metal-organic etched species on a GaAs surface. Generally the RIBE operating pressure is lower by an order of 10 to 100 times than that of RIE. There is a possibility that the species may be detected at such pressures and also, as the plasma is not in the same

chamber as the sample, the species life time may be longer due to the confinement of the plasma.

8.2.3 Electrical characterization

The optimum CH_4 volume concentration in H_2 alters when process parameters are varied. This includes changes in temperature and area of the substrate. For this reason a systematic program of experimentation should be carried out to characterize electrically the GaAs samples which where etched under different conditions. For this, both I-V and C-V techniques can be used to characterise a large number of diodes fabricated on the etched n and p type GaAs samples. This could be performed at different temperatures, including at room temperature (300 K), liquid nitrogen temperature (77 K) and liquid helium temperature (4 K). Also deep level transient spectroscopy (DLTS) can be performed.

Both n and p type GaAs etched samples could be compared for ideality factor and barrier height values. These could be measured as a function of depth. After RIE, diode fabrication and electrical measurements, the diodes on the surface and a layer from the surface of the sample (about 25 nm) could be removed by wet etching. Diodes could then be fabricated on the same sample again and electrical measurements taken. Annealing of the samples is also important. The samples could be annealed either isochronally or isothermally. In the case of isochronal annealing the samples etched at the same conditions could be annealed at different temperatures for constant time. For the case of isothermal annealing the samples which were etched at the same conditions could be annealed at the same temperature but for different times.

Generally good annealing should be possible for both cases. For the case of isochronal annealing damage to the semiconductor should be repaired at high temperature but short time. For the later case the temperature of

annealing could be low but the time of annealing would be long.

8.2.4 Surface and bulk analysis

It is important to analyze the surface and bulk of the etched GaAs samples. There are methods for detecting surface deposition, impregnation of semiconductors by foreign constituents and amorphous layers. Many methods are available. These include Auger electron spectroscopy (AES), high resolution transmission electron microscopy (HR-TEM), scanning tunnelling electron microscopy (STEM) and light element elastic recoil detection analysis (LE-ERDA).

AES could be used for investigation of surface deposition. In this case the deposited film would be a carbon or hydrocarbon polymeric film on the surface due to CH_4 plasma. AES could detect elemental carbon but not hydrogen. If the surface of the semiconductor sample is gallium or arsenic-rich, this method can show it up to a certain distance from the surface so some indication of amorphous layer depth and stoichiometric disturbance could be detected near the surface.

HR-TEM could be used to take micrographs of the amorphous and disturbed layer. GaAs etched at different conditions could be used for this method to discover the depth of the damaged layers.

STEM could be used for surface roughness measurements. Techniques such as surface profiling and scanning electron microscopy (SEM) are not able to show accurate roughness of the surface of the CH_4/H_2 etched samples. This is because the surfaces of the GaAs samples etched in such mixtures are very smooth and the sensitivity of such instruments cannot determine the roughness. It may be possible to use the STEM technique because it can be sensitive to atomic layers on the surface.

The LE-ERDA system can be used to detect hydrogen up to 2 μm into the GaAs bulk. This method is a kind of Rutherford back scattering system. The helium ions may knock any light element out of the GaAs surface which then will be detected. If the depth of hydrogen, implanted or in-diffused, is more than 2 μm, then methods such as secondary ion mass spectroscopy (SIMS) could be used. In this case such systems cannot detect hydrogen but they can detect deuterium (D_2 or $^2H_2$).

APPENDIX I
LIST OF SYMBOLS

Symbol	Description	Unit
a	Area	cm^2
A_f	Degree of anisotropy	
A^*	Richardson constant for semiconductors	A cm^{-2} K^{-2}
A^{**}	Richardson constant for semiconductors with quantum mechanical reflection and phonon back-scattering	A cm^{-2} K^{-2}
C	Capacitance	F
D	Deposition rate	nm min^{-1}
h	Planck constant	J s
I	Current	A
I_o	Saturation current	A
k	Boltzmann constant	J K^{-1}
m_o	Electron rest mass	kg
m^*	Effective mass	kg
m^*_x	(= m^*/m_0). [x= e, lh, hh][@]	
n	Ideality factor of Schottky diode	
N	Carrier concentration	cm^{-3}
N_c	Density of states in conduction band	cm^{-3}
N_v	Density of states in valence band	cm^{-3}
P_d	Power density	W cm_{-2}
p	Pressure	Pa
q	Electronic charge	C
Q	Total flow rate	Pa m^3 sec^{-1}
Q_x	Partial flow rate. [x= Gas]	Pa m^3 sec^{-1}
R	Etch rate	nm min^{-1}
t_x	Vertical depth. [x= Material]	nm
T	Temperature	K
V	Applied voltage	V
V_{bi}	Built-in voltage	V
V_{self}	DC self bias voltage	V
V_p	Plasma Volume	m^3
$V_{\%x}$	Percent volume concentration of gas. [x= Gas]	
W_d	Depletion width	µm
x	Lateral etch depth	nm

Symbol	Description	Unit
y	Vertical etch depth. [= t_x for Material]	nm
ξ	Activation energy	eV $mole^{-1}$
ε_x	Relative permittivity. [x= Material]	
ε_o	Permittivity of free space	F cm^{-1}
ε_s	Permittivity of semiconductor	F cm^{-1}
θ	Angle of Anisotropy	°
τ	Etching time	min
τ_r	Residence time of gas in vacuum chamber	s
ϕ	Barrier height	V

@ - [e = electron, lh = light hole and hh = heavy hole.]

APPENDIX II
PROCESS CONDITIONS

System 1 -----> Electro Gas Systems SILOX EG 8/2 APCVD.

System 2 -----> Plasma-Therm PK 2430 PD PECVD.

System 3 -----> Nanotech Plasma Prep 100.

System 4 -----> Electrotech Plasmafab 340.

	System 1	System 2	System 3	System 4
Base Pressure	----	20 mtorr	100 mtorr	10 mtorr
Pressure	760 torr	600 mtorr	800 mtorr	45 mtorr
Power	----	40 W	100 W	75 W
Gas Flow 1	O_2 200 cc/min	NH_3 50 sccm	O_2 15000 cc/min	CHF_3 40 sccm
Gas Flow 2	N_2/SiH_4 95%/5% 60 cc/min	N_2/SiH_4 95%/5% 800 sccm	----	----
Gas Flow 3	N_2 8000 cc/min	----	----	----
Plate Temp.	450 °C	300 °C	----	----
Time	15 min	20 min	5 min	3 min
Material	SiO_2	Si_3N_4	N-45*, C^+	SiO_2, Si_3N_4
Process	Deposition ~ 170 nm	Deposition ~ 130 nm	Removing C or N-45	Removing SiO_2/Si_3N_4

* - N-45 is Merck negative photoresist. + - C or C polymers.

APPENDIX III
PHOTORESIST MASKING PROCEDURE

Merck negative photoresist N-45

Process step	Conditions
Substrate dehydration pretreatment	200 °C, 1 hour
Spin coating	5000 rpm ⇒ 0.4 µm thick
Pre-bake	80 °C, 10 minutes
Irradiation with high pressure mercury vapour lamp HB O: 200 W	2 seconds
Development with Selectiplast N-2	First bath 45 seconds Second bath 5 seconds
Rinsing with n-butyl acetate MOS Selectipur	First bath 45 seconds Second bath 5 seconds
Post-bake	170 °C, 30 minutes
Pattern transfer	Wet or dry etching
Removal of photoresist with O_2 plasma	5 minutes

APPENDIX IV
CHARACTERISTICS OF GASES USED FOR REACTIVE ION ETCHING

	ARGON	FREON 23	METHANE	HYDROGEN
FORMULAE	Ar	CHF_3	CH_4	H_2
GRADE	Electronic N 4.85	VLSI N 4.8	Research N 4.5	Research N 5.5
PURITY (%)	99.9985	99.998	99.995	99.9995
FLAMMABLE LIMIT IN AIR (%)	Non Flammable	Non Flammable	5-15	4-74.5
CONVERSION FACTOR*	1.42	0.50	0.72	1.01
MAIN CHARACTERISTICS	Chemically Inert, Asphyxiant	Asphyxiant	Flammable, Asphyxiant	Highly Flammable, Asphyxiant
CONTENTS IN CYLINDER	Gas	Liquefied Gas	Gas	Gas
BOILING POINT (°C)	-185.9	-82.1	-161.5	-252.77
Typical Impurities	O_2, N_2, CO_2, CO, H_2, H_2O, HC.	Air, H_2O, Acidity, Freons.	O_2, N_2, Ar, CO_2, H_2O.	O_2, N_2, CO_2, CO, H_2O, HC.

*- Conversion factor relative to N_2.

APPENDIX V
CONVERSION GRAPH FOR MASS FLOW CONTROLLERS

1 sccm = (101333.33 Pa)/((1 X10^6 m^3) X (60 sec)) = 1.69 X 10^{-3} Pa m^3/ sec.

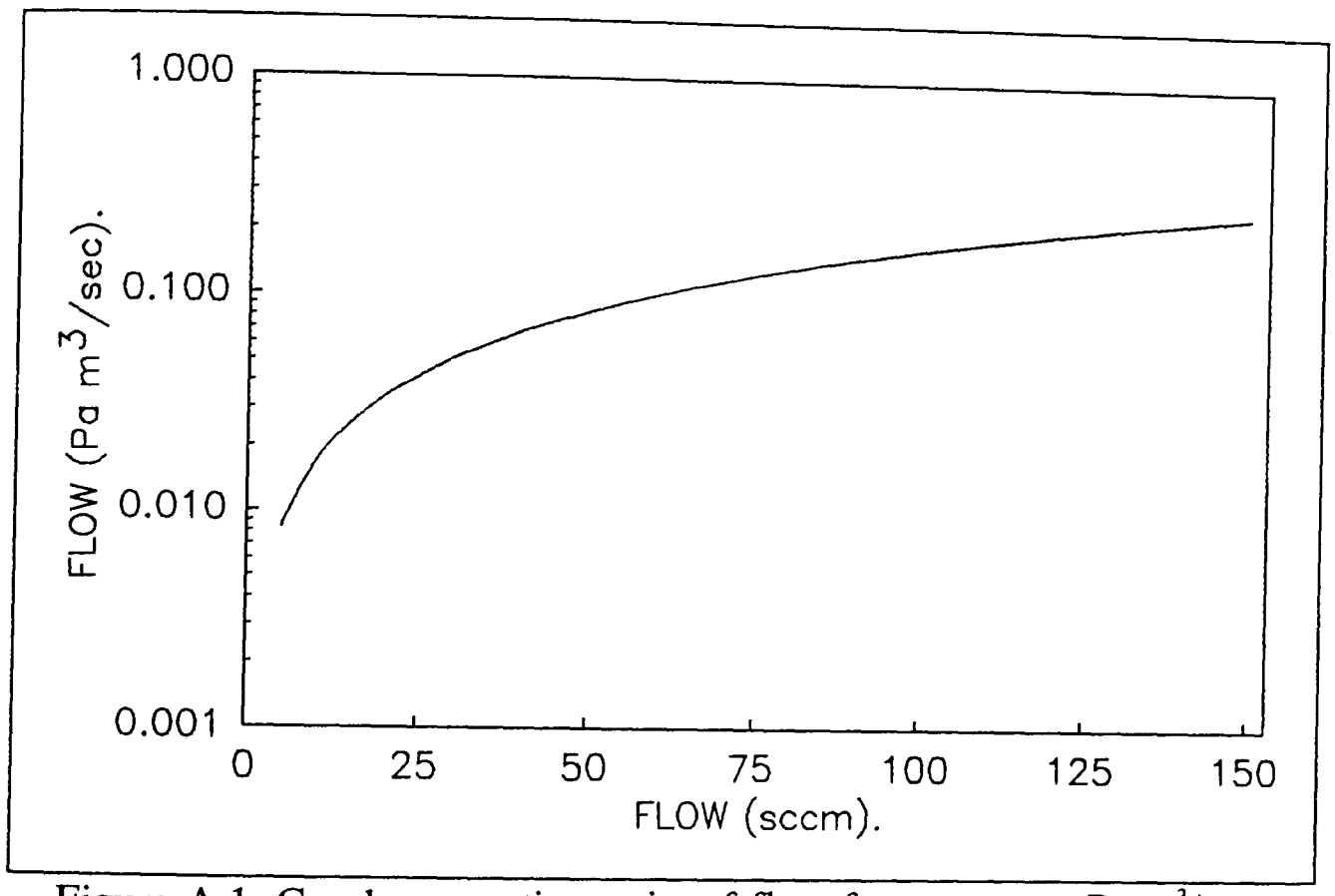

Figure A.1. Graph converting units of flow from sccm to Pa m^3/sec.

Table presenting conversion of values from sccm to Pa m^3/sec.

sccm	Pa m^3/sec (X 10^{-2})	sccm	Pa m^3/sec (X 10^{-2})
10	1.7	60	10.1
20	3.4	70	11.8
30	5.1	80	13.5
40	6.8	90	15.2
50	8.5	100	16.9

APPENDIX VI
TABLES OF CONSTANTS

Physical constants

Quantity	Symbol	Value	Unit
Boltzmann's constant	k	1.38066×10^{-23}	$J\ K^{-1}$
Electronic charge	q	1.60218×10^{-19}	C
Electronic rest mass	m_o	0.91095×10^{-30}	kg
Permittivity in vacuum	ε_o	8.85418×10^{-14}	$F\ cm^{-1}$
Plank's constant	h	6.62617×10^{-34}	J s
Thermal voltage at 300 K	kT/q	0.0259	V

Properties of GaAs at 300 K

Properties	Symbol	Value	Unit
Relative permittivity of GaAs	ε_{GaAs}	13.1	
Permittivity of GaAs	ε_s	1.15935×10^{-12}	$F\ cm^{-1}$
Effective density of states in conduction band	N_c	4.7×10^{17}	cm^{-3}
Effective density of states in valence band	N_v	7.0×10^{18}	cm^{-3}
Electron effective mass	m^*_e	0.067	
Hole (light) effective mass	m^*_{lh}	0.082	
Hole (Heavy) effective mass	m^*_{hh}	0.45	
Energy gap at 300 K	E_g	1.42	eV

APPENDIX VII
CURRENT-VOLTAGE CHARACTERISTICS OF SCHOTTKY DIODES

From thermionic-emission theory (Rhoderick and Williams, 1988), the current I is given by,

$$I = I_o \exp\left(\frac{qV}{nkT}\right), \tag{1A7}$$

where, q = electronic charge
V = applied voltage
k = Boltzmann's constant
T = temperature which was taken as 300 K
n = ideality factor
I_o = saturation current. (See appendix VI for values of constants).

From (1A7),

$$\ln I = \ln I_o + \left(\frac{q}{nkT}\right)V, \tag{2A7}$$

The above equation yields a straight line from which n can be calculated from the gradient,

$$n = \left(\frac{q}{kT}\right)\frac{\partial(\ln I)}{\partial V}, \tag{3A7}$$

where $\partial(\ln I)/\partial V$ is the gradient of the graph. The saturation current I_o can be found from the y intercept of the graph and is given by,

$$I_o = A^{**} T^2 a \exp\left(-\frac{q\phi}{kT}\right), \tag{4A7}$$

where a is the surface area of the diode, A^{**} is the Richardson constant. (see appendix VIII) and ϕ is the barrier height. From (4A7),

$$\phi = \frac{kT}{q} \ln\left(\frac{A^{**}aT^2}{I_o}\right), \qquad (5A7)$$

n and ϕ can then be calculated from above equations.

APPENDIX VIII
CALCULATION OF RICHARDSON CONSTANT

The Richardson constant for semiconductors is given approximately by.

$$A^* = \frac{4\pi q m^* k^2}{h^3}, \qquad (1A8)$$

With quantum mechanical reflections and phonon scattering the formula is changed to,

$$A^{**} = (f_Q f_P) A^*, \qquad (2A8)$$

where the constant ($f_Q f_P$)=0.5, (Shur, 1987) and h is the Planck's constant. The effective mass is given by,

$$m^* = m_0 m_x^*, \qquad (3A8)$$

where

$$m_x^* = m_e^*,$$

for electrons and

$$m_x^* = m_{lh}^* + m_{hh},$$

for holes respectively.

Richardson constant calculated for GaAs.
Units of A cm^{-2} K^{-2}.

	A^*	A^{**}
n-type	9.5	4.8
p-type	75.5	37.8

APPENDIX IX
CAPACITANCE-VOLTAGE CHARACTERISTICS OF SCHOTTKY DIODES

For a metal-semiconductor barrier (Look, 1989) the depletion width W_d is given by,

$$W_b = \sqrt{\frac{2\epsilon_s}{qN}\left(V_{bi} - V - \frac{kT}{q}\right)}, \tag{1A9}$$

The depletion layer capacitance C is given by,

$$C = \frac{\epsilon_s a}{W_d}, \tag{2A9}$$

where, N = carrier concentration

ε_s = Permittivity of semiconductor (= $\varepsilon_o\varepsilon_{GaAs}$, where ε_o is permittivity in free space and ε_{GaAs} is the GaAs relative permittivity).

V_{bi} = built-in voltage. (See appendix VI for values of constants).

From (1A9) and (2A9),

$$\frac{1}{C^2} = \frac{2}{qNa^2\epsilon_s}\left(V_{bi} - V - \frac{kT}{q}\right), \tag{3A9}$$

Graphs of $1/C^2$ against V would yield a straight line if N is uniform throughout the semiconductor. In the case of a non-uniform carrier concentration, N should be plotted against the W_d. N is given by;

$$N = \frac{2}{qa^2\epsilon_s}\left(-\frac{1}{d(1/C^2)/dV}\right), \tag{4A9}$$

APPENDIX X
DC SELF BIAS VOLTAGE

The negative charge accumulated on the cathode in a RIE system causes the DC self bias voltage . This is due to the fast mobility of the electrons compared with other particles present in the chamber during RIE. Figure A.2 (a), shows a simplified diagram of the chamber with the plasma and the insulating material covering the cathode. Its equivalent circuit diagram is presented in figure A.2 (b). Figure A.2 (c) shows the voltage at α, (The wave form is presented in square shape for simplicity). At β the wave form is as shown in figure A.2 (d). This is because of the accumulation of charge per cycle on the cathode.

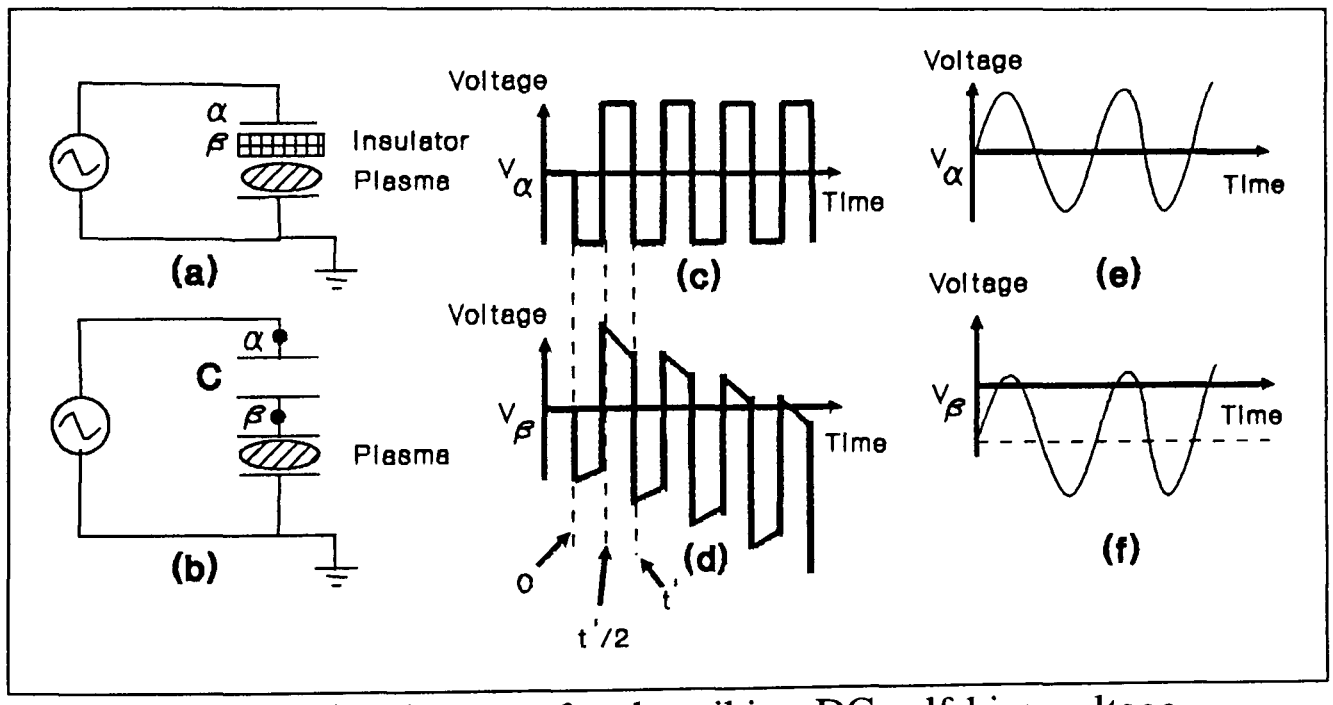

Figure A.2. Diagrams for describing DC self bias voltage.

If the wave form at α, is a sinusoid as presented in figure A.2 (e), then at β this wave form would be offset by a negative amount as shown in figure A.2 (f).

APPENDIX XI
REFLECTED POWER OF RF GENERATORS

When a RF generator supplies power to a load (plasma vacuum chamber), some power is reflected back to the RF generator. This is called the reflected power.

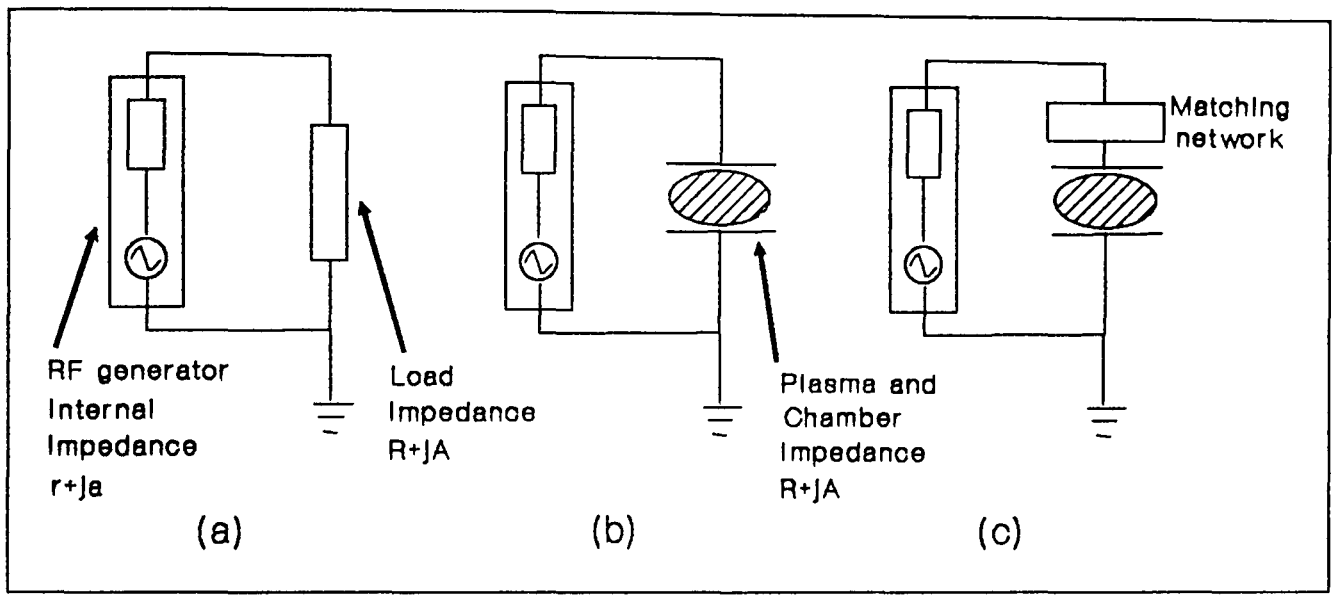

Figure A.3. Diagrams showing RF generator with internal impedance and load.

Figure A.3 (a) shows a RF generator with an internal impedance of (r+ja) which is connected to a load of impedance (R+jA). It is important for the generator to have a maximum power dissipation on load so that power is not be reflected back to the RF generator, (i.e. a large current does not flow round the circuit back to the generator). The mean power over one cycle <P> for the circuit shown in figure A.3 (a) is given by;

$$<P> = \frac{R(V_{rms})^2}{[(r+R)^2+(a+A)^2]} \qquad (1A11)$$

where V_{rms} is the root mean square voltage generated by the RF generator. The power dissipation in the load can change when the impedance of the circuit is changed. The minimum value of power dissipated in load is found by;

$$\frac{d<P>}{dR} = \frac{(V_{rms})^2 [(r+R)^2+(a+A)^2] - 2R(r+R)}{[(r+R)^2 +(a+A)^2]^2} \qquad (2A11)$$

From equation (2A11) it can be noted that power dissipation in the load will be a maximum when A=-a and R=r.

Figure A.3 (b), shows the same arrangement as before but the load is the chamber with plasma. In this case to minimise the reflected power a matching network is needed such that the combined impedance of the plasma chamber and the matching network is equal to that of the generator. This is shown in figure A.3 (c).

APPENDIX XII
IONIZATION POTENTIAL AND BOND STRENGTH OF SELECTED ELEMENTS AND MOLECULES

Ionization energy of molecules (eV)		**Ionization energy of elements (eV)**		**Bond Strength of molecules (eV)**	
Molecule	Energy	Element	Energy	Molecule	Energy
H_2	15.4	H	13.6	H-H	4.5
CH_4	12.6	C	11.3	H-CH_3	4.6
CH_3	9.8	Ar	15.8	H-CH_2	4.8
CH_2	10.4	Ne	21.6	H-CH	4.4
CH	11.1	He	24.6	H-C	3.5

Divide by 96.49 to convert from eV to kJ/mol.

Values from CRC Handbook of Chemistry and Physics, 67th Edition, 1986-1987, CRC Press.

PUBLICATIONS AND PRESENTATIONS

[1] **Sahafi, H.F.**, Goldspink, G.F., Rezazadeh, A.A., Webb, A.P. and Carter, M.A. (1992). "Damage induced in p-GaAs due to RIE in CH_4/H_2 mixtures", 'Electronics Letters', Vol. 28, December, No. 25, pp 2300-2302.

[2] **Sahafi, H.F.**, Goldspink, G.F., Webb, A.P. and Carter, M.A. "Effect of flow rate on reactive ion etching of GaAs in CH_4/H_2 plasma", Accepted for publication in 'Vacuum'.

[3] **Sahafi, H.F.**, Webb, A.P., Carter, M.A. and Goldspink, G.F. "Effect of process parameters on dc self-bias voltage in CH_4/H_2 RIE of GaAs", Accepted for publication in 'Microelectronics Journal'.

[4] **Sahafi, H.F.**, Webb, A.P., Carter, M.A. and Goldspink, G.F. "Reactive ion etching of GaAs in CH_4/H_2 plasma", Poster presented at Dry Etching Symposium, 'Technology and Application of Ion Beams Conference', Loughborough University of Technology, April 8th 1992.

REFERENCES

Akita, K., Sugimoto, Y. and Kawanishi, H. (1991). "Electron-beam-induced maskless HCl pattern etching of GaAs", Semiconductor Science and Technology, Vol. 6, pp 934-936.

Ali, F., Bahl, I. and Gupta, A. (Editors), (1989). "Microwave and millimeter-wave heterostructure transistors and their applications", (Artech House).

Aoyagi, Y., Shinmura, K., Kawasaki, K., Tanaka, T., Gamo, K., Namba, S. and Nakamoto, I. (1992). "Molecular layer etching of GaAs", Applied Physics Letters, Vol. 60, February, No. 8, pp 968-970.

Asakawa, K., Takadoh, N., Uchida, M. and Yuasa, T. (1987). "GaAs reactive ion beam etching and surface cleaning using enclosed ultrahigh-vacuum processing system", NEC Research and Development, October, No. 87, pp 1-13.

Ashburn, P. and Rezazadeh, A.A. (1988). "Comparison of silicon bipolar and GaAlAs/GaAs hetrojunction bipolar technologies using a propagation delay expression", GEC Journal of Research, Vol. 6, No. 3, pp 176-182.

Broydo, S. (1983). "Important considerations in selecting anisotropic plasma etching equipment", Solid State Technology, April, pp 159-165.

Carter, A.J., Thomas, B., Morgan, D.V., Bhardwaj, J.K., McQuarrie, A.M. and Stephens, M.A. (1989). "Dry etching of GaAs and InP for optoelectronic devices", IEE Proceedings, Vol. 136, February, Pt. J, No. 1, pp 2-5.

Carter, M.A. (1988). "Dry etch development for silicon processing within a teaching institution", Vacuum, Vol. 38, No. 8-10, pp 873-876.

Chakrabarti, U.K., Pearton, S.J. and Ren, F. (1991). "Sidewall roughness during dry etching of InP", Semiconductor Science and Technology, Vol. 6, pp 408-410.

Chang[b], R.P.H., Chang, C.C. and Darack, S. (1982). "Summary abstract: Hydrogen plasma etching of semiconductors and their oxides", Journal of Vacuum Science and Technology, Vol. 20, March, No. 3, pp 490-491.

Chang[a], R.P.H., Chang, C.C. and Darack, S. (1982). "Hydrogen plasma etching of semiconductors and their oxides", Journal of Vacuum Science and Technology, Vol. 20, January, No. 1, pp 45-50.

Chaplart, J., Fay, B. and Linh, N.T. (1983). "Reactive ion etching of GaAs using CCl_2F_2 and the effect of Ar addition", Journal of Vacuum Science and Technology B, Vol. 1, October/December, No. 4, pp 1050-1052.

Chapman, B.N. (1980). "Glow discharge processes", Wiley (Pub.).

Chapman, B.N. and Minkiewicz, V.J. (1978). "Flow rate effects in plasma etching", Journal of Vacuum Science and Technology, Vol. 15, March/April, No. 2, pp 329-332.

Chen, C.L. (1982). "Gate formation in GaAs MESFET's using ion-beam etching technology", IEEE Transactions on Electron Devices, Vol. ED-29, October, No. 10, pp 1522-1529.

Cheung, R., Thoms, S., McIntyre, I., Wilkinson, C.D.W. and Beaumont (1988). "Passivation of donors in electron beam lithographically defined nanostructures after methane/hydrogen reactive ion etching", Journal of Vacuum Science and Technology B, Vol. 6, November/December, No. 6, pp 1911-1915.

Cheung, R., Thoms, S., Beaumont, S.P., Doughty, G., Law, V. and Wilkinson, C.D.W. (1987). "Reactive ion etching of GaAs using a mixture of methane and hydrogen", Electronics Letters, Vol. 23, July, No. 16, pp 857-859.

Coburn, J.W. (1982). "Plasma-assisted etching", Plasma Chemistry and Plasma Processing, Vol. 2, No. 1, pp 1-41.

Collot, P. and Gaonach, C. (1990). "Electrical damage in n-GaAs due to methane-hydrogen RIE", Semiconductor Science and Technology, Vol. 5, pp 237-241.

Cooper III, C.B., Salimian, S. and Day, M.E. (1989). "Dry Etching for the Fabrication of Integrated Circuits in III-V Compound Semiconductors", Solid State Technology, January, pp 109-112.

Darbyshire, D.A. and Pitt, C.W. (1990). "Ion-assisted processing of GaAs for optical devices", Vacuum, Vol. 40, No. 4, pp 351-355.

Dautremont-Smith, W.C. (1988). "Hydrogen in III-V semiconductors", Materials Research Society Symposium Proceedings, Vol. 104, pp 313-323.

Donnelly, V.M., Flamm, D.L., Tu, C.W. and Ibbotson, D.E. (1982). "Temperature dependence of InP and GaAs etching in a chlorine plasma", Journal of Electrochemical Society: Solid-State Science and Technology, Vol. 129, November, No. 11, pp 2533-2537.

Doughty, G.F., Thoms, S., Law, V. and Wilkinson, C.D.W. (1986). "Dry etching of indium phosphide", Vacuum, Vol. 36, No. 11-12, pp 803-806.

Duffin, W.J. (1980). "Electricity and magnetism", 3rd Edition, McGraw-Hill (Pub.), London, UK.

Ephrath, L.M. (1982). "Dry Etching for VLSI-A Review", Jornal of Electrochemical Society: Reviews and News, Vol. 129, March, No. 3, pp 62C-66C.

Field, D., Song, Y.P., Klemperer, D.F. and Day, A.P. (1990). "Etch diagnostics for new III-V and other semiconductors", Vacuum, Vol. 40, No. 4, pp 357-361.

Flamm, D.L., Donnelly, V.M. and Ibbotson, D.E. (1983). "Basic chemistry and mechanisms of plasma etching", Journal of Vacuum Science and Technology B, Vol. 1, January/March, No. 1, pp 23-30.

Flamm, D.L. and Donnelly, V.M. (1981). "The design of plasma etchants", Plasms Chemistry and Plasma Processing, Vol. 1, No. 4, pp 317-363.

Fonash[b], S.J. (1985). "Damage Effects in Dry Etching", Solid State Technology, April, pp 201-205.

Fonash[a], S.J. (1985). "Advances in dry etching processes-A review", Solid State Technology, January, pp 150-158.

Foxon, C.T. (1978). "Molecular beam epitaxy", Acta Electronica, Vol. 21, No. 2, pp 139-150.

Gottscho, R.A., Smolinsky, G. and Burton, R.H. (1982). "Carbon tetrachloride plasma etching of GaAs and InP: A kinetic study utilizing nonperturbative optical techniques", Journal of Applied Physics, Vol. 53, August, No. 8, PP 5908-5919.

Hayes[b], T.R., Dreisbach, M.R., Thomas, P.M. and Dautremont-Smith, W.C., (1989). "Reactive ion etching of InP using CH_4/H_2 mixtures: Mechanisms of etching and anisotropy", Journal of Vacuum Science ond Technology B, Vol. 7, September/October, No. 5, pp 1130-1140.

Hayes[a], T.R., Dautremont-Smith, W.C., Luftman, H.S. and Lee, J.W. (1989). "Passivation of acceptors in InP resulting from CH_4/H_2 reactive ion etching", Applied Physics Letters, Vol. 55, July, No. 1, pp 56-58.

Henry, L., Vaudry, C. and Granjoux, P. (1987). "Novel process for integration of optoelectronic devices using reactive ion etching without chlorinated gas", Electronics Letters, Vol. 23, November, No. 24, pp 1253-1254.

Herbst, L.T. (Editor), (1992). "The heterojunction bipolar transistor in high speed digital electronics", Prentice-Hall International (Pub.), UK.

Hikosaka, K., Mimura, T. and Joshin, K. (1981). "Selective dry etching of AlGaAs/GaAs heterojunction", Japanese Journal of Applied Physics, Vol. 20, November, No. 11, pp L847-L850.

Hilton, K.P., Woodward, J., Dawsey, J.R., Ball, G. and Gill, S.S. (1989). "Damage-free reactive ion etching of GaAs FET gate recess", Electronics Letters, Vol. 25, November, No. 24, pp 1617-1618.

Hilton, K.P. and Woodward, J. (1988). "Surface patterning of GaAs by CCl_2F_2 reactive ion etching", Vacuum, Vol. 38, No. 7, pp 519-525.

Hipwood, L.G. and Wood, P.N. (1985). "Dry etching of through substrate via holes for GaAs MMIC's", Journal of Vacuum Science and Technology B, Vol. 3, January/February, No. 1, pp 395-397.

Hirano, M. and Asai, K. (1991). "GaAs taper etching by mixture gas reactive ion etching system", Japanese Journal of Applied Physics, Vol. 30, December, No. 12B, pp L2136-L2138.

Horwitz, C.M. (1983). "RF sputtering-voltage division between two electrodes" Journal of Vacuum Science and Technology A, Vol. 1, January/March, No. 1, pp 60-68.

Howes, M.J. and Morgan, D.V. (1986). "Gallium arsenide, materials, devices and circuits", Wiley (Pub.), UK.

Ibbotson[b], D.E. and Flamm, D.L. (1988). "Plasma etching for III-V compound devices: Part II", Solid State Technology, November, pp 105-108.

Ibbotson[a], D.E. and Flamm, D.L. (1988). "Plasma etching for III-V compound devices: Part I", Solid State Technology, October, pp 77-79.

Jacko, M.G. and Price, S.J.W. (1964). "The pyrolysis of trimethylindium", Canadian Journal of Chemistry, Vol. 42, pp 1198-1205.

Jacko, M.G. and Price, S.J.W. (1963). "The pyrolysis of trimethyl Gallium", Canadian Journal of Chemistry, Vol. 41, pp 1560-1567.

Knoedler, C.M. and Kuech, T.F. (1986). "Selective GaAs/$Al_xGa_{1-x}As$ reactive ion etching using CCl_2F_2", Journal of Vacuum Science and Technology B, Vol. 4, September/October, No. 5, pp 1233-1236.

Kobayashi, R., Fujii, K. and Hasegawa, F. (1991). "Etching of GaAs by atomic hydrogen generated by a tungsten filament", Japanese Journal of Applied Physics, Vol. 30, August, No. 8B, pp L1447-L1449.

Law, V.J. and Jones, G.A. (1992). "Chloromethane-based reactive ion etching of GaAs and InP", Semiconductor Science and Technology, Vol. 7, pp 281-283.

Law[b], V.J., Ingram, S.G. and Jones, G.A.C. (1991). "ECR/magnetic mirror coupled plasma etching of GaAs using CH_4:H_2:Ar", Semiconductor Science and Technology, Vol. 6, pp 945-947.

Law[a], V.J., Ingram, S.G., Tewordt, M. and Jones, G.A.C. (1991). "Reactive ion etching of GaAs using CH_4: in He, Ne, and Ar", Semiconductor Science and Technology, Vol. 6, pp 411-413.

Law[c], V.J., Jones, G.A.C. and Tewordt, M. (1990). "Propane: hydrogen MORIE of GaAs", Semiconductor Science and Technology, Vol. 5, pp 1001-1003.

Law[b], V.J., Jones, G.A.C., Patel, N.K. and Tewordt, M. (1990). "Loading effects in CH_4 and H_2 MORIE of GaAs", Microelectronic Engineering, Vol. 11, pp 611-614.

Law[a], V.J., Jones, G.A.C. and Tewordt, M. (1990). "Substrate temperature dependence of GaAs etch rates in CH_4:H_2 MORIE", Semiconductor Science and Technology, Vol. 5, pp 281-283.

Law, V.J., and Jones, G.A.C. (1989). "Obtaining high etch rates of GaAs/$Al_{0.3}Ga_{0.7}As$ using methane:hydrogen MORIE and organic photoresist masks", Semiconductor Science and Technology, Vol. 4, pp 833-835.

Law, V.J., Jones, G.A.C., Ritchie, D.A., Peacock, D.C. and Frost, J.E.F. (1989). "Selective metalorganic reactive ion etching of molecular-beam epitaxy GaAs/$Al_xGa_{1-x}As$", Journal of Vacuum Science and Technology B. Vol. 7, November/December, No. 6, pp 1479-1482.

Lecrosnier, D., Henry, L., Le Corre, A. and Vaudry, C. (1987). "GaInAs junction FET fully dry etched by metal organic reactive ion etching technique", Electronics Letters, Vol. 23, November, No. 24, pp 1254-1255.

Lee, B.S. and Baratte, H. (1990). "Reactive ion etching of GaAs in chlorine and resulting surface damage", Journal of Electrochemical Society, Vol. 137, March, No. 3, pp 980-983.

Li, J.Z., Adesida, I. and Wolf, E.D. (1985). "Evidence of crystallographic etching in (100)GaAs using $SiCl_4$ reactive ion etching", Journal of Vacuum Science and Technology B, Vol. 3, January/February, No. 1, pp 406-409.

Li, J.Z., Adesida, I. and Wolf, E.D. (1984). "Orientation dependent reactive ion etching of GaAs in $SiCl_4$", Applied Physics Letters, Vol. 45, October, No. 8, pp 897-899.

Look, D.C. (1989). "Electrical characterization of GaAs materials and devices" Wiley (Pub.), UK.

Madams, C.J., Morgan, D.V. and Howes, M.J. (1975). "Outmigration of Gallium from Au-GaAs interface", Electronics Letters, Vol. 11, November, No. 24, pp 574-575.

Matsui, T., Sugimoto, H., Ohishi, T. and Ogata, H. (1988). "Reactive ion etching of III-V compounds using C_2H_6/H_2", Electronics Letters, Vol. 24, June, No. 13, pp 798-800.

McNabb, J.W., Craighead, H.G., Temkin, H. and Logan, R.A. (1991). "Anisotropic reactive ion etching of InP in methane/Hydrogen based plasma", Journal of Vacuum Science and technology B, Vol. 9. November/December, No. 6, pp 3535-3537.

McQuarrie, A.D. (1988). "Practical alternative to ion beam milling", European Secmiconductor, March, pp 34-35.

Miers, T.H. (1982). "Schottky contact fabrication for GaAs MESFET's", Journal of Electrochemical Society: Solid-State Science and Technology, Vol. 129, August, No. 8, pp 1795-1799.

Moss, R.H. (1983). "Metallo-organic compounds", Chemistry in Britain, September, pp 733-737.

Mullins, C. (1982). "Single Wafer Plasma Etching, 2. SiO_2: Etching Mechanisms and Characteristics", Solid State Technology, August, pp 88-92.

Niggebrügge, U., Klug, M. and Garus, G. (1985). "A novel process for reactive ion etching on InP using CH_4/H_2", Institute of Physics Conference, Serial No. 79, Ch. 6, pp 367-372.

Olsen, G.H. and Zamerowski, T.J. (1983). "Double-barrel III-V compound vapour-phase epitaxy systems", RCA Review, Vol. 44, June, pp 270-285.

Pang, S.W. (1986). "Surface damage on GaAs induced by reactive ion etching and sputter etching", Journal of Electrochemical Society: Solid-State Science and Technology, Vol. 133, April, No. 4, pp 784-787.

Pang, S.W. (1984). "Dry etching induced damage in Si and GaAs", Solid State Technology, April, pp249-256.

Pearton, S.J., Chakrabarti, U.K., Katz, A., Ren, F. and Fullowan, T.R. (1992). "High-rate anisotropic dry etching of InP in HI-based discharges". Applied Physics Letters, Vol. 60, February, No. 7, pp 838-840.

Pearton, S.J. and Hobson, W.S. (1991). "Electron cyclotron resonance microwave plasma etching of $In_{0.2}Ga_{0.8}As$-GaAs quantum well laser structures", Semiconductor Science and Technology, Vol. 6, pp 948-951.

Pearton[b], S.J. and Hobson, W.S. (1989). "Elevated temperature reactive ion etching of GaAs and AlGaAs in C_2H_6/H_2", Journal of Applied Physics, Vol. 66, November, No. 10, pp 5018-5025.

Pearton[a], S.J. and Hobson, W.S. (1989). "Etch rates and surface chemistry of GaAs and AlGaAs reactive ion etched C_2H_6/H_2", Journal of Applied Physics, Vol. 66, November, No. 10, pp 5009-5017.

Pearton, S.J., Dautremont-Smith, W.C., Lopata, J., Tu, C.W. and Abernathy, C.R. (1987). "Dopant-type effects on the diffusion of deuterium in GaAs", Physical Review B, Vol. 36, September, No. 8, pp 4260-4264.

Rhoderick, E.H. and Williams R.H. (1988). "Metal-semiconductor contacts", 2nd Edition, Oxford (Pub.), New York, USA.

Salimian, S. and Cooper III, C.B. (1988). "Selective dry etching of GaAs over AlGaAs in $SF_6/SiCl_4$ mixtures", Journal of Vacuum Science and Technology B, Vol. 6, November/December, No. 6, pp 1641-1644.

Sato, M. and Nakamura, H. (1982). "Reactive Ion Etching of Aluminum using $SiCl_4$", Journal of Vacuum Science and Technology, Vol. 20, February, No. 2, pp 186-190.

Scherer, A., Craighead, H.G. and Beebe, E.D. (1987). "Gallium arsenide and aluminum gallium arsenide reactive ion etching in boron trichloride/argon mixtures", Journal of Vacuum Science and Technology B, Vol. 5, November/December, No. 6, pp 1599-1605.

Schwartz, G.C. and Schaible, P.M. (1980). "Reactive ion etching in chlorinated plasmas", Solid State Technology, November, pp 85-91.

Seaward, K.L., Moll, N.J. and Coulman, D.L. (1987). "An analytical study of etch and etch-stop reactions for GaAs on AlGaAs in CCl_2F_2 plasma", Journal of Applied Physics, Vol. 61, March, No. 6, pp 2358-2364.

Semura, S., Saitoh, H. and Asakawa, K. (1984). "Reactive ion etching of GaAs in CCl_4/H_2 and CCl_4/O_2", Journal of Applied Physics, Vol. 55, April, No. 8, pp 3131-3135.

Shur, M. (1987). "GaAs devices and circuits", Plenum (Pub.), New York, USA.

Singer, P.H. (1988). "Today's Plasma Etch Chemistries", Semiconducror International, March, pp 68-73.

Singh, J. (1991). "Magnetron ion etching of InP using mixture of methane and hydrogen and its comparison with reactive ion etching", Journal of Vacuum Science and Technology B, Vol. 9, July/August, No. 4, pp 1911-1919.

Smolinsky, G., Gottscho, R.A. and Abys, S.M. (1983). "Time-dependent etching of GaAs and InP with CCl_4 or HCl Plasmas: Electrode material and oxident addition effects", Journal of Applied Physics, Vol. 54, June, No. 6, pp 3518-3523.

Smolinsky, G., Chang, R.P. and Mayer, T.M. (1981). "Plasma etching of III-V compound semiconductor materials and their oxides", Journal of Vacuum Science and Technology, Vol. 18, January/February, No. 1, PP 12-16.

Sonek, G.L. and Ballantyne, J.M. (1984). "Reactive ion etching of GaAs using BCl_3", Journal of Vacuum Science and Technology B, Vol. 2, October/December, No. 4, pp 653-657.

Spicer, W.E., Eglash, S., Lindau, I, Su, C.Y. and Skeath, P.R. (1982). "Development and confirmation of the unified model for the Schottky barrier formation and MOS interface states on III-V compounds", Thin Solid Films, Vol. 89, pp 447-460.

Spicer, W.E., Lindau, I., Skeath, P. and Su, C.Y. (1980). "Unified defect model and beyond", Journal of Vacuum Science and Technology, Vol. 17, September/October, No. 5, pp 1019-1027.

Stern, M.B. and Liao, P.F. (1983). "Reactive ion etching of GaAs and InP using $SiCl_4$", Journal of Vacuum Science and Technology B, Vol. 1, October/December, No. 4, PP 1053-1055.

Sugata, S. and Asakawa, K. (1987). "GaAs and AlGaAs crystallographic etching with low-pressure chlorine radicals in an ultrahigh-vacuum system", Journal of Vacuum Science and Technology B, Vol. 5, July/August, No. 4, pp 894-901.

Sze, S.M. (Editor), (1985). "VLSI Technology", McGraw-Hill (Pub.), Singapore.

Sze, S.M. (1981). "Physics of Semiconductor Devices", 2nd Edition, Wiley (Pub.), New York, USA.

Tachibana, K., Nishida, M., Harima, H. and Urano, Y. (1984). "Diagnostics and modelling of a methane plasma used in the chemical vapour deposition of amorphous carbon film", Journal of Physics D: Applied Physics, Vol. 17, pp 1727-1742.

Thomas, H., Morgan, D.V., Thomas, B., Aubrey, J.E. and Morgan, J.B. (Editors), (1986). "Gallium Arsenide for Devices and Integrated Circuits". Proceedings of the 1986 UWIST GaAs School, Peter Peregrinus Ltd. (Pub.), London , on behalf of the IEE.

Thompson, G.H.B. and Kirkby, P.A. (1974). "Liquid phase epitaxial growth of six-layer GaAs/(GaAl)As structures for injection lasers with 0.04 μm thick centre layer", Journal of Crystal Growth, Vol. 27, pp 70-85.

Thoms, S., McIntyre, I., Beaumont, S.P., Al-Mudares, M., Cheung, R. and Wilkinson, C.D.W. (1988). "Fabrication of quantum wires in GaAs/AlGaAs heterolayers", Journal of Vacuum Science and Technology B, Vol. 6, January/February, No. 1, pp 127-130.

Tirtowidjojo, M. and Pollard, R. (1986). "Equilibrium gas phase species for MOCVD of $Al_xGa_{1-x}As$", Journal of Crystal Growth, Vol. 77, pp 200-209.

Van Daele, P., Lootens, D. and Demeester, P. (1990). "Dry etching of III-V semiconductors: influence of temperature on the anisotropy and induced damage", Vacuum, Vol. 41, No. 4-6, pp 906-908.

Van Gurp, G.J., Jacobs, J.M., Binsma, J.J.M. and Tiemeijer, L.F. (1989). "InGaAsP/InP Lasers with two reactive ion etched mirror facets", Japanese Journal of Applied Physics, Vol. 28, July, No. 7, pp L1236-L1238.

Van Roijen, R., Kemp, M.B.M., Bulle-Lieuwma, C.W.T., Van Ijzendoom, L.J. and Thijssen, T.L.G. (1991). "Surface analysis of reactive ion-etched InP", Journal of Applied Physics, Vol. 70, October, No. 7, pp 3983-3985.

Van Roosmalen, A.J. (1984). "Review: dry etching of silicon oxide". Vacuum, Vol. 34, No. 3-4, pp 429-436.

Vawter, G.A., Coldren, L.A., Merz, J.L. and Hu, E.L. (1987). "Nonselective etching of GaAs/AlGaAs double heterostructure laser facets by Cl_2 reactive ion etching in a load-locked system", Applied Physics Letters, Vol. 51, September, No. 10, pp 719-721.

Vodjdani, N. and Parrens, P. (1987). "Reactive ion etching of GaAs with high aspect ratios with Cl_2-CH_4-H_2-Ar mixtures", Journal of Vacuum Science and Technology B, Vol. 5, November/December, No. 6, pp 1591-1598.

Yamada, H., Ito, H. and Inaba, H. (1985). "Anisotropic Reactive Ion Etching Technique of GaAs and AlGaAs Materials for Integrated Optical Device Fabrication", Journal of Vacuum Science and Technology B, Vol. 3, May/June, No. 3, pp 884-888.

Yuba, Y., Ishida, T., Gamo, K. and Namba, S. (1988). "Characterization of ion beam etching induced defect in GaAs", Journal of Vacuum Science and Technology B, Vol. 6, January/February, No. 1, pp 253-256.